



# ALT'19

**INTERNATIONAL CONFERENCE**

**Advanced Laser Technologies**



## Book of Abstracts

**Prague, Czech Republic**



---

15-20 September 2019

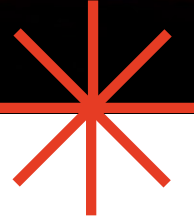




# ALT'19

**INTERNATIONAL CONFERENCE**

**Advanced Laser Technologies**



## Plenary Speakers

**Prague, Czech Republic**



---

15-20 September 2019

**P-I****Laser optics to uncover mysteries of early development***I.V. Larina*<sup>1</sup><sup>1</sup>*Molecular Physiology and Biophysics, Baylor College of Medicine, Houston, Texas, USA*

Over the last decades, developments in laser-based technologies significantly contributed to multiple areas of biomedicine; however, their application in developmental biology still has a lot of area for exploration. Early mammalian development is of very dynamic and dramatic structural changes, happening on different spatial scales, these ranging from subcellular to the whole organism. Because embryonic development happens deep within the female body, our current understanding of its dynamics is derived from static histological analysis, low-resolution visualizations, and studies of invertebrate models (e.g. sea urchin) and, as a result, do not necessarily represent what really happens. In our pursuit of building a comprehensive understanding of mammalian developmental dynamics *in vivo*, we took advantage of multiple laser-based technologies and developed a series of imaging methods and protocols combining functional optical coherence tomography (OCT), vital fluorescence reporters, optogenetic control, non-linear microscopy, intravital imaging approaches and mouse models of human developmental defects. We established functional OCT imaging methods providing information about transferring of oocytes/embryos, the contraction of the oviduct muscle, distribution of the frequency of cilia beat, as well as sperm behavior in the ampulla. These new observations revealed never-before-seen dynamic events which contradicted current views in scientific community and suggesting a role for cilia dynamics in the regulation of sperm movements. We are also investigating biomechanical regulation of cardiovascular development and cardiodynamics in live culture. We developed techniques for volumetric heart imaging at cellular resolution, blood flow analysis and 4-D angiography in the heart. These methods were applied to analysis of the pumping mechanism of early hearts and characterization of mutant phenotypes mimicking human congenital heart defects, suggesting regulatory role of heart contractions in cardiogenesis. We are now developing optogenetics to non-invasively manipulate cardiodynamics and second harmonic generation analysis of collagen to define the role of cardiac forces in maintaining mechanical homeostasis. Laser-based technologies have great potential to answer many important biological questions, leading to a better understanding, prevention, and treatment of congenital defects and embryonic failures in humans. Additionally, highly dynamic and diverse developmental processes with variety of challenging and exciting questions provide a great platform for laser physicists and optical engineers to develop new imaging and manipulation methods, pushing forward technological developments in optical engineering.

**P-II****New prospects in multiphysics modeling and simulations of matter dynamics of laser induced solid-to-plasma phase transitions**

*V. Dimitriou*<sup>1</sup>

*<sup>1</sup>Hellenic Mediterranean University- Greece, Institute of Plasma Physics & Lasers - IPPL, Rethymnon, Greece*

Femtosecond and nanosecond laser pulses are used for matter excitation. The common numerical approximation schemes, for the simulation of the excited matter dynamics, are analyzed and presented. Emphasis is given on their multiphysics character and their ability to include the phase transitions. The differences of the approximations of laser induced energy on solid targets by ns and fs laser pulses, are discussed. The cases of interest, where a global numerical scheme is able to monitor the matter dynamics, from ultrashort to nanoscale time ranges, are highlighted. The new prospects in multiphysics modeling and simulations of matter dynamics, of laser induced solid-to-plasma phase transitions, are discussed, focused on combinatorial models, able to simulate the spatiotemporal scales of interest. Representative models lying on various numerical approximation schemes, combined with macroscopic models, based on the Finite Element Method (FEM), are presented. The FEM models may offer clear insights into the volume and on the boundaries of the target, and realistically represent the dynamic response mechanisms that follow ultrashort laser irradiation. Representative applications, that may be used to monitor and detect the structural and mechanical characteristics of solids, are demonstrated.

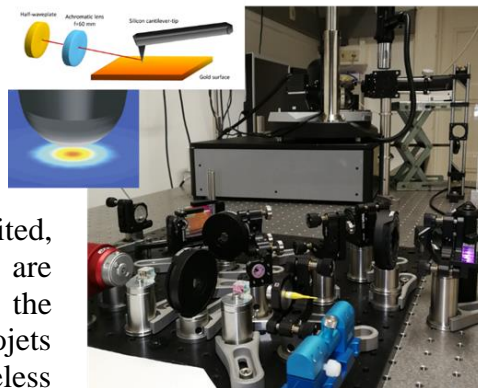
### P-III Laser-induced processes on condensed matter

W. Kautek<sup>1</sup>

<sup>1</sup>University of Vienna, Department of Physical Chemistry, Vienna, Austria

Fundamentals and recent research in the laser-driven physical chemistry at condensed matter interfaces will be presented [1,2]. This will include nanosecond pulse work in respect to 3D depth profiling by laser-induced breakdown spectroscopy [3-5] and the laser generation of colloidal nanoparticles for medical applications [6-8].

Femtosecond investigations with bandwidth-limited, temporally shaped pulses, are reviewed. Recent examples are the laser-driven synthesis of graphene nanosheets, the deterministic nanostructuring of solids generating e.g. nanojets in the far field [9], and nanolithography in the apertureless femtosecond scanning near-field (Figure) [10,11]. An outlook for new projects and applications will be presented.



#### References

- [1] W. Kautek and O. Armbruster, Springer Series in Materials Science 191 (2014) 43-66.
- [2] M.V. Shugaev, C. Wu, O. Armbruster, A. Naghilou, N. Brouwer, D.S. Ivanov, T.J.-Y. Derrien, N. M. Bulgakova, W. Kautek, B. Rethfeld, L.V. Zhigilei, MRS Bulletin 41 (2016) 960–968.
- [3] T. Nagy, U. Pacher, A. Giesriegl, L. Soyka, G. Trettenhahn, W. Kautek, Appl. Surf. Sci. 302 (2014) 184–188.
- [4] E. Paulis, U. Pacher, M.J.J. Weimerskirch, T.O. Nagy, W. Kautek, Appl. Phys. A 123 (2018) 790.
- [5] U. Pacher, M. Dinu, T.O. Nagy, R. Radvan, W. Kautek, Spectrochim. Acta B 146 (2018) 36-40.
- [6] N. Lasemi, U. Pacher, C. Rentenberger, O. Bomati Miguel, W. Kautek, ChemPhysChem 18 (2017) 1118–1124.
- [7] N. Lasemi, U. Pacher, L.V. Zhigilei, O. Bomati-Miguel, R. Lahoz, W. Kautek, Applied Surface Science 433 (2018) 772–779.
- [8] N. Lasemi, O. Bomati Miguel, R. Lahoz, V.V. Lennikov, U. Pacher, C. Rentenberger, W. Kautek, ChemPhysChem (2018) DOI: 10.1002/cphc.201701214.
- [9] A. Naghilou, M. He, J.S. Schubert, L.V. Zhigilei, W. Kautek, Phys. Chem. Chem. Phys. 21 (2019) 11846-11860
- [10] I. Falcón Casas, W. Kautek, Nanomaterials 8 (2018) 20-31.
- [11] I. Falcón Casas, W. Kautek, in “Laser micro-nano-nanomanufacturing and 3D microprinting”, A. Hu (Ed.), Springer, „Apertureless scanning near-field optical lithography“, in press.

## P-IV

### Pioneering pulsed laser synthesis of colloids

*A. Fojtik*<sup>1</sup>

<sup>1</sup>*NRNU MEPhI - Institut of Engineering Physics for Biomedicine, Moscow, Russia and Czech Technical University, Prague, Czech Republic*

In the year 1991 it has been assumed, that all substantial facts and technologies regarding nanoparticles were already known. We have been using all available methods. What more was left? Could lasers be put to a good use? Attempts were made, but without any particular breakthrough... At that time, we aimed to new type of nanostructures and we really had not expected that usage of lasers could bring us something revolutionary. But there was a surprise waiting around the corner...We hoped that by an absorption of intense laser beam by a solid state material, producing temperature of plasma of many thousands kelvins (similar like in sonochemistry, where several thousand kelvins are reached in oscillating gas bubbles in a liquids [1]), similar effects could be reached. Nothing more, nothing less. Initiating plasma by a focused laser beam (694nm Ruby laser flash) to thin film of solid state material thus creates conditions similar to a plasma discharge and cause ablation condition. When some liquid surrounds „hot plasma spot”, evaporated products are very quickly cooled down and very small nanoparticles can be produced. We hoped that maybe under these conditions new colloidal particles and clusters could be produced. Perhaps even some new form of nanostructures? All was working. What we had learnt from this experiment? We concluded that smaller particles are formed with increasing laser energy. Relatively broad size distribution was found in all experiments at laser synthesis of colloids. (At that time we did not expect that this idea would have such an enthusiastic following). Presently, situation for such a field of research, i.e., „Nanoparticle Generation by Lasers in Liquids”, is becoming a much hotter topic due to availability of picosecond and femtosecond lasers. Where are we now and what’s next? Open the research mainly for biomedical and biomedicine applications. For example, only this way can be prepare Fe /Ag magnetic nanoparticles, with high purity, which are at top interest for research against HIV virus and strategically defence against gram-positive bacteria like anthrax (our attempt). See the lecture.

### References

- [1] A. Fojtik, A. Henglein, Laser Ablation of Films and Suspended particles in a Solvent: Formation of Cluster and Colloid Solutions, Ber. Buns. Phys. Chem., Vol.97, No.9, 1993, p.252.

**P-V****Terahertz photonics of multiphase thermodynamic systems: from gas to liquid***A.P. Shkurinov*<sup>1</sup><sup>1</sup>*Department of physics and International Laser Center, Lomonosov Moscow State University, Russia*

A spark was the first source of man-made electromagnetic radiation (EMR) obtained by Hertz [1], later by Bose [2], Lebedev [3] and others. While the initial experiments used electric breakdown in air, the later ones [4] switched to the use of liquid, namely oil. This resulted in the increase in stability and intensity of radiation, although its physical mechanism was not studied at the time. The study of the source of THz EMR on the basis of a laser spark follows the same pattern - from air [5] to liquid [6]. In this paper an experiment in which a liquid, namely, water was used for the conversion of femtosecond radiation into the THz one. Being a polar liquid, water has considerable absorption in the THz frequency range and the authors of previously published works had to use very thin water films of a few hundred micrometer thickness in their experiments. The source of electromagnetic radiation in the THz band on the basis of laser spark was firstly presented earlier. Laser experiment was carried out in which a liquid, namely, water was used for the conversion of femtosecond radiation into the THz. Water is a polar liquid which has high absorption in the THz frequency range and the authors of previously published works have to use for the experiments the very thin water films. Unlike water, considerable absorption both in THz and NIR ranges is absent in liquid nitrogen. We describe broadband generation of THz radiation first obtained in liquefied gas. In comparison with THz radiation in air plasma, THz radiation from LN reacts in a very different way to the change in the length of the pulse and the intensity of laser radiation. We demonstrated that both the ionization of the medium and its nonlinear susceptibility play a considerable role in the generation of THz radiation in LN. We assumed that the mobility of ions and electrons in liquid can play an essential role, forming quasi-static electric field by means of ambipolar diffusion mechanism. This quasi-stationary field can be an additional factor which could increase the effectiveness of transformation of optical radiation into the THz one. NLO susceptibility of the third order, which is much higher in nitrogen compared to air, enables us to carry out polarization control of THz radiation with the help of polarization parameters of femtosecond lasers.

**References**

- [1] H. Hertz, On electromagnetic waves in air and their reflection, vol. Electric Waves, Chap. 8 (D.E. Jones translation, London, Macmillan and Co., London, 1893).
- [2] D. T. Emerson, "The work of Jagadis Chandra Bose: 100 years of millimeter-wave research," IEEE Trans. Microwave Theo. Techn. 45, 2267 (1997).
- [3] P. Lebedev, "The double refraction of electric waves," Ann. Phys. Lpz. 56, 1 (1895).
- [4] A. Glagolewa-Arkadewa, "Short electromagnetic waves of wave-length up to 82 microns," Nature 113, 640 (1924).
- [5] H. Hamster, A. Sullivan, S. Gordon, W. White, and R. W. Falcone, "Subpicosecond, electromagnetic pulses from intense laser-plasma interaction," Phys. Rev. Lett. 71, 2725–2728 (1993).
- [6] Q. Jin, Y. E. K. Williams, J. Dai, and X.-C. Zhang, "Observation of broadband terahertz wave generation from liquid water," Applied Physics Letters 111, 071103 (2017).

**P-VI****Laser synthesis of colloidal metal and alloy colloids – fundamentals, scalability and alloy phase structure***S. Barcikowski*<sup>1</sup><sup>1</sup>*Technical Chemistry I and Center for Nanointegration Duisburg-Essen (CENIDE), University of Duisburg-Essen, Germany*

Integration of the “nano-function” into products is still limited due to drawbacks of gas phase and chemical synthesis methods regarding particle aggregation and contamination by adsorbates causing deactivation of the building blocks’ surface. In addition, thermodynamically - controlled synthesis methods naturally face limited access to alloy nanoparticle systems with miscibility gaps. As an alternative synthesis route, nanoparticle generation by pulsed laser ablation in liquids has proven its capability to generate ligand-free colloidal nanoparticles with high purity for a variety of materials [1,2]. Good reproducibility and significant up-scaling of nanoparticle generation were achieved recently by a continuous flow synthesis using a high-power ultrafast laser system leading to productivities of 4 g/h (equivalent to > 15 l/h) colloidal nanoparticles [3]. The transferability of this synthesis route to a variety of materials and liquids further enabled high-throughput screening of molar fraction series of e.g. water oxidation catalysts [4]. Alloy nanoparticles series (i.e., AgAu, NiMo, AuFe, AgNi, FeNi) were synthesized and their phase structure as well as their application potential will be discussed. Interestingly, on the one hand, phase diagram seems to play a role in ruling the nanoparticles crystal structure and phase segregation, but at the same time, unusual structures difficult to access by conventional synthesis methods are yielded, indicating kinetic control [5]. In this talk, laser synthesis of colloids will be introduced at the example of metal and alloy nanoparticles, including the resulting material properties. Application of these laser-generated nanoparticles by supporting them on carrier structures for heterogeneous catalysis 2, or in biomedicine [6] will be demonstrated.

**References**

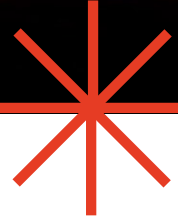
- [1] D. Zhang, B. Gökce, S. Barcikowski, *Chemical Reviews* 2017, 117, 3990.
- [2] a) G. Marzun, A. Levish, V. Mackert, T. Kallio, S. Barcikowski, P. Wagener, *J. Coll. Int. Sc.* 2017, 489, 57. // b) Dong, W. ; Reichenberger, S. ; Chu, S. ; Weide, P. ; Ruland, H. ; Barcikowski, S.; Wagener, P. ; Muhler, M. *Journal of Catalysis*, 330 (2015), S. 497-506.
- [3] R. Streubel, S. Barcikowski, B. Gökce, *Optics Letters* 2016, 41, 1486.
- [4] a) Hunter, B. M.; Gray, H. B.; Müller, A. M.: *Chem. Rev.* 2016, 116 // b) Hunter, B. M.; Blakemore, J. D.; Deimund, M.; Gray, H. B.; Winkler, J. R.; Müller, A. M. *J. Am. Chem. Soc.* 2014, 136, 13118–13121.
- [5] a) G. Marzun, C. Streich, S. Jendrzey, S. Barcikowski, P. Wagener, *Langmuir* 2014, 30, 11928. // b) O. Prymak, J. Jakobi, C. Rehbock, M. Epple, S. Barcikowski, *Materials Chemistry and Physics*, 207 (2018) 442-450. // c) P. Wagener, J. Jakobi, C. Rehbock, V.S.K. Chakravadhanula, C. Thede, U. Wiedwald, M. Bartsch, L. Kienle, S. Barcikowski, *Scientific Reports*, 6 (2016) 12. // d) A. Neumeister, J. Jakobi, C. Rehbock, J. Moysig, S. Barcikowski, *PCCP*, 16 (2014) 23671-23678.
- [6] a) Streich, C. ; Akkari, L. ; Decker, C. ; Bormann, J. ; Rehbock, C. ; Mueller-Schiffmann, A. ; Niemeyer, F. C. ; Nagel-Steger, L. ; Willbold, D. ; Sacca, B. ; Korth, C. ; Schrader, T. ; Barcikowski, S.: *ACS Nano* 10 (2016), S. 7582-7597 b) Kalus, M.-R. ; Rehbock, C. ; Baersch, N.; Barcikowski, S.: *Materials Today: Proc.* 4 (2017), 2, S. 93-S100



# ALT'19

**INTERNATIONAL CONFERENCE**

**Advanced Laser Technologies**



## **LASER-MATTER INTERACTION**

**Prague, Czech Republic**



---

15-20 September 2019

**LMI-I-1****On the role of plasma phase during Pulsed Laser Ablation in liquid for nanoparticles production**

*A. De Giacomo<sup>1</sup>, V. Motto-Ros<sup>2</sup>, F. Pelascini<sup>3</sup>, I. Gornushkin<sup>4</sup>, M. Dell'Aglio<sup>5</sup>*

*<sup>1</sup>University of Bari, Department of Chemistry, Bari, Italy*

*<sup>2</sup>Université Lyon 1, Institut Lumière Matière UMR 5306, Lyon, France*

*<sup>3</sup>Cetim Grand Est, Cetim Grand Est, Schiltigheim, France*

*<sup>4</sup>BAM Federal Institute for Material Research and Testing, Berlin, Germany*

*<sup>5</sup>Consiglio Nazionale delle Recirche-CNR, Instiuto di Nanotecnologie- CNR-NANOTEC, Bari, Italy*

In this paper experimental temperature and density maps of the laser induced plasma in water during Pulsed Laser ablation in Liquid (PLAL) for the production of metallic nanoparticles (NPs) has been determined. A detection system based on the simultaneous acquisition of two emission images at 515 and 410 nm has been constructed and the obtained images have been processed simultaneously by imaging software. The results of the data analysis show a variation of the temperature between 4000 and 7000 K over the plasma volume. Moreover, by the study of the temperature distribution and of the number densities along the plasma expansion axis it is possible to observe the condensation zone of the plasma where NPs can be formed.

Finally, the time associated to the electron processes is estimated and the plasma charging effect on NPs is demonstrated. The set of observations retrieved from these experiments allows a new insight about the nature of LIP in water during PLAL for the production of NPs and about the mechanism of NP formation as well as the releasing of NPs from the bubble to the solution.

**LMI-I-2****Comparative study of the electron photoemission from dielectrics, semiconductors, and metals induced by femtosecond laser pulses**

*G. Duchateau<sup>1</sup>, N. Fedorov<sup>2</sup>, B. Chimier<sup>1</sup>, H. Jouin<sup>3</sup>, P. Martin<sup>3</sup>*

*<sup>1</sup>CELIA- Universite de Bordeaux, IFCIA, Talence, France*

*<sup>2</sup>CELIA- Universite de Bordeaux, golf, Talence, France*

*<sup>3</sup>CELIA- Universite de Bordeaux, xuv, Talence, France*

The interaction of femtosecond laser pulses with materials is a topic of great interest since this interaction is only partially understood and applications are numerous including material laser processing. Therefore there is a need for further studies of this interaction to improve our knowledge and provide routes for applications. For that purpose, we have studied the electron photoemission from various materials induced by 25-femtosecond laser pulses at 800 nm with intensities below the damage threshold. Conventional dielectrics (SiO<sub>2</sub>, Al<sub>2</sub>O<sub>3</sub>, etc), semiconductors (Si, Ge, etc) and metals (Au, Pt, etc) are studied.

The experimental observations, i.e. the electron energy distribution depending on the material and the laser intensity, are analyzed within the framework of the state-of-the-art model of the electron dynamics in solids induced by femtosecond laser pulses. That includes the photo-ionization, the impact ionization, free electron heating by single and multiple photon absorption through intra- and inter-band processes, and electron relaxation through electron-electron and electron-phonon collisions.

Despite various shapes of the electron energy distribution depending on the material class, all observed behaviors can be explained within this model framework. It turns out that the present interaction exhibit an universal behavior in the sense where the electron dynamics is driven by the same processes whatever the material kind. Depending on the bandgap value, the photo-ionization rate evolves, providing different timescale for the laser heating of free electrons. This simple consideration allows to account for the various shapes of electron energy distributions. A corollary conclusion is that the information on the detailed electronic band structure of materials is lost during the interaction.

## LMI-I-3

### Internal structuring of silicon using ultrafast lasers

*D. Grojo*<sup>1</sup>

<sup>1</sup>*CNRS / Aix-Marseille University, LP3, Marseille, France*

An important challenge in the field of three-dimensional (3D) ultrafast laser processing is to achieve permanent modifications in the bulk of silicon (Si) and narrow-gap materials. High-energy infrared femtosecond laser pulses fail when conventional laser machining configurations are used [1,2].

By comparisons between ultrafast plasma images, 3D energy density maps inside the samples and nonlinear propagation simulations of tightly focused infrared pulses [3], we identify the strong nonlinear and plasma effects in the pre-focal region causing a strict clamping of the intensity that can be delivered inside Si [4].

To circumvent this limitation, we describe a solution inspired by solid-immersion microscopy to achieve hyper-tight focusing of the pulses. We describe the details of a proof-of-concept experiment demonstrating femtosecond optical breakdown inside Si and discuss the associated local refractive index changes measured by infrared phase microscopy [4].

The complexity of these optimizations in the space domain suggests that more practical solutions may likely arise with the use of longer pulses for reduced beam power. We concentrate our attention on the picosecond regime for which non linear effects persist and cause a non-monotonic evolution of the peak delivered fluence as a function of the incoming pulse of the energy. This is a situation somehow more complex than the clamping of the intensity observed in the femtosecond regime. However, we also find reduced energy thresholds for 3D writing inside silicon that is highly desirable.

Finally, we describe the range of possibilities that are already accessible with the fabrication of optical waveguides [5] and diffraction grating [6], structures based on positive- and negative-tone laser-assisted chemical etching [7] and a demonstration of 3D data inscription deep inside silicon using nanosecond and picosecond lasers. This directly translates in Si some of the 3D writing technologies originally developed in transparent dielectrics and has the potential to change the way Si microsystems are today designed and fabricated.

### Acknowledgments

This project has received funding from the European Research Council (ERC) under the European Union's Horizon 2020 research and innovation program (Grant Agreement No. 724480).

### References

- [1] A. Mouskeftaras, A. V. Rode, R. Clady, M. Sentis, O. Utéza, and D. Grojo, *Appl. Phys. Lett.* 105, 191103 (2014).
- [2] D. Grojo, A. Mouskeftaras, P. Delaporte, and S. Lei, *J. Appl. Phys.* 117, 153105 (2015).
- [3] V.Y. Fedorov, M. Chanal, D. Grojo, and S. Tzortzakis, *Phys. Rev. Lett.* 117, 43902 (2016).
- [4] M. Chanal, V.Y. Fedorov, M. Chambonneau, R. Clady, S. Tzortzakis, and D. Grojo, *Nature Communications* 8, 773 (2017).
- [5] M. Chambonneau, Q. Li, M. Chanal, N. Sanner, and D. Grojo, *Opt. Lett.* 41, 4875 (2016).
- [6] M. Chambonneau, D. Richter, S. Nolte, and D. Grojo, *Opt. Lett.* 43, 6069 (2018).
- [7] M. Chambonneau, X. Wang, Q. Yu, Q. Li, D. Chaudanson, S. Lei, and D. Grojo, *Opt. Lett.* 44, 1619 (2019).

**LMI-I-4****Maxwell+TDDFT multiscale method for light-propagation in solids***M. Uemoto<sup>1</sup>, A. Yamada<sup>1</sup>, K. Yabana<sup>1</sup>**<sup>1</sup>University of Tsukuba, Center for Computational Sciences, Tsukuba, Japan*

To describe interaction between an intense laser pulse and solids, we are developing an ab-initio Maxwell+TDDFT multiscale simulation method [1]. The method combines two simulations of different spatial scales. In the microscopic scale, dynamics of electrons and ions is described using the time-dependent density functional theory (TDDFT). The time-dependent Kohn-Sham (TDKS) equation for Bloch orbitals is solved in real time using 3D Cartesian spatial grids. It describes electron dynamics in a unit cell of solids under a spatially uniform, time-dependent electric field. In the macroscopic scale, we solve the Maxwell equations, again in real time for vector potentials that describe the light propagation in solids. Both equations are solved simultaneously to describe the coupled dynamics of light propagation, electron dynamics, and atomic motion. In our simulation method, various nonlinearities in light-matter interaction can be incorporated since we solve the TDKS equation without any perturbative approximation. The descriptions of nonlinearities include  $\chi^{(2)}$  and  $\chi^{(3)}$  [3], saturable absorption [4], and multiphoton/tunneling ionizations [5].

In my presentation, I will show several recent applications of our method. Energy transfer from an intense laser pulse to electrons in dielectrics by multiphoton/tunneling ionization mechanisms is an important quantity to investigate the early stage of laser processing. We have compared our calculated results for SiO<sub>2</sub> with the measurement using attosecond streaking method [6], showing that the onset of the energy transfer can be reasonably described. We have also carried out an estimation of damage threshold and crater depth from our calculation and compared them with those by a single-shot femtosecond laser pulse [7], which shows a reasonable agreement. Recently, we have extended to include microscopic ionic motion as well as electron dynamics employing the Ehrenfest molecular dynamics, namely, “Maxwell+TDDFT+MD” [2]. It can describe the generations of coherent phonon and stimulated Raman wave. We have also extended the method to three-dimensional nonlinear nano-optics, solving 3D-Maxwell equation coupled with microscopic TDDFT.

Finally, we would like to mention that our computational code is made open to public as an open source software, SALMON (Scalable Ab-initio Light-Matter simulator for Optics and Nanoscience) [8], downloadable from our website, <http://salmon-tddft.jp>.

**References**

- [1] K. Yabana et.al, Phys. Rev. B (2012).
- [2] M. Uemoto et al, J. Chem. Phys. 150, 094101 (2019).
- [3] M. Uemoto et al, CLEO, OSA Technical Digest (online) (Optical Society of America, 2017), paper JTh2A.26.
- [4] A. Yamada, K. Yabana, Euro. Phys. J. D73, 87 (2019).
- [5] A. Sommer et.al, Nature 534, 86 (2016).
- [6] S.A. Sato et.al, Phys. Rev. B92, 205413 (2015).
- [7] A. Yamada, K. Yabana, Phys. Rev. B99, 245103 (2019).
- [8] M. Noda et al. Comm. Compt. Phys. 235, 356 (2019).

**LMI-I-5****Simulations of the energy spectrum of conduction band electrons for a better understanding of free-electron-mediated modifications of biomolecules, and fs laser materials processing***X.X. Liang<sup>1,2</sup>, Z.X. Zhang<sup>2</sup>, A. Vogel<sup>1</sup>**<sup>1</sup>University of Luebeck, Institute of Biomedical Optics, Luebeck, Germany**<sup>2</sup>Xi'an Jiaotong University, Institute of Biomedical Analytical Technology and Instrumentation, Xi'an, China*

Short-pulse lasers are widely used for plasma-mediated material processing, and photomodification of biomolecules. The thresholds for phase transitions and ablation in transparent dielectrics depend on conduction band (CB) electron density  $n_{\text{total}}$  and the resulting volumetric energy density  $U$ . Exact knowledge of the average kinetic electron energy  $\varepsilon_{\text{avg}}$  would create a more precise link between  $n_{\text{total}}$  and  $U$ , and the energy distribution of CB electrons determines which chemical changes may be induced by free electrons,  $e^-$ . Thus, knowledge of the energy spectrum is pivotal for a better understanding of free-electron-mediated modifications of biomolecules, and fs laser materials processing.

We study the energy spectrum of laser-induced conduction band (CB) electrons in water by multi-rate equations (MRE) with different impact ionization schemes. Rethfeld's MRE model [1] enables tracking the evolution of the energy distribution of CB electrons during femtosecond breakdown and deriving an asymptotic single-rate equation (SRE) suitable for the calculation of energy deposition at longer (picosecond to nanosecond) pulse durations. However, the impact ionization scheme neglects the excess energy remaining after collisional ionization of valence band electrons. This shortcoming is overcome by an energy splitting scheme introduced by Christensen and Balling [2], but the corresponding rate equations are computationally very expensive.

We introduce a simplified splitting scheme and corresponding rate equations that still agree with energy conservation but enable the derivation of an asymptotic SRE. This approach is well suited for the calculation of energy spectra at long pulse durations and high irradiance, and for combination with spatiotemporal beam propagation/plasma formation models. Using the energy-conserving MREs, we present the time-evolution of CB electron density and energy spectrum during femtosecond breakdown as well as the irradiance dependence of free-electron density, energy spectrum, volumetric energy density, and plasma temperature.

These data are relevant for understanding photodamage pathways in nonlinear microscopy, free-electron-mediated modifications of biomolecules in laser surgery, and laser processing of transparent dielectrics in general.

**References**

- [1] Rethfeld B., Physical Review Letters 92(18), 187401 (2004).
- [2] Christensen, B.H. and Balling P. Physical Review B 79(15), 155424 (2009).

**LMI-I-6****Multistep phase transitions in X-ray free-electron-laser irradiated solids***N. Medvedev*<sup>1</sup>*<sup>1</sup>Institute of Physics Czech Academy of Sciences, Department of Radiation and Chemical Physics, Prague, Czech Republic*

This talk will briefly review the results of our theoretical research on damage mechanisms in various materials irradiated with femtosecond X-ray free-electron-laser pulses at fluences ranging from mild excitation of the target to warm dense matter formation. Various damage mechanisms are discussed on examples of insulators (e.g. diamond [1]), semiconductors (e.g. silicon [2]), metals (e.g. gold). They are studied with the developed hybrid approach, XTANT (X-ray-induced Thermal And Nonthermal Transitions [3]), which includes nonequilibrium kinetics of electrons modeled within a combination of the Monte Carlo simulation and Boltzmann kinetic approach, nonthermal effects in the atomic system traced within tight-binding molecular dynamics, and nonadiabatic coupling between the systems.

We analyze the effects of thermal melting of targets as a result of electron-ion energy exchange; nonthermal phase transitions due to modification of the interatomic potential (such as nonthermal melting in silicon or solid-solid phase transition in irradiated diamond); spallation or ablation at higher fluences due to detachment of sample fragments; and a complex multistep kinetics of warm dense matter formation [4]. As a result, we demonstrate that diamond upon femtosecond pulse irradiation turns into graphite within 150-200 fs, in a very good agreement with experimental data [1]. Silicon [2], as well as AlAs [5], can melt both, thermally or nonthermally, into two different liquid phases. We also find that the electron-ion (electron-phonon) coupling parameter can be accessed in highly-excited samples via pump-probe time-resolved measurements of optical properties [2].

**References**

- [1] F. Tavella, H. Höppner, V. Tkachenko, N. Medvedev, F. Capotondi, T. Goltz, Y. Kai, M. Manfredda, E. Pedersoli, M. J. Prandolini, N. Stojanovic, T. Tanikawa, U. Teubner, S. Toleikis, and B. Ziaja, *High Energy Density Phys.* 24, 22 (2017).
- [2] N. Medvedev, Z. Li, V. Tkachenko, and B. Ziaja, *Phys. Rev. B* 95, 014309 (2017).
- [3] N. Medvedev, V. Tkachenko, V. Lipp, Z. Li, and B. Ziaja, *4open* 1, 3 (2018).
- [4] N. Medvedev and B. Ziaja, *Sci. Rep.* 8, 5284 (2018).
- [5] N. Medvedev, Z. Fang, C. Xia, and Z. Li, *Phys. Rev. B* 99, 144101 (2019).

## LMI-I-7

## Investigating energy deposition of ultrashort lasers at the surface of solids at the femtosecond scale

*O. Uteza<sup>1</sup>, T. Genieys<sup>1</sup>, C. Pasquier<sup>1</sup>, M. Sentis<sup>1</sup>, N. Sanner<sup>1</sup>*  
<sup>1</sup>LP3 - CNRS - AMU, LP3, Marseille, France

Ultrashort laser pulses ( $\ll 100$  fs) offer remarkable capabilities for laser-matter interaction, especially for ablation of transparent dielectric materials [1,2]. However, achievement of those performances requires precise evaluation and understanding of the optical response of the material under laser irradiation. In this context, determination of laser-induced damage or/and ablation thresholds (LIDT/LIAT) of materials and measurement and understanding of energy deposition are mandatory to calibrate material transformation upon laser excitation. This is particularly crucial, for instance in view of laser damage certification of optical components or of development of micromachining processes [2,3].

By convenience or because it corresponds to their actual routine use, those optics or processes are in general set in operation in air. However, focusing ultrashort laser pulses in air implies natural limitations to linear beam propagation because of the development of nonlinearities related to Kerr effect and air ionization prior the target.

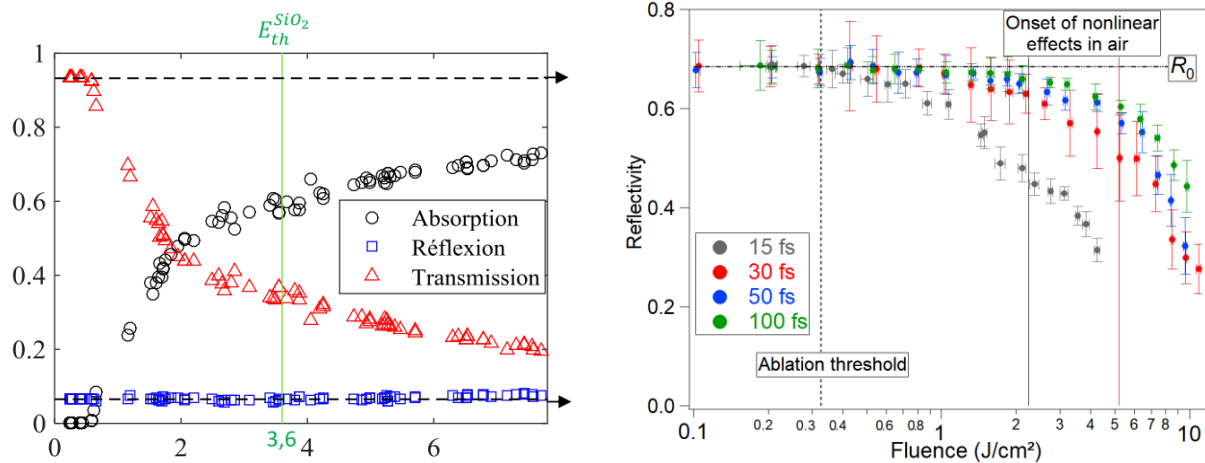


**Fig. 1.** Evolution of reflection (R), transmission (T) and absorption (A, deduced from energy conservation) as a function of incident energy for fused silica measured at 15 fs (a) and evolution of reflectivity vs fluence and pulse duration for nickel (b).  $E_{th, SiO_2}$  indicates the ablation energy threshold of fused silica ( $w_{0, exp} = 11 \mu m$ ). The corresponding ablation thresholds (expressed in peak fluence) are:  $F_{th, SiO_2} = 1.8 J/cm^2$  and  $F_{th, Ni} = 0.33 J/cm^2$  for pulse duration ranging from 15 to 100 fs.

In this context, we first analyze the spatial, spectral and temporal properties of the ultrashort laser beam to characterize its propagation till the focal plane where the target is located [4]. We further couple this information to the surface ablation of dielectrics and metals of scientific and industrial interest (fused silica sapphire, aluminum, nickel, copper and tungsten), inferring precise LIDT/LIAT evaluation in a pulse duration range (15 – 100 fs) little explored yet. In operating conditions for which the beam propagation is not affected by nonlinearities in air, we further extend our experimental investigations to the determination of the energy coupling at the surface of those

materials using pulse-time-integrated measurements of reflectivity and transmissivity performed for different pulsed durations and at fluences below and above the ablation threshold. Examples of those energy balance measurements are shown below (Figure 1) for metals (nickel) and dielectrics (fused silica). The main results obtained will be detailed and discussed providing valuable insights of laser energy deposition and transformation of solid materials in the ultrashort irradiation regime.

## References

- [1] K. Sugioka, Progress in ultrafast laser processing and future prospects, *Nanophotonics* 6 (2), 393–413, (2017).
- [2] O. Utéza, N. Sanner, A. Brocas, B. Chimier, N. Varkentina, M. Sentis, P. Lassonde, F. Légaré, J-C. Kieffer, Control of material removal of fused silica with single pulses of few optical cycles to sub-picosecond duration, *Applied Physics A* 105, 131-141, (2011).
- [3] M.E. Shaheen, J.E. Gagnon, J.B. Fryer, Femtosecond laser ablation behavior of gold, crystalline silicon, and fused silica: a comparative study, *Laser Phys.* 24, 106102 (2014).
- [4] C. Pasquier, P. Blandin, R. Clady, N. Sanner, M. Sentis, O. Utéza, Y. Li, S. Yan long, Handling beam propagation in air for nearly 10-fs laser damage experiments, *Optics Comm.* 355, 230–238, (2015).

**LMI-I-8****Wavelength dependent energy transfer to semiconductors and dielectrics irradiated by ultrashort laser pulses**

*T. Apostolova*<sup>1,2</sup>

<sup>1</sup>*Institute for Nuclear Research and Nuclear Energy, Cyclotron physics, Sofia, Bulgaria*

<sup>2</sup>*Institute for Advanced Physical Studies, New Bulgarian University, Sofia, Bulgaria*

Femtosecond laser-induced energy absorption and optical breakdown of silicon and germanium is studied for laser wavelengths in the near- and mid-infrared spectral regions using the Time dependent Schrodinger equation in one electron approximation<sup>1,2</sup>. The dependence of the photoelectron density and deposited energy on the laser intensity and wavelength are obtained. For Si irradiated by mid-IR wavelengths and low laser field strength, material-specific threshold for the onset of energy absorption into the bulk is found, while for near-IR wavelengths the energy transfer to electrons occurs via multiphoton absorption. For high driving field strength, absorption of energy becomes wavelength independent and increases linearly with increase of the laser intensity. During the irradiation, part of the energy stored in the electronic system is transferred back to the radiation field via high harmonic generation. We obtain clean harmonic peaks generated during the irradiation with near-IR laser pulse, while quasi-continuous bremsstrahlung radiation is generated during the irradiation with mid-IR wavelengths. Dielectric breakdown thresholds are discussed in terms of the total laser energy coupled to ultrafast electron excitations in the materials and sufficient to cause melting of the solid and the onset of laser-induced DC currents after the end of the driving pulse.

**References**

[1] S. Lagomarsino et. al, Phys. Rev. B 93, 085128, 2016.

[2] T. Apostolova, et. al, Applied Surface Science, 427, 334, 2018.

**LMI-I-9****High-Speed surface functionalization using interference-based laser processes - From prediction to technological applications**

*T. Kunze<sup>1</sup>, T. Steege<sup>1</sup>, S. Alamri<sup>1</sup>, B. Krupop<sup>1</sup>, A. Madelung<sup>1</sup>, A. Aguilar-Morales<sup>1</sup>, F. Schell<sup>1</sup>, F. Hundertmark<sup>1</sup>, V. Lang<sup>1,2</sup>, A.F. Lasagni<sup>1,2</sup>*

*<sup>1</sup>Fraunhofer IWS Dresden, Microtechnology, Dresden, Germany*

*<sup>2</sup>Technische Universität Dresden, Institute for Manufacturing Technology, Dresden, Germany*

Functional laser surface texturing arose in recent years to a very powerful tool for tailoring the surface properties of parts and components. The design of these textured surfaces often follows a biomimetic approach motivated by living organisms. The laser-textured surfaces, typically exhibiting well-defined features (e.g. periodic structures), can show outstanding properties such as self-cleaning, optimized tribological properties as well as an increased biocompatibility. With the increasing capabilities in functional laser surface texturing, the prediction of surface properties become more and more important in order to reduce the development time of those functionalities. Therefore, advanced approaches for the prediction of the properties of laser-processed surfaces – the so called predictive modelling – are required and in the scope of current research activities. The industrialization of functional laser surface texturing necessitates an efficient production of laser-textured surfaces which still represents one of the greatest technical challenges. In this context, Direct Laser Interference Patterning (DLIP) has been identified as an outstanding technology for the efficient fabrication of tailored surface structures. The DLIP approach can show impressive processing speeds (up to 1 m<sup>2</sup>/min) as well as a superior flexibility in achieving extremely versatile surface structures.

This work gives an overview about recent developments of the DLIP technology by focusing on the topics: structure flexibility, prediction, process productivity, technical implementations and recent examples of achieved surface functionalities. The work especially focuses on novel ways to predict surface functionalities using machine learning approaches as well as on large-area structuring with surfaces exceeding that of an A4 sheet.

**LMI-I-10****Energetic-beam induced regular surface structuring: Comparison of ultra-short laser pulses vs. ion beams**

*J. Reif<sup>1</sup>*

*<sup>1</sup>BTU Cottbus-Senftenberg, Fak 1, Cottbus, Germany*

In the laser materials processing community, the modification of target surface morphology by impact of intense laser pulses has been of continuing prominence. In particular regular Laser-induced periodic surface structures (LIPSS) have been the subject of intensive research, aiming not only at the structure formation, specifically, but also on a broad range of applications, such as wettability modification, coloring, tribology etc.

Much less known in the laser community is, however, the fact that similar, almost identical structures are also obtained by ion sputtering, when energetic ion beams are incident on the surface.

The presentation will shortly present some results of ion induced periodic surface structuring. Then these will be compared to LIPSS, elaborating similarities and differences. Finally models for both interactions will be reviewed and compared.

**LMI-I-11****Modelling of the ultrafast dynamics and surface plasmon properties of silicon upon irradiation with mid-IR femtosecond laser pulses***G. Tsibidis*<sup>1</sup><sup>1</sup>*FORTH, Institute of Electronic Structure and Laser, Heraklion, Greece*

We present a theoretical investigation of the yet unexplored ultrafast processes and dynamics of the produced excited carriers upon irradiation of Silicon with femtosecond pulsed lasers in the mid-infrared (mid-IR) spectral region. The evolution of the carrier density and thermal response of the electron-hole and lattice subsystems are analysed for various wavelengths  $\lambda_L$  in the range between 2.2  $\mu\text{m}$  and 3.3  $\mu\text{m}$  where the influence of two and three-photon absorption mechanisms is explored. The role of induced Kerr effect is highlighted and it manifests a more pronounced influence at smaller wavelengths in the mid-IR range. Elaboration on the conditions that leads to surface plasmon (SP) excitation indicate the formation of weakly bound SP waves on the material surface. The lifetime of the excited SP is shown to rise upon increasing wavelength yielding a larger than the one predicted for higher laser frequencies. Calculation of damage thresholds for various pulse durations  $\tau_p$  show that they rise according to a power law ( $\sim$ ) where the increasing rate is determined by the exponent  $\zeta(\lambda_L)$ . Investigation of the multi-photon absorption rates and impact ionization contribution at different  $\tau_p$  manifests a lower damage for  $\lambda_L=2.5 \mu\text{m}$  compared to that for  $\lambda_L=2.2 \mu\text{m}$  for long  $\tau_p$ .

**References**

- [1] Petrakakis E., Tsibidis G.D., and Stratakis E., Modelling of the ultrafast dynamics and surface plasmon properties of silicon upon irradiation with mid-IR femtosecond laser pulses' *Physical Review B* 99, 195201 (2019).

**LMI-I-12****Femtosecond laser-induced periodic surface structures: from light localization to applications**

*J. Bonse<sup>1</sup>, C. Florian<sup>1</sup>, S.V. Kirner<sup>1</sup>, J. Krüger<sup>1</sup>*

*<sup>1</sup>Bundesanstalt für Materialforschung und -prüfung BAM, 6.4 Nanomaterial Technologies, Berlin, Germany*

This presentation reviews the current state in the field of *Laser-induced Periodic Surface Structures* (LIPSS). These surface nanostructures are a universal phenomenon and can be generated on almost any material by irradiation with intense linearly polarized laser radiation [1]. LIPSS are formed in a “self-ordered” way and are often accompanying material processing applications. They can be produced following a single-step process and enable surface functionalization through the adaption of optical, mechanical and chemical surface properties. Their structural sizes typically range from several micrometers down to less than 100 nanometers exhibiting a clear correlation with the polarization direction of the laser radiation. Various types of surface structures are classified, relevant control parameters are identified, and their material specific formation mechanisms are analyzed for different types of inorganic solids, i.e., metals, semiconductors, and dielectrics, through time-resolved optical experiments [2-4] and theoretical simulations [4,5]. Finally, technological applications featuring surface functionalization in the fields of optics, fluidics, medicine, and tribology are discussed [6].

**References**

- [1] J. Bonse, S. Höhm, S.V. Kirner, A. Rosenfeld, J. Krüger., “Laser-induced periodic surface structures – a scientific evergreen”, *IEEE Journal of Selected Topics in Quantum Electronics* 23 (2017), 9000615.
- [2] K. Sokolowski-Tinten, A. Barty, S. Boutet, U. Shymanovich, H. Chapman, M. Bogan, S. Marchesini, S. Hau-Riege, N. Stojanovic, J. Bonse, Y. Rosandi, H.M. Urbassek, R. Tobey, H. Ehrke, A. Cavalleri, S. Düsterer, H. Redlin, M. Frank, S. Bajt, J. Schulz, M. Seibert, J. Hajdu, R. Treusch, C. Bostedt, M. Hoener, T. Möller, “Short-pulse laser induced transient structure formation and ablation studied with time-resolved coherent XUV-scattering”, *AIP Conference Proceedings* 1278 (2010), 373.
- [3] S. Höhm, A. Rosenfeld, J. Krüger, J. Bonse, “Femtosecond diffraction dynamics of laser-induced periodic surface structures on fused silica”, *Applied Physics Letters* 102 (2013), 054102.
- [4] A. Rudenko, J.-P. Colombier, S. Höhm, A. Rosenfeld, J. Krüger, J. Bonse, T.E. Itina, “Spontaneous periodic ordering on the surface and in the bulk of dielectrics irradiated by ultrafast laser: a shared electromagnetic origin”, *Scientific Reports* 7 (2017), 12306.
- [5] Y. Fuentes-Edfuf, J.A. Sánchez-Gil, C. Florian, V. Giannini, J. Solis, J. Siegel, “Surface plasmon polaritons on rough metal surfaces: role in the formation of laser-induced periodic surface structures”, *ACS Omega* 4 (2019), 6939.
- [6] J. Bonse, S.V. Kirner, S. Höhm, N. Epperlein, A. Rosenfeld, J. Krüger, “Applications of laser-induced periodic surface structures (LIPSS)”, *Proceedings of SPIE* 10092 (2017), 100920N.

**LMI-I-13****Ultrafast-Laser generated nanoacoustic waves and their applications on material diagnosis***N. Papadogiannis*<sup>1</sup><sup>1</sup>*Hellenic Mediterranean University, Institute for Plasma Physics and Lasers, Rethymnon, Greece*

When ultrafast laser pulses interact with the metallic thin-film transducer of a nanostructured composed material, the free electrons of the metal absorb the laser photons and excited either in high energy states or in the continuum. Then, the overwhelming majority of the excited electrons transfer their excess energy in to the lattice or in to other electrons via non-radiative processes named electron-lattice and electron-phonon scattering. In later time localized high temperature and high pressure field is appeared in the interaction volume which generates a localized and fast moving mechanical nano-strain pulse outwards from the interaction region. Depending on the laser pulse characteristics and the nature of the materials involved in the process, different type of mechanical waves are generated and different physical phenomena occur. Above that, the phase of the material may change during the interaction process or during the mechanical wave propagation.

The physics and the applications of ultrafast-laser generated nanoacoustic waves on metal thin films transducers mounted on dielectric (or semiconductor) substrates will be presented for different laser pulse excitation characteristics. Both, Rayleigh-type surface mechanical waves, and longitudinal phononic acoustical strains propagated normally to the surface, will be explored. State of the art pump-probe experimental techniques based on whole field dynamic laser nano-imaging or degenerated transient reflectivity methods will be analyzed and discussed. Theoretical models that describe the laser-material interaction processes and the generation and propagation of mechanical waves for different laser characteristics and different materials seem to be validated. Finally, successful optical coherent control of nanostrains in semiconductor materials, of the laser-generated mechanical waves will be shown using sophisticated initial electron excitation.

**References**

- [1] Y. Orphanos, K. Kosma, E. Kaselouris, V. Dimitriou, M. Bakarezos, N. Vainos, M. Tatarakis and N. A. Papadogiannis, *Femtosecond laser generated surface acoustic waves in Au thin films deposited on glass substrates*, Appl. Phys. A: Mat. Sc. and Proc. 125, 269 (2019).
- [2] M. Bakarezos, E. Tzianaki, S. Petrakis, G. D. Tsibidis, P. A. Loukakos, V. Dimitriou, C. Kosmidis, M. Tatarakis and N. A. Papadogiannis, *Ultrafast laser pulse chirp effects on laser-generated nanoacoustic strains in Silicon*, Ultrasonics 86C, 14 (2018).
- [3] E. Kaselouris, V. Dimitriou, I. Ftilis, A. Skoulakis, G. Koundourakis, E. L. Clark, M. Bakarezos, I. K. Nikolos, N. A. Papadogiannis, M. Tatarakis, Nature Communications 8, 1713, (2017).
- [4] E. Tzianaki, M. Bakarezos, G. D. Tsibidis, S. Petrakis, P. A. Loukakos, C. Kosmidis, M. Tatarakis and N. A. Papadogiannis, *Controlling nanoscale acoustic strains in Silicon using chirped femtosecond laser pulses*, Applied Physics Letters 108, 254102 (2016).
- [5] E. Kaselouris, E. Skarvelakis, I. K. Nikolos, G. E. Stavroulakis, Y. Orphanos, E. Bakarezos, N. A. Papadogiannis, M. Tatarakis, V. Dimitriou, *Simulation of the Transient Behavior of Matter with Characteristic Geometrical Variations & Defects Irradiated by Nanosecond Laser Pulses Using FEA*, Key Engineering Materials 665, 157 (2016).
- [6] E. Kaselouris, I.K. Nikolos, Y. Orphanos, M. Bakarezos, N.A. Papadogiannis, M. Tatarakis and V. Dimitriou, *Elastoplastic study of nanosecond-pulsed laser interaction with metallic films using 3D multiphysics fem modeling*, International Journal of Damage Mechanics 25, 42 (2016).

- [7] E. Makis Bakarezos, G. D. Tsididis, Y. Orphanos, P. A. Loukakos, C. Kosmidis, P. Patsalas, M. Tatarakis, and N. A. Papadogiannis, *High acoustic strains in Si through ultrafast laser excitation of Ti thin-film transducers*, Optics Express 23, 17191 (2015).
- [8] V. Dimitriou, E. Kaselouris, Y. Orphanos, M. Bakarezos, N. Vainos, I.K. Nikolos, M. Tatarakis, and N.A. Papadogiannis, *The thermo-mechanical behavior of thin metal films under nanosecond laser pulse excitation above the thermoelastic regime*, Applied Physics A: Materials Science and Processing 739, 118 (2015).
- [9] E. Kaselouris, I.K. Nikolos, Y. Orphanos, M. Bakarezos, N.A. Papadogiannis, M. Tatarakis and V. Dimitriou, *A review of simulation methods of laser matter interaction focused on nanosecond laser pulsed systems*, Journal of Multiscale Modelling 5, 1330001, (2013).
- [10] V. Dimitriou, E. Kaselouris, Y. Orphanos, M. Bakarezos, N. Vainos, M. Tatarakis and N.A. Papadogiannis, *Three dimensional transient behaviour of thin films surface under pulsed laser excitation*, Applied Physics Letters 103, 114104 (2013).
- [11] Y. Orphanos, V. Dimitriou, E. Kaselouris, M. Bakarezos, N. Vainos, M. Tatarakis and N.A. Papadogiannis, *An integrated method for material properties characterization based on pulsed laser generated surface acoustic waves*, Microelectronic Engineering 112, 249 (2013).

## LMI-I-14

### Laser made random and solitary surface structures

*N. Inogamov<sup>1,2</sup>, V. Zhakhovsky<sup>1</sup>, S. Anisimov<sup>2</sup>, Y. Petrov<sup>2</sup>, V. Khokhlov<sup>2</sup>*

*<sup>1</sup>The Dukhov Research Institute of Automatics,*

*The Centre for Fundamental and Applied Research, Moscow, Russian Federation*

*<sup>2</sup>Landau Institute for Theoretical Physics of the Russian Academy of Sciences,*

*Lasers and Plasma, Chernogolovka- Moscow region, Russian Federation*

Studies in physics of a laser-matter interaction are necessary for optimization for several modern technologies. There are printing technologies like LIFT (laser induced forward transfer) and LIBT (laser induced backward transfer) [1]; LAL - laser ablation in liquid as the ecologically clean way for nanoparticles production [2]; LSP - laser shock peening for improvement of quality of materials; and fabrication of multipurpose metasurfaces [3]. There are two ways of fabrication of the metasurfaces. One of them is connected with creation of a tiny (its size along a target surface is  $\sim$  micron) solitary "cupola" by a diffraction limited ultrashort laser action; we use a term "cupola" here as the generalizing name because it may be a cupola, or cupola with a jet above in its tip, or hole in a film; usually a target is a thin film mounted on dielectric substrate. We create a matrix of the cupolas repeating placing of them on a film in the desired points. This matrix changes surface properties of a target thus transferring the usual surface into a metasurface.

Wide beam and ultrashort action are used on the second way to fabricate a metasurface. In this case (illuminating above an ablation threshold) a random surface micro- nano-structures appears first described in the papers by Vorobyev and Guo [4]. Creation of solitary and random structures are connected with many physical processes: there are hydrodynamic and dynamic of deformable solids phenomena including strong heating and cooling with phase transitions which convert (a) solids to liquid therefore the capillary effects become dynamically important, (b) rarefactions, tensile stress, fragmentation, formation of the three-phase (solid-liquid-vapour) mixtures, evaporation, foaming of hot liquid metals, (c) conductive cooling, re-crystallization in motion.

Laser action inevitably creates shocks. The LSP technologies are based on that. The shocks have to be strong enough (above limits of plasticity) to cause the irremovable deformation in solids. Therefore physics of laser initiated shocks in elastic-plastic media (ductile metals) have to be studied [5].

Laser ablative action in liquid generates a chain of processes covering many orders of magnitudes in space and time. Initial stages significantly depend on duration of a pulse and absorbed energy. They cause foaming of metal in the case of picosecond pulses. While in the case of a nanosecond action the foam is absent. To produce nanoparticles the heating have to be strong. There are significant differences between the situations when a target is heated below its critical parameters and above. In the last case the surface tension at a contact boundary between a target material and liquid disappears. Thus mutual diffusion is enhanced. The dissolved target atoms filling the diffusion layer are cooled down (because the surrounding liquid is colder) and begin to condense [2].

## References

- [1] C. Unger et al., Opt. Express 20, 24864 (2012); N. Inogamov et al., Journal of Experimental and Theoretical Physics, Vol. 120, No. 1, pp. 15–48 (2015)

- [2] D. Zhang et al., *Chem Rev.* 117(5), 3990-4103 (2017). doi:10.1021/acs.chemrev.6b00468; Yu. Petrov et al., *Contributions to Plasma Physics*, e419, First published: 15 May 2019. doi: 10.1002/ctpp.201800180 (2019); arXiv:1812.09929; arXiv:1812.09109; arXiv:1811.11990
- [3] A. Kuchmizhak et al., *Nanoscale* 8, 12352-12361 (2016). DOI: 10.1039/C6NR01317AN; Inogamov et al., *Applied Physics A: Material Science and Processing* 122, 432 (9 pages) (2016). DOI 10.1007/s00339-016-9942-9X; Wang et al., *Phys. Rev. Appl.* 8, 044016 (2017)
- [4] A. Vorobyev and C. Guo, *J Appl Phys* 110, 043102 (2011)
- [5] M. Agranat et al., *JETP Lett.* 91 (9), 471-477 (2010); S. Ashitkov et al., *JETP Lett.* 92 (8), 516-520 (2010); V. Zhakhovskii and N. Inogamov, *JETP Lett.*, 92 (8), 521-526 (2010); N. Inogamov et al., *JETP Letters*, v. 93 (4), 226-232 (2011); V. Zhakhovsky et al., *Phys. Rev. Lett.*, v. 107, 135502 (2011); B. Albertazzi et al., *Sci. Adv.* 3, e1602705 (2017)

**LMI-I-15****Production of wear resistant surface zones with high power laser technologies**

*M. Seifert<sup>1</sup>, S. Kuehn<sup>1</sup>, M. Barbosa<sup>2</sup>, S. Nowotny<sup>2</sup>, C. Leyens<sup>3</sup>*

*<sup>1</sup>Fraunhofer IWS Dresden, Heat Treatment and Plating, Dresden, Germany*

*<sup>2</sup>Fraunhofer IWS Dresden, Thermal Coating, Dresden, Germany*

*<sup>3</sup>Fraunhofer IWS Dresden, Director, Dresden, Germany*

Surface engineering to increase the wear resistance of components is required in any kind by almost all industrial sectors. This is often achieved by applying thermal surface treatments or wear-resistant coatings. Which process, or which coating material, to choose will depend not only on the required surface properties but also on economic and technical challenges. Additionally, there is an increasing demand for more cost-efficient processes and materials.

This contribution gives an overview over different high-performance laser surface technology solutions (laser hardening, laser cladding and laser shock peening). Even if the basic mechanisms of the laser based technologies are fully different, the aim to increase the wear resistance and lifetime of parts is the same.

In laser hardening the microstructure of steel or cast iron components is modified by thermal processing in the solid state. Advantages of this technology over conventional heat treatment processes are its high precision combined with very short process time, low energy consumption and low heat input, which results in low distortion and reduced efforts to finish the final contour in the process chain. The basics of the laser hardening technology and new concepts of process control are presented.

Laser cladding with modern laser types and process-specific laser heads covers applications from the micro to macro scale today. Powder or wire can be used as feedstock to deposit various materials for applications in surface cladding and repair. The advantages and some best practices of the actual laser cladding technology will be shown for industrial relevant applications.

One aim of the laser shock peening technology similar to other laser technologies is also to strengthen metallic surfaces (i.e. at steel, aluminum or titanium components) by using a laser induced mechanical shock wave. But often more relevant for applications is its strong influence on residual stresses at and near the treated surface. This makes the shock peening technology ideal for post-treatment of surfaces after previous manufacturing steps like welding, cladding or local heat treatment. First results of laser peening of laser heat treated steel grades are presented.

**LMI-I-16****Prospects for the application of vortex beams of mid- and far-infrared ranges in surface plasmonics**

*B. Knyazev<sup>1</sup>, Y. Choporova<sup>1</sup>, O. Kameshkov<sup>2</sup>, A. Nikitin<sup>3</sup>, N. Osintseva<sup>1</sup>, V. Pavelyev<sup>4</sup>*

<sup>1</sup>*Budker Institute of Nuclear Physics SB RAS, Free Electron Laser, Novosibirsk, Russian Federation*

<sup>2</sup>*Novosibirsk State University, Physics, Novosibirsk, Russian Federation*

<sup>3</sup>*Scientific and Technology Center of Unique Instrumentation, Terahertz Laboratory, Moscow, Russian Federation*

<sup>4</sup>*Samara University, Nanotechnology, Samara, Russian Federation*

Photonics and plasmonics are the most rapidly developing areas of modern optics. The current state and prospects of further development of these areas of science are vividly described in articles [1] and [2]. Surface plasmon polaritons, electromagnetic waves coupled to conductive surfaces, and vector and vortex beams of light are objects studied in plasmonics and photonics. They are used in many applications such as surface sensing and processing, communication systems, and so on. In a number of works (see, e. g. [3]), vortex beams illuminated a system of spiral slots in thin metal films to form radially converging surface plasmons carrying orbital angular momentum. In several papers (see, e. g., [4]), the propagation of rotating plasmons along cylinders with a screw thread has been demonstrated. Although such plasmons can be called vortex plasmons, the sign and magnitude of their topological charge are determined by the geometry of the conductor and cannot be changed. Cylindrical waveguides, along which a superposition of plasmons with different orbital moments is transmitted, can be used in different material applications, as well as in multiplex communication lines in photonic devices. Since the path length of plasmons in the visible range are only tens of microns, it is beneficial to use plasmons of mid- and far-infrared ranges. To implement such systems in these ranges, it is necessary to have an appropriate radiation source, create a system for launching surface plasmons, study the propagation characteristics of vortex plasmons, and create mixers and sorters for multimode beams. In this paper, we report the results of numerical and experimental studies of several variants of devices for the formation, transportation and investigation of vortex plasmon polaritons at wavelengths of 140, 47 and 8.5 micrometers, using the Novosibirsk free electron laser and the quantum cascade laser as radiation sources. To launch plasmons by end-fire-coupling technique or using diffraction elements, Gaussian and Bessel beams of different orders are used [5-9].

This work was supported in parts by RSF grants 19-12-00103 and 19-72-20202. The experiments were carried out at the unique facility "Novosibirsk free electron laser" using the equipment of the Siberian Center of Synchrotron and Terahertz Radiation.

**References**

- [1] H. Rubinsztein-Dunlop, et al. Roadmap on structured light, *J. Opt.*, V. 19, 013001 (2017).
- [2] M. I. Stockman, et al. Roadmap on plasmonics, *J. Opt.*, V. 20, 043001 (2018).
- [3] Seung-Yeol Lee, et al. Controlling the state of surface plasmon vortex by changing the topological charge and polarization state, *Proc. SPIE*, V. 7757, 77573G (2010).
- [4] H.-Z. Yao, S. Zhong, Wideband circularly polarized vortex surface modes on helically grooved metal wires, *IEEE Photonics J.*, V. 7, 4600707 (2015).

- [5] B. A. Knyazev, Y. Y. Choporova, M. S. Mitkov, V. S. Pavelyev, B. O. Volodkin, Generation of terahertz surface plasmon polaritons using nondiffractive Bessel beams with orbital angular momentum. *Phys. Rev. Lett.*, V. 115, 163901 (2015).
- [6] Y. Y. Choporova, B. A. Knyazev, G. N. Kulipanov, et al., High-power Bessel beams with orbital angular momentum in the terahertz range. *Phys. Rev. A*, V. 96, 023846 (2017). [7] B. Knyazev, V. Serbo, Beams of photons with a nonzero projection of the orbital angular momentum - new results, *Phys. Usp.*, V. 61, 449 (2018).
- [8] V. S. Pavelyev, B. O. Volodkin, K. N. Tukmakov, B. A. Knyazev, Yu. Yu. Choporova, Transmissive diffractive micro-optics for high-power THz laser radiation. In *AIP Conf. Proc.*, V. 1989, No. 1, p. 020025 (2018).
- [9] B. A. Knyazev, V. V. Gerasimov, A. K. Nikitin, I. A. Azarov, Yu. Yu. Choporova, Propagation of terahertz surface plasmon polaritons around a convex metal-dielectric interface, *JOSA B*, v. 36, 1684 (2019).

**LMI-I-17****Ionization-event harmonics: basic mechanisms and characterization of ionization dynamics**

*A. Husakou<sup>1</sup>, P. Jurgens<sup>2</sup>, B. Liewehr<sup>3</sup>, B. Kruse<sup>3</sup>, C. Peltz<sup>3</sup>, W. Engel<sup>4</sup>, M. Ivanov<sup>1</sup>,  
M. Vrakking<sup>2</sup>, T. Fennel<sup>3</sup>, A. Mermillod-Blondin<sup>2</sup>*

<sup>1</sup>*Max Born Institute, Division T, Berlin, Germany*

<sup>2</sup>*Max Born Institute, Department A, Berlin, Germany*

<sup>3</sup>*University Rostock, Institute of Physics, Rostock, Germany*

<sup>4</sup>*Max Born Institute, Department B, Berlin, Germany*

The nonlinearity of different materials in the strong pulsed optical field is ubiquitous in modern optics and plays a critical role in key applications such as generation of new frequency components, pulse compression, attosecond science, spectroscopy, metrology, material processing and so on. Up to now, three main background mechanisms were considered responsible for the optical nonlinearities in the rarefied media, in particular gases. First of them is the Kerr-type nonlinearity which is based on the anharmonicity of the bound electron motion. Second is high-order harmonics generation by the three-step process. Finally, the Brunel mechanism of the nonlinearity is associated with stepwise increase of the free-electron density during the photoionization and the associated subcycle phase modulation. In this contribution, we investigate additional and novel mechanisms of nonlinearity and harmonic generation which are based on the previously overlooked peculiarities of the photoionization process.

First, we show that the photoionization electron occurs as a free electron at the finite distance (photoionization displacement, PD) from the parent ion, which leads to ultrafast buildup of the polarization and associated light emission. This effect was neglected up to now. The semiclassical theory of the PD harmonic emission is presented, and we connect the obtained expression of the PD to the photoionization energy losses. We analyze the resultant formalism for the harmonic generation and investigate its contribution as a function of the pump parameters such as intensity and wavelength. The regimes where the PD contribution plays a dominant role compared to the three previously known mechanisms are identified. The possibilities to benchmark the above semiclassical theory by solving the time-dependent Schrödinger equation are discussed. Also, the phase of the PD contribution is investigated analytically and numerically, paving the way to detect and characterize this contribution experimentally.

Second, we show that in addition to the PD contribution, the electrons are photoionized with nonzero velocity (photoionization velocity, PV). The corresponding term in the polarization was also up to now completely neglected. Similarly to the PD term, a semiclassical, strong-field theory will be presented for the PV contribution based on a formalism related to the formalism of the three-step mechanism. The dependence of the PV contribution on the pump parameters will be analyzed. The phase of the PV contribution, in contrast to that of the PD contribution, significantly depends on the pump parameters, which on one hand leads to difficulties in experimental detection and characterization, on the other hand, opens new possibilities with respect to phase matching. In summary, in this contribution we discuss and analyze, based on the semiclassical theory, two new fundamental contributions to the optical nonlinearity, which are related to the displacement and initial velocity of an electron after the photoionization.

## LMI-I-18

### Frequency conversion in nanocomposites

*O. Fedotova<sup>1</sup>, O. Khasanov<sup>1</sup>, R. Rusetski<sup>1</sup>, T. Smirnova<sup>2</sup>*

*<sup>1</sup>Scientific-Practical Materials Research Centre NAS Belarus, Laboratory of Theory of Solids, Minsk, Belarus*

*<sup>2</sup>International Sakharov Environmental Institute BSU, Department of Environmental Information Systems, Minsk, Belarus*

We consider ultrashort laser pulse interaction with nanocomposite consisted of semiconductor quantum dots (QD) incorporated into nonlinear dielectric matrix. Value, angular distribution and spatial dispersion of permanent dipole moments (PDM) are taken into account. The three-level system resonant to pump pulse at the lowest transition between QD exciton states is analyzed. The Hamiltonian describing the light-matter interaction includes fast oscillating diagonal elements due to PDM that impedes to apply traditional approach to calculate medium responses on pulsed excitation. Transformed Hamiltonian is involving QD interaction with fields at multiple frequencies. In result, we get generalized two-level system in rotating reference frame without fast oscillating terms, suitable for one- and two-quantum transitions, and Bloch equations for the QD with PDM in SVEA. The macroscopic photoinduced polarization contains multiple harmonics, which can be a source of responses at corresponding frequencies for the nanocomposite.

THz generation is shown to increase under phase-matching conditions (PMC) due to Zakharov-Benney resonance between THz and pump waves. When PDM is weak and one-photon transitions predominate, the THz field dependence on the pump pulse field is quadratic, in this case THz efficiency does not exceed 0.1%. With increasing PDM magnitude the underlying two-photon transitions (2PT) result in stronger dependence of THz harmonic on the pump pulse providing more efficient frequency conversion. For prevailing 2PT, THz efficiency reaches 16-17%. Second harmonic (SH) generation is a parametric process of the same order as a frequency down-conversion in noncentrosymmetric media. As a result, the solutions for pump pulse and its effect on generated harmonics in both cases are similar. However, the frequency up-conversion process provides substantially larger harmonic yield than low frequency generation, so SH attains 70% under proper PMC.

We compute photon echo (PE) signals under two-pulsed excitation taking into account excitation-induced shift (EIS) of absorption frequency. In addition to signals at resonant frequency under PMC, we establish the responses on two-pulse excitation at multiple frequencies. The spatial synchronism conditions of new responses will differ from those for the primary PE signal. The signals at multiple frequencies and THz responses are originated from PDM interaction with excitation pulses and depend strongly on its angular distribution. The most intensive signals appear at doubled and THz frequencies. Local field effect such as EIS parametrically generates different PE signals at resonant frequency with corresponding PMC. The larger order of PE signal the less its intensity. Spatial dispersion of PDM influences only on even responses. For short time delay between excitation pulses the nonresonant nonlinear matrix will contribute to the time-resolved four wave mixing signals mainly to resonant, SH and THz range. Having optimized the response on the parameters of radiation and materials, highly efficient frequency conversion to THz and SH has been established.

**LMI-I-19****Free-electron-mediated effects of single femtosecond pulses and pulse series in the (irradiance/fluence) parameter space***A. Vogel<sup>1</sup>, X.X. Liang<sup>1</sup>, S. Freidank<sup>1</sup>, N. Linz<sup>1</sup>**<sup>1</sup>University of Luebeck, Institute of Biomedical Optics, Luebeck, Germany*

Laser-induced plasma generation by single and multiple femtosecond laser pulses is used surgically and constitutes also a source of unwanted photodamage in nonlinear microscopy. The irradiance threshold at which transient vapor bubbles in water are produced by single pulses is 20 times higher than the irradiance used for nonlinear microscopy. However, photodamage in multiphoton microscopy already starts, when the irradiance is raised 1.5 times above the value used for autofluorescence imaging. Thus, there is a huge realm of low-density plasma effects between the multi-pulse damage threshold and the single-pulse surgical regime, which has been little explored to date. The talk will provide a systematic overview over laser applications in this regime and the irradiance and radiant exposure dependence of the laser effects.

Single-pulse effects are used for flap-cutting in corneal refractive laser surgery, for cataract surgery, and in cell surgery. The bubble threshold is here determined by a temperature threshold above which a phase transition occurs.

Pulse-series effects, in which a few fs pulses of lower energy overlap, are used for gentle flap-cutting in refractive surgery. Here, dissection relies on molecular disintegration of biomolecules by the interaction with electrons of the low-density plasma, and the bubble produced contains non-condensable gas rather than water vapor. The underlying process is a nonlinear chemical rate process, and the character of the threshold is thus fundamentally different from the single-pulse threshold.

At even lower pulse energies, fs laser irradiation can be employed to create refractive index changes of the corneal tissue for non-ablative treatment of myopia or hyperopia [1]. The n-changes have been attributed to free-electron-induced generation of reactive oxygen species in water, which then create crosslinks in collagen molecules. However, calculations of the free-electron energy spectrum using our model [2] revealed that electrons have sufficient energy to also directly modify collagen molecules.

Photodamage in multiphoton microscopy was explored for various cell types and tissues using physical indicators that enable real-time-monitoring of the photodamage kinetics. We established algorithms that can evaluate the transition from unchanged tissue (emitting 2-photon-excited autofluorescence) to slightly changed tissue (hyperfluorescence), drastically changed tissue (plasma luminescence) and disintegrated biomolecules (gas bubble formation). Series of scans at different irradiance values,  $I$ , were evaluated to determine the radiant exposure values,  $H$ , for the onset of hyperfluorescence, plasma luminescence, and bubble formation. By plotting these threshold values in  $(H, I)$  space, a “safe” region can be identified, in which nonlinear microscopy without photodamage is possible, and the photomodification regime can be delineated.

Altogether, we created a comprehensive picture of photomodification kinetics and mechanisms by fs single- and multipulse irradiation in the realm of low-density plasmas. Exploration of this regime implies many opportunities for novel applications in the future.

**References**

- [1] Wang C., Fomovsky M., Miao G., Zyablitskaya M. and Vukelic, S. *Nat. Photon.* 12:416–422 (2018).
- [2] Liang X.-X., Zhang Z., and Vogel A. *Optics Express* 27:4672 (2019)

**LMI-I-20****Dynamics of water ionization under intensive femtosecond irradiation***V. Konov<sup>1</sup>, V. Kononenko<sup>1</sup>, V. Gololobov<sup>1</sup>**<sup>1</sup>General Physics Institute, Natural Sciences Center, Moscow, Russian Federation*

Temporal variation of water optical properties (transmittance  $T$  and refractive index  $n$ ) induced by intense 100 fs pulses of Ti:Sa ( $\lambda=800$  nm) laser was studied. Beam intensity  $\approx 10^{12}$  W/cm<sup>2</sup> was sufficient for strong multi-photon ionization of water. For focal area visualization as well as measurements of  $n(t)$  and  $T(t)$ , pump-probe interferometric technique was applied (Fig.1).

In contrast to our similar investigations with solids and gases no negative refractive index values, determined by free carriers generation, could be monitored.

During the laser pulse action this effect can be explained by the fast ( $<100$  fs) drop of free carriers concentration caused by solvation process. At the same time Kerr effect, resulting in positive growth of  $n(t)$ , is strong both in the original and solvated water. In the latter case the observed higher  $n(t)$  amplitude can be explained by higher non-linear properties of solvated water and by self-focusing of the laser beam.

After pulse termination non-monotonous behavior of  $n(t)$  was found. Two additional peaks with  $\Delta n=4 \times 10^{-3}$  and  $6 \times 10^{-3}$  at 3 ps and 1 ns delay times are clearly seen in Fig.1b. We consider this effect is determined by a combination of solvated electrons interaction with water molecules and thermodynamic phenomena.

This work was supported by RSF grant N 19-12-00255.

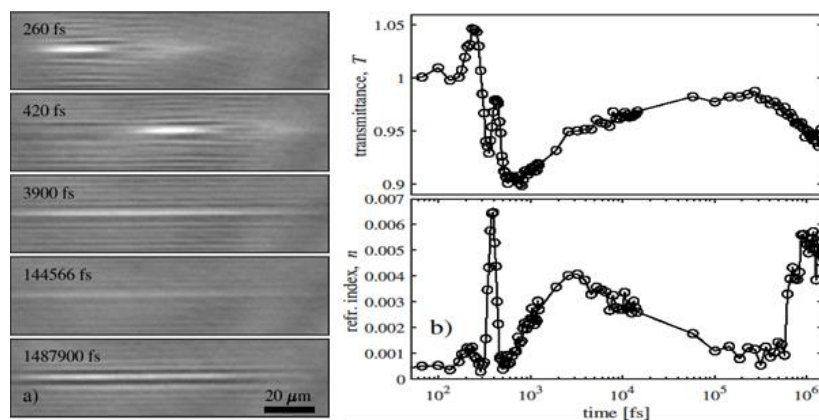


**Fig.1.** Modification of water optical properties during and after fs pulse action  
a) Snapshots with marked delays b) Dynamics of transmittance and refractive index

**LMI-I-21****Nuclear nanomedicine: laser ablated nanoparticles in new generation radiopharmaceuticals**

*I.N. Zavestovskaya<sup>1</sup>, A. Kabashin<sup>2</sup>, V. Petriev<sup>3</sup>*

*<sup>1</sup>MEPHI, BHSPH, Moscow, Russian Federation*

*<sup>2</sup>Aix-Marseille Univ. - CNRS, Laser Lab, Marseille, France*

*<sup>3</sup>National Medical Research Centre of radiology of the Ministry of Health of the Russian Federation, Nuclear Medicine, Obninsk, Russian Federation*

The results in *nuclear nanomedicine* which utilizes nanoparticles (NPs) as carriers of radionuclides are presented. We propose silicon NPs (Si\*NPs) synthesized by pulsed laser ablation in liquids. One can use these methods to make stable colloidal dispersions of Si\*NPs in both organic and aqueous media, which are suitable for a multitude of applications across the important fields of health care. Size tailoring allows production of Si\*NPs with efficient photoluminescence that can be tuned across a broad spectral range from the visible to near-IR by varying particle size and surface functionalization. These applications encompass several types of bioimaging and various therapies, including photodynamic therapy, RF thermal therapy, and radiotherapy. The uniqueness of such Si\*NPs is based on their biodegradability, which makes possible rapid elimination of these structures from the organism within several days under absence of any toxic effects.

Synthesized nanoparticles were tested as carries for promising radionuclides, as well as sensitizers in radiation therapy. We demonstrate the possibility for fast PEGylation and conjugation of laser-synthesized Si\*NPs with Rhenium-188 (<sup>188</sup>Re) radionuclide, which is one of most promising generator-type therapeutic beta-emitters with the energy of positron emission of 1.96 MeV (16.7%) and 2.18 MeV (80%) and half-decay time of 17 hours. We show that such conjugates can efficiently deliver the radionuclide through the blood stream and retain it in the tumor region. We also show that Si NPs ensure excellent retention of <sup>188</sup>Re in tumor, not possible with the salt, which enables one to maximize therapeutic effect, as well as a complete time-delayed conjugate bioelimination. Finally, our tests on rat survival demonstrate excellent therapeutic effect (72% survival compared to 0% of the control group). Combined with a series of imaging and therapeutic functionalities based on unique intrinsic properties of Si\*NPs, the proposed biodegradable complex promises a major advancement of nuclear nanomedicine.

**LMI-I-22****Damage effects in metals induced by short and ultrashort laser pulses: Comparison of air and water environments**

*A.V. Bulgakov<sup>1,2</sup>, S.V. Starinskiy<sup>2</sup>, M. Stehlík<sup>1,3</sup>, I. Mirza<sup>1</sup>, Y.G. Shukhov<sup>2</sup>, C. Liberatore<sup>1</sup>, N.M. Bulgakova<sup>1</sup>*

*<sup>1</sup>HiLASE Centre, Institute of Physics of the Czech Academy of Sciences, Dolní Břežany, Czech Republic*

*<sup>2</sup>S.S. Kutateladze Institute of Thermophysics, Siberian Branch of RAS, Novosibirsk, Russian Federation*

*<sup>3</sup>FNSPE, Czech Technical University in Prague, Prague, Czech Republic*

Pulsed laser ablation in liquids (PLAL) is an efficient and flexible technique for nanoparticle production and surface nanostructuring. Although PLAL is simple in realization, the process itself is very complicated and still poorly understood. The complexity of the PLAL process can be illustrated by the example of the laser-induced damage threshold (DT), a well-defined parameter which can be unequivocally measured and serve as a reference for understanding and modelling of the PLAL process. However, available data on DTs in liquids are rather contradictory, provide threshold fluences higher, equal to, or lower than the corresponding values in air, and various mechanisms are invoked to explain the difference. In this work, we have systematically investigated the DTs of a number of metals (gold, silver, gold-silver alloys, titanium) irradiated by IR laser pulses in water. The experiments were carried out with nano-, pico- and femtosecond pulses in single-shot and multi-short irradiation regimes. The results are compared with data obtained under identical irradiation conditions in air. The influences of the pulse duration, surface reflectivity, focusing conditions, water superheating and nucleation, accumulation effects and non-linear effects during laser pulse propagation in water are discussed.

**LMI-I-23****Ionization-field instabilities and nanograting formation in optical breakdown processes***V. Gildenburg<sup>1,2</sup>, I. Pavlichenko<sup>1,2</sup>**<sup>1</sup>Institute of Applied Physics RAS, Plasma physics department, Nizhny Novgorod, Russian Federation**<sup>2</sup>University of Nizhny Novgorod, Radiophysics department, Nizhny Novgorod, Russian Federation*

The ionization-field instability developing due to the mutual enhancement of the electric field and plasma density perturbations in the processes of the optical and microwave breakdown of different media can lead, as is well known, to formation of small-scale periodic ionization structures instead the homogeneous plasma seemingly corresponding to the initially homogeneous ionizing radiation [1-5]. During the last decade, the interest in such structures has been renewed in connection with their growing applications for the production of the subwavelength nanogratings in the optical materials, in particular, in the fused silica, by the series of repeated laser pulses [6-8]. The creation of such nanogratings is considered now as a promising technique of the material optical properties modification and compact writing and storage of the optical information. Nevertheless, the physical mechanisms predetermining these structures appearance are not revealed completely and remain the subject of discussion.

In the presented report, the spatiotemporal evolution of the field and plasma in the optical breakdown induced in the volume of transparent dielectric (fused silica) by fs laser pulse is studied under condition of the so-called plasma-resonance-induced ionization instability that results in the deep small-scale periodic modulation of the breakdown plasma parameters in the direction of the laser polarization. We address two essentially different models of optical discharge created (i) in the homogeneous dielectric with a slight (modeling the seed perturbation) periodic modulation of the permittivity [9,10] and (ii) in the dielectric with multiple randomly placed and easily ionized ellipsoidal inclusions (modeling small voids and atomic structure defects) [11-13]. For the second model we calculate the effective permittivity of the nano-dispersive media based on the Maxwell Garnett theory. The optical electric field is calculated with allowance for the effects influencing both its long-scale structure (the beam focusing accounted for in the given-ray-tube approximation) and the small-scale one (quasi-static enhancement in the plasma resonance regions). The plasma density evolution is described by the rate equation taking into account the photoionization, avalanche ionization, and ambipolar diffusion. Based on the fulfilled numerical calculations, we have described the main types of the plasma-field structures formed in one laser pulse and have found the laser pulse intensity range where the instability evolving from seed perturbations leads to the formation of the contrast subwavelength periodic structure containing the number of the narrow zones with overcritical plasma density and enhanced energy deposition. The latter allows us to consider this structure formed in one pulse as underlying the nanograting formation observed experimentally in the fused silica irradiated by series of repeated fs pulses.

**References**

- [1] V.B. Gildenburg and A.V. Kim, Sov. Phys. JETP, V. 47, P. 72 (1978).
- [2] M. Lontano, G. Lampis, A.V. Kim, and A.M. Sergeev, Phys. Scripta, V. T63, P. 141 (1996)
- [3] V.B. Gildenburg, A.G. Litvak, and N.A. Zharova, Phys. Rev. Lett., 78, 2968 (1997).
- [4] T.M. Antonsen, and Z. Bian, Jr., Phys. Rev. Lett., V. 82, P. 3617 (1999).

- [5] V.B. Gildenburg and N.V. Vvedenskii, *Phys. Plas.*, V. 8, P. 1953 (2001).
- [6] Y. Shimotsuma, P. Kazansky, J. Qiu, and K. Hirao, *Phys. Rev. Lett.*, V. 91, 247405 (2003).
- [7] C. Hnatovsky, R.S. Taylor, P.P. Rajeev, E. Simova, V.R. Bhardwaj, D.M. Rayner, and P.B. Corkum, *Appl. Phys. Lett.*, V. 87, 014104 (2005).
- [8] N. M. Bulgakova, V. Zhukov, Y. Meshcheryakov, *Appl. Phys. B*, V. 113, P. 437 (2013).
- [9] V.B. Gildenburg and I.A. Pavlichenko, *Phys. Plas.*, V. 23, 084502 (2016).
- [10] V.B. Gildenburg and I.A. Pavlichenko, *Opt. Lett.*, V. 44, P. 2534 (2019).
- [11] R. Buschlinger, S. Nolte, and U. Peschel, *Phys. Rev. B*, V. 89, 184306 (2014).
- [12] A. Rudenko, J.-P. Colombier, and T.E. Itina, *Phys. Rev. B*, V. 93, 075427 (2016).
- [13] A. Rudenko, J.-P. Colombier and T.E. Itina, *Phys. Chem. Chem. Phys.*, V. 20, P. 5887 (2018).

**LMI-I-24****High-precision simulations of interaction of ultrashort laser pulses with bulk bandgap materials***V. P. Zhukov<sup>1,2,3</sup>, N. M. Bulgakova<sup>1</sup>**<sup>1</sup>HiLASE Centre, Institute of Physics of the Czech Academy of Sciences, Dolní Břežany, Czech Republic**<sup>2</sup>Institute of Computational Technologies, Siberian Branch RAS, Novosibirsk, Russian Federation**<sup>3</sup>Novosibirsk State Technical University, Physical-Technical Faculty, Novosibirsk, Russian Federation*

Numerical modeling has proven to be a powerful tool for investigations of laser-matter interaction. It enables to gain insight into dynamic interplay of multiplicity of processes triggered by laser light and to identify the main factors and processes influencing efficient laser energy coupling to materials. In this report, modeling aspects of interaction of femtosecond laser pulses with transparent materials will be discussed for the regimes of volumetric modification. The advantages of the model based on nonlinear Maxwell's equations supplemented by the hydrodynamic equations for free electron plasma [1,2] will be addressed. The typical difficulties of such kind models associated with the construction of the finite-difference scheme, the boundary conditions for incoming laser beam (especially for the cases of tight focusing inside the bulk and very short pulse durations), the description of elementary processes in the conductive zone where free-electron plasma is excited (collision time, photo- and impact ionization, recombination) will be outlined. The problems of accuracy of numerical schemes will be touched and the limiting factors for the application of a simplified approach based on nonlinear Schrödinger equation will be analyzed [3]. Finally, the possibilities and peculiarities of simulations of laser beam propagation in transparent materials will be considered for the cases of multi-pulse irradiation [2] as well as for dichromatic laser pulses.

**References**

- [1] N. M. Bulgakova, V. P. Zhukov, S.V. Sonina, and Y. P. Meshcheryakov, Modification of transparent materials with ultrashort laser pulses: What is energetically and mechanically meaningful? *J. Appl. Phys.* 118, 233108 (2015).
- [2] V.P. Zhukov, S. Akturk, N. M. Bulgakova, Asymmetric interactions induced by spatio-temporal couplings of femtosecond laser pulses in transparent media, *J. Opt. Soc. Am. B* 36, 1556-1564 (2019).
- [3] V. P. Zhukov, N. M. Bulgakova, M. P. Fedoruk, Nonlinear Maxwell's and Schrodinger equations for describing the volumetric interaction of femtosecond laser pulses with transparent solid dielectrics: effect of the boundary conditions, *J. Opt. Technol.* 84, 439-446 (2017).

**LMI-I-25****Laser technologies in the diagnostics of heterogeneous substances with supercritical fluidic components**

*D. Zimnyakov<sup>1</sup>, S. Yuvchenko<sup>1</sup>*

*<sup>1</sup>Yury Gagarin State Technical University of Saratov, Physics, Saratov, Russian Federation*

Laser diagnostic technologies are an effective tool for characterizing the structure and dynamics of complex heterogeneous systems on a microscopic scale. Among such heterogeneous systems, two-phase and multiphase systems with supercritical fluid (SCF) components are of particular interest from the viewpoint of the synthesis of novel functional materials for biomedical, photonic and electronic applications. We present the theoretical and experimental results of applying various laser-based diagnostic technologies, such as the diffusing-wave spectroscopy, swept-source low-coherence reflectometry, and laser polarimetry, to analysis of the structural and dynamic properties of SCF-synthesized and modified highly porous polymer matrices. The fundamental features of the laser light transfer in such random multiple scattering systems are discussed; in particular, the remarkable correlations in the mutual positions of neighboring pores cause a significant decrease in the anisotropy of laser light scattering in the matrices. This effect appears when the volume fraction of the polymer in the matrix is in the range from 0.3 to 0.1. Further reduction of the polymer volume fraction in the SCF-synthesized porous matrices leads to the “optical inversion” of these multiple scattering systems (dramatic changes in the physical mechanism of laser light scattering related to transition from scattering by an unordered ensemble of voids in a polymer matrix to scattering by an ensemble of polymer films and their intersections in a gas matrix). The transport mean free path of propagation of the probe laser light in the synthesized matrices is strictly determined by the average size of pores and the volume fraction of the condensed phase (polymer). This makes it possible to evaluate these structural parameters with acceptable accuracy using analysis of the signal decay rate in the low-coherence reflectometric system with a frequency-modulated laser (the swept-source reflectometer). The study of dynamic multiple scattering of laser light in synthesized matrices allows the characterization of the kinetics of pore formation and development in the expanding polymer foams. The potential of laser diagnostic methods in characterizing unstable and quasi-stable heterogeneous two-phase systems is illustrated by experimental data on foaming of bioresorbable polymers (polylactides) using supercritical carbon dioxide.

In addition, supercritical fluids can be considered as efficient immersion agents easily controlled by variations in the temperature and pressure. This opens up possibilities for the practical use of the refractive index tuning (RIT) method in laser diagnostics of micro- and nanostructured composite materials.

This work is supported by the RFBR grant # 18-29-06024.

**LMI-I-26****Self-organization and laser structuring beyond diffraction limit***R. Stoian<sup>1</sup>, J.P. Colombier<sup>1</sup>, A. Rudenko<sup>1</sup>, A. Aguilar<sup>1</sup>, C. Mauclair<sup>1</sup>**<sup>1</sup>CNRS Université Lyon, Laboratoire Hubert Curien, St. Etienne, France*

Material structuring represents today the base for rapidly growing application areas in emerging technologies. Ultrafast lasers contribute essentially to the development of micro/nanotechnologies, being able to structure materials with utmost precision [1]. They hold in this context unique advantages as rapid, flexible, non-contact processing tools. These advantages originate specifically in the strong ability of laser pulses to confine light energy in nonlinear interactions and to suppress thermal effects, reducing thus collateral damage. The question of resolution is crucial for further industrial insertion and a lot of interest is devoted to the capacity of reaching the nanoscale. The scale of structuring, the minimal feature size, and the resulting morphologies and topographies define then the function that can be attached to the structured material and optical and mechanical functionalization was demonstrated.

With respect to the achievable feature size, optical processing is typically limited by diffraction to scales comparable to the wavelength. Therefore structuring in the nanoscale should rely on a specific material response to laser radiation, experiencing not an optical limit but a material organization limit which, for a large range of material phenomena, lies one order of magnitude below. We will discuss ultrafast laser irradiation concepts capable of achieving structuring features with sub-wavelength characteristic sizes and self-organized in periodic patterns on excited materials. They reflect a capacity of mutual influence between material and optical landscapes resulting from scattering, the emergence of surface waves or the self-organization capacity of hydrodynamic instabilities [2]. We will show the effects of far and near-field scattering and coherent superposition of wavelets in generating light patterns of various complexity. The scenario can be applied for 2D surface and 3D volume structures. New classes of evanescent surface waves have a dominant role in setting light patterns for a large range of materials. Coupling electromagnetic and hydrodynamic models we establish a dynamic interplay between light and material surfaces generating cavitation and material displacements and thus the positive feedback for ordered nanoscale structuring. We equally indicate advanced optical methods to resolve in-situ irradiation pattern and the growth of nanostructures [3] beyond diffraction limit, corroborating light scattering scenarios. The stability of patterns during growth validate the hydrodynamically-enforced electromagnetic origin of periodic patterns.

**References**

- [1] K. Sugioka and Y. Cheng, Ultrafast lasers-reliable tools for advanced materials processing, *Light: Sci. Appl.* 1, e149 (2014).
- [2] A. Rudenko, C. Mauclair, F. Garrelie, R. Stoian, and J. P. Colombier, Self-organization of surfaces on the nanoscale by topography-mediated selection of quasi-cylindrical and plasmonic waves, *Nanophotonics*, <https://doi.org/10.1515/nanoph-2018-0206> (2019).
- [3] A. Aguilar, C. Mauclair, N. Faure, J. P. Colombier, and R. Stoian, In-situ high-resolution visualization of laser-induced periodic nanostructures driven by optical feedback, *Sci. Repo.* 7, 16509 (2017).

**LMI-I-27****Intrapulse dynamics of plasma formation in fs-laser irradiated dielectrics**

*A. Mermillod-Blondin<sup>1</sup>, P. Jürgens<sup>1</sup>, B. Liewehr<sup>2</sup>, C. Peltz<sup>2</sup>, B. Kruse<sup>2</sup>, T. Fennel<sup>2</sup>, A. Husakou<sup>1</sup>, M.J.J. Vrakking<sup>1</sup>*

*<sup>1</sup>Max Born Institute for Nonlinear Optics and Short Pulse Spectroscopy, A: Attosecond Physics, Berlin, Germany*

*<sup>2</sup>University of Rostock, Institute of Physics, Rostock, Germany*

Focusing an intense (in the TW/cm<sup>2</sup> range) ultrashort (sub-ps) laser pulse in the bulk of a transparent material leads to permanent structural modifications of the lattice in the irradiation region. Such structural modifications alter the samples properties including its refractive index. Based on laser-induced refractive index changes, fs laser-direct writing of optical microstructures in solid dielectrics has rapidly become a standard process.

Because structural re-arrangements of the lattice require energy, understanding the mechanisms of laser energy deposition into the sample is of prime importance to describe, control and optimize the laser matter interaction. The energy transfer between the laser beam and the lattice proceeds through the promotion of electrons from the valence to the conduction band resulting in the formation of an underdense (density of ca.  $10^{19}$ - $10^{20}$  cm<sup>-3</sup>) electron-hole plasma. Strong-field ionization and electron-electron impact ionization have been identified as the two fundamental processes governing the free carrier generation. However, the relative contribution of these two channels remains an open question.

In this talk, we report on the emission of low-order harmonics during laser irradiation in amorphous fused silica and show that when the laser-intensity approaches the permanent modification threshold, the low-order harmonic formation is due to the transport of the free carriers across the bandgap. The nonlinearity of strong field ionization dominates by far all other possible sources of nonlinearities, including Kerr-type, intraband, interband as well as the so-called Brunel contributions. These results enable to detect optically the onset of strong-field ionization and provide unprecedented insights into the laser-induced plasma formation in microprocessing conditions.

**LMI-I-28****New insights to femtosecond excitation of solids with mid-IR laser fields***F. Potemkin<sup>1</sup>**<sup>1</sup>M.V. Lomonosov Moscow State University, Faculty of Physics, Moscow, Russian Federation*

Direct fabrication of nanoscale structures in bulk material (dielectric or semiconductor) is of significant importance for miniaturization of photonic and optoelectronic devices. Ultrafast lasers are a promising tool for direct writing of nanometer defects due to highly nonlinear nature of process [1,2]. Being defined as the ratio of total absorbed energy to the laser impact area, deposited energy density (DED) serves as a key parameter in the process of the femtosecond laser pulse energy delivery into the bulk of the solids during microstructuring [3]. Thus, in order to control the morphology of residual modifications inside solids one has to find the ways for increasing absorption of incident laser energy under conditions of laser impact area shrinking. However, due to diffraction limit, the minimal size of the structures obtained under single color excitation is still of the order of  $\lambda/NA$ ,  $\lambda$  is laser wavelength and NA is numerical aperture of the focusing optics. In contrast multi-color laser beams allow for precise control of structuring by dividing the excitation process into two steps [3,4]. Firstly, shorter wavelength pulse (visible or UV for dielectric and near-IR for semiconductor) creates seed electrons. Subsequently infrared (from near to mid-IR) pulse arrives and induces damage through efficient initiation of avalanche ionization. The significant importance of this approach is the capability of reaching high deposition energy density simultaneously with minimal defect sizes since energy of both pulses (visible and IR) is below the damage threshold [6].

In this paper we present our latest experimental and theoretical results aiming on the optimization of laser pulses parameters (energy, wavelength, polarization) and uncovering new features of femtosecond excitation of solids with mid-IR laser fields. We have investigated the effect of laser wavelength on the plasma formation and laser-induced damage threshold under femtosecond excitation of solids ( $\text{SiO}_2$ ,  $\text{MgF}_2$ ,  $\text{ZnSe}$ ) tuning the wavelength from visible (0.62  $\mu\text{m}$ ) to mid-IR (4.4  $\mu\text{m}$ ). For all the samples lowering plasma formation and damage threshold was observed scaling laser driver wavelength to mid-IR. The simulation of the electron plasma density dynamics, via MRE, show that using mid-IR laser pulses with shorter pulse durations leads to significant decreasing of the LIDT threshold that is in excellent agreement with experimental observations. Also we show that the highest deposited energy is reached when the energy of both pulses is close to single color threshold of plasma generation. The use of the second pulse with longer wavelength significantly increases absorbed energy due to more efficient heating of the quasi-free electrons in the conduction band. Elliptical polarization of the long wavelength pulse is additionally increase absorbed energy.

**References**

- [1] R. R. Gattass and E. Mazur, "Femtosecond laser micromachining in transparent materials," *Nat. Photonics* 2(4), 219–225 (2008).
- [2] M. Ali, T. Wagner, M. Shakoor, P. A. Molian, "Review of laser nanomachining," *J. Laser Appl.* 20(3), 169–184 (2008).
- [3] F. V. Potemkin et al. "Overcritical plasma ignition and diagnostics from oncoming interaction of two color low energy tightly focused femtosecond laser pulses inside fused silica," *Laser Physics Letters* 13(4), 045402 (2016).

- [4] F. V. Potemkin et al. "Enhancing nonlinear energy deposition into transparent solids with an elliptically polarized and mid-IR heating laser pulse under two-color femtosecond impact," *Laser Physics Letters* 14(6), 065403 (2017).
- [5] F. Potemkin et al. "Controlled energy deposition and void-like modification inside transparent solids by two-color tightly focused femtosecond laser pulses." *Applied Physics Letters* 110(16), 163903 (2017).

**LMI-I-29****Periodically poled crystals for nonlinear optical conversions and controlling of coherent light**

*V. Shur<sup>1</sup>, A. Akhmatkhanov<sup>1</sup>, A. Esin<sup>1</sup>, V. Pavelyev<sup>2</sup>*

*<sup>1</sup>Ural Federal University, Institute of Natural Sciences and Mathematics, Ekaterinburg, Russian Federation*

*<sup>2</sup>Samara University, Department of Nanoengineering, Samara, Russian Federation*

We present the recent achievements in periodical poling in MgO doped single crystals of lithium niobate (LN), lithium tantalate (LT) and potassium titanyl phosphate (KTP) and the design and realization of various LN based diffraction optical elements (DOE) based on the experimental study of the domain structure evolution by the complementary high-resolution domain visualization methods [1].

The crystals with tailored periodically poled domain structures (PPLN and PPLT) produced with nano-scale period reproducibility have been used for Second Harmonic Generation (SHG) and Optical Parametric Oscillation (OPO) based on quasi-phase-matched nonlinear optical wavelength conversion. The wide range of wall velocities with two orders of magnitude difference was observed for switching in a uniform electric field [2,3]. The kinetic maps allowed analyzing the spatial distribution of the wall motion velocities and classifying the walls by velocity ranges. The distinguished slow, fast, and superfast domain walls in KTP and LN differed by their orientation [3,4]. The deep knowledge of the domain structure evolution at elevated temperatures and relaxation of the high bulk conductivity along the charged domain walls MgO:LN and MgO:LT allowed us to optimize the periodical poling technique and to produce high-fidelity domain patterns.

The fan-out periodical domain structures created in 3-mm-thick MgO:LN wafers allowed us to realize the widely tunable OPO generation with the signal wave from 2.5 to 4.5  $\mu\text{m}$  using the 1.053  $\mu\text{m}$  pump. The possibility of producing the elements with thickness up to 10 mm for high-power application has been discussed. The periodical domain structure with period of 40  $\mu\text{m}$  was created in KTP single crystals for OPO generation at 2.4  $\mu\text{m}$  using the 1.053  $\mu\text{m}$  pump. The abilities and perspectives of producing the elements with submicron periods has been discussed. The ferroelectric domains with opposite values of spontaneous polarization possess also the opposite values of the linear electrooptic effect, which allowed to demonstrate the electrical field controlled optical beam deflectors [5-7], diffusers [8], Fresnel zone plates [9] and Shack-Hartmann sensors [10]. The operation range of the created diffraction elements was limited by 200°C due to essential decrease of the threshold fields for ferroelectric domain switching. The possibility of continuous tuning of diffraction efficiency of the elements has been demonstrated. It was shown that the DOE response time is less than 0.1  $\mu\text{s}$ .

The following tunable diffraction elements have been produced: (1) the hexagonal zone plate with focus distance 150 mm and aperture 1.7 mm and (2) the 2D diffraction grating with period 20  $\mu\text{m}$ . The hexagonal zone plate has focused up to 25% of the laser light into a spot of 130  $\mu\text{m}$  in diameter. The 2D diffraction grating has allowed decreasing the zero-order diffraction maximum intensity by 80%. The transparency range of the DOEs was 320-1800 nm.

**LMI-O-2****Time-resolved pump-probe microscopy of the complete ablation dynamics in ultrashort laser pulse irradiated aluminum and stainless steel**

*J. Winter<sup>1,2</sup>, S. Rapp<sup>1</sup>, M. Spellaug<sup>1</sup>, M. Schmidt<sup>2</sup>, H.P. Huber<sup>1</sup>*

*<sup>1</sup>Lasercenter Munich University of Applied Sciences, Department of Applied Sciences and Mechatronics, Munich, Germany*

*<sup>2</sup>Friedrich-Alexander University Erlangen-Nürnberg, Erlangen, Germany; Institute of Photonic Technologies, Erlangen, Germany*

Metals irradiated with ultrashort laser pulses pass through a sequence of physical processes that occur over a wide range of timescales, from femtoseconds to microseconds. The complete laser ablation process for the industrially relevant metals, aluminium (Al) and stainless steel (AISI 304) is tracked from the initial pulse absorption to the material removal occurring on a microsecond time scale.

The time-resolved ellipsometry [1,2] reveals changes in the real and imaginary part of the refractive index for the first tens of picoseconds and complementary time-resolved microscopy [3] gives access to changes of the relative reflectivity from the initial femtosecond pulse impact to the final state at 10  $\mu$ s. The changes in optical indices imply an ultrafast decrease [2] in the density connected to the pressure unloading process in the first picoseconds and reveal spallation as the dominant mechanism for laser ablation in bulk Al and stainless steel at the applied fluences. The study demonstrates that the energy specific ablation volume is kept at an optimum when the ablation is initiated with ultrafast pulses within the pressure unloading process and is able to evolve over eight orders of magnitude without perturbation from subsequent pulses to the final state. These results advance our understanding of a key aspect of the laser–material interaction pathway and can lead to optimization of associated applications ranging from material processing to laser surgery.

**References**

- [1] S. Rapp, M. Kaiser, M. Schmidt, H. P. Huber, Ultrafast pump-probe ellipsometry setup for the measurement of transient optical properties during laser ablation, *Opt. Express* 24 (2016) 17572.
- [2] J. Winter, S. Rapp, M. Schmidt, H. Huber, Ultrafast laser processing of copper: A comparative study of experimental and simulated transient optical properties, *Appl. Surf. Sci.* 417 (2017) 2-15.
- [3] M. Domke, S. Rapp, M. Schmidt, H. P. Huber, Ultrafast pump-probe microscopy with high temporal dynamic range, *Opt. Express* 20 (2012) 10330–10338.

**LMI-O-3****Effect of the ablation plume pre-formed by ASE on the characteristics of intense femtosecond laser-plasma interactions**

*V. Tcheremiskine*<sup>1,2</sup>, *O. Ranjbar*<sup>3</sup>, *A. Volkov*<sup>3</sup>

<sup>1</sup>*Aix-Marseille University - CNRS, LP Laboratory, Marseille, France*

<sup>2</sup>*Lebedev Physics Institute, Photochemical Processes Laboratory, Moscow, Russian Federation*

<sup>3</sup>*University of Alabama, Department of Mechanical Engineering, Tuscaloosa, USA*

Experimental data collected in recent studies of the Hard X-ray emission produced by intense ( $10^{16}$ - $10^{19}$  W/cm<sup>2</sup>) femtosecond (30 fs) Ti-Sa laser pulses interacting with a bulk molybdenum target [1,2] are re-examined applying an original method of the multi-pixel treatment of X-ray photon absorption events registered by CCD camera. Absolute energetic spectra of generated Hard X-ray pulses are reconstructed, and dependencies of the energetic conversion efficiency of laser radiation into Mo K $\alpha$  line emission at 17.4 keV on the laser peak intensity are obtained for various values of the laser pulse temporal contrast ( $10^6$ ,  $10^8$ , and  $10^9$ ) with respect to the intensity of amplified spontaneous emission (ASE) pedestal. The latter exhibits ~2 ns duration and precedes the main femtosecond laser pulse, which is P-polarized and hits the target at 45°. The obtained dependencies allow estimating the fraction of laser energy, which is transferred to hot electrons accelerated in the intense laser field to energies of the order of laser ponderomotive potential. These dependencies are strongly influenced by the target ablation. They provide important information on the character and physical conditions of laser-plasma interaction.

The derived conclusions are supported by results of numerical simulations of the target ablation by the ASE, which are based on a semi-kinetic model of the plasma plume formation, where the absorption of incident radiation occurs due to inverse bremsstrahlung. Our simulations reproduce well the ablation threshold of molybdenum at the ASE fluence reaching ~2 J/cm<sup>2</sup>, which corresponds to the ASE pedestal intensity of  $\sim 1 \times 10^9$  W/cm<sup>2</sup>. They also show a kind of self-regulated shielding by the ablation plume of the target surface with respect to the incoming ASE due to the collisional absorption of incident radiation in the plume at fluences exceeding the ablation threshold. It results in relatively similar shapes of density profiles for heavy particles (atoms and ions) and for electrons, which are pre-formed near the target surface at fixed laser pulse intensity but at different pulse contrast and correspond to a time instant, when the rising edge (with characteristic duration <10 ps) of the femtosecond laser pulse reaches the target. This is seen in the experiment by close values of the laser peak intensity of  $\sim 6 \times 10^{17}$  W/cm<sup>2</sup> observed at different pulse contrast for the onset of steepening of the electron density profile under influence of the laser radiation pressure. This effect occurs at the surface of critical electron density, where the dominant fraction of laser radiation is absorbed and reflected. Similar shapes of the pre-formed density profiles for electrons and for heavy particles lead to the similar shapes of the electron density profiles resulted due to the ionisation of heavy particles by intense optical field of the femtosecond laser pulse.

**References**

[1] V. Tcheremiskine and Y. Azamoum, arxiv preprint 1710.07125 (2017).

<http://arxiv.org/abs/1710.07125>

[2] Y. Azamoum, PhD thesis, Aix-Marseille University (2016). <http://www.theses.fr/en/s161735>

**LMI-O-4****Dynamic optical response of gold to ultrafast laser action: modeling of damage threshold and comparison with experiment**

*S.A. Lizunov<sup>1,2</sup>, I. Mirza<sup>1</sup>, M. Stehlik<sup>1</sup>, N.M. Bulgakova<sup>1,2</sup>, A.V. Bulgakov<sup>1,2</sup>*

*<sup>1</sup>HiLASE Centre, Institute of Physics of the Czech Academy of Sciences, Dolní Břežany, Czech Republic*

*<sup>2</sup>S.S. Kutateladze Institute of Thermophysics, Siberian Branch of RAS, Novosibirsk, Russian Federation*

Ultrashort (femtosecond and picosecond) lasers have proven to be a great tool for processing of any kind of materials. Due to minimized heat diffusion effects during the action of such pulses, it is possible to create nanosized surface modifications with higher accuracy and smaller energy input as compared to nanosecond and longer pulses. However, because of complexity and multiplicity of the processes triggered in materials by the laser action, the laser-matter interaction phenomenon as a whole and contributions of individual processes to material response on laser light remain challenging. Further advances of ultrafast laser processing demand further thorough studies using both theoretical and experimental approaches and comparison between them.

The optical response of metal surfaces to high-power laser excitation is one of the important topics of laser-matter interaction. As was shown in our recent studies [1], it swiftly changes during laser pulse action and strongly depends on the amount of absorbed energy, which in its turn depends on the optical response. Such interrelation is very complex and cannot be understood based on available experimental techniques. A combination of numerical simulation and experimental probing of laser-induced processes performed for the same irradiation conditions is likely to be the most efficient way of gaining deep insights into the rapid structural and phase transformations of materials triggered by ultrashort laser pulses. Many numerical models have been proposed with different estimations of optical and thermophysical parameters. However, all these models give satisfactory agreement with measurements only for limited ranges of applied laser fluences that calls for further studies.

In this work, results of numerical simulations of ultrashort laser irradiation of gold are reported for a wavelength of 800 nm at a pulse duration of 124 fs and a wavelength 1030 nm at pulse durations of 260 fs and 7 ps. The core of the model is the two-temperature approach supplemented with models of optical response. Several optical models were tested in the simulations. The dynamic changes of thermophysical parameters of gold (both for electronic and lattice subsystems) were taken into account, based on existing literature data. For every optical model and every set of thermophysical properties, the melting threshold fluences were calculated and compared with the experiments. Based on the comparison, the roles of the electron-phonon coupling factor and ballistic electrons will be discussed.

**References**

- [1] M.V. Shugaev, M. He, S.A. Lizunov, Y. Levy, T. J.-Y. Derrien, V.P. Zhukov, N.M. Bulgakova, L.V. Zhigilei, Insights into Laser-Materials Interaction Through Modeling on Atomic and Macroscopic Scales, In: Advances in the Application of Lasers in Materials Science, Springer Series in Materials Science, Ed. P.M. Ossi, Vol. 274, Chapter 5 (Springer, 2018). – P. 107-148.

**LMI-O-5****Conversions of optical angular momentum in the processes of sum-frequency and second-harmonic generation from the surface of the isotropic chiral medium with nonlocal nonlinear response.**

*K. Grigoriev<sup>1</sup>, V. Makarov<sup>1</sup>*

*<sup>1</sup>Lomonosov Moscow State University, Faculty of Physics, Moscow, Russian Federation*

Optical angular momentum (AM) has been a hot topic of investigation since early nineties [1]. Conventionally, the AM of a paraxial light beam is separated into two parts: spin and orbital. The first one is an intrinsic feature of a light field related to its polarization state, while the second is a more extrinsic one and originates from the transverse flow of the Poynting vector of the beam and the vortices of this flow. As a rule, nonlinear optical processes of frequency conversion are achieved when the input and output beams have well defined polarization state and mainly the orbital angular momentum conversions is studied. However, it has been repeatedly shown that, for example, sum-frequency and second-harmonic generation can be performed even in isotropic chiral medium in the case when its optical response is nonlocal in space. It was shown in [2] that the interplay between spin and orbital parts of the AM of input beams plays a key role in this kind of processes. The paper [2] only considered the part of nonlinear signal which was generated during the propagation of the input beams in the bulk of the medium, leaving the surface effects out of the scope of investigation. The present research is an attempt to account for the surface effects in these processes and to see how the AM of the light beams is transformed in them.

We considered the geometry of normal incidence of the input beams. All mentioned nonlinear processes were earlier shown to be forbidden in plane wave approximation in a given geometry. However, real laser beams, especially tightly focused ones, have a longitudinal components of their electric field as well. The interaction of transverse and longitudinal fields provides a sum-frequency generation even in the case when all the signal comes from the bulk response of the medium. We have shown analytically that the reflected signal beam consists of the modes, the angular momentum of which is strictly related to the AM of the input beams. Neither sum spin momentum, nor sum orbital momentum projections on the normal to the medium surface are conserved, but only the total AM (the sum of spin and orbital) is. These rules are not broken even if we take into account the surface response of the medium, the symmetry of which is much lower in comparison with its bulk. The very same rules are applicable for the process of second-harmonic generation driven by the nonlocal response of the medium, which, in its turn, also has more complicated form of its material tensor.

The authors acknowledge the support of Russian Foundation for Basic Research, Grant No. 19-02-00069 and the Foundation for the Development of Theoretical Physics and Mathematics “Basis”.

**References**

- [1] L. Allen, M. Beijersbergen, R. Spreeuw, and J. Woerdman, Phys. Rev. A (1992).
- [2] K.S. Grigoriev, I.A. Perezhogin, V.A. Makarov, Opt. Letters, (2018).

**LMI-O-6****Fragmentation of a liquid tin droplet by a short laser pulse**

*S. Grigoryev<sup>1</sup>, V. Zhakhovsky<sup>1</sup>, S. Dyachkov<sup>1</sup>, B. Lakatosh<sup>2</sup>, V. Medvedev<sup>3</sup>*

*<sup>1</sup>All-Russia Research Institute of Automatics VNIIA, Center for Fundamental and Applied Research, Moscow, Russian Federation*

*<sup>2</sup>Moscow Institute of Physics and Technology, Moscow Institute of Physics and Technology, Moscow, Russian Federation*

*<sup>3</sup>Institute for Spectroscopy RAS, Institute for Spectroscopy- RAS, Troitsk, Russian Federation*

Fragmentation mechanisms of a micrometer-sized liquid tin droplet irradiated by a short laser pulse are studied. Our experiments show either symmetric or asymmetric expansion of the droplet depending on laser pulse intensity. To reveal the underline processes we perform simulations complying with the experiments using the smoothed particle hydrodynamics. It is demonstrated that, as a result of fast laser energy deposition, a strong shock wave followed by a tensile wave is formed and propagates from the frontal side to the rear side of droplet. Convergence of such waves inside the droplet induces cavitation nearby the center, which causes the droplet to expand symmetrically. Reflection of a shock wave from the rear side of droplet may lead to spallation producing a thin layer moving in the laser pulse direction, which results in the asymmetrical expansion. The calculated laser intensity threshold for the rear-side spallation is higher than a threshold required for the central cavitation. The corresponding expansion velocities and thresholds agree well with the experimental results in both regimes of droplet expansion.

**LMI-O-8****Angular momentum of elliptically polarized cnoidal waves and breathers in a nonlinear gyrotropic medium with frequency dispersion**

*K. Grigoriev<sup>1,2</sup>, V. Petnikova<sup>1</sup>, V. Makarov<sup>1,2</sup>*

*<sup>1</sup>Lomonosov Moscow State University, Faculty of physics, Moscow, Russian Federation*

*<sup>2</sup>Lomonosov Moscow State University, International Laser Center, Moscow, Russian Federation*

We have analyzed expressions for the spin part of the density vector of the angular momentum of elliptically polarized cnoidal waves and elliptically polarized breathers propagating along  $z$  axis in an isotropic gyrotropic medium with second order frequency dispersion and spatial dispersion of cubic nonlinearity. A peculiar feature of the obtained analytical expressions for  $z$  component of the density vector of the angular momentum is the variety of forms of their dependence on the running time  $t$  and of the nonlinear gyrotropic medium parameters. For all degenerate solutions of both elliptically polarized cnoidal waves and breathers, the density vector of the spin part of the angular momentum is proportional to the nonlinear gyration parameter and differs from zero only in an isotropic medium with spatial dispersion of cubic nonlinearity.

The frequency of oscillations of Jacobi elliptic functions determining the solution in the form of elliptically polarized cnoidal waves is high enough to produce real sample oscillations. The time-averaged contribution of these oscillations is proportional to the nonlinear gyration parameter. The  $z$  component of the density vector of the angular momentum of elliptically polarized Akhmediev breather and the Kuznetsov – Ma soliton also depend on  $t$  and  $z$ . For the Akhmediev breather, it is periodic in  $t$  and soliton-like in  $z$ , and for the Kuznetsov – Ma soliton, it is soliton-like in  $t$  and periodic in  $z$ . The values of the spin part of the angular momentum averaged over time and propagation coordinate for Akhmediev breather and the Kuznetsov – Ma soliton are nonzero only in the medium with spatial dispersion of cubic nonlinearity.

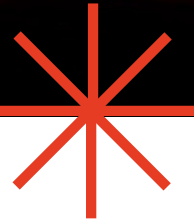
This work was supported by the Russian Foundation for Basic Research (Grant No. 19-02-00069).



# ALT'19

**INTERNATIONAL CONFERENCE**

**Advanced Laser Technologies**



**ADVANCED LASER PROCESSING  
AND LASER SYNTHESIS OF MATERIALS**

**Prague, Czech Republic**



---

15-20 September 2019

**LP-I-1 (Keynote)****Effect of plasma parameters modification on the properties of pulsed laser deposited thin films**

*J.G. Quiñones-Galvan<sup>1</sup>, E. Camps<sup>2</sup>, M.A. Santana Aranda<sup>1</sup>, A. Perez Centeno<sup>1</sup>, G. Gomez Rosas<sup>1</sup>, A. Chavez Chavez<sup>1</sup>, S. Saracho Gonzalez<sup>3</sup>, A. Estrada Lopez<sup>4</sup>, J.A. Guerrero de Leon<sup>4</sup>, L.P. Rivera<sup>1</sup>*

*<sup>1</sup>Universidad de Guadalajara, Physics, Guadalajara, Mexico*

*<sup>2</sup>Instituto Nacional de Investigaciones Nucleares, Physics, Ocoyoacac, Mexico*

*<sup>3</sup>Instituto Tecnológico y de Estudios Superiores de Occidente, Mathematics and Physics, Guadalajara, Mexico*

*<sup>4</sup>Universidad de Guadalajara, Projects Engineering, Guadalajara, Mexico*

Pulsed laser deposition (PLD) has proven to be a versatile technique for growing thin films of a wide range of materials, for a broad of different applications. One of the most used control parameter to grow films by PLD is the fluence, which depends on the output laser energy and the spot size; nevertheless, when using fluence as control parameter, experimental variations can produce uncontrolled properties of the films. On the other hand, reactive laser ablation or multicomponent targets are commonly used for deposition of compound or composite materials; which often results in films with compositions differing from planned. These result in problems with reproducibility.

An alternative to attain reproducibility of chemical composition, as well as physical properties of pulsed laser deposited thin films, is the diagnostic and control of plasma parameters (mean kinetic energy and density of the ions), by means of electrostatic Langmuir probes. In the present work, results on the influence of plasma parameters on the properties and reproducibility of compound thin films for different applications are presented.

**LP-I-2****Laser-induced forward transfer for paper electronics applications**

*P. Serra<sup>1</sup>, P. Sopeña<sup>1</sup>, J.M. Fernández-Pradas<sup>1</sup>, J. Sieiro<sup>2</sup>, J.M. López-Villegas<sup>2</sup>*

*<sup>1</sup>Universitat de Barcelona, Applied Physics, Barcelona, Spain*

*<sup>2</sup>Universitat de Barcelona, Electronic and Biomedical Engineering, Barcelona, Spain*

Paper electronics represents a new concept within the broader field of printed electronics. It combines the technologies and materials employed in the fabrication of electronic devices with the use of paper as the substrate onto which the devices are supported. Paper is by far the cheapest and most widely used substrate in everyday life. In addition, it is flexible, wearable and biocompatible, not to mention that it is renewable and recyclable. All those characteristics provide paper with promising technical, economic and environmental advantages over other flexible substrates for the fabrication of devices like smart labels, RFID tags, wearable sensors or point-of-care systems in applications ranging from smart packaging or health care to safety.

In this work we prove the feasibility of laser-induced forward transfer (LIFT) for printing electronic devices on cellulose paper. Unlike inkjet printing, its major digital competitor, LIFT is a technique with few restrictions concerning the rheological properties of the printable inks. This makes this technique specially suited for printing high solid content inks, an important requirement in the fabrication of conductive pads: the low sheet resistances needed can hardly be achieved with the typical low solid contents of inkjet printing inks. For paper electronics there is an additional advantage: it is possible to print on regular paper. Thanks to the high viscosity of high solid content inks there is no need to submit the substrates to the planarization treatments so characteristic of inkjet printing on paper, and thus minimize the use of additives, with the benefits that this represents both in terms of cost and impact on the environment.

**LP-I-3****Direct laser synthesis of two-dimensional transition metal dichalcogenides in ambient conditions**

*S. Mailis<sup>1</sup>, O. Abbas<sup>2</sup>, A.H. Lewis<sup>2</sup>, N. Aspiotis<sup>2</sup>, C.C. Huang<sup>2</sup>, I. Zeimpekis<sup>2</sup>, D. Hewak<sup>2</sup>, P. Sazio<sup>2</sup>*  
*<sup>1</sup>Skolkovo Institute of Science and Technology, Photonics and Quantum Materials, Moscow, Russian Federation*

*<sup>2</sup>University of Southampton, Optoelectronics Research Centre, Southampton, United Kingdom*

The emergence of nanomaterials with their often superior mechanical, electronic, magnetic and optical properties compared with bulk, demands a mature and robust technology that can synthesize, modify and pattern both scalably and cost effectively. This can be fulfilled via laser processing protocols which produce such materials with both high precision and excellent spatial controllability [1]. Direct laser synthesis of nanomaterials such as graphene and nano-structured metal oxides have been explored thoroughly for a wide range of applications [2,3]. However, to date, there are only a few reports associated with the laser processing of two-dimensional transition metal dichalcogenides (2D-TMDCs) [4]. These mainly utilize laser radiation for thinning thick TMDC films through sublimation down to a single molecular layer [1]. However, this top-down approach is not practical for large-area and scalable production. In addition, further processing steps such as micro-patterning are then required for discrete device fabrication.

Here we present a novel method for the local synthesis and patterning of MoS<sub>2</sub> and WS<sub>2</sub> 2D layers. The synthesis of these materials is achieved by spatially selective, visible laser irradiation of suitable precursors, which are deposited, on the surface of planar substrates under ambient, room temperature conditions. The non-exposed precursor regions are then completely removed in a single step, revealing the synthesised 2D material. This method can produce micro-patterned films with lateral dimensions that can be as narrow as the diffraction limit of the focussed laser beam permits. An example of such laser synthesised MoS<sub>2</sub> tracks can be seen in the optical microscopy image of Figure 1(a). Using this method we have achieved local synthesis of MoS<sub>2</sub> and WS<sub>2</sub> with thickness down to three layers for MoS<sub>2</sub> and monolayer WS<sub>2</sub> on various glass and crystalline substrates. The quality and thickness of the resulting films can be tuned by modifying the precursor chemistry and laser parameters. Different microprobe and spectroscopic techniques, such as optical microscopy, stylus profilometry, Raman spectroscopy, photoluminescence spectroscopy (PL) and X-ray photoelectron spectroscopy (XPS) have been used to assess the quality and thickness of the deposited MoS<sub>2</sub> and WS<sub>2</sub> structures. Finally, we have demonstrated the electronic functionality of our films by fabricating a thin film transistor (TFT). The transfer characteristics of such a TFT (source-drain current vs gate voltage) using a laser-synthesised MoS<sub>2</sub> channel is shown in Figure 1(b).

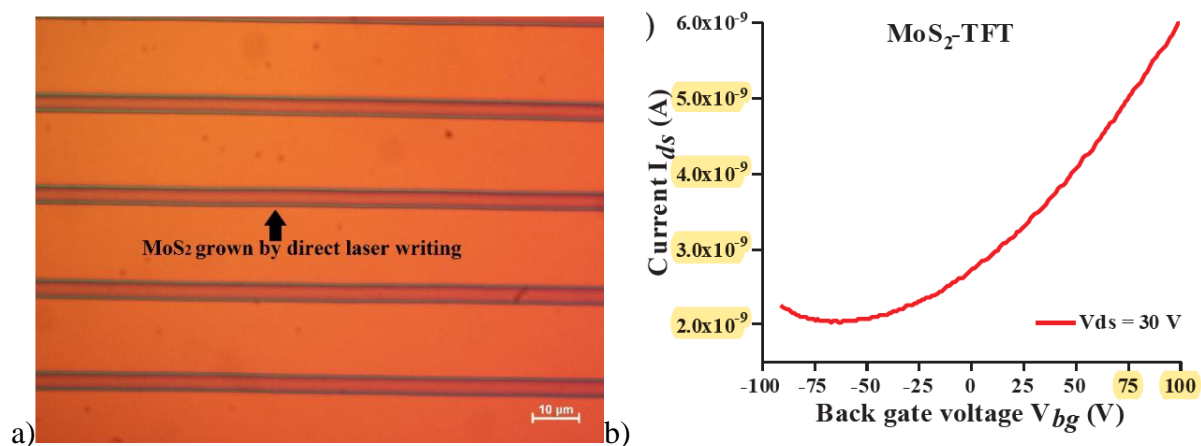


**Fig. 1.** (a) optical microscopy image of MoS<sub>2</sub> tracks deposited by direct laser synthesis on SiO<sub>2</sub>/Si substrate. (b) transfer characteristics (source-drain current vs gate voltage) of a back-gate thin film transistor (TFT) using a laser synthesised MoS<sub>2</sub> channel.

## References

- [1] S. Hong, H. Lee, J. Yeo, and S. H. Ko, “Digital selective laser methods for nanomaterials: From synthesis to processing,” *Nano Today*. 11, 547–564 (2016).
- [2] M. F. El-Kady and R. B. Kaner, “Direct Laser Writing of Graphene Electronics,” *ACS Nano*. 8, 8725–8729 (2014).
- [3] H. Palneedi, J. H. Park, D. Maurya, M. Peddigari, G. T. Hwang, V. Annapureddy, J. W. Kim, J. J. Choi, B. D. Hahn, S. Priya, K. J. Lee, and J. Ryu, “Laser Irradiation of Metal Oxide Films and Nanostructures: Applications and Advances,” *Adv. Mater.* 30, 1705148 (2018).
- [4] M. Samadi, N. Sarikhani, M. Zirak, H. Zhang, H. L. Zhang, and A. Z. Moshfegh, “Group 6 transition metal dichalcogenides nanomaterials: Synthesis, applications and future perspectives,” *Nanoscale Horiz.* 3, 90–204 (2018).

**LP-I-4****Laser-ablative synthesis of novel functional nanoformulations for biomedical applications***A. Kabashin*<sup>1,2</sup><sup>1</sup>*Aix-Marseille Univ.- CNRS, LP3, Marseille, France*<sup>2</sup>*MEPHI, Institute of Engineering Physics for Biomedicine PhysBio, Moscow, Russian Federation*

The presentation will overview our on-going activities on laser ablative synthesis of novel biocompatible colloidal nanomaterials and their testing in biomedical tasks. Our original approach is based on ultra-short (fs) laser ablation from a solid target or already formed water-suspended colloids to fabricate “bare” (ligand-free) nanoparticles (NPs) with well-controlled size characteristics [1-3], as well as coating of nanomaterials by functional molecules (dextran, PEG etc.) during the ablation process [4] or afterwards [5]. The presentation will describe different approaches to achieve appropriate characteristics of plasmonic (Au, TiN) and semiconductor (Si-based structures) nanomaterials and overview their biomedical applications. In particular, we show that bare laser-synthesized Au NPs can provide unique opportunities as SERS probes for identification of biological species such as yeast [6] and bacteria (*Listeria innocua* and *Escherichia coli*) [7] based on strong local electric field enhancement and exceptional purity of laser-synthesized NPs. We also show that bare metal nanoparticles synthesized by laser ablation can provide an order of magnitude better response in glucose oxidation tasks, which promises their use as electrocatalysts in bioimplantable therapeutic devices [8], as well as overview applications of plasmonic nanomaterials (TiN) in phototherapy tasks [9]. We finally overview applications of Si NPs, which exhibit a unique combination of biocompatibility and biodegradability options. In particular, we show that laser-synthesized NPs can be used as efficient markers in tasks of linear [10] and non-linear [11] optical bioimaging. In addition, these nanoparticles can be used in mild cancer therapies, e.g. as sensitizers of radiofrequency radiation-based hyperthermia [12] and as carriers of therapeutic <sup>188</sup>Re radionuclide in nuclear nanomedicine tasks [5].

**References**

- [1] A. V. Kabashin and M. Meunier, *J. Appl. Phys.*, Vol. 94, pp. 7941 (2003).
- [2] K. Maximova, A. I. Aristov, M. Sentis, and A. V. Kabashin, *Nanotechnology*, Vol. 26, pp. 065601 (2015).
- [3] T. Baati, A. Al-Kattan, M.-A. Estève, L. Njim, Y. Ryabchikov, F. Chaspoul, M. Hammami, M. Sentis, A. V. Kabashin, D. Braguer, *Sci. Rep.*, Vol. 6, pp. 25400 (2016).
- [4] F. Correard, K. Maximova, M.-A. Estève, C. Villard, A. Al-Kattan, M. Sentis, M. Roy, M. Gingras, A. V. Kabashin and D. Braguer, *Int. J. Nanomedicine*, Vol. 9, pp. 5415 (2014).
- [5] V. M. Petriev et al., *Sci. Rep.*, Vol. 9, pp. 2017 (2019).
- [6] S. Uusitalo et al, *J. Food Eng.*, Vol. 212, pp. 47 (2017).
- [7] M. Kögler et al, *J. Biophotonics*, Vol. 11, pp. e201700225 (2018).
- [8] S. Hebie et al, *ACS Catal.*, Vol. 5, pp. 6489 (2015).
- [9] A. A. Popov et al, *Sci. Rep.*, Vol. 9, pp. 1194 (2019).
- [10] M. B. Gongalsky et al., *Sci. Rep.*, Vol. 6, pp. 24732 (2016).
- [11] A. Kharin et al, *Adv. Opt. Mater.*, Vol. 7, pp. 1801728 (2019).
- [12] K. P. Tamarov et al, *Sci. Rep.*, 4, 7034 (2014).

**LP-I-5****Synthesis by pulsed laser ablation in liquid of noble metal-based colloids to detect anti-epileptic drugs**

*E. Fazio*<sup>1</sup>

<sup>1</sup>*Università di Messina, Dipartimento di Scienze Matematiche ed Informatiche, Scienze Fisiche e Scienze della Terra MIFT, Messina, Italy*

Noble metal nanoparticles (NPs) as thin films, or in colloidal state are widely studied, due to their surface plasmon resonances (SPR) of interest for biological sensing. Given the distinctive characteristics of epilepsy, the measurement of the concentration of Anti-Epileptic Drugs (AEDs) in the blood serum of a patient is essential for a positive clinical treatment to prevent seizures by adopting the suitable drug posology [1]. This procedure, that is named Therapeutic Drug Monitoring (TDM), is helpful to improve the life quality of the epileptic patients. TDM output is strongly patient-dependent and required to personalize therapy and to adjust the posology for variable pharmacokinetics.

Nowadays, state of the art TDM of AEDs (including Perampanel – PER, the Active Pharmaceutical Ingredient (API) of Fycompa®), employs reliable, but expensive and time-consuming analytical methods (immunoassay and chromatographic techniques). In recent years we proposed and tested a complementary TDM spectroscopic approach based on Surface Enhanced Raman Spectroscopy (SERS) using ad hoc engineered noble metal based plasmonic substrates [2].

In this contribution, we discuss noble metal-based substrates obtained by spraying colloids prepared by the Pulsed Laser Ablation in Liquid (PLAL) technique. Such substrates were tested as SERS sensors focusing on PER. Sensors with tunable SPR position can be produced by PLAL, analyzing the different experimental conditions to optimize the SERS intensity. The successful SERS measurement of PER is promising toward clinical application.

**References**

- [1] P.N. Patsalos PN1, E. P. Spencer, D.J. Berry, *Ther. Drug Monit.* 40(5), 526-548 (2018).
- [2] M. Tommasini et al., *Nanomaterials*, 9, 677 (2019).

**LP-I-6****Nanohybrids for multiphotons excitation. PLA synthesis and properties***W. Marine<sup>1</sup>**<sup>1</sup>HiLASE Centre, Institute of Physics of the Czech Academy of Sciences, Dolní Břežany, Czech Republic*

We present the development of a new approach for fabrication and assembly of nanohybrid (NH) systems consisting of a semiconducting metal oxide core with increased and controlled multi-photon absorption and functional organic molecules attached to the core surface. The core nanoparticles produced by Infra-Red femtosecond laser ablation in an organic solvent reacts with the anchoring group (carboxylic (-COOH) and isothiocyanate (-C=N=S)) of the functional organic molecules in the same solvent during ablation or after it. Potential applications of the NH materials are based on the charge transfer between the inorganic and organic components (multi-photon bioimaging, information storage) and vice versa (photovoltaic devices).

The results of new experimental studies of physical mechanisms of the nanoparticle formation during femtosecond PLA in different liquids demonstrating how the laser parameters and composition of the liquid medium affect the condensation and growth processes.

The properties of NH systems were tailored and improved by two independent ways: by fine tuning of the nanoparticle band gaps via doping (ZnO vs ZnO:Mg<sup>2+</sup>), by PLA synthesis and by utilisation of new organic molecules with varying electron donating and accepting properties. Nanoparticles and NH materials were characterized by conventional and time resolved spectroscopic methods and by hyper Rayleigh light scattering together with Transmission Electronic Microscopy observations.

Finally, we report on the new nonlinear optical properties of the nanohybrid materials: modified two-photon absorption and enhanced by more than one order of magnitude charge transfer from the ZnO/Zn<sub>1-x</sub>Mg<sub>x</sub> core excited by one- or multi-photon absorption to the attached rhodamine derived dyes.

**LP-I-7****Selective ablation of nano-layer thin films by single-pulse femtosecond laser irradiation**

*B. Gaković<sup>1</sup>, S. Petrović<sup>1</sup>, S. Kudryashov<sup>2</sup>, P. Danilov<sup>2</sup>, E. Skoulas<sup>3</sup>, G. Tsibidis<sup>3</sup>, A. Ionin<sup>2</sup>, E. Stratakis<sup>3</sup>*

<sup>1</sup>*Vinča Institute of Nuclear Sciences- University of Belgrade, Atomic Physics Department, Belgrade, Serbia*

<sup>2</sup>*Lebedev Physical Institute, Basov Quantum Electronics Department, Moscow, Russian Federation*

<sup>3</sup>*Foundation for Research and Technology-Hellas FORTH, Institute of Electronic Structure and Laser, Heraklion, Greece*

Laser processing of materials is a unique method, which allows their morphological and composition alterations. In the case of ultra-short laser pulses, laser processing is extremely precise. Irradiation of materials by femtosecond laser enables removal or change of their surface at nano/micro level. Nano layer thin films (NLTF) are attractive composite materials due to their properties that cannot be obtained in the case of materials of the same bulk constituents. Selective ablation of the upper layer of the nano-layer thin film, with little or no damage to the layer or the substrate beneath, is significant for application and theory<sup>1-3</sup>.

In this talk, we are discussing results concerning the selective ablation of a layer/layers from the surface of several NLTF by femtosecond laser pulses. Experimental samples, composed of metallic bilayers (Ni/Ti, Cr/Ti, and Zr/Ti), were prepared by ion sputtering on a Si substrate. Single-pulse irradiations were done in the air with focused and linearly polarized Gaussian laser beams - 515 nm or 1026 nm wavelength and 200 fs or 170 fs pulse duration, respectively. One-step selective ablations of the upper layer, from NLTFs at low laser pulse energies, and complete ablation of the thin films from the Si substrate at higher pulse energies, were registered. The effects of laser-induced morphological and composition changes were monitored by scanning electron microscopy (SEM&EDS) and profilometry. Spallation is appointed to be one of the main mechanisms that caused selective ablation of the upper layers from the NLTF.

**References**

- [1] B. Gaković, G. D. Tsibidis, E. Skoulas, S.M. Petrović, B. Vasić, and E. Stratakis, *Journal of Applied Physics* 122 (2017) 223106.
- [2] S.A. Romashevskiy, P.A. Tsygankov, S.I. Ashitkov, M.B. Agranat, *Applied Physics A*, 124 (2018) 376.
- [3] S.I. Kudryashov, B. Gaković, P. A. Danilov, S.M. Petrović, D. Milovanović, A.A. Rudenko, A.A. Ionin, *Applied Physics Letters*, 112 (2018) 023103.

**LP-I-8****Generation of nanoparticles of unique morphologies by laser ablation in liquids***G. Shafeev<sup>1</sup>**<sup>1</sup>Prokhorov General Physics Institute of RAS, Wave Research Center, Moscow, Russian Federation*

The review of experimental results is presented on the morphology of nanoparticles generated by laser ablation in liquids. Single-step formation of elongated Au nanoparticles with high aspect ratio is described under laser ablation of a bulk Au target in aqueous solutions of divalent cations ( $\text{Ca}^{2+}$ ,  $\text{Be}^{2+}$ ,  $\text{Mg}^{2+}$ , etc.). Extinction spectra of elongated Au nanoparticles in water are characterized by longitudinal plasmon resonance whose position depends on their aspect ratio and may protrude to near-infrared region of spectrum. External permanent magnetic field up to 7 Tesla causes orientation and further elongation of Au chains, which is attributed to interaction of magnetic field with that of longitudinal electrons oscillations.

Results are presented on the formation of core-shell nanoparticles (Co@Al, Fe@Al, Ti@Al) under laser exposure of the mixture of individual respective nanoparticles in ethanol. The mechanism of their formation is discussed from the viewpoint of difference in melting temperature of components. Possible applications of Al and Ti@Al nanoparticles for hydrogen storage are discussed.

**LP-I-9****Photoinduced formation of inorganic nanoparticles in polymer matrix: mechanisms and laser structuring**

*N. Bityurin<sup>1</sup>, A.A. Smirnov<sup>1</sup>, A. Afanasiev<sup>1</sup>, A. Pikulin<sup>1</sup>*

*<sup>1</sup>Institute of Applied Physics RAS, Nonlinear dynamics and optics, Nizhny Novgorod, Russian Federation*

Destruction of specially introduced precursor molecules may result in the formation of inorganic nanoparticles in a polymer matrix. The destruction can be caused by heating and/or photochemical effect of UV/laser radiation.

Among such photoinduced nanocomposites the most popular are plasmonic ones with metallic nanoparticles. Recently, the composites with semiconductor nanoparticles have attracted attention of the investigators because of their luminescent properties.

We selected an organic-inorganic compound that can serve as a soluble precursor of CdS nanoparticles in a PMMA matrix [1]. UV LED operating at a wavelength of 365 nm appeared to be very useful to study the kinetics of UV mediated CdS nanoparticle growth in these materials. In situ monitoring of the optical absorption evolution accompanying the nanoparticle growth by means of UV laser or white LED allows acquiring experimental data [1,2] that are sufficient to construct a theoretical model [3] and discuss the interrelation between homogeneous and heterogeneous nucleation processes.

Laser irradiation is a promising tool for originating structures within photoinduced nanocomposites. Experimental examples of the laser-induced nanostructuring of these materials are demonstrated. We discuss generation of nanoparticles in photoinduced nanocomposites by the focused laser light from a point of view of possible localization and shell-structure printing phenomena.

We also consider the possibility of obtaining core-shell nanoparticles at laser irradiation of photoinduced nanocomposites with precursors of two different kinds and the combined effect of laser and UV LED irradiation of composites with single and two precursors.

The authors thank the Russian Foundation for Basic Researches (Grant No. 19-02-00694 a) for financial support.

**References**

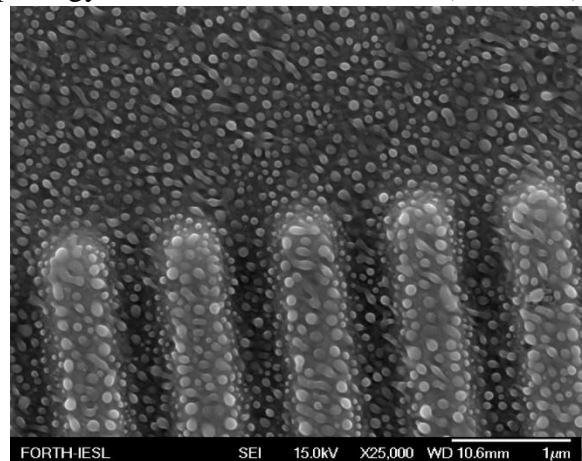
- [1] A.A. Smirnov, A. Afanasiev, S. Gusev, D. Tatarskiy, N. Ermolaev and N. Bityurin, Exposure dependence of the UV initiated optical absorption increase in polymer films with a soluble CdS precursor and its relation to the photoinduced nanoparticle growth, *Opt. Mater. Express*, 8(6), 1603-1612 (2018).
- [2] A. A. Smirnov, A. Kudryashov, N. Agareva, A. Afanasiev, S. Gusev, D. Tatarskiy, N. Bityurin, *In-situ* monitoring of the evolution of the optical properties for UV LED irradiated polymer-based photoinduced nanocomposites, *Applied Surface Science* 486 (2019) 376-382.
- [3] N. Bityurin, A.A. Smirnov, Model for UV induced growth of semiconductor nanoparticles in polymer films, *Applied Surface Science* 487 (2019) 678-691.

**LP-I-10****Laser micro- and nanostructuring of solids by sub-nanosecond laser pulses***E.V. Barmina*<sup>1</sup>*<sup>1</sup>Prokhorov General Physics Institute of the Russian Academy of Sciences,  
Wave Research Center, Moscow, Russian Federation*

Controlling the interactions of light with matter is crucial for the success and scalability of materials processing applications at micro and nano-scale. When lasers are used as light sources, the optimal interplay between the laser and material parameters may allow the fabrication of features with dimensions of the order or smaller than the laser wavelength diffraction limit. This report will focus on laser-assisted micro/nano structuring (NS) of surfaces and controlling materials properties via this process. A variety of different material responses have been achieved depending on the material system and the laser parameters, allowing processes to be designed and optimized to permanently alter the material's surface chemistry, crystal structure, and morphology to suite its desired function. The unique aspect of this for many applications is that the material modifications can occur over many different length scales, adding complexity to the surface and a new dimension to surface optimization. As a result, direct irradiation of materials by ultrafast laser pulses in controlled atmosphere often induces modifications leading to complex micro- and nano-scale surface structures, which are often found to have different and by far superior properties to those of the bulk materials. Indeed, we demonstrate that laser micro/nanostructured materials can be exploited for diverse emerging applications opening up new, exciting possibilities. Furthermore, laser initiation of phase transitions at the solid-liquid interface results in the formation of self-organized micro- and/or nanostructures and high-spatial-frequency laser-induced periodic surface structures (HSFL) on the solid surface.

Formation of NS is assigned to the instability of evaporation of the liquid that surrounds the irradiated target. In comparison HSFL occurs due to the development of thermocapillary instability of the melt layer on the target surface. The morphology of NS generated on various metallic as well as non-metallic bulk solids is studied as a function of laser parameters and target material.

The aim of this report is to show the evolution morphology of the surface from micro (1-10  $\mu\text{m}$ ) to nanoscale (till 10 nm) as different unique types of micro and nanostructures are formed under laser ablation of target. Laser nanotechnologies presented in this topic found a lot of applications such as enhancement of external applied field up to  $10^4$  times, change of antifriction properties, development of the structured surface as ultra-black absorbers with unique optical properties. Besides presenting recent advances on the elucidation of the possible mechanisms behind the formation of the structures obtained by these techniques, it will also delineate existing limitations and discuss emerging possibilities and future prospects.

**Fig. 1.**

**LP-I-11****Nanosecond laser treatment and fluoropolymer deposition for control of silicon surface wettability**

*S. Starinskiy<sup>1,2</sup>, A. Safonov<sup>1</sup>, E. Gatapova<sup>1</sup>, N. Miskiv<sup>1</sup>, E. Bochkareva<sup>1</sup>, V. Sulyeva<sup>3</sup>,  
A. Rodionov<sup>1,2</sup>, Y. Shukhov<sup>1</sup>, A. Bulgakov<sup>1,4</sup>*

<sup>1</sup>*Institute of Thermophysics, Sb RAS, Novosibirsk, Russian Federation*

<sup>2</sup>*Novosibirsk State University, Physical Department, Novosibirsk, Russian Federation*

<sup>3</sup>*Institute of Inorganic Chemistry, Sb RAS, Novosibirsk, Russian Federation*

<sup>4</sup>*HiLASE Centre, Institute of Physics of the Czech Academy of Sciences, Dolní Břežany, Czech Republic*

The extreme wettability surfaces (superhydrophilic and superhydrophobic) is very perspective for different application in textile industry, creating surfaces with anti corrosion and self-cleaning property, in separation filters, antifogging materials, heat exchangers, biosensors and biochips, etc. Recently, there has been a particular interest in material with a sharp boundary between superhydrophilicity and superhydrophobicity due to the particular behavior of the liquid along the contact line on such so-called biphilic materials. There are two main approaches to achieve extreme surface wettability. The first one suggests changing the surface texture (roughness) while the second one is based on varying the surface free energy by its functionalization. In this work, we combine this approaches by laser treatment of silicon and following HW CVD of fluoropolymer. We found a narrow range of conditions of nanosecond ablation by IR laser of silicon in which the two-level morphology of the surface is formed. It are pores at the nanoscale and self-organized periodic hills structure at the microscale. The surface enrichment with oxygen is observed in addition to changes in morphology, that leads to supehydrophilicity of silicon. The smooth transition from supehydrophilicity to superhydrophobicity achieved by gradually deposition of fluoropolymer. Thus, a silicon with an arbitrary apparent contact angle within the range from  $\sim 0^\circ$  to  $170^\circ$  can be obtained. The wettability properties were controlled by varying the thickness of fluoropolymer coating. It is demonstrated further functionalization of obtained materials by local removal of fluoropolymer by laser in the mode of preservation of superhydrophilic properties of silicon. The possibility of using the obtained biphilic samples in the problem of droplet evaporation is considered.

The work was supported by the Russian Science Foundation (project No. 18-79-10119).

**LP-I-12****Laser modification of silicon for creation of light emitting structures with dislocations related luminescence**

*D. Polyakov<sup>1</sup>, V. Veiko<sup>1</sup>, N. Sobolev<sup>2</sup>, A. Kalyadin<sup>2</sup>, V. Vdovin<sup>3</sup>*

*<sup>1</sup>ITMO University, Faculty of Laser Photonics and Optoelectronics, Saint-Peterburg, Russian Federation*

*<sup>2</sup>Ioffe Institute, Laboratory of Physics of Semiconductor Devices, Saint-Petersburg, Russian Federation*

*<sup>3</sup>Rzhanov Institute of Semiconductor Physics, Laboratory of Nano-diagnostic and Nanolithography, Novosibirsk, Russian Federation*

The problem of creation of effective silicon-based light emitter is one of the most important for optoelectronic technology. There are several approaches to solve this problem: implantation of erbium ions into silicon [1], using of silicon nanostructures [2], formation of strained germanium layers on silicon [3] etc. The promising way is to use so called dislocation-related luminescence (DRL), since the most intensive DRL line in silicon (D1) «survive» at room temperature and correspond to the transparency window of fiber optics ( $\sim 1.55 \mu\text{m}$ ) [4]. Several researches show that laser treatment of silicon lead to the creation of dislocations [5], however it's luminescence properties were not studied in details. Thus the aim of this work is to investigate the structural and luminescence properties of silicon after laser irradiation and optimization of laser processing modes for creation light-emitting structures with intense luminescence at wavelength  $\sim 1.55 \mu\text{m}$ . In our experiments we use different laser processing modes: multipulse irradiation by nanosecond pulses (with various pulse fluences, pulse durations, total irradiation doses etc) that allows to introduce dislocations into surface layers, irradiation in CW mode that allows to introduce the dislocation throughout the thickness of the plate, irradiation by femtosecond pulses. Plates of Cz-Si and Cz-Si/SiO<sub>2</sub> structures were used as samples.

The structural properties after irradiation were studied by transmittance electron microscopy and atomic force microscopy. Luminescent properties were studied at different temperatures from helium temperatures up room temperatures. The photoluminescence spectrum obtained on Si/SiO<sub>2</sub> structure after irradiation by series of nanosecond pulses is shown at fig.1. One can see the appearance of DRL. Properties of obtained spectrums were studied in details at different temperatures.

Our research shows that laser irradiation of silicon can be considered as a perspective technological tool for the controlled introduction of optically active extended defects into silicon for further creation of light emitting diodes.

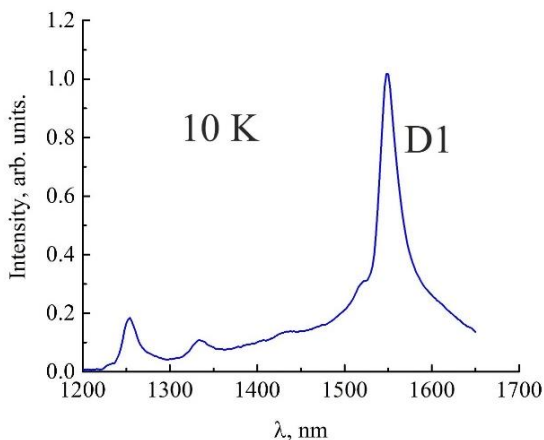


**Fig. 1.**

**References**

[1] A.J. Kenyon. Erbium in silicon// *Semicond. Sci. Technol.*, V.20. pp. R65-R84, 2005.

- [2] F. Priolo, T. Gregorkiewicz, M. Galli, T. F. Krauss. Silicon nanostructures for photonics and photovoltaics// *Nature Nanotechnology*, V. 9, pp. 19 – 32, 2014.
- [3] Camacho - Aguilera R.E., Cai Y., Patel N. et al. An electrically pumped germanium laser // *Opt. Express*, V.20, p.11316, 2012.
- [4] Sobolev N.A. Defect engineering in implantation technology of silicon light-emitting structures with dislocation-related luminescence // *Semiconductors. Springer*, V.. 44, pp. 1–23, 2010.
- [5] Skvortsov A.M., Veiko V.P., Huynh C., Polyakov D.S., Tamper A.M. Modification of the SiO<sub>2</sub>/Si interface by pulsed fibre laser radiation//*Quantum Electronics*, V. 47, pp. 503-508, 2017.

**LP-I-13****Optical response of metals to ultrashort laser pulses: A puzzle for optical models**

*N.M. Bulgakova<sup>1</sup>, S.A. Lizunov<sup>1,2</sup>, V.P. Zhukov<sup>1,3,4</sup>, A.V. Bulgakov<sup>1,2</sup>*

*<sup>1</sup>HiLASE Centre, Institute of Physics of the Czech Academy of Sciences, Dolní Břežany, Czech Republic*

*<sup>2</sup>S.S. Kutateladze Institute of Thermophysics, Siberian Branch of RAS, Novosibirsk, Russian Federation*

*<sup>3</sup>Institute of Computational Technologies, Siberian Branch of RAS, Novosibirsk, Russian Federation*

*<sup>4</sup>Novosibirsk State Technical University, Physical-Technical Faculty, Novosibirsk, Russian Federation*

The interaction of ultrashort laser pulses with solid surfaces involves a wealth of the physical processes, depending on the material kind and laser light properties. Even within the same material family, considerably different modifications of material properties can be achieved when applying similar laser pulses. Improvement in understanding of the physical mechanisms of laser-induced material modification/ablation and contributions of individual processes is of a vital need for further advance of ultrafast laser processing techniques for a broad range of applications, including micro- and optoelectronics, surface nanostructuring, and photovoltaics.

The optical response of metal surfaces to ultrashort laser excitation is one of important topics of laser-matter interaction. It is known that many metals, which are highly reflective at normal conditions, become considerably absorbing during ultrashort laser pulse action but understanding of the dynamic variation of their optical properties remains to be challenging. On the other hand, namely dynamic change of metal reflectivity determines the amount of the energy absorbed by metal and, hence, its post-irradiation evolution. Numerous optical models have been proposed to describe this effect and to link the actually absorbed laser energy with the incident laser energy. This includes variations of the Drude and Drude-Lorenz models, contribution of plasma-like response of free electrons in metal, as well as attempts of ab initio simulations of the optical response (see overview in [1]). However, all these models require adjusting parameters and give a reasonable agreement with experiments for limited ranges of irradiation conditions.

In this talk, the existing models of the optical response of metals will be overviewed with critical assessment of their applicability to the conditions of ultrashort laser irradiation, based on direct comparison with experimental data for several metals. The results of two-temperature modeling (TTM) of femtosecond laser irradiation of a number of metals by fs laser pulses, combined with simulations of dynamic change of optical properties, will be reported and compared with available data on measured reflectivity behavior. Strong interconnection between optical and thermodynamic properties of the irradiated metals will be demonstrated. A collective behavior of free electrons in metals subjected to ultrashort laser action will be discussed. A question about the effect of decoherence of free electrons on metal reflectivity at different laser intensities and pulse durations will be raised.

**References**

[1] M.V. Shugaev, M. He, S.A. Lizunov, Y. Levy, T. J.-Y. Derrien, V.P. Zhukov, N. M. Bulgakova, L. V. Zhigilei, Insights into Laser-Materials Interaction Through Modeling on Atomic and Macroscopic Scales, In: Advances in the Application of Lasers in Materials Science, Springer Series in Materials Science, Ed. P.M. Ossi, Vol. 274, Chapter 5 (Springer, 2018). – P. 107-148.

**LP-I-14****Three-step model of the laser-induced periodic surface structures (LIPSS) formation on metal surfaces**

*E. Gurevich<sup>1</sup>, S. Maragkaki<sup>2</sup>, Y. Levy<sup>3</sup>, T. Derrien<sup>3</sup>, N. M. Bulgakova<sup>3</sup>*

*<sup>1</sup>Ruhr-University Bochum, Applied Laser Technologies, Bochum, Germany*

*<sup>2</sup>IESL-FORTH, Ultrafast Laser Micro and Nano Processing, Heraklion, Greece*

*<sup>3</sup>HiLASE Centre, Institute of Physics of the Czech Academy of Sciences, Dolní Břežany, Czech Republic*

Although laser-induced periodic surface structures (LIPSS) are studied for more than 50 years, the physical background of the periodic pattern formation is still under discussion. Here we consider femtosecond single-pulse ablation of metals. Each laser pulse modifies the sample surface in three consequent steps: (1) the incident light energy heats the electrons; (2) the hot electrons heat the lattice; (3) liquid melt appears and resolidifies on the sample surface. In frames of the suggested model, the observed period of the LIPSS is influenced by all these three processes [1,2,3]. Here we report our experimental results of the on LIPSS upon laser ablation of copper in different liquids [4] and test the influence of the liquid environment on the hydrodynamic instabilities, which can develop in the melt. The theoretical results are compared with the experimental findings.

**References**

- [1] E. L. Gurevich, Mechanisms of femtosecond LIPSS formation induced by periodic surface temperature modulation. *Applied Surface Science* 374, 56-60 (2016).
- [2] E. L. Gurevich, Y Levy, SV Gurevich, N. M. Bulgakova, Role of the temperature dynamics in formation of nanopatterns upon single femtosecond laser pulses on gold. *Physical Review B* 95, 054305 (2017).
- [3] S. Maragkaki, T. J.Y. Derrien, Y. Levy, N. M. Bulgakova, A. Ostendorf, E. L. Gurevich, Wavelength dependence of picosecond laser-induced periodic surface structures on copper. *Applied Surface Science* 417, 88-92 (2017).
- [4] S. Maragkaki, A. Elkalash, E. L. Gurevich, Orientation of ripples induced by ultrafast laser pulses on copper in different liquids. *Applied Physics A* 123, 721 (2017).

**LP-I-15****Thermochemical laser-induced periodic structures formation on metals and semiconductors surfaces**

*A. Dostovalov<sup>1,2</sup>, K. Bronnikov<sup>1,2</sup>, K. Okotrub<sup>3</sup>, V. Terentyev<sup>1</sup>, T.J.Y. Derrien<sup>4</sup>, S. Lizunov<sup>4</sup>, T. Mocek<sup>4</sup>, V. Korolkov<sup>5</sup>, N. M. Bulgakova<sup>4</sup>, S. Babin<sup>1,2</sup>*

*<sup>1</sup>Institute of Automation and Electrometry SB RAS, Fiber optics lab, Novosibirsk, Russian Federation*

*<sup>2</sup>Novosibirsk State University, The Department of Physics, Novosibirsk, Russian Federation*

*<sup>3</sup>Institute of Automation and Electrometry SB RAS, Laboratory of Condensed Matter Spectroscopy, Novosibirsk, Russian Federation*

*<sup>4</sup>HiLASE Centre, Institute of Physics of the Czech Academy of Sciences, Dolní Břežany, Czech Republic*

*<sup>5</sup>Institute of Automation and Electrometry SB RAS, Laboratory of Diffraction Optics, Novosibirsk, Russian Federation*

The formation of thermochemical laser-induced periodic surface structures (TLIPSS) featured by high ordering in contrast to the ablative structures was recently demonstrated [1]. These structures are formed due to the oxidation of the metal surface illuminated with ultrashort laser pulses and are characterized by the elevation of the relief, forming parallel oxide protrusions. In contrast to the more studied ablative LIPSS, they are oriented parallel to the polarization of incident radiation and highly uniform over the period and height.

The results of TLIPSS formation on chromium films with a thickness of  $d_f = 28 \div 350$  nm, a Gaussian laser beam with a wavelength  $\lambda = 1026$  nm, a pulse duration of 232 fs, a repetition rate of 200 kHz was obtained. The growth of the structures period from 678 nm to 950 nm with increasing film thickness was found [2]. It was also observed that with increasing  $v_s$  up to several hundred  $\mu\text{m/s}$ , the formation of the main structure with a period of the order of  $\lambda$  is replaced by the formation of a structure with a period of  $\sim 200\text{-}250$  nm, oriented perpendicular to the polarization of the radiation. To explain formation of the LIPSS, a rigorous numerical approach for modeling surface electromagnetic waves in thin-film geometry has been developed [3]. The TLIPSS fabrication productivity increase by 2 orders of magnitude on chromium films with an astigmatic Gaussian beam in comparison with a radially symmetric Gaussian beam is demonstrated [4].

Also, the results of TLIPSS formation on silicon films with a thickness of  $d_f = 60 \div 370$  nm, at processing speeds  $v_s = 1 \div 100$   $\mu\text{m/s}$ , will be presented. On thin films ( $d_f = 60$  and 100 nm), an ordered structure with a period of  $\sim 700$  nm and orientation along the polarization of the incident radiation is observed at  $v_s \leq 5$   $\mu\text{m/s}$ . With increasing thickness, the period increases to  $\sim 1$   $\mu\text{m}$  ( $d_f = 180$  nm), and an ordered structure is formed at  $v_s \leq 25$   $\mu\text{m/s}$ . With a further increase in thickness, the period of structures formed on films with  $d_f = 300$  and 370 nm does not change significantly and at low scanning speeds of 1–5  $\mu\text{m/s}$  has a different morphology from previous cases (Fig. 1).

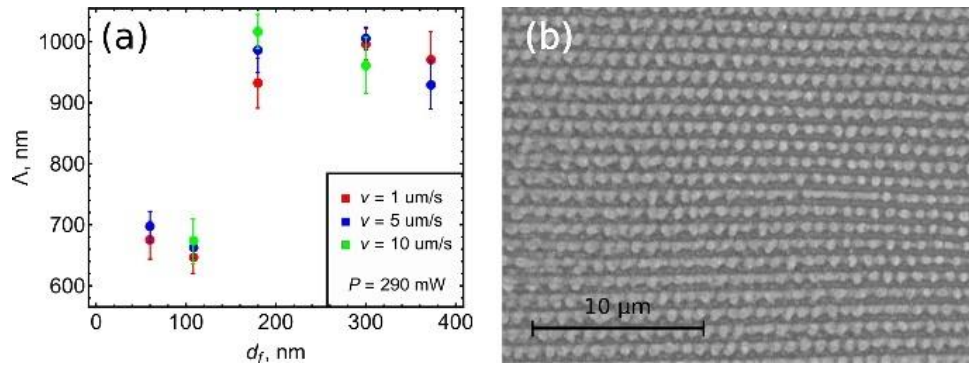


Fig. 1.

## References

- [1] B. Öktem, I. Pavlov, S. Ilday, H. Kalaycıoğlu, A. Rybak, S. Yavaş, M. Erdoğan, and F. Ö. Ilday, "Nonlinear laser lithography for indefinitely large-area nanostructuring with femtosecond pulses," *Nat. Photonics* 7, 897–901 (2013).
- [2] A. V. Dostovalov, V. P. Korolkov, K. A. Okotrüb, K. A. Bronnikov, and S. A. Babin, "Oxide composition and period variation of thermochemical LIPSS on chromium films with different thickness," *Opt. Express* 26, 7712–7723 (2018).
- [3] A.V. Dostovalov, T. J.-Y. Derrien, S.A. Lizunov, F. Peučil, K.A. Okotrüb, T. Mocek, V. P. Korolkov, S. A. Babin, N.M. Bulgakova, "LIPSS on thin metallic films: New insights from multiplicity of laser-excited electromagnetic modes and efficiency of metal oxidation," *Applied Surface Science*, (2019) (in press).
- [4] A. V. Dostovalov, K. A. Okotrüb, K. A. Bronnikov, V. S. Terentyev, V. P. Korolkov, and S. A. Babin, "Influence of femtosecond laser pulse repetition rate on thermochemical laser-induced periodic surface structures formation by focused astigmatic Gaussian beam," *Laser Phys. Lett.* 16, 026003 (2019).

**LP-I-16****Laser-induced crystallization of titanium dioxide nanotubular layers for photocatalytic applications**

*I. Mirza<sup>1</sup>, H. Sopa<sup>2</sup>, J.M. Macák<sup>2</sup>, A.V. Bulgakov<sup>1</sup>, N.M. Bulgakova<sup>1</sup>, O. Novák<sup>1</sup>, H. Turčičová<sup>1</sup>, A. Endo<sup>3</sup>, T. Mocek<sup>1</sup>*

<sup>1</sup>*HiLASE Centre, Institute of Physics of the Czech Academy of Sciences, Dolní Břežany, Czech Republic*

<sup>2</sup>*Centre of Materials and Nanotechnologies, Faculty of Chemical Technology, University of Pardubice, Pardubice, Czech Republic*

<sup>3</sup>*Faculty of Science and Engineering, Waseda University- Shinjuku-ku, Tokyo, Japan*

During the last two decades, the photocatalytic application of titanium dioxide (TiO<sub>2</sub> or titania) has received much attention for water purification and other environmental problem [1,2]. For such applications, the crystalline structure of material is a crucial parameter, since the amorphous phase may contain various kinds of defects in large quantity. These defects lead to recombination and trapping of photo-generated electron-hole pairs well before they can be involved in a chemical reaction [3]. Titanium dioxide has three main crystalline phases, anatase, rutile and brookite [4]. It has been shown that the anatase phase of nanocrystalline particles is much more functional in dye-sensitized solar cells [5]. Among titania nanomaterials, nanotube layers are one of the most promising structures, which represent several mm long nanotube (NTs) arrays with large surface areas.

Highly ordered Titania NT layers can be grown in fluoride ion containing electrolytes and as-formed anodic nanotubes have an amorphous structure [6]. Their dimensions (length and diameter) can be significantly varied by adjusting the growth conditions. Thermal annealing is one of the most frequently used methods for crystallization of amorphous TiO<sub>2</sub> nanomaterials. However, it is an energy-intensive method and needs several hours of treatment at a few hundred degrees Celsius. Under thermal annealing, amorphous titania transforms typically to a mixture of anatase and rutile. Increasing the annealing temperature leads to a higher rutile fraction in the mixed rutile-anatase phase [6,7]. Therefore, a fast energy-efficient method, which can crystallize NT layers into desired anatase phase in a non-destructive way, is highly beneficial in this field. In this work, we will present the results of laser-induced crystallization and photoelectrochemical properties of crystallized titania NT layers. For crystallization of NT samples, picosecond UV pulses with accumulative dose of few kJ cm<sup>-2</sup> were applied. X-ray diffraction and Raman spectroscopy analysis of NT layers show the anatase phase with a negligible fraction of rutile under optimal irradiation conditions. Influence of laser processing parameters (laser fluence, accumulative energy dose, repetition rate) will be discussed.

**References**

- [1] O'Regan, B. & Grätzel, M. A low-cost, high-efficiency solar cell based on dye-sensitized colloidal TiO<sub>2</sub> films. *Nature* 353, 737–740 (1991).
- [2] Fujishima, A., Rao, T. N. & Tryk, D. A. Titanium dioxide photocatalysis. *J. Photochem. Photobiol. C Photochem. Rev.* 1, 1–21 (2000).
- [3] Ohtani, B., Ogawa, Y. & Nishimoto, S. Photocatalytic activity of amorphous-anatase mixture of titanium (IV) oxide particles suspended in aqueous solutions. *J. Phys. Chem. B* 101, 3746–3752 (1997).
- [4] Diebold, U. The Surface science of titanium dioxide. *Surf. Sci. Rep* 48, 53–229 (2003).

- [5] O'Regan, B. & Grätzel, M. A low-cost, high-efficiency solar cell based on dye-sensitized colloidal TiO<sub>2</sub> films. *Nature* 353, 737–740 (1991).
- [6] Macak, J. M., Tsuchiya, H., Ghicov, A., Yasuda, K., Hahn, R., Bauer, S., Schmuki, P. TiO<sub>2</sub> nanotubes: Self-organized electrochemical formation, properties and applications. *Curr. Opin. Solid State Mater. Sci.* 11, 3-18 (2007).
- [7] Sugapriya, S., Sriram, R. & Lakshmi, S. Effect of annealing on TiO<sub>2</sub> nanoparticles. *Opt. - Int. J. Light Electron Opt.* 124, 4971–4975 (2013).

**LP-I-17****New super-resolution method of direct laser writing on Zr films**

*V. Korolkov<sup>1</sup>, S. Mikerin<sup>2</sup>, R. Kuts<sup>1</sup>, A. Malyshev<sup>1</sup>*

*<sup>1</sup>Institute of Automation and Electrometry SB RAS, Diffractive optics laboratory, Novosibirsk, Russian Federation*

*<sup>2</sup>Institute of Automation and Electrometry SB RAS, Laboratory of laser physics, Novosibirsk, Russian Federation*

The thermochemical effect of laser radiation on metal films has been studied for a long time. Laser-induced surface oxidation of thin chromium films with subsequent selective liquid etching is used for the manufacture of diffractive elements with a minimal feature of about 0.5-0.7  $\mu\text{m}$  [1]. However, the modern trend in optical design requires further increase the resolution to the level of 100-200 nm. To jump over the gap a regime of through oxidation can be used. The regime is easier to get when using pyrophoric metals (for example Ti, Hf, Zr) having small thermal diffusivity, quite high hardness, the high melting temperature of the metal and the oxide [2]. We have found out that Zr film sputtered on fused silica substrates is optimal to make nanostructured regions on surfaces of optical components by through oxidation.

Here we demonstrate periodic gratings wrote on Zr films with 80 nm thickness by using circular laser writing system CLWS-300IAE. The system scans focused beam (700 nm diameter) of green CW DPSS laser at different scanning speeds and laser powers (in range of 10-30 mW).

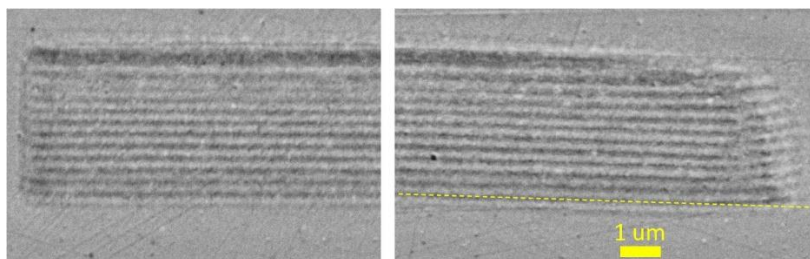


**Fig. 1.** SEM image of the grating with 300 nm period: (a) the edge of the grating where the beam was switched off; (b) the edge of the grating when the beam was switched on. The yellow line is parallel to the scanning direction. Scanning speed – 276 mm/s, beam power – 13 mW.

Fig. 1 shows an SEM image of the grating recorded with a period of 300 nm. From fig. 1b, it is obvious that the black track is formed along the contour of the thermal distribution since when the beam is turned on, it gradually shifts from the spot center to the periphery following the expansion of the heated area. In our opinion, the black tracks are cracks or deformations formed at the boundary between the metal film and the oxide track due to the high stress caused by the sharp thickening of the film after oxidation and different thermal expansion. Contour mechanism is confirmed at writing with laser pulses having a duration of 440 ns. However, in this case, the black contour is formed across the direction of beam scanning.

The revealed writing mechanism can be used to fabricate nanostructured optical components, since the phase of reflected light changes significantly.

**References**

- [1] V.P. Korolkov, A.G. Sedukhin, D.A. Belousov, R.V. Shimansky, V.N. Khomutov, S.L. Mikerin, E.V. Spesivtsev, R.I. Kutz, "Increasing the spatial resolution of direct laser writing of diffractive structures on thin films of titanium group metals," Proc. SPIE 11030, 110300A (23 April 2019).

**LP-I-18****Laser interactions with low density porous matter - experiment and modelling***J. Limpouch<sup>1</sup>**<sup>1</sup>Czech Technical University in Prague, Faculty of Nuclear Sciences and Physical Engineering, Praha 8, Czech Republic*

Porous solid media enable decreasing and tuning the average density of solid materials. Laser interactions with porous matter have a broad range of applications. Laser interaction with porous layers may be used both in direct-drive and in indirect-drive inertial confinement fusion (ICF). Enhancement of shock wave pressure by low density layers is used in studies of equation of state. Long homogeneous plasmas created from porous materials may be used as an efficient X-ray source and also for investigation of physics relevant to shock ignition of ICF; nearly critical plasmas are used for laser-driven ion acceleration and radiation sources.

We will briefly describe various available types of porous matter. Then, several interaction experiments will be reviewed and I shall present preliminary results of our recent experiment in the PALS laboratory where foam homogenization was studied.

Numerical modelling of laser interactions with porous materials is a very difficult task due to large differences in the scales involved – solid elements thickness typically of order tens of nanometres, pore dimension of order of a few microns and macroscopic interaction scale typically of order hundreds of microns. Moreover, typical porous materials have three-dimensional structure. Thus, including detailed structure of a porous material into numerical simulations of macroscopic experiments is beyond present capabilities. On the other hand, simple substitution of porous matter by a homogeneous material of the same average density leads to large discrepancies between experiment and simulations due to omission of the homogenization process. Our and other models for including the homogenization process into fluid simulations of laser-target interactions are described and simulation results are compared with experiments.

**LP-I-19****Modeling of thermodynamic properties and phase transitions of refractory metals under conditions of intense pulsed influences**

*K.V. Khishchenko*<sup>1</sup>

*<sup>1</sup>Joint Institute for High Temperatures RAS, Moscow, Russia*

Models of thermodynamic properties and phase transitions of materials are required for numerical simulations of time-dependent physical processes at laser technologies. In the present work, an equation of state for a refractory metal (rhenium) is proposed with taking into account melting and evaporation effects. As distinct from the previously known multiphase equation of state, new expressions for the thermodynamic potentials are formulated. Those provide for a more correct thermal contribution of ions in the liquid phase under extension. A critical analysis of calculated results is made in comparison with available data from experiments with intense pulsed influences upon the metal. The equation of state can be used efficiently in simulations of intense laser-material interactions.

The work is supported by the Russian Science Foundation (grant No. 19-19-00713).

**LP-O-1****Time-resolved shadowgraphy imaging of LIFT ejections, induced by pico- and nanosecond UV laser pulses**

*J. Miksys<sup>1</sup>, G. Arutinov<sup>2</sup>, G.W. Römer<sup>1</sup>*

<sup>1</sup>*University of Twente- Chair of Laser Processing,*

*Department of Mechanics of Solids- Surfaces & Systems, Enschede, Netherlands*

<sup>2</sup>*TNO, Holst Centre, Eindhoven, Netherlands*

In the field of printed electronics well know and established material deposition techniques, like screen printing, inkjet or dispensing are being pushed to its limits. Therefore, there is an increasing need for a new digital, more flexible and versatile technology, which allows high yield printing of depositions in the micrometer range and would be applicable to the wide range of materials. Laser-induced Forward Transfer (LIFT) already proved to be a potential technique meeting these demands [1]. LIFT is a digital, non-contact, nozzle-free technique, applicable for deposition of a wide range of materials, including pure metals, polymers, ceramics, semiconductors and biomaterials [2]. However, LIFT printing of complex materials, like silver nanoparticle inks remain challenging, due to the viscosity dependence of the shear rate of these materials. The complex nature of such materials narrows the range of the laser processing parameters of the well controlled LIFT ejections [3]. This has a key impact on the clean and reproducible depositions printing. Therefore, better understanding of the physical phenomena of the LIFT process is needed.

In this work, we present a comparative study on the effect of laser pulse duration on the ejections of donor material as well as on the influence to the deposition dimensions of viscous silver nanoparticle inks. In order to capture the dynamics of the LIFT jets, we employed time-resolved shadowgraphy (Figure 1) in both pico- and nanosecond LIFT setups. We found that in the lower laser fluence range, donor material is ejected at higher velocities when picosecond laser pulses are used, than when nanosecond pulses are used. However, as the fluence level is increased nanosecond laser pulses become as efficient, from an energy point of view, than when picosecond pulses are used. This trend is observed in time-resolved LIFT ejection dynamics, as well as in the analysis of depositions. These differences are attributed to a difference in heat dissipation in the donor material, as well as to the shear-thinning property of the silver nanoparticle ink.

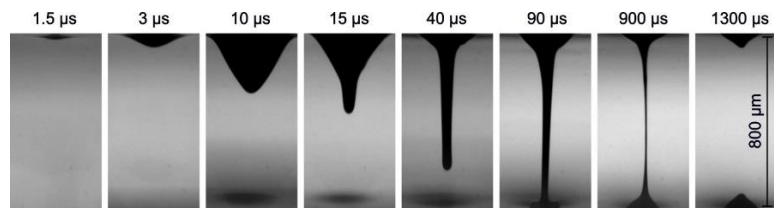


**Fig. 1.** Time-resolved shadowgraphy image sequence of LIFT of silver nanoparticle ink.

**References**

- [1] M. Morales, D. Munoz-Martin, A. Marquez, S. Lauzurica, C. Molpeceres, *Laser-Induced Forward Transfer Techniques and Applications*, Second Edi, Elsevier Ltd., 2017.
- [2] A. Piqué, P. Serra, *Laser Printing of Functional Materials: 3D Microfabrication, Electronics and Biomedicine*, 2018.
- [3] C. Boutopoulos, I. Kalpyris, E. Serpetzoglou, I. Zergioti, Laser-induced forward transfer of silver nanoparticle ink: Time-resolved imaging of the jetting dynamics and correlation with the printing quality, *Microfluid. Nanofluidics*. 16 (2014) 493–500.

**LP-O-2****Laser processing of antimicrobial peptides releasing thin films for the inhibition of microbial attachment and biofilms formation on medical implants**

*R. Cristescu<sup>1</sup>, I. Negut<sup>1</sup>, A. Visan<sup>1</sup>, D. Istrati<sup>2</sup>, D.E. Mihaiescu<sup>2</sup>, M. Popa<sup>3</sup>, M.C. Chifiriuc<sup>3</sup>, R.J. Narayan<sup>4</sup>, D.B. Chrisey<sup>5</sup>*

*<sup>1</sup>National Institute for Lasers- Plasma and Radiation Physics, Lasers Department, Bucharest-Magurele, Romania*

*<sup>2</sup>Politehnica University of Bucharest, Faculty of Applied Chemistry and Materials Science, Bucharest, Romania*

*<sup>3</sup>Faculty of Biology- Research Institute of the University of Bucharest - ICUB, Microbiology Immunology Department, Bucharest, Romania*

*<sup>4</sup>University of North Carolina, Department of Biomedical Engineering, Chapel Hill, USA*

*<sup>5</sup>Tulane University, Department of Physics and Engineering Physics, New Orleans, USA*

Antimicrobial peptides (AMPs) promise an efficient solution to the devastating global health threat of drug-resistant bacteria. In this work, we report on the fabrication of composite thin films based on AMPs nanoencapsulated in mesoporous magnetic nanoparticles using the Matrix Assisted Pulsed Laser Evaporation (MAPLE) technique; these materials may have a role in antibiotic releasing implant coatings. Investigation by SEM, TEM, and XRD revealed coating uniformity, nanoparticle shape, and crystallinity of the thin films; the chemical functional groups and bonding of the target (starting material) and thin films were compared using FT-IR, IR-spectroscopy and HR-MS. The antimicrobial activity was evaluated with “antibiotic immune” ESKAPE bacterial strains using culture-dependent, quantitative methods, which are based on the dynamic assessment of the planktonic growth as well as adherence and biofilm development in the presence of the tested surface. The biocompatibility of the obtained thin films was investigated using *in vitro* models. The results of our studies reveal that the mesoporous magnetic nanoparticle composite thin films fabricated by MAPLE are biocompatible and release the nanoencapsulated AMPs in active form. This approach has a promising potential for use in designing combination products and devices such as drug delivery devices and medical device surfaces with antimicrobial activity.

**LP-O-3****Fabrication of plasmonic titanium nitride nanoparticles by femtosecond laser ablation in water and organic solvents**

*A. Popov<sup>1</sup>, G. Tselikov<sup>2</sup>, A. Al-Kattan<sup>2</sup>, N. Dumas<sup>3</sup>, C. Berard<sup>3,4</sup>, J. Nicola<sup>5</sup>, A. Da Silva<sup>6</sup>, D. Braguer<sup>3,4</sup>, M.A. Estève<sup>3,4</sup>, A. Kabashin<sup>1,2</sup>*

*<sup>1</sup>MEPhI, Institute of Engineering Physics for Biomedicine PhysBio-Bio-nanophotonics Laboratory, Moscow, Russian Federation*

*<sup>2</sup>Aix-Marseille University, CNRS, LP3 laboratory, Marseille, France*

*<sup>3</sup>Aix-Marseille University, CNRS, INP- Inst. Neurophysiopathol., Marseille, France*

*<sup>4</sup>Assistance Publique – Hôpitaux de Marseille, Hôpital Timone, Marseille, France*

*<sup>5</sup>Aix-Marseille University, CNRS, Centrale Marseille, LMA, Marseille, France*

*<sup>6</sup>Aix-Marseille University, CNRS, Centrale Marseille, Institut Fresnel, Marseille, France*

Exhibiting a red-shifted absorption/scattering feature compared to conventional plasmonic metals, titanium nitride nanoparticles (TiN NPs) look as very promising candidates for biomedical applications, but these applications are still underexplored despite the presence of extensive data for conventional plasmonic counterparts. Here, we present the fabrication of ultrapure, size-tunable crystalline TiN NPs by methods of femtosecond laser ablation in liquids. We demonstrate the possibility to tune size of NPs between 5 and 40 nm by varying laser fluence and ablation strategies. We show that so prepared TiN NPs demonstrate strong and broad plasmonic peak around 640–700 nm with a significant tail over 800 nm even for small NPs sizes (<7 nm), which is a very important fact, since this band lies within the region of relative tissue transparency, therefore laser-synthesized TiN NPs promise the advancement of biomedical modalities employing plasmonic effects, including absorption/scattering contrast imaging, photothermal therapy and photoacoustic imaging.

**LP-O-4****Wurzite CdTe thin films deposited by PLD under different atmosphere gas and pressures**

*M.Á. Santana-Aranda<sup>1</sup>, S. Saracho-González<sup>2</sup>, A. Pérez-Centeno<sup>1</sup>, G. Gómez-Rosas<sup>1</sup>, A. Chávez-Chávez<sup>1</sup>, E. Camps<sup>3</sup>, J.G. Quiñones-Galván<sup>1</sup>*

*<sup>1</sup>Centro Universitario de Ciencia Exactas e Ingenierías- Universidad de Guadalajara, Departamento de Física, Guadalajara, Mexico*

*<sup>2</sup>ITESO- Universidad Jesuita de Guadalajara, Departamento de Matemáticas y Física, San Pedro Tlaquepaque, Mexico*

*<sup>3</sup>Instituto Nacional de Investigaciones Nucleares, Departamento de Física, Ciudad de México, Mexico*

A set of CdTe thin films was grown by Pulsed Laser Deposition under different working atmospheres. After a background pressure of  $5.0 \times 10^{-6}$  Torr was obtained, the working pressure was varied between  $1.0 \times 10^{-5}$  and  $1.0 \times 10^{-2}$  Torr, using either pure N<sub>2</sub>, pure Ar, and O<sub>2</sub> 20% balance Argon. As initial conditions at base pressure, the plasma parameters were fixed to 85 eV and  $2.0 \times 10^{13}$  cm<sup>-3</sup>, prior to the deposition of each sample; then, the chamber pressure was set, using the corresponding ambient gas. Laser ablation was performed using the fundamental 1064 nm line of a Nd:YAG laser, with a 5 ns pulse width at a repetition rate of 10 Hz, during 30 minutes. Thus obtained thin films exhibit hexagonal phase, showing a predominant orientation into the (110) direction, with texture variations. The bandgap energy showed some fluctuations around 1.45 eV, with the largest breach obtained under Argon atmosphere at  $1.0 \times 10^{-2}$  Torr.

**LP-O-5****Pulsed laser deposition under low background gas pressure**

*M. Kostejn<sup>1</sup>, R. Fajgar<sup>1</sup>, V. Drinek<sup>1</sup>, V. Jandova<sup>1</sup>, M. Klementova<sup>2</sup>, S. Bakardijeva<sup>3</sup>*

*<sup>1</sup>Institute of Chemical Process Fundamentals of the CAS- v. v. i., Department of laser chemistry, Prague, Czech Republic*

*<sup>2</sup>Institute of Physics CAS, Department of Material Analysis, Prague, Czech Republic*

*<sup>3</sup>Institute of Inorganic Chemistry CAS, Centre of Instrumental Techniques, Husinec-Řež, Czech Republic*

Properties of the layers prepared by pulsed laser deposition (PLD) was modified by background gas pressure. The background pressure is additional parameter of the deposition which is easily controllable. In dependence on the type of the gas, a chemical reaction or a nucleation of nanoparticles was initiated in evolving plume.

For initiating of a chemical reaction, a reactive gas SiH<sub>4</sub> or GeH<sub>4</sub> was used during a transition metal (Mn, Cr, etc.) ablation. The molecules of the reactive gas are decomposed by abundant energy of particles spreading from the target and material with mixed composition is formed. Variation of background pressure from 1 to 4 Pa of SiH<sub>4</sub>, resp. from 1 to 2 Pa of GeH<sub>4</sub>, resulted in deposition of compact layers with metal content from 20 to 50 at.%. Growth rate of this deposition was found between 5 and 15 nm/min in dependence on conditions. Annealing of these layers led to production of silicide and germanide nanostructures exhibiting ferromagnetic behaviour up to the room temperature.

The nucleation of nanoparticles was applied during gold deposition onto TiO<sub>2</sub> layers. For nucleation, up to 10 Pa of inert gas (argon) was used. Argon molecules efficiently helped to cool temperature of evolving plume and initiated the nucleation which resulted in deposition of gold nanoislands. Gold nanoparticles incorporated in TiO<sub>2</sub> layers provided plasmonic properties. Au/TiO<sub>2</sub> layers were used for water splitting as proved by photoelectrochemical measurements.

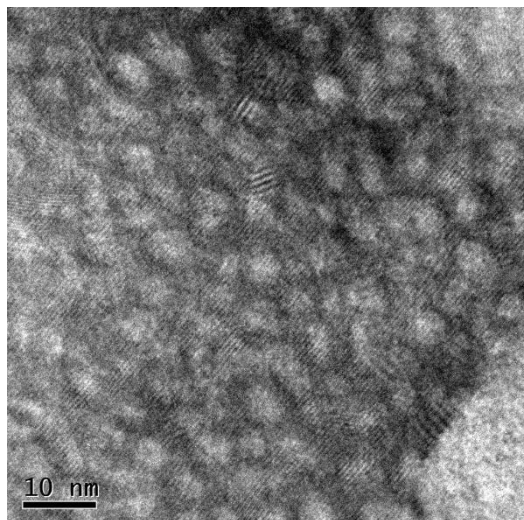


**Fig. 1.**

**LP-O-6****Direct writing in transparent materials using ultra short laser pulses: towards functionalization by controlling the induced phase shift***B. Ancelot<sup>1</sup>, L. Gemini<sup>1</sup>, M. Faucon<sup>1</sup>, R. Kling<sup>1</sup>**<sup>1</sup>ALPhANOV, Laser Processing, Talence, France*

In the past years, the process of direct writing in transparent materials by femtosecond laser pulses has been thoroughly studied [1,2] and greatly developed thanks to its wide range of application fields such as optical waveguides generation [2-4], to mention only a few. Indeed, the use of ultra-short laser pulses combined to a tight laser beam focusing allows the generation of a permanent and local index change in the area of the focal point within the bulk of transparent materials [5]. However, the possibility to exploit this local refractive index change into functionalized components still faces substantial challenges since the induced laser phase shift must be controlled precisely.

The purpose of this work is to quantitatively evaluate the influence of laser parameters on the induced phase shift and its homogeneity within the bulk of polymers and fused silica for different laser patterns: 0D (single laser shot), 1D (single laser line), 2D (multiple laser lines) and 3D (multiple laser lines at different z positions). An example of a single laser line phase shift measurement is illustrated on the figure 1.

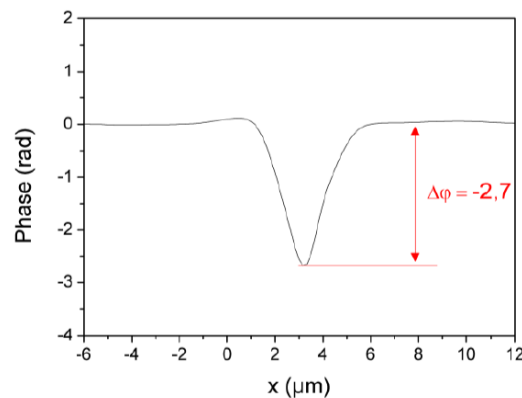


**Fig. 1.** Example of a single laser line phase shift measurement.

Influence of the pulse energy (from 0.1  $\mu\text{J}$  to 2  $\mu\text{J}$ ), pulse to pulse overlap, focusing conditions and laser trajectory on the induced refractive index change is firstly investigated and a prototype for high-resolution fluorescence imaging application is finally realized in silica glass.

The wavelength and pulse duration of the laser employed in the study are 1030 nm and 350 fs, respectively. The wavelength is converted to 515 nm for the trials within polymers bulk. Phase shift characterization is carried by a quantitative phase imaging camera.

**References**

- [1] V.P. Zhukov, N.M. Bulgakova and M.P. Fedoruk, *J. Opt. Technol.*, Vol 84, 439-446 (2017).
- [2] R. R. Gattass and E. Mazur, *Nature Photonics*, Vol 2, 219–225 (2008).
- [3] K. Itoh, W. Watanabe, S. Nolte and C.B. Schaffer, *MRS Bulletin*, Vol.31, 620-625 (2006).
- [4] W.M. Patzold, A. Demircan and U. Morgner, *Optics Express*, Vol 25, 263-270 (2017).
- [5] S.S. Mao, F. Quéré, S. Guizard, X. Mao, R.E. Russo, G. Petite and P. Martin, *Applied Physics A*, Vol. 79, 1695-1709 (2004).

**LP-O-7****High-performance perforation of thin titanium plates with fiber laser**

*A. Lyukhter<sup>1</sup>, T. Kononenko<sup>2</sup>, K. Skvortsov<sup>1</sup>, V. Konov<sup>2</sup>, V. Vermel<sup>3</sup>*

*<sup>1</sup>Vladimir State University named after Alexander Grigorievich and Nikolai Grigorievich Stoletovs, Scientific and educational center for the introduction of laser technology, Vladimir, Russian Federation*

*<sup>2</sup>Natural Sciences Center, General Physics Institute, Moscow, Russian Federation*

*<sup>3</sup>Central Aerohydrodynamic Institute, Research and production complex, Zhukovsky, Russian Federation*

Currently, laser perforation technology is used in various industrial fields, from the food processing to the aerospace industry [1]. In the world, there are already a lot of laser-based perforation systems introduced successfully into a batch production [2], however, it is still an important and relevant task to increase the process performance while maintaining the high quality of holes with a typical diameter of several tens of microns.

To secure a laminar stream of airflow, special chambers with a field of microscopic holes have to be built into the wings and the tail of mainline airliners.

The chambers are manufactured from 0.5 mm thick plate of Titanium Grade 5 and the perforation should meet several strong requirements:

- Whole diameter is  $50 \pm 10 \mu\text{m}$ .
- Ratio of inlet diameter to output diameter is below 1.3;
- Density of holes is larger than 9 holes per sqmm;
- Surface roughness of the panel is less than  $2 \mu\text{m}$ ;
- Productivity – more than 90000 holes per one working shift.

The main objectives of this work were to obtain experimental data in order to access the impact of different processing parameters on a through-hole formation in a titanium plate and to develop and provide well-grounded recommendations for selecting an optimal commercial laser system for highly productive perforation.

It reports on the results of titanium plate drilling with different laser pulse duration - from 400 fs to 100 ns. The dynamics of through hole formation under the irradiation of picosecond laser pulses with a different repetition frequency (30-300 kHz) is considered. The research revealed the ambiguous influence of the heat accumulation effect induced by high repetition rate of the laser pulses on quality and productivity of laser perforation [3].

While preparing a technical proposal for a high-performance laser system that provides the production of a perforated panel with overall dimensions of 1.5-2.5 m, the author's team, in addition to technological tasks, addresses a number of design ones. Such as: how to select commercially available laser and optical equipment, positioning and fixing system(-s), real-time hole quality monitoring system(-s) and how to set up and manage sub-processes, run at post-processing of holes.

For industrial enterprises specialized in perforated metal plates production it is important to have access to laser systems with higher productivity, higher efficiency rate (not less than 40%) and a longer service interval. Ytterbium fiber laser sources satisfy meet all these criteria. This type of laser sources is the best option for integration into the complex for high-performance sheet metal perforation.

## References

- [1] Review “Industrial Laser Solutions for manufacturing” January-February 2016. pp.6-8.
- [2] A. Stephen, High speed laser micro drilling for aerospace applications. New Production Technologies in Aerospace Industry - 5th Machining Innovations Conference (MIC 2014) Procedia CIRP 24 (2014) pp. 130 – 133.
- [3] T. V. Kononenko et al. Influence of pulse repetition rate on percussion drilling of Ti-based alloy by picosecond laser pulses. Optics and Lasers in Engineering 103 (2018) pp.65–70.

**LP-O-8****Nonlinear femtosecond optical lithography for the micro- and nano-structuring***N. Minaev<sup>1</sup>, M. Tarchov<sup>2</sup>**<sup>1</sup>Federal Scientific Research Centre "Crystallography and Photonics" of Russian Academy of Sciences, Institute of Photon Technologies, Moscow- Troitsk, Russian Federation**<sup>2</sup>Institute of Nanotechnologies of Microelectronics of the Russian Academy of Sciences, Department of development and research of micro- and nanosystems, Moscow, Russian Federation*

It presents results of research of the possibilities a new approach to optical laser photolithography, carried out at the unique femtosecond laser complex of the Institute of Photonic Technologies of the Federal Research Center "Crystallography and Photonics" of the Russian Academy. We used method of nonlinear femtosecond optical lithography (NFOL) [1] with help of them, due to the high localization of the process of nonlinear absorption of femtosecond laser radiation, we managed to form in standard commercially available polymer resistive materials a structure with a resolution not limited by the diffraction limit (up to 100 nm). The parameters of the process irradiating samples of various resistive materials in the mode of nonlinear femtosecond optical lithography, allowing to achieve high resolution during the formation of structures in thin resistive layers, are determined. A series of test matrix structures with different topologies was created and analyzed, using as example the maximum possible resolution in the proposed resistive materials using the developed method. The achieved repeatable resolution on several resistive materials ranges from 100 to 200 nm, on individual samples it was possible to obtain a resolution in individual elements less than 100 nm (up to 50 nm). Selected modes were used in the formation of prototypes of full-functional sensitive elements of superconducting nanowire single-photon detectors, as well as large planar structures of a centimeter scale. When combining the proposed method with additive two-photon femtosecond microstereolithography technology, it is possible to create prototypes of complex optoelectronic devices on laboratory scale, in fact, using a single femtosecond laser microstructuring setup.

This work was supported by the Ministry of Science and Higher Education within the State assignment FSRC «Crystallography and Photonics» RAS, Russian Science Foundation (Project No. 18-07-01052), Ministry of Education and Science of the Russian Federation (Project No. 0004-2019-0004).

**References**

- [1] Minaev N. V, Tarkhov M.A., Dudova D.S., Timashev P.S., Chichkov B.N., Bagratashvili V.N. Fabrication of superconducting nanowire single-photon detectors by nonlinear femtosecond optical lithography // Laser Phys. Lett. IOP Publishing, - 2018. - Vol. 15 - № 2. - P. 1–6. 10.1088/1612-202X/aa8bd1.

**LP-O-9****Structuring of Kapton surface with ultrashort laser pulses**

*J. Hrabovský<sup>1,2,3</sup>, C. Liberatore<sup>1</sup>, I. Mirza<sup>1</sup>, J. Sládek<sup>1</sup>, J. Beránek<sup>1</sup>, V. Hájková<sup>4</sup>, A.V. Bulgakov<sup>1</sup>, N.M. Bulgakova<sup>1</sup>*

*<sup>1</sup>HiLASE Centre, Institute of Physics of the Czech Academy of Sciences, Dolní Břežany, Czech Republic*

*<sup>2</sup>Faculty of Mathematics and Physics, Charles University in Prague, Prague, Czech Republic*

*<sup>3</sup>Faculty of Chemical Technology, University of Pardubice, Pardubice, Czech Republic*

*<sup>4</sup>Czech Technical University in Prague, Faculty of Nuclear Sciences and Physical Engineering, Prague, Czech Republic*

Nowadays there is huge demand for high precision processing of biocompatible polymers and, in particular, of polyimide for medical, electronics and industry applications. Pulsed laser ablation (PLA) is a well established method for surface processing and modification of polymers of different kinds. This process has extensively been investigated for UV region of electromagnetic spectra mainly with nanosecond laser pulses. However, polymer ablation in IR, Near- and Mid-IR spectral ranges is not widely been studied, especially in the regimes of ultrashort laser pulses when non-linear phenomena can play an important role in laser energy absorption. In this contribution, we report on a comparative study of surface structuring of polyimide (Kapton) by pico- and femtosecond laser pulses of 1030 nm wavelength. Accurate structuring of this biocompatible polymer is of importance for direct applications in prosthesis and other medical instruments. The ablation was performed with three lenses of different focal distances and the ablation thresholds have been determined. It was shown that femtosecond laser pulses are much more advantages for high-precision surface structuring compared to picosecond pulses.



# ALT'19

**INTERNATIONAL CONFERENCE**

**Advanced Laser Technologies**



**LASER SYSTEMS AND MATERIALS**

**Prague, Czech Republic**



---

15-20 September 2019

**LS-I-1****Femtosecond-laser-written 2- $\mu\text{m}$  waveguide lasers**

*X. Mateos*<sup>1</sup>, *E. Kifle*<sup>1</sup>, *P. Loiko*<sup>2</sup>, *C. Romero*<sup>3</sup>, *J. R. Vázquez de Aldana*<sup>3</sup>, *U. Griebner*<sup>4</sup>, *V. Petrov*<sup>4</sup>,  
*M. Aguiló*<sup>1</sup>, *F. Díaz*<sup>1</sup>

<sup>1</sup>*Universitat Rovira i Virgili, Inorganic and Physical Chemistry, Tarragona, Spain*

<sup>2</sup>*Université de Caen Normandie, Centre de recherche sur les Ions, les Matériaux et la Photonique, Caen, France*

<sup>3</sup>*University of Salamanca, Aplicaciones del Láser y Fotónica, Salamanca, Spain*

<sup>4</sup>*Max Born Institute for Nonlinear Optics and Short Pulse Spectroscopy, Berlin, Germany*

This work reviews our recent achievements on fabrication, optical characterization and continuous-wave and passively Q-switched 2- $\mu\text{m}$  laser operation of active waveguides (WGs) produced by femtosecond direct laser writing (fs-DLW) in thulium and holmium doped low-symmetry (monoclinic) crystals. Various depressed-index photonic micro-structures were fabricated, such as buried channel WGs with circular and hexagonal (lattice-like) cladding, surface WGs with a half-ring cladding, and straight WGs and Y-branch splitters.

As active materials for emission near 2  $\mu\text{m}$ , monoclinic double tungstate crystals,  $\text{KRE}(\text{WO}_4)_2$  singly doped and codoped with  $\text{Tm}^{3+}$  and  $\text{Ho}^{3+}$  ions were studied. The WGs were characterized by confocal laser microscopy,  $\mu$ -Raman and  $\mu$ -luminescence spectroscopy, confirming well preserved crystallinity of their cores [1].

As for Tm-doped WGs, the best CW laser output was achieved using a circular-cladding Tm:KLu(WO<sub>4</sub>)<sub>2</sub> WG which generated 1.07 W at 1.84  $\mu\text{m}$  with a slope efficiency of 69.5% (fundamental mode, linearly polarized emission). An in-band pumped Holmium WG laser was scaled to 0.21 W at 2.06  $\mu\text{m}$  with a slope efficiency of 67.2%.

Passive Q-switching of Tm WG lasers was achieved using “fast” (graphene, MoS<sub>2</sub>, single-walled carbon nanotubes - SWCNTs) and “slow” saturable absorbers (Cr<sup>2+</sup>:ZnS). Surface functionalization of Tm WGs by SWCNTs lead to generation of nanosecond pulses through evanescent-field-interaction [2].

**References**

- [1] E. Kifle, X. Mateos, J. R. Vázquez de Aldana, A. Ródenas, P. Loiko, S. Y. Choi, F. Rotermund, U. Griebner, V. Petrov, M. Aguiló, and F. Díaz, Femtosecond-laser written Tm:KLu(WO<sub>4</sub>)<sub>2</sub> waveguide lasers. *Opt. Lett.* Vol., 42, 1169 (2017).
- [2] E. Kifle, P. Loiko, J. R. V. de Aldana, A. Ródenas, S. Y. Choi, F. Rotermund, V. Zakharov, A. Veniaminov, M. Aguiló, F. Díaz, U. Griebner, V. Petrov, and X. Mateos, Passively Q-switched fs-laser-written thulium waveguide laser based on evanescent field interaction with carbon nanotubes. *Phot. Res.* 6, 971 (2018).

**LS-I-2****Sub-100 fs OPA in the 6-10  $\mu\text{m}$  range pumped by a 100 kHz Yb laser, and its application to vibrational spectroscopy***Z. Heiner<sup>1</sup>**<sup>1</sup>Humboldt Universität zu Berlin, School of Analytical Sciences Adlershof SALSA, Berlin, Germany*

Nonlinear spectroscopy is one of the numerous applications being revolutionized by commercial diode-pumped (sub-)picosecond Yb-lasers exhibiting exceptional average power scalability. On the one hand, frequency down-conversion of Yb-laser pulses to the mid-infrared spectral region between 2.5 and 12.5  $\mu\text{m}$  has an enormous potential in vibrational spectroscopic applications, especially vibrational sum-frequency generation (VSFG) and 2D-IR spectroscopy, where the high repetition rate can significantly improve the sensitivity and signal-to-noise ratio (SNR) even at drastically reduced acquisition times. On the other hand, standard Ti:Sapphire-pumped vibrational spectrometers operating beyond 5  $\mu\text{m}$  rely on multiple frequency conversion stages, including a difference frequency generation stage, severely limiting the conversion efficiency. Employing an OPA with an output above 5  $\mu\text{m}$  pumped directly at  $\sim 1$   $\mu\text{m}$  is a promising solution. This requires a nonlinear crystal that is both highly transparent at these long mid-IR wavelengths and also has sufficiently large bandgap and damage threshold.

Recently, we constructed the first high-resolution, broadband VSFG spectrometer operating at laser repetition rates up to 100 kHz between 2.8 and 3.6  $\mu\text{m}$  but the long wavelength edge of the spectrum was limited by the absorption edge of the amplifying material to  $\sim 4.5$   $\mu\text{m}$  [1,2]. Here, we present the first 100-kHz VSFG spectrometer operating at an extended mid-IR spectral region. The MIR source is based on a single-stage OPA pumped directly at 1  $\mu\text{m}$  delivering carrier-envelope-phase-stable, sub-100 fs, 0.5  $\mu\text{J}$ , and spectrally tunable pulses in the region of 6-10  $\mu\text{m}$  [3]. To demonstrate the capability and sensitivity of our 100-kHz VSFG spectrometer, vibrational spectra of biomolecules at air-solid and air-liquid interfaces will be demonstrated in the fingerprint region, yielding very high SNR's within short acquisition times ( $\ll 1$  min). The obtained results can bring new insight into laser-matter interaction of biomolecules at high repetition rates up to 100 kHz.

**References**

- [1] Z. Heiner, V. Petrov, M. Mero, APL Photonics 2, 066102 (2017).
- [2] F. Yesudas, M. Mero, J. Kneipp, Z. Heiner, J. Chem. Phys. 148, 104702 (2018).
- [3] Z. Heiner, L. Wang, V. Petrov, M. Mero, Opt. Exp. 27, 15289-15297 (2019).

**LS-I-3****OPOs for standoff gas sensing**

*A. Godard<sup>1</sup>, G. Walter<sup>1</sup>, T. Hamoudi<sup>1,2</sup>, Q. Berthomé<sup>1,3</sup>, J.B. Dherbecourt<sup>1</sup>, J.M. Melkonian<sup>1</sup>, R. Santagata<sup>1</sup>, M. Raybaut<sup>1</sup>*

<sup>1</sup>*DPHY, ONERA, Université Paris-Saclay, Physics Instrumentation Environment Space Department, Palaiseau, France*

<sup>2</sup>*Laboratoire Charles Fabry, Institut d'Optique Graduate School, CNRS, Université Paris-Saclay, Lasers group, Palaiseau, France*

<sup>3</sup>*Teem Photonics, Research & Development Department, Meylan, France*

Multispecies gas detection, quantification, and localization in the atmosphere has become a growing concern for various applications from environmental and air quality monitoring, to warfare agents detection for defense, through industrial security. For these purposes, laser absorption spectroscopy in the mid-infrared from 1.5  $\mu\text{m}$  to 15  $\mu\text{m}$  is an extremely valuable tool due to the presence of atmospheric transmission windows as well as intense and well separated absorption lines of the species of interest. Depending on the application, the required laser spectral range can be either 1.6–2.2  $\mu\text{m}$  for spaceborne monitoring of greenhouse gases, 3–5  $\mu\text{m}$  for hydrocarbons and volatile organic compounds sensing, or 6–14  $\mu\text{m}$  for hazardous chemicals detection. There is consequently a significant need for broadly tunable laser sources in the mid-infrared exhibiting high spectral purity, narrow linewidth, as well as compactness and robustness for field campaign deployment.

We will present our work on the development of novel optical parametric sources and their integration in gas sensing instruments that have been carried for that purpose. In particular, we have introduced the nested cavity optical parametric oscillator (NesCOPO) scheme that enables to deliver a single frequency tunable emission with a much simpler and more compact device than usual narrow-linewidth OPOs. Its high potential was demonstrated for multiple-gas sensing, either for point measurements or standoff gas detection using lidar instruments [1]. For long range applications, the compact NesCOPO is implemented in a master oscillator power-amplifier (MOPA) architecture [2].

The presentation will especially focus on our latest development on high energy infrared emitters (mJ level) for long range (km) differential absorption LIDAR (DIAL) applications. These developments either address the 1.6  $\mu\text{m}$  – 2.0  $\mu\text{m}$  range for the detection of greenhouse gases ( $\text{CO}_2$ ,  $\text{CH}_4$ , and  $\text{H}_2\text{O}$ ) [3,4], and the 8.0  $\mu\text{m}$  – 12  $\mu\text{m}$  region for the detection of toxic agents [5]. Most of these systems were implemented as transportable optical benches that were deployed for outdoor field test in representative facilities. Emitters' performances, LIDAR instrument capabilities, as well as experimental demonstration results will be discussed during the presentation.

**References**

- [1] Godard, M. Raybaut, M. Lefebvre, Encyclopedia of Analytical Chemistry (2017)
- [2] E. Cadiou et al, Opt. Lett. 42, 4044–47 (2017).
- [3] E. Cadiou et al, Imaging and Applied Optics 2018, OSA Technical Digest (Optical Society of America, 2018), paper LTu5C.5.
- [4] J. Dherbecourt et al, Conference on Lasers and Electro-Optics, OSA Technical Digest (Optical Society of America, 2019), paper ATu3K.1.
- [5] J. Armougom et al, Imaging and Applied Optics 2018, OSA Technical Digest (Optical Society of America, 2018), paper LTu5C.6.

**LS-I-4****Millijoule level, sub 8 cycle, 7  $\mu\text{m}$  OPCPA on a tabletop: design, applications and routes for future development.**

*L. Maidment<sup>1</sup>, U. Elu<sup>1</sup>, D. Sánchez<sup>1</sup>, T. Steinle<sup>1</sup>, K. Zawilski<sup>2</sup>, P. Schunemann<sup>2</sup>, G. Matras<sup>3</sup>, C. Simon-Boisson<sup>3</sup>, J. Biegert<sup>1,4</sup>*

<sup>1</sup>*ICFO - Institut de Ciències Fotoniques, The Barcelona Institute of Science and Technology, 08860 Castelldefels- Barcelona, Spain*

<sup>2</sup>*BAE Systems, MER15-1813- P.O. Box 868, Nashua- New Hampshire 03061, USA*

<sup>3</sup>*THALES Optronique S.A.S, Laser Solutions Unit- 2 avenue Gay-Lussac, 78995 Elancourt Cedex, France*

<sup>4</sup>*ICREA, Pg. Lluis Companys 23, 08010 Barcelona, Spain*

Carrier-to-envelope phase (CEP) stable ultrashort and intense mid-infrared pulses promise applications such as multi-kilo-electron-volt coherent X-ray generation [1] and the study of strong field physics [2]. However, above 5- $\mu\text{m}$  wavelength it has typically been challenging to generate intense few cycle pulses as no practical laser materials with sufficient gain bandwidth exist and most commonly used nonlinear materials are opaque [3].

We present the development of a 7  $\mu\text{m}$  optical parametric chirped pulse amplifier (OPCPA) based on zinc germanium phosphide. Pulses at 100 Hz with 0.70-mJ energy and 188-fs duration after compression (8 optical cycles) are produced. An intermediate chirp inversion stage is used to permit pulse compression with 93.5% efficiency in bulk  $\text{BaF}_2$ . Additionally, the 7  $\mu\text{m}$  seed to the OPCPA is generated through difference frequency generation between two beams from the same source, making the mid-infrared beam passively CEP stable.

As an application demonstration, the output is used to generate high harmonics in ZnSe spanning the near infrared into the visible spectral region, reaching harmonic order 13. We also present plans for energy scaling of the system. The high intensity, passively CEP stable mid-infrared pulses make this table-top source a key enabling tool for strong field physics and keV-level coherent x-ray sources.

**References**

- [1] T. Popmintchev et al., “Bright coherent ultrahigh harmonics in the keV x-ray regime from mid-infrared femtosecond lasers,” *Science* 336(6086), 1287–1291 (2012).
- [2] B. Wolter et al., “Strong-field physics with Mid-IR fields,” *Phys. Rev. X* 5(2), 1–16 (2015).
- [3] V. Petrov, “Frequency down-conversion of solid-state laser sources to the mid-infrared spectral range using non-oxide nonlinear crystals,” *Prog. Quantum Electron.* 42, 1–106 (2015).

**LS-I-5****Nonlinear conversion of broadband mid-IR laser radiation into the wavelength range of ~2 - 20 micron**

*A. Ionin<sup>1</sup>, I. Kinyaevskiy<sup>1</sup>, Y. Klimachev<sup>1</sup>, A. Kotkov<sup>1</sup>, A. Kozlov<sup>1</sup>, A. Sagitova<sup>1</sup>, D. Sinitsyn<sup>1</sup>, L. Seleznev<sup>1</sup>*

*<sup>1</sup>P.N. Lebedev Physical Institute of the Russian Academy of Sciences, Division of Quantum Radiophysics, Moscow, Russian Federation*

The mid-IR laser sources operating within the molecular fingerprint region (the wavelengths of ~2-20  $\mu\text{m}$ ) are being actively developed for various important applications. To cover the mid-IR range with discrete bright spectral lines, a frequency conversion of high-peak power mid-IR molecular gas lasers in different nonlinear crystals was studied.

A hybrid laser system based on repetitively pulsed multiline carbon monoxide (CO) and carbon dioxide (CO<sub>2</sub>) lasers including slab RF discharge lasers with synchronous Q-switching was developed. Its spectrum is presented in Fig.1. Multiline Q-switched CO laser emitted simultaneously up to 150 spectral lines within 5.0-7.5  $\mu\text{m}$  in a single microsecond pulse. Multiline Q-switched CO<sub>2</sub> laser emitted simultaneously up to 9 spectral lines within 9.25-9.59  $\mu\text{m}$  in a single microsecond pulse as well. To extend the laser system spectrum down to 2.5-3.7  $\mu\text{m}$  range, broadband sum frequency (SF) generation of CO laser radiation in ZnGeP<sub>2</sub> crystal was implemented (CO\_SF). In turn, CO\_SF emission lines were mixed with the residual CO laser lines in the same crystal, which resulted in generation of difference frequencies within 4.3-5.0  $\mu\text{m}$  and 7.5-8.3  $\mu\text{m}$  spectral ranges (CO\_DF).

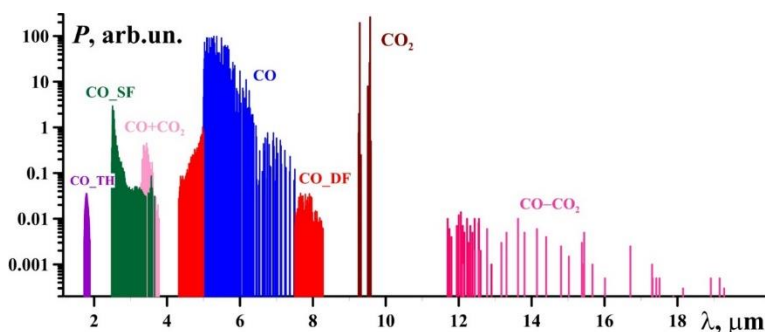


**Fig. 1.**

To extend the laser system spectrum toward the near-IR range of 1.7-1.9  $\mu\text{m}$ , third harmonic generation of CO laser (CO\_TH) in BaGa<sub>2</sub>GeSe<sub>6</sub> crystal was performed (sum frequency generation of CO\_SF lines and the residual CO laser lines). Sum frequency generation of multiline CO and CO<sub>2</sub> lasers radiation in GaSe crystal (CO+CO<sub>2</sub>) covered 3.3-3.8  $\mu\text{m}$  range. The highest efficiency of difference frequency generation between CO and CO<sub>2</sub> lasers lines (CO-CO<sub>2</sub>) was obtained in PbIn<sub>6</sub>Te<sub>10</sub> crystal, which allowed us to cover 11.5-19.3  $\mu\text{m}$  range by dozens of narrow spectral lines.

The research was supported by the Russian Science Foundation (Project No 16-19-10619).

**LS-I-6****Progress in high-power, 100 kHz mid-infrared OPCPA's***M. Mero*<sup>1</sup><sup>1</sup>*Max Born Institute for Nonlinear Optics and Short Pulse Spectroscopy,  
A3 Ultrafast Lasers and Nonlinear Optics, Berlin, Germany*

Technologically mature, diode-pumped picosecond and sub-picosecond Yb lasers have become the main workhorses behind high-average-power, ultrafast optical parametric amplifiers (OPA's) operating in the near-infrared (0.8-3  $\mu\text{m}$ ) and at the short-wave edge of the mid-infrared (MIR, 3-30  $\mu\text{m}$ ). In the 1.5-4  $\mu\text{m}$  spectral range, where various wide-bandgap oxide nonlinear optical crystals are commercially available, the exceptional power scalability of Yb lasers has already enabled average powers well beyond 10 W at multi-GW peak powers with pulses lasting only a few optical cycles [1]. Extension of the wavelength range above 5  $\mu\text{m}$  is traditionally achieved by employing an OPA-DFG (difference frequency generation) cascade at an overall pump-to-MIR energy conversion efficiency of only  $< 0.5\%$  at 8  $\mu\text{m}$ . Using novel wide-bandgap non-oxide nonlinear crystals that can be pumped directly at  $\sim 1$   $\mu\text{m}$  without detrimental one- and two-photon absorption of pump radiation, the DFG step can be eliminated leading to a significant increase in the overall conversion efficiency and the attainable average and peak power beyond 5  $\mu\text{m}$ . Despite their utmost importance, properties of nonlinear optical crystals affecting OPA performance at repetition rates above a few kHz are rarely investigated or considered in the OPA design. Depending on the choice of crystal, such material properties can lead to a complicated interplay of thermal lensing, non-permanent photorefractive damage, and self- and cross-phase modulation of the interacting pulses. Here we review some of the important material properties of nonlinear optical crystals that can be employed in ultrafast, high-repetition-rate, Yb-laser-pumped MIR OPA's operating either below or above 4  $\mu\text{m}$  and present examples of OPA's for each case [1,2].

**References**

- [1] M. Mero, Z. Heiner, V. Petrov, H. Rottke, F. Branchi, G. M. Thomas, and M. J. J. Vrakking, "43 W, 1.55  $\mu\text{m}$  and 12.5 W, 3.1  $\mu\text{m}$  dual-beam, sub-10 cycle, 100 kHz optical parametric chirped pulse amplifier," *Opt. Lett.* 43, 5246 (2018).
- [2] Z. Heiner, L. Wang, V. Petrov, and M. Mero, "Broadband vibrational sum-frequency generation spectrometer at 100 kHz in the 950-1750  $\text{cm}^{-1}$  spectral range utilizing a LiGaS<sub>2</sub> optical parametric amplifier," *Opt. Express.* 27, 15289 (2019).

**LS-I-7****Spectroscopic and laser properties of Fe<sup>2+</sup> ions in several AIBVI crystals of solid solutions like Zn<sub>1-x</sub>Mn<sub>x</sub>Se, Zn<sub>1-x</sub>Mg<sub>x</sub>Se, Zn<sub>1-x</sub>Mn<sub>x</sub>Te and Cd<sub>1-x</sub>Mn<sub>x</sub>Te***M. Doroshenko*<sup>1</sup>*<sup>1</sup>A.M. Prokhorov General Physics Institute Russian Academy of Sciences, Laser Materials and Photonics, Moscow, Russian Federation*

Fe<sup>2+</sup> doped materials are attracting growing interest as a source of tunable radiation in mid IR (4-6 μm) spectral region. Highly efficient pulsed and CW operation of Fe<sup>2+</sup> ions in ZnSe crystals have been already demonstrated [1,2]. The 5.1 μm limit of Fe<sup>2+</sup> ions tuning range in ZnSe crystal can be overcome by using different Se-based solid solutions like Zn<sub>1-x</sub>Mn<sub>x</sub>Se, Zn<sub>1-x</sub>Mg<sub>x</sub>Se or Te-based solid solutions like Zn<sub>1-x</sub>Mn<sub>x</sub>Te, Cd<sub>1-x</sub>Mn<sub>x</sub>Te. Results on influence on matrix composition as well as excitation wavelengths on spectroscopic and laser properties of Fe<sup>2+</sup> ions for a wide range of Mn concentrations *x* and temperatures will be presented and discussed. Applying of solid-solutions technique will be shown to allow Fe<sup>2+</sup> ions central oscillation wavelength shift from 4.5 μm in ZnSe crystal up to 5800 nm in Se-based and up to 5950 nm in Te-based solid solutions at room temperature. Advantages of solid solutions for Cr<sup>2+</sup> co-doping allowing to obtain efficient Cr<sup>2+</sup>-Fe<sup>2+</sup> energy transfer for further Fe<sup>2+</sup> ions lasing will be discussed.

**References**

- [1] A.A. Voronov, V.I. Kozlovsky, Yu.V. Korostelin, A.I. Landman, Yu.P. Podmar'kov, Ya.K. Scasyrsky, M.P. Frolov, A continuous wave Fe<sup>2+</sup>:ZnSe laser, *Quantum Electronics*, 38(12), 1113-1116 (2008).
- [2] K.N. Firsov, M.P. Frolov, E.M. Gavrishchuk, S.Yu. Kazantsev, I.G. Kononov, Yu.V. Korostelin, A.A. Maneshkin, S.D. Velikanov, I.M. Yutkin, N.A. Zaretsky, E.A. Zotov, Laser on single-crystal ZnSe:Fe<sup>2+</sup> with high pulse radiation energy at room temperature, *Laser Phys. Lett.*, 13, 015002 (2016).

**LS-I-8****Large-aperture quasi-phase-matching stacks of multiple GaAs plates fabricated with the room-temperature bonding for high-power wavelength conversion in mid-IR region***I. Shoji<sup>1</sup>**<sup>1</sup>Chuo University, Department of Electrical, Electronic, and Communication Engineering, Tokyo, Japan*

GaAs is an attractive material for mid-infrared wavelength conversion owing to its high optical nonlinearity and transparency up to 17  $\mu\text{m}$ . Since GaAs is optically isotropic, quasi-phase matching (QPM) is essential for highly efficient wavelength conversion. Although epitaxially grown GaAs QPM devices have been reported [1], it is difficult to fabricate thick devices for high-power wavelength conversion. On the other hand, diffusion bonded stacks of GaAs plates were reported as large-apertures QPM devices [2]. However, the high-temperature process degraded the crystal quality and the transmittance. In this work, we report on fabrication of large-aperture QPM stacks of multiple GaAs plates using the room-temperature bonding (RTB) and their wavelength-conversion properties.

The GaAs plates used for bonding were (111) plates with the size of 5.5 mm  $\times$  5.0 mm  $\times$  106  $\mu\text{m}$ , the thickness of which corresponds to the first-order QPM second-harmonic generation (SHG) period for the fundamental wavelength of 10.6  $\mu\text{m}$ . Two plates are set face to face in the vacuum chamber, and their surfaces are irradiated by Ar atom beams to be activated. Then the two plates are atomically bonded when they are touched and pressed, and another plate is supplied by the translation stage after the bonded plates are pulled up. We have succeeded in fabricating a 53 plate-stacked structure, the photograph of which is shown in Fig. 1. The whole thickness is about 5.6 mm.

We performed the SHG measurement using a CO<sub>2</sub> laser as a fundamental light source. Figure 1 shows the dependence of the SH power on the fundamental power for the 53-stacked and the previously fabricated 9-stacked devices. The SH power from the 53-plate stack (open circles) was 29 times higher than that from the previously fabricated 9-plate stack (open squares) [3]. We expect to obtain higher conversion efficiency and higher output power by increasing the number of plates.

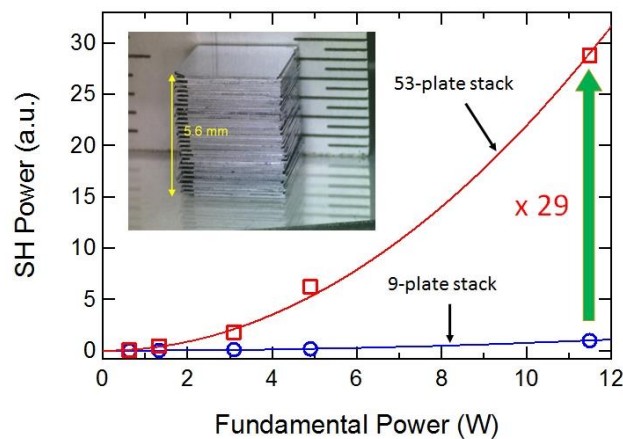


**Fig. 1.** SH power vs. fundamental power. Inset: 53-plate QPM GaAs stack.

## References

- [1] S. Koh, T. Kondo, M. Ebihara, T. Ishiwada, H. Sawada, H. Ichinose, I. Shoji, and R. Ito, "GaAs/Ge/GaAs sublattice reversal epitaxy on GaAs (100) and (111) substrates for nonlinear optical devices," *Jpn. J. Appl. Phys.* 38, L508 (1999).
- [2] L. A. Gordon, G. L. Woods, R. C. Eckardt, R. K. Route, R. S. Feigelson, M. M. Fejer, and R. L. Byer, "Diffusion bonded stacked GaAs for quasiphase-matched second-harmonic generation of a carbon dioxide laser," *Electron. Lett.* 29, 1942 (1993).
- [3] T. Kubota, H. Atarashi, and I. Shoji, "Fabrication of quasi-phase-matching stacks of GaAs plates using a new technique: room-temperature bonding," *Opt. Mater. Express* 7, 932 (2017).

**LS-I-9****Advances in 2 micron lasers for non-linear conversion into the Mid-IR**

*M. Eichhorn<sup>1</sup>, P. Forster<sup>2</sup>, C. Romano<sup>2</sup>, C. Kieleck<sup>2</sup>, S. Güntert<sup>2</sup>, B. Luwe<sup>2</sup>, M. Gross<sup>2</sup>*

*<sup>1</sup>Fraunhofer IOSB, Divisional Director, Ettlingen, Germany*

*<sup>2</sup>Fraunhofer IOSB, LASer Technology LAS, Ettlingen, Germany*

Laser sources around 2  $\mu\text{m}$  and non-linear converters covering the mid-infrared (Mid-IR) spectral range are important for a large variety of applications like in environmental sensing, detection and ranging, optical free-space communication, optical countermeasures, medical treatments and surgery, and fundamental physics research. Especially recent developments in two-micron pulsed thulium and thulium-holmium doped fiber lasers allow for significant average-power and energy scaling of mid-IR OPOs based on  $\text{ZnGeP}_2$  or OP-GaAs conversion crystals thereby broadening the scope of various applications. The presentation gives an overview of fundamental concepts, recent achievements as well as novel results in the field.

**LS-I-10****Stimulated Brillouin scattering phase conjugate mirror (SBS-PCM) using the fused silica for the high average power laser**

*H.J. Kong<sup>1</sup>, S. Cha<sup>1</sup>*

*<sup>1</sup>KAIST, Department of Physics, Daejeon, Republic of Korea*

Coherent beam combining using stimulated Brillouin scattering phase conjugate mirrors (SBS-PCM) is expected as one of the most promising technique to develop a high average laser system [1]. Its feasibility was successfully demonstrated at the low power of 1 W (100 mJ @ 10 Hz) class in 2010 by using SBS-PCM with the liquid medium, HT-70 [2]. One of the remaining issues to apply the SBS-PCM for high average power laser is the thermal issue in the SBS cell [3]. Absorbed input laser beam can cause the convection and the boiling of the liquid medium. These effects disrupt the wavefront compensation and cause jiggling effect in the reflected beam pattern.

To resolve this issue, fused silica is proposed for the SBS medium at the high input power. The fused silica has the high thermal conductivity of 1.38 W/m K and the low absorption coefficient of  $10^{-6}/\text{cm}$ , which is higher than the thermal conductivity of the liquid medium by a factor of 20 and smaller than the absorption coefficient of the liquid medium by a factor of 300. The calculated temperature difference for the input energy of 10 J at 1 kHz operation was 0.007 K after 0.3 seconds. By curve fitting, the maximum temperature difference is expected to be less than 0.011 K.

Now the experiment with the SBS-PCM using the fused silica has been on the progress. To test the SBS-PCM using the fused silica, Kumgang laser system will be utilized. The result will be shown in the conference.

**References**

- [1] H. J. Kong, S. Park, S. Cha, and M. Kalal, *Opt. Mater. (Amst)*. 35, 807–811 (2013).
- [2] J. S. Shin, S. Park, H. J. Kong, and J. W. Yoon, *Appl. Phys. Lett.* 96, 3–5 (2010).
- [3] M. Nakatsuka, H. Yoshida, Y. Fujimoto, K. Fujioka, and H. Fujita, *JKPS* 43, 607-615 (2003).
- [4] H. J. Kong, S. Park, S. Cha, H. Ahn, H. Lee, J. Oh, B. J. Lee, S. Choi, and J. S. Kim, *High Power Laser Sci. Eng.* 3, e1 (2015).

**LS-I-11****New strategies for the fabrication of photonic devices by direct inscription with femtosecond laser pulses**

*C. Romero<sup>1</sup>, J. G. Ajates<sup>2</sup>, X. Mateos<sup>3</sup>, A. Ródenas<sup>4,5</sup>, P. Moreno<sup>1</sup>, F. Cheng<sup>6</sup>,  
J. R. Vázquez de Aldana<sup>1</sup>*

<sup>1</sup>*Universidad de Salamanca, Aplicaciones del láser y fotónica, Salamanca, Spain*

<sup>2</sup>*Spanish Center for Pulsed Lasers, Technical Division, Villamayor, Spain*

<sup>3</sup>*Universitat Rovira i Virgili- Departament Química Física i Inorgànica, Física I Cristal·lografia de Materials i Nanomaterials FicMA-FicNA-EMaS, Tarragona, Spain*

<sup>4</sup>*Universidad de La Laguna, Departamento de Física, Santa Cruz de Tenerife, Spain*

<sup>5</sup>*Universidad de La Laguna, Instituto Universitario de Estudios avanzados en Atómica, Molecular y Fotónica IUDEA, Santa Cruz de Tenerife, Spain*

<sup>6</sup>*School of Physics, Shandong University, Jinan, China*

Femtosecond laser inscription has already been proved to be a powerful and flexible tool for the manufacture of 3D photonic devices [1] in dielectric materials. The short temporal duration of the laser-matter interaction and the large intensity that can be achieved in the focal region, are responsible to produce local and controllable modifications, as for example a change in the refractive index. In other words, the target material can be processed, at arbitrary depths, with minimal affection of the neighboring region. This fact has opened the door to the fabrication of 3D photonic devices [2], based on optical waveguides, by direct inscription in the substrate, i.e. without the need of post-processing.

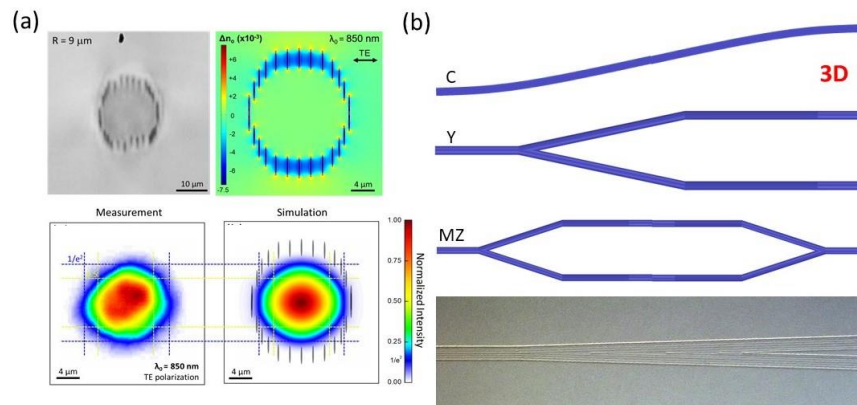


**Fig. 1.** (a) Typical section of a circular depressed cladding waveguide and modal profile ( $\text{LiNbO}_3$ ). The refractive index reconstruction and modal simulation are also shown [3]. (b) Schematics of different implemented photonic structures: curved connector (C), Y-junctions (Y) and Mach-Zehnder interferometers (MZ). Microscope image of the transition area on the bottom.

Crystalline materials are very attractive for the integration of photonic devices, both in the passive and active regimes, as they possess excellent properties, such as a large transparency window, anisotropy, or non-linear behavior, among many others. However, such properties cause, at the same time, a large difficulty for the laser processing, thus requiring the development of specific strategies. In many crystals, the refractive index modification that can be induced by femtosecond laser irradiation is only negative (refractive index decreases at the focal spot), effect

that is linked to a local amorphization of the material. In this context, depressed-cladding waveguides [4], that consist of a cladding with low refractive index modified by femtosecond laser irradiation and a core with unmodified properties, were developed as an efficient and universal technique for waveguide inscription in transparent crystals. In this work we present our recent advances [3,5] on this technique with the aim of inscribing 3D photonic elements in any crystalline dielectric. Our results suggest that depressed-cladding waveguides are key structures for integration of complex 3D photonic devices (waveguide lasers, beam-shapers).

## References

- [1] R. R. Gattass, E. Mazur, Femtosecond laser micromachining in transparent materials, *Nat. Photonics* 2, 219–225 (2008).
- [2] R. Osellame, G. Cerullo, and R. Ramponi, *Femtosecond Laser Micromachining: Photonic and Microfluidic Devices in Transparent Materials*, Springer Science & Business Media, New York (2012).
- [3] J. Ajates, J. R. Vázquez de Aldana, F. Chen, A. Ródenas, Three-dimensional beam-splitting transitions and numerical modelling of direct-laser-written near-infrared LiNbO<sub>3</sub> cladding waveguides, *Opt. Mat Express* 8, 1890-1901 (2018).
- [4] A. G. Okhrimchuk, A. V. Shestakov, I. Khrushchev, and J. Mitchell, Depressed cladding, buried waveguide laser formed in a YAG:Nd<sup>3+</sup> crystal by femtosecond laser writing, *Opt. Lett.* 30, 2248-2250 (2005).
- [5] G. Li, H. Li, R. Gong, Y. Tan, J. R. Vázquez de Aldana, Y. Sun and F. Cheng, Intracavity biosensor based on the Nd:YAG waveguide laser: tumor cells and dextrose solutions, *Phot. Research* 6, 728-732 (2017).

**LS-I-12****Cobalt-doped transparent ceramics and glass-ceramics for saturable absorbers of erbium lasers**

*P. Loiko<sup>1</sup>, O. Dymshits<sup>2</sup>, A. Belyaev<sup>3</sup>, I. Alekseeva<sup>2</sup>, M. Tsenter<sup>2</sup>, V. Vitkin<sup>4</sup>, D. Shemchuk<sup>2</sup>, A. Zhilin<sup>2</sup>*

<sup>1</sup>*ITMO University, Center for Physics of Nanostructures, Saint-Petersburg, Russian Federation*

<sup>2</sup>*S.I. Vavilov State Optical Institute, Laboratory of Optical Glass-ceramics, Saint-Petersburg, Russian Federation*

<sup>3</sup>*G.G. Devyatikh Institute of Chemistry of High-Purity Substances IHPS of the Russian Academy of Sciences, Laboratory of High-purity Oxygen-free Glasses, Nizhny Novgorod, Russian Federation*

<sup>4</sup>*ITMO University, Faculty of Laser Photonics and Optoelectronics, Saint-Petersburg, Russian Federation*

Cobalt ions ( $\text{Co}^{2+}$ , electronic configuration:  $[\text{Ar}]3d^7$ ) embedded in tetrahedral ( $T_d$ ) sites are known for their absorption around  $1.5 \mu\text{m}$  due to the  ${}^4A_2 \rightarrow {}^4T_1({}^4F)$  transition. The high ground-state absorption cross-sections inherent for transition-metal ions in  $T_d$ -sites and a spectral overlap between the  $\text{Co}^{2+}$  absorption and emission of eye-safe erbium (Er) lasers make  $\text{Co}^{2+}$ -doped materials attractive for saturable absorbers (SAs) of such lasers. The SAs feature a decreased absorption (bleaching) with increasing incident laser fluence and they are used to generate ns pulses under passive Q-switching (PQS) operation regime. Among the known crystals with  $\text{Co}^{2+}$  ions in  $T_d$  sites, the most widespread is the cubic spinel,  $\text{MgAl}_2\text{O}_4$ .  $\text{Co}^{2+}:\text{MgAl}_2\text{O}_4$  single-crystals are the state-of-the-art SAs for lasers based on  $\text{Er}^{3+}, \text{Yb}^{3+}$ -codoped phosphate glasses emitting at  $\sim 1.54 \mu\text{m}$ .

The drawbacks of  $\text{Co}^{2+}:\text{MgAl}_2\text{O}_4$  single-crystals are the complicated growth method, polarization-anisotropy of nonlinear properties and an abrupt drop of absorption at above  $1.6 \mu\text{m}$ , where the emission from Er crystalline lasers ( $\text{Er}^{3+}:\text{Y}_3\text{Al}_5\text{O}_{12}$ ) is observed. Thus, other materials such as transparent ceramics and glass-ceramics (GCs) based on various spinels and doped with  $\text{Co}^{2+}$  ions were proposed. The ceramics contain  $\mu\text{m}$ -sized crystalline grains while the GCs contain nm-sized crystals uniformly distributed in the residual glassy matrix. The linear and nonlinear properties of ceramics resemble those of the single-crystals [1]; some specific spinels (e.g.,  $\text{Co}^{2+}:\text{ZnAl}_2\text{O}_4$ ) can be prepared in the ceramic form [2]. Transparent GCs based on spinel nanocrystals are produced in different systems. Their properties are dependent on both the composition of initial Co-doped glasses and the regime of their secondary heat-treatments leading to formation of nanocrystals.

In the present work, we review our achievements in developing SAs using transparent ceramics and GCs based on various spinels. Regarding  $\text{Co}^{2+}$ -doped ceramics, we describe  $\text{MgAl}_2\text{O}_4$  and  $\text{ZnAl}_2\text{O}_4$  ones sintered by Hot Isostatic Pressing (HIPing) [2]. We also focus on transparent GCs containing  $\text{MgAl}_2\text{O}_4$ ,  $\text{Mg}(\text{Al},\text{Ga})_2\text{O}_4$ ,  $\text{Li}(\text{Al},\text{Ga})_5\text{O}_8$  or  $\text{Co}:\gamma\text{-Ga}_2\text{O}_3$  nanocrystals [3,4]. Furthermore, we propose GCs with novel host crystals for  $\text{Co}^{2+}$  ions in  $T_d$  sites, such as ZnO (zinc oxide) or  $\beta\text{-Zn}_2\text{SiO}_4$  ( $\beta$ -willemite) [5].

The  $\text{Co}^{2+}$ -doped ceramics and GCs are studied with respect to their microstructure (by SEM or TEM and X-ray diffraction), vibronic properties (by Raman spectroscopy), linear optical properties (absorption and luminescence) and nonlinear properties. The absorption saturation characteristics and the recovery times are determined. The laser-induced damage threshold of

ceramics and GCs is compared. Finally, SAs made of various  $\text{Co}^{2+}$ -doped GCs are applied in PQS lasers based on  $\text{Er}^{3+}$ ,  $\text{Yb}^{3+}$ -codoped glasses generating ns-long pulses with mJ-level pulse energies at  $\sim 1.54 \mu\text{m}$  [4].

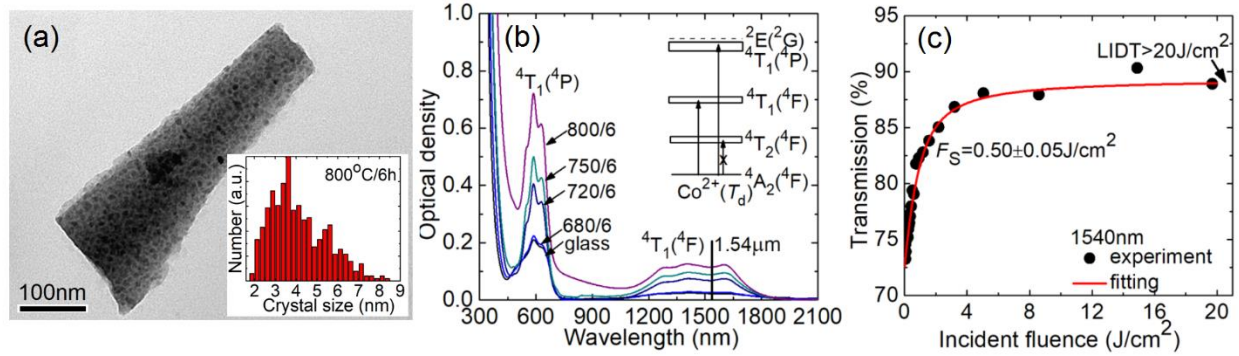


**Fig. 1.** Transparent GCs based on  $\text{Co}^{2+}:\text{Li}(\text{Al,Ga})_5\text{O}_8$  nanocrystals: (a) TEM image, *inset* - size distribution of the nanocrystals; (b) Absorption spectra of the initial glass and GCs, *inset* – energy levels of  $\text{Co}^{2+}$  ions ( $T_d$  sites); (c) absorption saturation curve at  $1.54 \mu\text{m}$ .

## References

- [1] A. Goldstein, P. Loiko, Z. Burshtein, N. Skoptsov, I. Glazunov, E. Galun, N. Kuleshov, and K. Yumashev, “Development of saturable absorbers for laser passive Q-switching near  $1.5 \mu\text{m}$  based on transparent ceramic  $\text{Co}^{2+}:\text{MgAl}_2\text{O}_4$ ,” *J. Amer. Ceram. Soc.* 99(4), 1324–1331 (2016).
- [2] P. Loiko, A. Belyaev, O. Dymshits, I. Evdokimov, V. Vitkin, K. Volkova, M. Tsenter, A. Volokitina, M. Baranov, E. Vilejshikova, A. Baranov, and A. Zhilin, “Synthesis, characterization and absorption saturation of  $\text{Co}:\text{ZnAl}_2\text{O}_4$  (gahnite) transparent ceramic and glass-ceramics: A comparative study,” *J. Alloys Compd.* 725, 998-1005 (2017).
- [3] P.A. Loiko, O.S. Dymshits, V.V. Vitkin, N.A. Skoptsov, A.A. Kharitonov, A.A. Zhilin, I.P. Alekseeva, S.S. Zapalova, A.M. Malyarevich, I.V. Glazunov, and K.V. Yumashev, “Glass-ceramics with  $\gamma\text{-Ga}_2\text{O}_3:\text{Co}^{2+}$  nanocrystals: Saturable absorber for  $1.5\text{--}1.7 \mu\text{m}$  Er lasers,” *Laser Phys. Lett.* 12(3), 035803-1-5 (2015).
- [4] V. Vitkin, P. Loiko, O. Dymshits, A. Zhilin, I. Alekseeva, D. Sabitova, A. Polishchuk, A. Malyarevich, and K. Yumashev, “Passive Q-switching of an Er,Yb:glass laser with  $\text{Co}:\text{Mg}(\text{Al,Ga})_2\text{O}_4$ -based glass-ceramics,” *Appl. Opt.* 56(8), 2142-2149 (2017).
- [5] P.A. Loiko, O.S. Dymshits, V.V. Vitkin, N.A. Skoptsov, A.A. Zhilin, D.V. Shemchuk, M.Ya. Tsenter, K. Bogdanov, A.M. Malyarevich, I.V. Glazunov, and K.V. Yumashev, “Saturable absorber: Transparent glass-ceramics based on a mixture of  $\text{Co}:\text{ZnO}$  and  $\text{Co}:\beta\text{-Zn}_2\text{SiO}_4$  nanocrystals,” *Appl. Opt.* 55(21), 5505-5512 (2016).

**LS-I-13****Direct generation of vortex beam from a Er:Y<sub>2</sub>O<sub>3</sub> ceramic laser at 2.7 μm***Y. Zhao*<sup>1</sup>, *M. Ding*<sup>2</sup>, *Y. Chen*<sup>2</sup>, *D. Shen*<sup>2</sup><sup>1</sup>*Shandong University, State Key Laboratory of Crystal Materials and Institute of Crystal Materials, Jinan, China*<sup>2</sup>*Jiangsu Normal University, Jiangsu Key Laboratory of Advanced Laser Materials and Devices, XuZhou, China*

Optical vortices characterized by doughnut-shaped intensity profile and helical phase front, carry orbital angular momentum (OAM) of  $l\hbar$  per photon, where  $l$  is topological charge [1]. Generation of vortex beams in the mid-infrared spectral range is now mainly focused on nonlinear frequency conversion technique [2], which suffers from low conversion efficiency and complex setups. In comparison, “direct generation” technique [3] using a robust laser cavity features with high beam quality, power scaling capability and low cost.

Here we demonstrate, to the best of our knowledge, the first vortex beam in the 3-micron spectral region from an Er:Y<sub>2</sub>O<sub>3</sub> ceramic laser pumped by a ring-shaped beam. The 7 at.% Er:Y<sub>2</sub>O<sub>3</sub> ceramic has a dimension of 3×4×14.5 mm<sup>3</sup>. A Brewster plate was inserted in the cavity to obtain linear polarized laser. Handedness of the scalar vortex lasers was controllable by introducing asymmetric cavity loss. To further improve the purity of generated vortex beam, an etalon was inserted in the cavity to reduce longitudinal modes. The topological charge ( $l$ ) was detected using a mid-infrared CCD camera and a home-made Mach–Zehnder interferometer, and was quantitatively analyzed by using a cylindrical lens. The  $l$  of LG<sub>0,-1</sub> was calculated to be -0.9878, and 0.9884 in the case of the LG<sub>0,+1</sub> mode, indicating a high purity of the generated vortex beams. The optical spectra were recorded by high resolution optical spectrum analyzer (OSA, AQ6376, YOKOGAWA). The central wavelength of LG<sub>0,+1</sub> mode was 2710.8 nm and 2710.5 nm for the LG<sub>0,-1</sub> laser mode.

**References**

- [1] L. Allen, M. W. Beijersbergen, R. J. C. Spreeuw, and J. P. Woerdman, “Orbital angular momentum of light and the transformation of Laguerre-Gaussian laser modes,” *Phys. Rev. A* 45, 8185–8189 (1992).
- [2] T. Yusufu, Y. Tokizane, M. Yamada, K. Miyamoto, and T. Omatsu, “Tunable 2-μm optical vortex parametric oscillator,” *Opt. Express* 20, 23666-23675 (2012).
- [3] Y. G. Zhao, Q. Y. Liu, W. Zhou, and D. Y. Shen, “~1 mJ pulsed vortex laser at 1645 nm with well-defined helicity,” *Opt. Express* 24, 15596-15602 (2016).

**LS-I-14****Generation of doughnut beam from self-Raman laser with or without optical vortex***W. Chen<sup>1</sup>, G. Zhang<sup>1</sup>**<sup>1</sup>Fujian Institute of Research on the Structure of Matter- Chinese Academy of Sciences, Crystal and laser physics, Fuzhou, China*

Characterizing the very original features of annular-ring transverse spatial profile and the twist of helical phase-front with carrying well-defined amount of orbital angular momentum (OAM) per photon [1], scalar first-order Laguerre-Gaussian beam has become a subject of great interest for applications in many cutting-edge fields of optical tweezers and spanners [2], multiple degrees classical [3] quantum communications [4], super resolution spectroscopy [5] and micro-particles manipulation [6]. Diode-pumped Solid-State Lasers (DPSSLs) incorporating Stimulated Raman Scattering (SRS) provides an efficient approach to access some hard-to-reach frequency regime [7].

Here we demonstrated a proof-of-concept experiment to explore the generation of first-Stokes optical vortex beam via stimulated Raman scattering (SRS) in a solid-state laser associated with spatially-matched pump gain distribution. This scheme has been applied to a diode-pumped Nd:YVO<sub>4</sub> self-Raman laser. Doughnut-like first-Stokes beam with or without optical vortex can be selectively excited without using any dedicated gyration selective element. The observation for phase front evolution characteristics of Stokes field confirmed that, first-order Laguerre-Gaussian first-Stokes beam with well-determined spiral phase front trajectory can only be excited by introducing non-axial symmetric cavity loss.

**References**

- [1] L. Allen, M. W. Beijersbergen, R. J. C. Spreeuw, and J. P. Woerdman, "Orbital angular momentum of light and the transformation of Laguerre-Gaussian laser modes," *Phys. Rev. A* 45, 8185-8189 (1992).
- [2] J. E. Curtis, B. A. Koss, and D. G. Grier, "Dynamic holographic optical tweezers," *Opt. Commun.* 207, 169-175 (2002).
- [3] A. E. Willner, H. Huang, Y. Yan, Y. Ren, N. Ahmed, G. Xie, C. Bao, L. Li, Y. Cao, Z. Zhao, J. Wang, M. P. J. Lavery, M. Tur, S. Ramachandran, A. F. Molisch, N. Ashrafi, and S. Ashrafi, "Optical communications using orbital angular momentum beams," *Adv. Opt. Photonics* 7, 66-106 (2015).
- [4] X.-L. Wang, X.-D. Cai, Z.-E. Su, M.-C. Chen, D. Wu, L. Li, N.-L. Liu, C.-Y. Lu, and J.-W. Pan, "Quantum teleportation of multiple degrees of freedom of a single photon," *Nature* 518, 516-519 (2015).
- [5] A. Y. Okulov, "Cold matter trapping via slowly rotating helical potential," *Phys. Lett. A* 376, 650-655 (2012).
- [6] J. W. R. Tabosa, and D. V. Petrov, "Optical Pumping of Orbital Angular Momentum of Light in Cold Cesium Atoms," *Phys. Rev. Lett.* 83, 4967-4970 (1999).
- [7] H. M. Pask, "The design and operation of solid-state Raman lasers," *Prog. Quant. Electron.* 27, 3-56 (2003).

**LS-I-15****Hollow-core fibers destruction under high power laser radiation**

*I. Bufetov<sup>1</sup>, A. Kolyadin<sup>1</sup>, A. Kosolapov<sup>1</sup>*

<sup>1</sup>*Fiber Optics Research Center of RAS, HCF Lab, Moscow, Russian Federation*

The first detailed quantitative study of the catastrophic destruction of hollow-core fibers under the action of pulsed (Q-switched + mode-locked) laser radiation containing evaluation of key physical processes will be presented. The propagation of an optical discharge (OD) along hollow-core optical fibers (HCFs) was investigated experimentally (Fig.1)

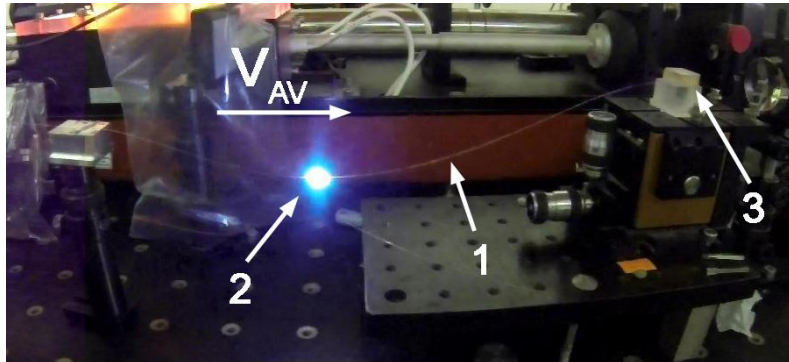


Fig1. Picture of an OD propagating through HCF. Numbers indicate HCF (1), OD (2), and laser radiation launch unit (3).

Outwardly this process looks very similar to the well-known fiber fuse effect in solid core fibers [1]. Silica-based revolver-type HCFs (RFs) filled with atmospheric air were used as test samples in our experiments [2]. We observed that the average propagation velocity of an OD along the RFs ( $V_{AV}$ ) depends on the properties of the medium around the silica structure of the RF. It is shown that the value of  $V_{AV}$  changes by approximately a factor of three, depending on whether the OD is moving along a polymer coated or uncoated RF (Fig.2).

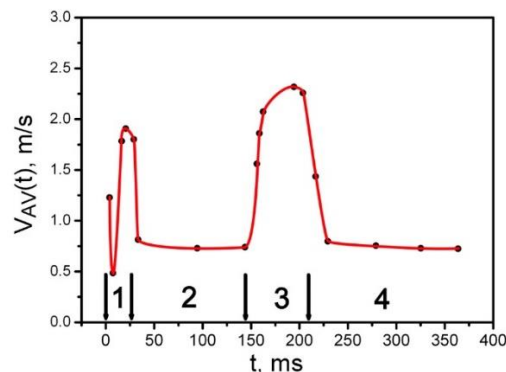


Fig.2.  $V_{AV}(t)$  for OD propagation through HCF. Numbers indicate regions of OD initiation (1), polymer coated HCF (2, 4), uncoated HCF (3).

The value of  $V_{AV}$  practically does not change when the polymer is replaced by an immersion liquid (such as glycerol) or liquid gallium. By analyzing the destruction region's patterns that appear in the fiber cladding after an OD propagation, we propose the physical picture of the phenomenon. A consistent physical picture of an OD propagating along an RF (as a version of

HCFs) in our experiments includes the following processes: 1. Initiation and propagation of a laser supported detonation wave under the action of a picosecond laser pulses. 2. Movement of the attenuating shock wave along a RF during the period between picosecond pulses. 3. The process of a iterated detonation wave initiation in front of the shock wave by the next picosecond pulse. 4. A special mode of OD self-initiation at spiky splinters of silica capillaries after ms time intervals between Q-switch laser pulses.

The study was supported by the Russian Foundation for Basic Research (Project No. 18-02-00324).

## References

- [1] R. Kashyap, "The Fiber Fuse - from a curious effect to a critical issue: A 25th year retrospective," *Opt. Express* 21(5), 6422-6441 (2013).
- [2] A. N. Kolyadin, A. F. Kosolapov, and I. A. Bufetov, "Optical discharge propagation along hollow-core optical fibres", *Quantum Electronics* 48(12), 1138-1142 (2018).

**LS-I-16 (Keynote)****Opportunities in Terahertz science open by state-of-the-art high-power ultrafast disk lasers***C. Saraceno<sup>1</sup>**<sup>1</sup>Ruhr University Bochum, Germany*

Terahertz time-domain spectroscopy (TDS) is nowadays well-established to study a variety of low-frequency motions in condensed matter. However, whereas immense progress has been made in the development of single-cycle THz sources for TDS, many studies continue to suffer from the low average power, that result in extremely poor signal-to-noise ratio and impractically long times. Increasing the average power of current THz-TDS sources calls for more powerful, state-of-the-art NIR ultrafast driving lasers. In this talk, we will present latest progress in high-power ultrafast disk oscillators, as well as their application for the generation of high average power THz radiation. We will report on record-high THz powers in the few to tens of milliwatts regime, and will present future applications enabled by these unique sources.

**LS-I-17****Photosensitivity of composite heavily erbium-doped phosphosilicate fibers**

*A. Rybaltovsky<sup>1</sup>, O. Egorova<sup>2</sup>, S. Vasiliev<sup>3</sup>, S. Zhuravlev<sup>1</sup>, O. Butov<sup>4</sup>, S. Semjonov<sup>5</sup>, B. Galagan<sup>6</sup>, S. Sverchkov<sup>6</sup>, B. Denker<sup>6</sup>*

<sup>1</sup>*Fiber Optics Research Center of Russian Academy of Sciences, Laboratory of Optical Fibers Technology, Moscow, Russian Federation*

<sup>2</sup>*Natural Sciences Center at Prokhorov General Physics Institute of the Russian Academy of Sciences, Force Fiber Optics Laboratory, Moscow, Russian Federation*

<sup>3</sup>*Fiber Optics Research Center of Russian Academy of Sciences, Laboratory of Fiber Optics, Moscow, Russian Federation*

<sup>4</sup>*Kotelnikov Institute of Radio Engineering and Electronics of Russian Academy of Sciences, Laboratory of Fiber Optic Technology, Moscow, Russian Federation*

<sup>5</sup>*Fiber Optics Research Center of Russian Academy of Sciences, Laboratory of Optical Fiber Technology, Moscow, Russian Federation*

<sup>6</sup>*Prokhorov General Physics Institute of the Russian Academy of Sciences, Laboratory of Concentrated Laser Materials, Moscow, Russian Federation*

Single frequency fiber lasers are attractive for many photonic applications. Narrowband emission of this laser type is usually provided by a relatively short (10-20 mm) Fabry-Perot structure (or phase-shifted fiber Bragg grating (FBG)) created in the fiber core. Two factors have key importance for short-length laser structures: high pump absorption (emission gain) per unit length and sufficient photosensitivity of the active fiber. A novel composite heavily erbium-doped phosphosilicate (24 mol. % of phosphorus oxide, 3 mol. % of aluminium oxide and 0.39 mol. % of erbium oxide) single-mode fiber has been recently developed using a rod-in-tube technique [1]. It was shown that the fiber has good lasing properties as well as rather high photosensitivity to 193-nm radiation, which allowed achieving a stable single frequency lasing using optical pump at 980 nm [2].

In this work the photosensitivity of this composite fiber was further investigated. Particularly, dose dependencies of modulation amplitude and mean index change have been measured for both pristine and hydrogen-loaded fiber samples. Thermal stability (temperature annealing) of the induced index change has been also analyzed. It was shown that the UV-induced index gradually decreases with temperature increase, nevertheless some magnitude of induced index remains unerasable until the core material melts (600-650°C).

A composite fiber with a core diameter of 5 μm (cut-off wavelength - 1.43 μm) has been used for investigation. An ArF excimer laser (Coherent COMPexPro) emitting 20-ns pulses at 193 nm (repetition rate - 10 Hz) was used for fiber side irradiation with the energy density of about 200 mJ/cm<sup>2</sup> per pulse. Low temperature hydrogen loading of fiber samples has been performed in gas chamber (H<sub>2</sub> pressure - 120 atm) at 90°C during 24 hours. FBGs were written via the 10-mm-long phase mask having a period of 1064 nm.

Dose dependences of UV-induced index modulation amplitude and average index change measured for both as prepared and H<sub>2</sub>-loaded fibers are shown in Fig.1. Similar to germane-silicate glass, molecular hydrogen dissolved in the phosphosilicate glass increases its photosensitivity greatly. The observed photosensitivity is enough to fabricate highly reflecting FBGs, necessary to create single-frequency laser cavities. Other results obtained in our experiments on induction and

erasure of refractive index in the core of the composite Er-doped phosphosilicate fiber will be presented at the Conference.

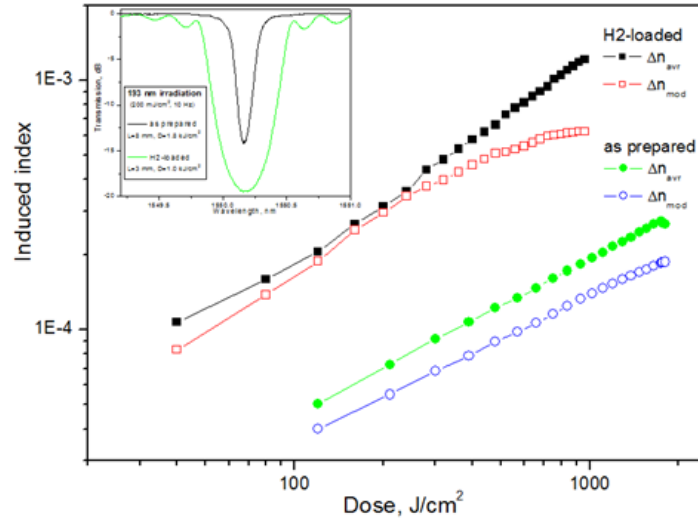


**Fig. 1.** Dose dependences of UV-induced index components for both pristine and H<sub>2</sub>-loaded composite phosphosilicate fiber (insert: FBG spectra measured at the end of UV-irradiation).

## References

- [1] O.N. Egorova, S.L. Semjonov, V.V. Velmskin, Yu.P. Yatsenko, S.E. Sverchkov, B.I. Galagan, B.I. Denker, and E.M. Dianov, "Phosphate-core silica-clad Er/Yb-doped optical fiber and cladding pumped laser", *Opt. Express* 22, 7632 (2014).
- [2] A.A. Rybaltovsky, O.N. Egorova, S.G. Zhuravlev, S.L. Semjonov, B.I. Galagan, S.E. Sverchkov, B.I. Denker, "Distributed Bragg reflector fiber laser directly written in a composite fiber manufactured by melting phosphate glass in a silica tube", to be published in *Optics Letters*.

## LS-I-18

### 100 Hz repeatable power laser

*J. Kawanaka<sup>1</sup>, S. Tokita<sup>1</sup>, J. Ogino<sup>1</sup>, K. Matsumoto<sup>1</sup>, H. Yoshida<sup>1</sup>, K. Tsubakimoto<sup>1</sup>, K. Fujioka<sup>1</sup>, Z. Li<sup>1</sup>, N. Morio<sup>1</sup>, S. Motokoshi<sup>2</sup>*

<sup>1</sup>*Osaka University, Institute of Laser Engineering, Osaka, Japan*

<sup>2</sup>*Institute for Laser Technology, Laser Technology Development, Osaka, Japan*

Recently petawatt lasers have been used in various plasma experiments for high field science. 10PW lasers have been developed in Romania and China, and 100PW project in China will start in earnest. On the other hands, realistic industrial applications using power laser is very few. Because the repetition rate below several hertz is not enough at all. The most significant problem to be resolved is thermal problem in such large aperture laser more than several centimeters.

An active mirror has excellent power scaling in both pulse energy and repetition rate (average power). The required pulse energy decides the aperture size to avoid optical damages of the materials. The thickness and the number of active mirrors are optimized for pulse energy and repetition rate. In addition, thermal improvement, often in order, of a laser material cryogenically cooled will increase repetition rate. To suppress and compensate phase front distortion for enlarged aperture size and increased number of the active mirrors is important. Using cryogenically cooled Yb:YAG in Fig.1, 100Hz, 10J nano-second pulse laser is under construction.[1] 10Hz operation has been already demonstrated with four active mirrors.

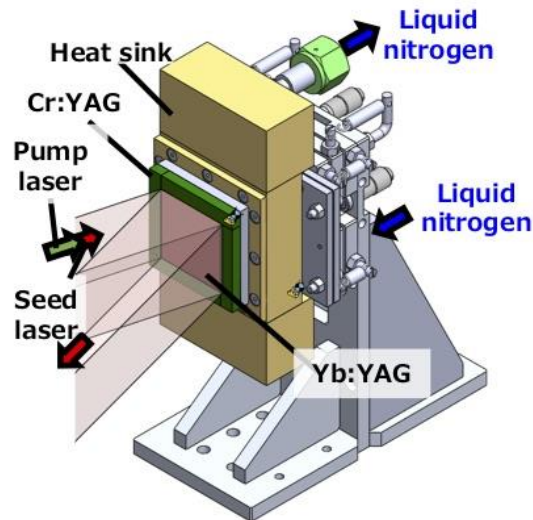


**Fig. 1.** Large-aperture active mirror with a cryogenic Yb:YAG ceramic disk.

## References

- [1] J. Kawanaka et. al., “Innovative power laser system developed at Osaka University,” ALPS 2019, Yokohama, Japan, April 2019.

**LS-I-19****One-Joule, 500 Hz cryogenic composite-disk laser amplifier**

L.E. Zapata<sup>1,2,3</sup>, S. Schweisthal<sup>1</sup>, J. Thesinga<sup>1</sup>, C. Zapata<sup>2</sup>, M. Schust<sup>1</sup>, M. Pergament<sup>1</sup>,  
F.X. Kaertner<sup>1</sup>

<sup>1</sup>*Deutsches Elektronen Synchrotron, Center for Free-Electron Laser Science-, Hamburg, Germany*

<sup>2</sup>*MAGiC Laser Technologies- LLC, Lasers, Palatka- Florida, USA*

<sup>3</sup>*Lumitron Technologies, High Power Lasers, Irvine- California, USA*

A cryogenic Yb:YAG composite-thin-disk laser driver demonstrated stable operation at 500 Hz with chirped 1-Joule 300-ps pulsed output [1, 2] earlier this year. The bandwidth of 0.35 nm, compressible to < 3 ps, was measured with 1.2 Joule pulses at 400 Hz. In the acceptance tests, the highly engineered alpha-level hardware exceeded its 100 Hz contractual requirement demonstrating constant and stable output in long-runs (up to 8 hrs) at over one-joule output and sustained repetition rates from 100 to 300 Hz. Testing was on a daily basis over the span of two weeks. The compiled run-time at high power is over 60 hrs to date. The laser system is capable of higher pulse energies (2-Joules) that will remain untested for the time being as the hardware is presently being incorporated into the AXISIS lab at DESY in Hamburg to provide the primary photons in an all optically driven, ICS x-ray source under development with ERC funding.

**References**

- [1] "One Joule 500 Hz cryogenic Yb:YAG Laser Driver", L. E. Zapata, S. Schweisthal, J. Thesinga, C. Zapata, M. Schust and F. X. Kaertner , © OSA Advanced Solid State Lasers ATu6A.1 Boston Nov. 2018.
- [2] "Joule-class 500 Hz Cryogenic Yb:YAG Chirped Pulse Amplifier", Luis E. Zapata, Simon Schweisthal, Jelto Thesinga, Collette Zapata, Matthias Schust, Liu Yizhou, Mikhail Pergament and Franz X. Kaertner, © OSA CLEO 2019, Chair's pick: SM4E.1, San Jose May 2019.

**LS-O-1****All-solid-state Fe:ZnSe mid-IR femtosecond laser operating at 4.4  $\mu\text{m}$  for driving extreme nonlinear optics***F.V. Potemkin<sup>1</sup>**<sup>1</sup>M.V.Lomonosov Moscow State University, Faculty of Physics, Moscow, Russian Federation*

Nowadays mid-IR photonics is a rapidly developing area due to their inspiring horizons both in fundamental and practical areas. During the last decades the most prospective way to reach high peak powers in mid-IR is the usage of optical parametric chirped pulse amplification (OPCPA) concept [1,2,3]. The alternative way to build mid-IR high power laser system is using the relatively new transition metal-doped crystal Fe:ZnSe which emission bandwidth supports to 50 fs pulse duration. In our previous papers we have developed an approach for the creation of high-power femtosecond laser system based on chirp pulse amplification of mid-IR seed in optically pumped Fe:ZnSe gain medium [4]. The amplification of nanosecond and femtosecond pulses in Fe:ZnSe was investigated in [5] and [6] correspondingly with further enhancing of the energy extraction from the amplifier up to 1.2 mJ [7].

In this contribution, we present complete laser system, which is based on hybrid parametric and laser amplification and delivers 3.5 mJ 150 fs laser pulses centered at 4.4  $\mu\text{m}$  [8]. To the best of our knowledge, this is the first CPA system that operates at wavelengths longer than 2.5  $\mu\text{m}$ .

To demonstrate the potential of the developed IR fs source we generate four-octave-spanning supercontinuum (SC) in xenon. Output beam from the system was focused by the  $\text{CaF}_2$  lens with focal length of 150 mm inside 8-cm-long gas chamber. We used only 2.5 mJ of the output energy in order to avoid self-phase modulation at the entrance of the 1-cm-thick  $\text{CaF}_2$  window.  $\text{CaF}_2$  lenses with 150 and 50 mm focal lengths were used to focus pump radiation and collimate generated supercontinuum (SC). Generated radiation was then directed into the scanning monochromator equipped with the set of diffraction gratings (150 – 3000 gr/mm) and detectors (PMT, Ge, PbSe and MG-32). We observed stable plasma channel and strong visible conical emission at 20 bar pressure. Generated supercontinuum covers the whole region from 350 nm to 5.5  $\mu\text{m}$ . We believe that careful adjustment of the pressure or/and cell length may also lead to filamentation assistant self-compression to few-cycle pulses.

**References**

- [1] G. Andriukaitis et al., “90 GW peak power few-cycle mid-infrared pulses from an optical parametric amplifier,” *Opt. Lett.* 36, 2755–2757 (2011); D. Sanchez et al., “7  $\mu\text{m}$ , ultrafast, sub-millijoule-level mid-infrared optical parametric chirped pulse amplifier pumped at 2  $\mu\text{m}$ ,” *Optica* 3, 147 (2016).
- [2] D. Sanchez et al., “7  $\mu\text{m}$ , ultrafast, sub-millijoule-level mid-infrared optical parametric chirped pulse amplifier pumped at 2  $\mu\text{m}$ ,” *Optica* 3, 147 (2016).
- [3] M. Bock et al., “Generation of Millijoule Few-Cycle Pulses at 5  $\mu\text{m}$  by Indirect Spectral Shaping of the Idler in an OPCPA,” *J. Opt. Soc. Am. B* 35, 18–21 (2018).
- [4] B. G. Bravy et al., “High-power mid-IR (4–5  $\mu\text{m}$ ) femtosecond laser system with a broadband amplifier based on  $\text{Fe}^{2+}$ :ZnSe,” *Bull. Russ. Acad. Sci. Phys.* 80, 444–449 (2016).
- [5] F. V. Potemkin et al., “Toward a sub-terawatt mid-IR (4–5  $\mu\text{m}$ ) femtosecond hybrid laser system based on parametric seed pulse generation and amplification in  $\text{Fe}^{2+}$ :ZnSe,” *Laser Phys. Lett.* 13, 015401 (2015).

- [6] F. V. Potemkin et al., "Mid-IR (4-5  $\mu\text{m}$ ) femtosecond multipass amplification of optical parametric seed pulse up to gigawatt level in  $\text{Fe}^{2+}:\text{ZnSe}$  with optical pumping by a solid-state 3  $\mu\text{m}$  laser," *Laser Phys. Lett.* 13, 125403 (2016).
- [7] F. V. Potemkin et al., "Gigawatt mid-IR (4-5  $\mu\text{m}$ ) femtosecond hybrid  $\text{Fe}^{2+}:\text{ZnSe}$  laser system," in *Proceedings of SPIE (The International Society for Optical Engineering, 2017)*, vol. 10238, pp.102308L.
- [8] E. Migal et al., "3.5-mJ 150-fs  $\text{Fe}:\text{ZnSe}$  hybrid mid-IR femtosecond laser at 4.4  $\mu\text{m}$  for driving extreme nonlinear optics," *Opt. Lett.* 44, 2550-2553 (2019).

**LS-O-2****Modulational instability at normal dispersion in microresonators with backscattering**

*N. Kondratiev<sup>1</sup>, V. Lobanov<sup>1</sup>, D. Skryabin<sup>1,2</sup>*

<sup>1</sup>*Russian Quantum Center, Coherent Microoptics and Ragiophotonics, Moscow, Russian Federation*

<sup>2</sup>*University of Bath, Department of Physics, Bath, United Kingdom*

In recent years, optical whispering gallery modes (WGM) microresonators have found wide application in various fields of science and technology. Due to high quality factor they represent the most promising platform for the creation of miniature, energy-efficient components for photonics and radiophotonics. The discovery of Kerr frequency combs and dissipative Kerr solitons (DKS) generation in microresonators [1] increased the interest to the WGM microresonator field. Several recent works showed that Rayleigh scattering inside a microresonator [2] can generate a backward wave to provide resonant feedback for the laser line stabilization via the self-injection locking effect [3,4]. Furthermore the generation of DKS was demonstrated by the multi-frequency laser locked by high-Q microresonator [5]. However, this backward wave also interacts nonlinearly with the forward wave and influence frequency comb dynamics. It was shown that the cross-phase modulation can lead to modulational instability for the copropagating waves [6-8]. Here we study this effect for the counter-propagating waves using numerical modeling and linear stability analysis.

First, we rigorously derived the coupled mode equations from the ab initio Maxwell equations to describe the resonator. For large enough finesse (the resonance frequency to inter-mode distance ratio) and the equations can be transformed to Lugiati-Lefever-like equations. We found that in the normal dispersion mode, the scanning of the main resonance does not generate additional spectral components. At the same time, modulation instability is observed at the second resonance, which provides a new mechanism for the generation of the frequency comb. While scanning the second branch branch and a certain detuning value is reached, the first sidebands appear, and then due to non-degenerate four-wave interaction, the remaining frequency components rise. Then, a chaotic regime is observed, corresponding to the generation of an incoherent comb, which then passes into a stable low-intensity single-mode mode.

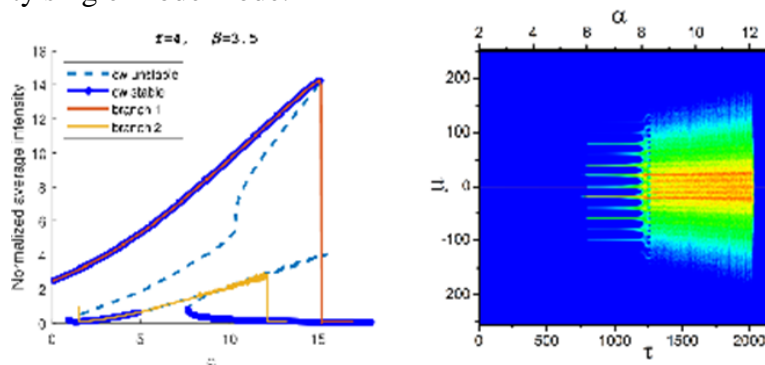


**Fig. 1.**

The parameters of the generated frequency comb also depend on the linear coupling coefficient of the forward and backward waves. It can be assumed that such a mechanism of frequency comb generation in the normal dispersion mode may be responsible for the generation of the platonic in

the self-injection locking regime [9]. The linear stability analysis was also performed to get the insight on the system regimes. This allows us to estimate the detuning and mode number at which the first sideband will appear during laser sweeping. We also note that the mode number and second order dispersion parameter appear in formulas as a united term giving out a simple square-root scaling for first sideband with dispersion.

This work was supported by the Russian Science Foundation (Project 17-12-01413).

## References

- [1] T. Herr, et.al., Temporal solitons in optical microresonators, *Nat. Photon.* 8, 145152 (2014).
- [2] M. L. Gorodetsky, et.al., Rayleigh scattering in high-Q microspheres, *J. Opt. Soc. Am. B* 17, 10511057 (2000).
- [3] N. M. Kondratiev, et.al., Self-injection locking of a laser diode to a high-Q WGM microresonator, *Opt. Express* 25, 2816728178 (2017).
- [4] R.R.Galiev, et.al., Spectrum collapse, narrow linewidth, and Bogatov effect in diode lasers locked to high-Q optical microresonators, *Opt. Express* 26, 3050930522 (2018).
- [5] N. G. Pavlov, et.al., Narrow linewidth lasing and soliton Kerr-microcombs with ordinary laser diodes, *Nat. Photon.* 12, 694698 (2018).
- [6] G. Agrawal, Modulation instability induced by cross-phase modulation, *Phys. review letters* 59, 880883 (1987).
- [7] T. Tanemura and K. Kikuchi, Unified analysis of modulational instability induced by cross-phase modulation in optical fibers, *J. Opt. Soc. Am. B* 20, 25022514 (2003).
- [8] L. Li, et.al., Modulation instability induced by intermodal cross-phase modulation in step-index multimode fiber, *Appl. Opt.* 58, 42834287 (2019).
- [9] V.Lobanov, et.al., Frequency combs and platicons in optical microresonators with normal GVD, *Opt. Express* 23, 77137721 (2015).

**LS-O-3****Progress on self-frequency-doubled Nd:Ca<sub>4</sub>GdO(BO<sub>3</sub>)<sub>3</sub> and Yb:Ca<sub>4</sub>YO(BO<sub>3</sub>)<sub>3</sub> crystal**

*H. Yu<sup>1</sup>, H. Zhang<sup>1</sup>, J. Wang<sup>1</sup>, Z. Hu<sup>2</sup>*

*<sup>1</sup>Shandong University,*

*State Key Laboratory of Crystal Materials and Institute of Crystal Materials, Jinan, China*

*<sup>2</sup>Tianjin University of Technology, Institute of Functional Crystal Materials, Tianjin, China*

Self-frequency-doubled (SFD) Nd:Ca<sub>4</sub>GdO(BO<sub>3</sub>)<sub>3</sub> (Nd:GdCOB) and Yb:Ca<sub>4</sub>YO(BO<sub>3</sub>)<sub>3</sub> (Yb:YCOB) crystal with different doping concentration has been grown by the Czochralski method. The thermal and fluorescence spectroscopic properties of Nd:GdCOB and Yb:YCOB crystals were studied. It was found that a dualwavelength laser output of 1060 and 1091 nm were obtained when pumped by the high power with Nd:GdCOB crystal. On the basis of Boltzmann Statistics, the number of electrons of lower level reduced with the increasing of the upper level, and the gain of 1060 nm decreased with the increase in the level of 1091 nm, leading to the increasing output of 1091 nm and the reducing output of 1060 nm. By optimizing the coating condition, the maximum output power of 3.01W at a wavelength of 545nm with an optical efficiency of 20.7% was obtained. The polarized fluorescence spectra with Yb:YCOB crystal showed that it had broad and anisotropic vibronic emission with a small peak at about 1130 nm. A watt-level self-frequency-doubled yellow laser at the 570 nm wavelength was realized by taking advantage of the vibronic emission of Yb:YCOB crystal cut along the optimized direction out of the principal planes with the maximum effective nonlinear coefficient. By employing the self-frequency-doubling behavior of Yb:YCOB, the self-frequency-doubled yellow laser was achieved with a maximum output power of 1.08 W at 570 nm.

**LS-O-4****Diode pumped cryogenic Yb:Lu<sub>2</sub>O<sub>3</sub> ceramic laser**

*S. Paul David<sup>1</sup>, V. Jambunathan<sup>1</sup>, F. Yue<sup>1</sup>, B. J Le Garrec<sup>2</sup>, A. Lucianetti<sup>1</sup>, T. Mocek<sup>1</sup>*

<sup>1</sup>*HiLASE Centre, Institute of Physics of the Czech Academy of Sciences, Dolní Břežany, Czech Republic*

<sup>2</sup>*Unité Mixte n° 7605 CNRS - CEA - Ecole Polytechnique - UPMC, Laboratoire pour l'Utilisation des Lasers Intenses LULI-, Saclay, France*

Cubic sesquioxides with a general formula RE<sub>2</sub>O<sub>3</sub> (RE=Y, Lu and Sc) have shown excellent thermal properties which make them attractive for high power solid state lasers. The challenges in achieving high quality sesquioxide single crystals have recently been solved by transparent ceramic technology. Among them, Lu<sub>2</sub>O<sub>3</sub> is more attractive because of its high thermal conductivity value of about 12.5 W/m/K which is least affected by the dopant ion [1]. Yb<sup>3+</sup> in Lu<sub>2</sub>O<sub>3</sub> ion with a low quantum defect and simple electronic structure is widely considered for generating high power lasers operating at 1 μm. Thermal issues of room temperature laser operation can be successfully overcome by cryogenically cooling the sample to achieve a good beam quality [2]. In this work, we studied Yb doped Lu<sub>2</sub>O<sub>3</sub> ceramic laser operated at cryogenic temperatures pumped by a laser diode.

Laser experiment was carried out using a 3 mm thick 2% Yb:Lu<sub>2</sub>O<sub>3</sub> circular ceramic disk of 20 mm diameter in a typical L-shaped plano-concave cavity with mirrors coated appropriately for pump and laser wavelengths. We employ a Volume Bragg Grating (VBG) stabilized laser diode emitting at 976 nm with a bandwidth of 0.40 nm to match the zero phonon line absorption peak of Yb:Lu<sub>2</sub>O<sub>3</sub>. Continuous wave (CW) laser characteristics of Yb:Lu<sub>2</sub>O<sub>3</sub> measured using various output coupler transmissions (TOC = 10, 20, 30 and 40%) and at various cryogenic temperatures. A highest output power of 11.24 W and a slope efficiency of 59.2% were achieved at 100K using a 40% output coupler transmission value. The slope efficiency was more than doubled when the sample is cooled down from the room temperature to 100 K as shown in Fig. 1. The highest power at 300K was only 4.44 W which was 2.5 times lower than that of 100K.

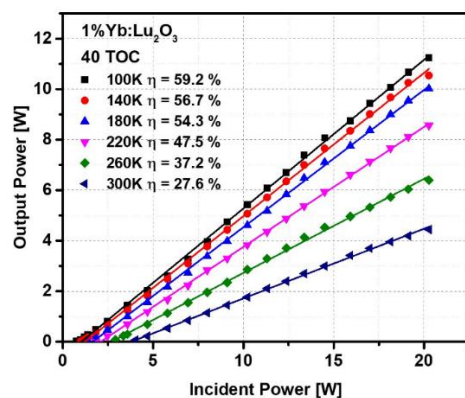


**Fig. 1.**

**References**

- [1] B. Le Garrec, V. Cardinali and G. Bourdet, Proc. of SPIE Vol. 8780 (2013) 87800E-1-12.  
 [2] V. Cardinali, E. Marmois, B. Le Garrec, G. Bourdet, Optical Materials 34 (2012) 990–994.

**LS-O-5****2.3  $\mu\text{m}$  and 4.4  $\mu\text{m}$  lasing in Cr,Fe:Zn<sub>1-x</sub>Mn<sub>x</sub>Se (x=0.3) single crystal pumped by Q-switched Er:YLF laser at 1.73  $\mu\text{m}$** 

*A. Říha<sup>1</sup>, M.E. Doroshenko<sup>2</sup>, H. Jelínková<sup>1</sup>, M. Němec<sup>1</sup>, M. Jelínek<sup>1</sup>, M. Čech<sup>1</sup>, D. Vyhlídal<sup>1</sup>, N.O. Kovalenko<sup>3</sup>, A.S. Gerasiemenko<sup>3</sup>*

<sup>1</sup>*Faculty of Nuclear Sciences and Physical Engineering, Czech Technical University in Prague, Břehová 7, 115 19 Prague, Czech Republic*

<sup>2</sup>*Laser Materials and Technology Research Center, General Physics Institute, Vavilov Str. 38, 119991 Moscow, Russian Federation*

<sup>3</sup>*Institute for Single Crystals, National Academy of Sciences of Ukraine, 60 Lenin Ave., Kharkiv, Ukraine*

Novel Cr<sup>2+</sup> and Fe<sup>2+</sup> co-doped Zn<sub>1-x</sub>Mn<sub>x</sub>Se (x = 0.3) crystal with Cr<sup>2+</sup> to Fe<sup>2+</sup> ions concentration ratio about 1:2 (both doping ions concentration were at the  $\sim 10^{18}$  cm<sup>-3</sup> level) with good optical quality was synthesized. Under pumping by a Q-switched Er:YLF laser at 1.73  $\mu\text{m}$  the oscillations of Cr<sup>2+</sup> ions at 2.3  $\mu\text{m}$  as well as Fe<sup>2+</sup> ions at 4.4  $\mu\text{m}$  were realized. Both regimes, i. e. intracavity pumping of Fe<sup>2+</sup> ions by Cr<sup>2+</sup> as well as excitation through Cr<sup>2+</sup>  $\rightarrow$  Fe<sup>2+</sup> ions energy transfer mechanism were demonstrated. The output energy for Cr<sup>2+</sup> ions lasing at 2.3  $\mu\text{m}$  was up to 900  $\mu\text{J}$  while Fe<sup>2+</sup> ions lasing at 4.4  $\mu\text{m}$  reached up to 60  $\mu\text{J}$  in the intracavity pumping mode. In the Cr<sup>2+</sup>  $\rightarrow$  Fe<sup>2+</sup> energy transfer mode, the maximum output energy was 20  $\mu\text{J}$  at 4.4  $\mu\text{m}$ . Laser generation at 2.3  $\mu\text{m}$  was observed up to 340 K while Fe<sup>2+</sup> ions oscillations stopped for temperatures above  $\sim 150$  K. Fe<sup>2+</sup> ions oscillation wavelength was observed to shift with temperature increase from  $\sim 4.4$   $\mu\text{m}$  at 78 K to  $\sim 4.5$   $\mu\text{m}$  at 150 K. The Fe<sup>2+</sup> ions output pulses were quite stable in amplitude and temporal domain in both excitation modes with beam profile close to fundamental transversal mode.

**LS-O-6****307 W high power 1018 nm monolithic tandem pump fiber source with effective thermal management***X. Chen<sup>1</sup>, Y. Yang<sup>1</sup>, B. He<sup>1</sup>**<sup>1</sup>Shanghai Institute of Optics and Fine Mechanics- Chinese Academy of Sciences, Shanghai Key Laboratory of All Solid-State Laser and Applied Techniques, Research Center of Space Laser Information Technology, Shanghai, China*

High power fiber lasers or amplifiers have attracted a lot of attention due to their outstanding characteristics, such as excellent beam quality, high efficiency, power scalability, and available high-power pumps [1-4]. Recent years, with the introduction of tandem-pumping technique, the ytterbium-doped fiber lasers (YDFLs) open up a new insight in available output laser power. Though the YDFLs have shown 5~6 orders of magnitude brightness enhancement by using tandem pump laser sources compared to that of the diode pump sources [1, 5-6], presenting compact high power tandem-pumping laser sources with high brightness is still challenging. Here, we report a monolithic 1018 nm fiber laser with total output power of 307 W, much higher than the reported tandem-pumping laser powers. The laser system is well designed to be suitable for an YDFL core-pumping setup. The cavity slope efficiency is up to 75.9% and the amplified spontaneous emission is suppressed by 54 dB. The measured beam quality has a  $M^2$  factor of 1.17. Heat dissipation of the key components is taken into account to achieve a stable laser operation. The power fluctuation is measured to be less than 0.8% of the maximum power during a measurement time of half an hour. This architecture can be an effective high brightness pump source of core-pumping high power fiber amplifiers.

**References**

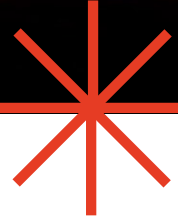
- [1] Y. Jeong, J. K. Sahu, D. N. Payne, and J. Nilsson, "Ytterbium-doped large-core fiber laser with 1.36 kW continuous-wave output power," *Opt. Express* 12(25), 6088-6092(2004).
- [2] V. Gapontsev, D. Gapontsev, N. Platonov, O. Shkurkhin, V. Fomin, A. Mashkin, M. Abramov, and S. Ferin, "2 kW CW ytterbium fiber laser with record diffraction limited brightness," in *Proceedings of the Conference on Lasers and Electro-Optics Europe*, (Optical Society of America, 2005).
- [3] B. He, J. Zhou, Q. Lou, Y. Xue, Z. Li, W. Wang, J. Dong, Y. Wei, and W. Chen, "1.75 kilowatt continuous-wave output fiber laser using homemade ytterbium-doped large-core fiber," *Microw. Opt. Technol. Lett.* 52(7), 1668-1671 (2010).
- [4] B. Y. Zhao, K. L. Duan, W. Zhao, C. Li, and Y. S. Wang, "Experimental study on high power all-fiber laser," *Chin. Opt. Lett.* 8(4), 404-406 (2010).
- [5] Y. Jeong, A. J. Boyland, J. K. Sahu, S. Chung, J. Nilsson, and D. N. Payne, "Multi-kilowatt single-mode ytterbium-doped large-core fiber laser," *J. Opt. Soc. Korea* 13(4), 416-422 (2009).
- [6] J. Nilsson, "Recent progress and limiting factors in high power fiber laser technology," in *Proceedings of the Conference on Lasers and Electro-Optics*, 2010 OSA Technical Digest Series (Optical Society of America, 2010), tutorial paper CTuC1.



# ALT'19

**INTERNATIONAL CONFERENCE**

**Advanced Laser Technologies**



**LASER DIAGNOSTICS  
AND SPECTROSCOPY**

**Prague, Czech Republic**



---

15-20 September 2019

**LD-I-1****Interaction of strong optical fields with diamond - towards ultrafast control of electronic excitations**

M. Kozák<sup>1</sup>

<sup>1</sup>*Charles University- Faculty of Mathematics and Physics,  
Department of Chemical Physics and Optics, Prague, Czech Republic*

Nonlinear interaction between few-cycle laser pulses with controlled carrier-envelope phase and solid-state materials allows to control the electron dynamics in matter on sub-femtosecond time scales. With increasing field amplitude of the driving light, the interaction changes from the classical perturbative regime to the non-perturbative, strong-field regime. In the latter, the electrons are excited by optical field-induced tunneling during a fraction of the optical cycle and further accelerated by the fields to high energies. The underlying electron dynamics can be studied using several observables as coherent high harmonic radiation, excited carrier population or transient changes of optical susceptibility.

In this contribution we discuss experimental observation and theoretical description of multiphoton absorption in diamond driven by few-cycle laser pulses and discuss its strong dependence on the polarization state of light [1]. We also experimentally demonstrate the dynamical Franz-Keldysh effect in diamond close to its direct band gap. Further, impact ionization of electrons in diamond driven by mid-infrared laser pulses is observed and studied in detail.

**References**

- [1] M. Kozák, T. Otobe, M. Zukerstein, F. Trojánek, and P. Malý, „Anisotropy and polarization dependence of multiphoton charge carrier generation rate in diamond,“ *Phys. Rev. B* 99, 104305 (2019).

## LD-I-2

## Pump-probe magneto-optical studies of thin-film ferromagnets and antiferromagnets

P. Nemeč<sup>1</sup><sup>1</sup>Charles University, Faculty of Mathematics and Physics, Prague 2, Czech Republic

Recent breakthroughs in electrical detection and manipulation of antiferromagnets have opened a new avenue in the research of non-volatile spintronic devices. Antiparallel spin sublattices in antiferromagnets lead to the insensitivity to magnetic field perturbations, multi-level stability and ultra-fast spin dynamics. However, these features also make the characterization of antiferromagnetic materials, in particular of thin metallic films suitable for spintronics, a major challenge [1]. In this contribution we show how the know-how, which we achieved in the pump-probe study of diluted ferromagnetic semiconductor (Ga,Mn)As [2,3], can be transferred to the research of thin films of compensated antiferromagnetic metal CuMnAs [4], where terahertz writing speed in a non-volatile antiferromagnetic memory device has been demonstrated recently [5].

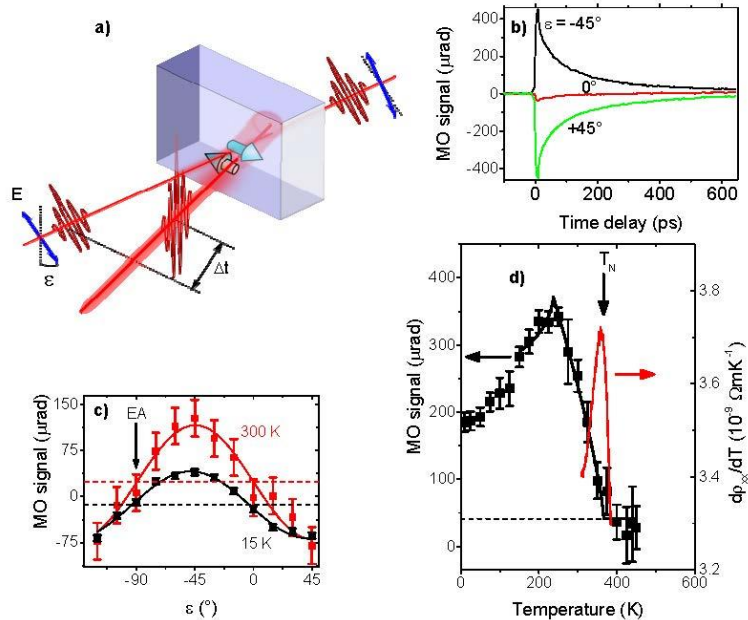


**Fig. 1.** Investigation of 10 nm thick film of compensated antiferromagnetic metal CuMnAs [4]. a) Schematic illustration showing how strong laser pulse-induced demagnetization leads to a reduction of Voigt effect-related probe polarization rotation, which is detected as a function of time delay  $Dt$  between pump and probe pulses for various probe pulses polarization plane orientations  $e$ , as shown in b). c) Probe-polarization dependence of pump-induced change of MO signal measured for  $Dt = 60$  ps at 15 K and 300 K, the vertical arrow depicts the position of the sample easy axis. d) Determination of the Néel temperature, depicted by a vertical arrow, from temperature dependence of MO signal (black). The red line is a temperature derivative of the sample resistivity.

## References

- [1] P. Nemeč, M. Fiebig, T. Kampfrath, and A. V. Kimel, *Antiferromagnetic opto-spintronics*, Nature Physics 14, 229 (2018).
- [2] P. Nemeč et al., *Experimental observation of the optical spin transfer torque*, Nature Physics 8, 411 (2012).
- [3] N. Tesařová, P. Nemeč et al., *Experimental observation of the optical spin-orbit torque*, Nature Photonics 7, 492 (2013).

- [4] V. Saidl, P. Němec et al., *Optical determination of the Néel vector in a CuMnAs thin-film antiferromagnet*, Nature Photonics 11, 91 (2017) .
- [5] K. Olejník, et al, *Terahertz electrical writing speed in an antiferromagnetic memory*. Science Advances 4, eaar3566 (2018).

**LD-I-3****Carbon nanotubes-localized surface plasmon fibre optic sensors for CO<sub>2</sub> gas detection**

*A. Rozhin<sup>1</sup>, T. Allsop<sup>1</sup>, R. Arif<sup>1</sup>, D. Webb<sup>1</sup>, R. Neal<sup>2</sup>*

*<sup>1</sup>Aston University, Electrical Engineering, Birmingham, United Kingdom*

*<sup>2</sup>University of Plymouth, Communications and Electronics, Plymouth, United Kingdom*

Single-Wall Carbon Nanotubes (SWNT) have a unique combination of optical, structural-surface properties making them promising for sensor and bio imaging applications [1]. A large number of electronic sensors based on chemical field effect transistors (FETs) and chemical resistors have been demonstrated over the past two decades [2]. Moreover, sensing on such platforms was achieved for different gases depending on the type of carbon nanotubes such as SWNT or Multi-Wall Carbon Nanotubes (MWNT) as well as for different functionalisation of their surface. Despite significant progress in the field, such sensors are of limited use in explosive environments due to a possible electrical sparks and alternative approaches are urgently needed.

In our report, we show a new type of sensor that uses optical gas detection with SWNT—Localized Surface Plasmon (LSP) platform. The LSP structure was developed on the surface of the D-shaped optical fibre by depositing thin layers (<40 nm) of Ge, SiO<sub>2</sub> and platinum. Subsequently, the resulting multi-layered structure was modified with a high power UV laser with a purpose to obtain an ordered array of nanowires, which supports the LSPs. Then, we deposited SWNTs functionalised by Polyvinylpyrrolidone (PVP) on the surface of the nanowires array. The resulting SWNTs-LSP platform showed excellent selectivity for detecting CO<sub>2</sub> with a sensitivity of about 150-500 ppm [3]. This method has a high potential for sensing of other gases, as well as for multiple gases detection depending on functionalisation of SWNTs and configurations of optical sensors.

**References**

- [1] I. Zaporotskova, et al., *Modern Electronic Materials* 2, p.95 (2016).
- [2] T. Zhang, et al., *Nanotechnology* 19, p. 332001 (2008).
- [3] T. Allsop, et al., *Light S&A* 5, e16036; doi: 10.1038/lsa.2015.36 (2016).

**LD-I-4****Laser methods in aerosol science**

*D.A. Czitrovsky<sup>1</sup>, A. Nagy<sup>1</sup>, M. Veres<sup>1</sup>, S. Kugler<sup>1</sup>, I. Kreisz<sup>2</sup>*

*<sup>1</sup>Wigner Research Centre for Physics of the Hungarian Academy of Sciences,  
Applied and Nonlinear Optics, Budapest, Hungary*

*<sup>2</sup>Lasram Engineering Ltd., R&D Management, Budapest, Hungary*

Non-contact laser methods for study of atmospheric, urban, industrial or pharmaceutical aerosols are widely used for determination of their parameters. The unique possibility of measurement of concentration, size distribution, flow velocity, absorption, refractive index, shape-factor and other characteristics of aerosol particles by remote sensing using lasers, gives a number of benefits in comparison with other measurement methods. After development of a dozen of different instruments for aerosol measurements using lasers – e.g. laser particle counters and sizers, aerosol spectrometers, laser Doppler velocimeters, aerosol analysers, we present an overview of modern techniques and their application in study of air contamination of the atmosphere, aerosol drug delivery in human airways, determination of filtration conditions in operating theatres and industrial firms, etc.

This work was supported by the Hungarian National Research, Development and Innovation Fund under grant No. KFI\_16-1-2016-0055.

**LD-I-5****Stimulated Raman spectroscopy with femtosecond laser and spectral focusing detection**

*M. Veres<sup>1</sup>, D. A. Czitovszky<sup>1</sup>, L. Himics<sup>1</sup>, R. Holomb<sup>1</sup>, A. Nagy<sup>1</sup>, I. Rigo<sup>1</sup>, T. Vaczi<sup>1</sup>*

*<sup>1</sup>Wigner Research Centre for Physics, Department of Applied and Non-linear Optics, Budapest, Hungary*

During the last decades Raman spectroscopy became a routinely used characterization technique for many fields and materials. It gives information on vibrational modes and so on the structure (bonds, composition, functional groups, etc.) of the investigated medium. Raman scattering is of relatively low probability, however, several approaches can be used to enhance its sensitivity, including resonant Raman scattering or surface enhanced Raman scattering. Non-linear Raman techniques, like stimulated Raman spectroscopy are also available and with state of the art instrumentation they can offer even for video rate imaging and real time monitoring of cellular activity, biochemical reactions etc.

Normal Raman scattering is an inelastic light scattering process, in which part of the energy of the monochromatic incident light goes for the excitation of fundamental vibrations of the medium. SRS utilizes two coherent, temporally and spatially synchronized light sources (pump and Stokes beams having higher and lower energies, respectively) and when the energy difference of the two beams is equal to the energy of a vibrational transition of the investigated medium, stimulated excitation of that vibration occurs. The intensity of the scattered light at the pump wavelength experiences a stimulated Raman loss, while that of the scattered light at the Stokes wavelength experiences a stimulated Raman gain. The cross-section of the SRS process is around six orders of magnitudes higher than conventional Raman scattering, and so it has much better sensitivity. SRS microscopy is capable of high-speed spectral imaging of samples ranging from single cells to human patient tissues. Here we report on the development of an imaging SRS system utilizing femtosecond lasers and spectral focusing detection.

A dual output Coherent Chameleon Discovery femtosecond laser was used as light source for the SRS system, which was coupled into a Femtonics FemtoSmart two-photon scanning microscope. Special optics have been incorporated between the laser and the microscope consisting of a motorized delay line in the Stokes beam for temporal synchronization, acousto-optic modulator for the pump beam (for lock-in detection) and dichroic mirror for collinear arrangement of the two beams before introducing them into the microscope. Both pump and Stokes beams were chirped to achieve dispersive pulse stretching. The amount of chirp was set so that equal chirp parameters were obtained for both beams. As a result the two pulses have equal energy difference allowing to excite the same vibrational transition for the whole duration of the pulse. The probed wavenumber can be tuned by changing the delay between the pulses. The SRS system was used to characterize different inorganic and biological samples.

This work was supported by the European Commission through the H2020 FET-OPEN project NEURAM (grant agreement 712821) and H2020 MSCA-RISE-2016 project VISGEN (grant agreement: 734862).

**LD-I-6****Characterization of the emission of laser deposition additive manufacturing process**

*A. Nagy<sup>1</sup>, S. Kugler<sup>1</sup>, I. Kreisz<sup>2</sup>, M. Veres<sup>1</sup>, A. Czitrovsky<sup>1</sup>*

*<sup>1</sup>H.A.S. Wigner Research Centre for Physics, Applied and Nonlinear Optics, Budapest, Hungary*

*<sup>2</sup>Lasram Engineering Ltd., R&D Management, Budapest, Hungary*

The laser metal deposition technology is becoming one of the most important manufacturing technologies in the industry, due to its capabilities when building-up new prototype parts, enhancing or repairing parts. While significant progress has been made in understanding additive manufacturing processes and the structure and properties of the fabricated metallic components, the possible health effects related to the generated smoke during the processes are not widely recognized. Metal powders produced by inert gas atomization, contain alveolar as well as inhalable dust fractions and may contain hazardous elements. It is of crucial importance to recognize the potential hazards and provide a safe environment for the exposed persons.

Different instruments were used to measure the properties of the generated smoke while building-up a part from different alloys with an AM machine. The number and mass concentrations of the particles were measured by an Optical Particle Counter (Grimm 1.109) with 31 size channels in the range of 0.3-32  $\mu\text{m}$ , an Aerodynamic Particle Sizer Spectrometer (TSI 3321) with 52 size channels in the range of 0.5-20  $\mu\text{m}$ , a Scanning Mobility Particle Sizer (Grimm ) with 64 size channels per decade in the range of 0.01-1  $\mu\text{m}$ . The particles were also sampled by a cascade impactor and microscopy were utilized to characterize the morphology of the particles.

The research was supported by the Hungarian National Research, Development and Innovation Fund under grant No. 2017-1.3.1-VKE-2017-00039.

**LD-I-7****Raman spectroscopy and spectrophotometry studies of silicon nanoparticles for biophotonics**

*S. Zobotnov<sup>1</sup>, A. Kolchin<sup>1</sup>, A. Pavlikov<sup>1</sup>, F. Kashaev<sup>1</sup>, D. Kurakina<sup>2</sup>, A. Khilov<sup>2</sup>, P. Agrba<sup>3</sup>, M. Kirillin<sup>2</sup>, L. Golovan<sup>1</sup>, P. Kashkarov<sup>1</sup>*

<sup>1</sup>*Lomonosov Moscow State University, Faculty of Physics, Moscow, Russian Federation*

<sup>2</sup>*Institute of Applied Physics RAS, Laboratory of Biophotonics, Nizhny Novgorod, Russian Federation*

<sup>3</sup>*Lobachevsky State University of Nizhny Novgorod, Faculty of Radiophysics, Nizhny Novgorod, Russian Federation*

Nowadays silicon nanoparticles (Si-NPs) produced by mechanical grinding of porous silicon are efficiently used in bioimaging and therapeutic applications [1,2]. We suggest employing an alternative technique consisting in pulsed laser ablation in liquids (PLAL) to fabricate small and chemically pure Si-NPs for biomedical applications.

Pico- and femtosecond laser radiation was used to form the Si-NPs via PLAL from porous silicon targets. In our experiments the Si-NPs are fabricated in water, ethanol and liquid nitrogen and characterized by sizes smaller than 100 nm. Raman spectroscopy revealed a presence of the lines for crystalline ( $520\text{ cm}^{-1}$ ) and amorphous ( $480\text{ cm}^{-1}$ ) silicon phases (Fig.1a). An analysis of the ratio of these lines integral intensities indicated that the volume fraction of the crystalline particles is higher than 87% for all types of the studied samples.

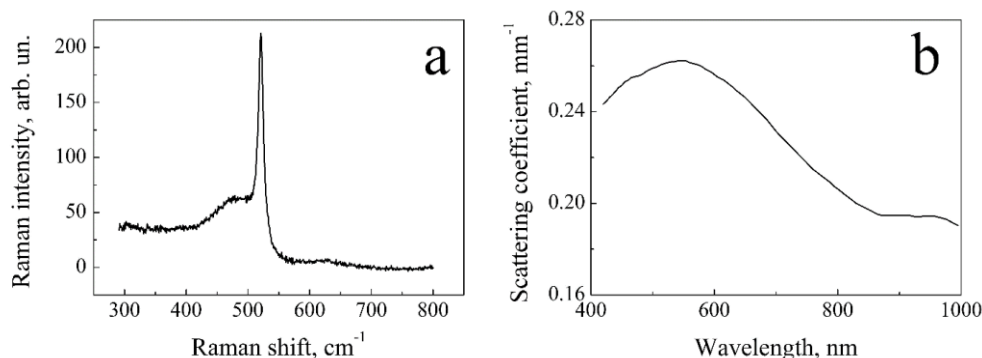


**Fig. 1.** Raman spectrum for Si-NPs ablated in water for excitation at 632 nm (a) and scattering coefficient spectrum for Si-NPs ablated in liquid nitrogen (b).

Spectrophotometry measurements of the ablated Si-NPs suspensions revealed that scattering coefficient value reaches up to  $0.3\text{ mm}^{-1}$  in the spectral range of 400 – 1000 nm (Fig.1b as example).

Optical coherence tomography imaging of the suspensions drops administered on agar gel surfaces indicated high efficiency of the Si-NPs as contrast agents providing the contrast up to 30 dB. Thus, the perspectives of the Si-NPs formed via PLAL in optical imaging are demonstrated. This work was supported by the Russian Science Foundation (project № 19-12-00192).

**References**

- [1] O.I. Ksenofontova, A.V. Vasin, V.V. Egorov, et al., *Tech. Phys.* 59, 66 – 77 (2014).
- [2] V. Stojanovic, F. Cunin, J.O. Durand, et al., *J. Mater. Chem. B* 4, 7050 – 7059 (2016).

**LD-I-8****Label-based and label-free optical nanoscopy of pathogenic bacterial species**

*M. Lucidi<sup>1</sup>, S.G. Stanciu<sup>2</sup>, D.E. Tranca<sup>2</sup>, R. Hristu<sup>2</sup>, A.M. Holban<sup>3</sup>, L. Nchele<sup>1</sup>, G.A. Stanciu<sup>2</sup>, G. Cincotti<sup>1</sup>*

<sup>1</sup>*University Roma Tre, Engineering, Rome, Italy*

<sup>2</sup>*University Politehnica of Bucharest, Center for Microscopy, Microanalysis and Information Processing, Bucharest, Romania*

<sup>3</sup>*University of Bucharest, Faculty of Biology, Microbiology and Immunology Department, Bucharest, Romania*

Nanoscopy techniques can overcome the Abbe's diffraction limit, which is about half the wavelength of the excitation light, and are capable to achieve resolutions of less than 50 nm. Stimulated Emission Depletion (STED) microscopy can increase the optical resolution of a conventional confocal microscope with up to one order of magnitude, by switching off the fluorescence of dye molecules positioned in the outer regions of the excitation area with an intense doughnut shaped laser beam that depletes the electrons from the excited levels [1]. In our work, we stained different pathogenic bacterial species using the Abberior<sup>®</sup> STAR RED NHS, which has been previously utilized in STED imaging of eukaryotic cells. To our knowledge, this is the first experimental demonstration on prokaryotes' staining with this dye, and the obtained results suggest that Abberior<sup>®</sup> STAR RED NHS is able to label the membranes of both Gram-positive and Gram-negative bacteria.

We also characterized the same bacterial species with scattering-type Scanning Near-field Optical Microscopy (s-SNOM), a label-free technique for optical nanoscale imaging that we used in combination with Atomic Force Microscopy (AFM) to place the optical information into a topographic context, which is relevant for the viability of the imaged organisms. s-SNOM relies on the fact that the interaction between the enhanced near-field at the tip apex, which results upon its illumination with a focused laser beam, and the sample volume underneath modifies both the amplitude and the phase of the scattered light [2]. Besides qualitative studies, s-SNOM was recently used to determine at nanoscale resolution the refractive index (RI) of human erythrocytes [3]. For the first time, we use the same approach to determine the RI of both commensal and pathogen bacteria, which is useful for understanding in detail their optical properties and morphology.

**References**

- [1] G. Vicidomini, P. Bianchini, A. Diaspro, STED super-resolved microscopy, *Nat Methods*, vol.15, pp. 173-182, (2018).
- [2] F. Keilmann, R. Hillenbrand, Near-field microscopy by elastic light scattering from a tip, *Philos Trans A Math Phys Eng Sci*, vol. 362, pp. 787-805, (2004).
- [3] D.E. Tranca, S.G. Stanciu, R. Hristu, B.M. Witgen BM, G.A. Stanciu, Nanoscale mapping of refractive index by using scattering-type scanning near-field optical microscopy, *Nanomedicine*, vol.1, pp. 47-50, (2018).

**LD-I-9****Laser photoacoustic detection of ethylene emission during germination and early seedling development of tomato seeds stimulated by non-thermal plasma**

*C.E. Matei<sup>1</sup>, M. Monica<sup>2</sup>*

*<sup>1</sup>National Institute for Laser- Plasma and Radiation Physics, Laser Department, Magurele, Romania*

*<sup>2</sup>National Institute for Laser- Plasma and Radiation Physics, Department of Plasma Physics and Nuclear Fusion, Magurele, Romania*

The sustainability chain in agriculture and environment requires today efficient technologies that enhance productivity and ensure the high quality of the crops, protecting in the same time the environment by reducing waste and chemical pollution. One of the clean alternative to enhance the quality of the seeding material is the treatment of the seeds by the means of non-thermal plasma, method that has been proved in different studies to increase the germination rate, vigor and nutrient absorption.

There is a large palette of characterization methods for monitoring the seed germination and the subsequently growth processes, but until today to our knowledge is unknown any study based on the quantification of the ethylene emission during these early stages applied to plasma treated seeds.

We exposed tomato seeds (*Lycopersicon esculentum* hybrid Belle F1 from Seminis company) to plasma generated in a dielectric barrier discharge (DBD) at atmospheric pressure, with high air flow, so that the seeds were held in suspension within the discharge zone, at a reduced average power (0.55-1.43W). The expected advantage of this fluidized bed reactor is the more uniform treatment of the seeds due to their continuous movement in the plasma region.

After the exposure, the seeds were germinated in controlled conditions and we used a sensitive CO<sub>2</sub> laser photoacoustic spectroscopic instrument to measure the low levels (ppb) of the ethylene concentration emitted over several days starting with the germination moment. In our paper we shall present the obtained data for different patches of treated seeds, as well the correlation with the known growth parameters, i.e. average length of roots (MRL) and sprouts (MSL).

**Acknowledgements:** This work has been financially supported by the Executive Agency for Higher Education, Research, Development and Innovation Funding (UEFISCDI), project number PN-III-P4-ID-PCE-2016-0152 and the Ministry of Research and Innovation, Program Nucleu - LAPLAS V/2018.

**LD-I-10****Spectral and temporal characteristics of silicon quantum dot luminescence and their application in light conversion***I. Sychugov<sup>1</sup>**<sup>1</sup>KTH Royal Institute of Technology, Applied Physics, Stockholm, Sweden*

Strong size-dependent properties of nanocrystal quantum dots stipulate targeting individual particles for the investigation of their basic properties [1]. In this talk fundamental parameters of the light emission from silicon quantum dots will be summarized as deduced from single-dot emission, absorption and lifetime measurements [2-7]. In particular, emission and absorption states in individual silicon nanocrystals were studied by temperature-dependent photoluminescence and photoluminescence excitation experiments. Both close-to-spherical and elongated particles were probed and the results were compared to first-principle calculation. The comparison revealed good agreement with theory, where the intermixing of direct and indirect states in nanostructured silicon takes place as a function of nanoparticle size, shape and photon energy. Next, some applications of silicon nanocrystal quantum dots in light-conversion applications will be summarized [8-10]. An important feature of such nanoparticles is a large Stokes shift, stemming from the bulk material energy structure. This property makes these fluorophores good candidates for some light converting applications, such as in luminescent solar concentrators [10]. We have prepared hybrid materials with different polymers, where enhancement of quantum yield up to 60-70% was recorded in case of off-stoichiometry thiols, attributed to dangling bond passivation by polymer radicals. The resulting nanoparticle-polymer hybrids were successfully integrated with glass and their stability over months was demonstrated [9].

**References**

- [1] I. Sychugov, J. Valenta, J. Linnros, Probing Silicon Quantum Dots by Single-dot Techniques, *Nanotechnology*, 28 (2017) 072002.
- [2] I. Sychugov, F. Pevere, J.W. Luo, A. Zunger, J. Linnros, Single-dot Absorption Spectroscopy and Theory of Silicon Nanocrystals, *Phys. Rev. B*, 93 (2016).
- [3] I. Sychugov, F. Sangghaleh, B. Bruhn, F. Pevere, J.-W. Luo, A. Zunger, J. Linnros, Strong Absorption Enhancement in Si Nanorods, *Nano Lett.*, 16 (2016) 7937-7941.
- [4] J.W. Luo, S.S. Li, I. Sychugov, F. Pevere, J. Linnros, A. Zunger, Absence of Red-shift in the Direct Band Gap of Silicon Nanocrystals with Reduced Size, *Nat. Nanotechnol.*, 12 (2017) 930-932.
- [5] F. Pevere, F. Sangghaleh, B. Bruhn, I. Sychugov, J. Linnros, Rapid trapping as the origin of non-radiative recombination in semiconductor nanocrystals, *ACS Photon.*, 5 (2018) 2990-2996.
- [6] F. Pevere, C. von Treskow, E. Marino, M. Anwar, B. Bruhn, I. Sychugov, J. Linnros, X-ray radiation hardness and influence on blinking in Si and CdSe quantum dots, *Appl. Phys. Lett.*, 113 (2018) 253103.
- [7] M. Greben, P. Khoroshyy, I. Sychugov, J. Valenta, Non-exponential decay kinetics: Correct assessment and description illustrated by slow luminescence of Si nanostructures, *Appl. Spectrosc. Rev.*, 54 (2019) 1-44.
- [8] A. Marinins, Z. Yang, H. Chen, J. Linnros, J.G.C. Veinot, S. Popov, I. Sychugov, Photostable Polymer/Si Nanocrystal Bulk Hybrids with Tunable Photoluminescence, *ACS Photon.*, 3 (2016) 1575.
- [9] A. Marinins, R. Shafagh, W. Van der Wijngaart, T. Haraldsson, J. Linnros, J.G.C. Veinot, S. Popov, I. Sychugov, Light Converting Polymer/Si Nanocrystal Composites with Stable 60-70% Efficiency and their Glass Laminates, *ACS Appl. Mater. Interfaces*, 9 (2017) 30267-30272.
- [10] I. Sychugov, Analytical Description of a Luminescent Solar Concentrator Device, arxiv:1903.03788, (2019).

**LD-I-11****Atomically-thin colloidal CdTe and CdSe nanosheets: effect of spontaneous folding and its impact on optical properties**

*R. Vasiliev<sup>1,2</sup>, D. Kurtina<sup>2</sup>, L. Kozina<sup>2</sup>, A. Garshev<sup>1,2</sup>, V. Zaytsev<sup>3</sup>, I. Vasil'eva<sup>4</sup>, V. Shubin<sup>4</sup>, A. Gaskov<sup>2</sup>*

*<sup>1</sup>Lomonosov Moscow State University, Department of Materials Science, Moscow, Russian Federation*

*<sup>2</sup>Lomonosov Moscow State University, Department of Chemistry, Moscow, Russian Federation*

*<sup>3</sup>Lomonosov Moscow State University, Department of Physics, Moscow, Russian Federation*

*<sup>4</sup>Research Center of Biotechnology of the Russian Academy of Sciences, Bach Institute of Biochemistry, Moscow, Russian Federation*

Two-dimensional semiconductors have unique electronic and optical properties that are different from those of bulk materials. In present work, we report an effect of spontaneous folding of 2D CdTe and CdSe nanosheets and analyze its impact on a structure and optical properties.

CdSe and CdTe nanosheets with a thickness of about 1 nm and extended lateral sizes up to 400 nm were grown by the colloid method [1, 2]. The native stabilizer – oleic acid was exchanged for various thiol ligands, including L- and D-acetylcysteine molecules. Analysis of the crystal structure, morphology, and composition was carried out using HRTEM, HAADF-STEM, SAED, XRD and FTIR methods in dependence on ligand type.

We show that initially flat CdTe nanosheets are uniformly rolled up when oleic acid is replaced by thiols. Detailed study shows nanosheet folding along [110] direction forming multiwall scroll-like structures. In contrast, CdSe nanosheets were found initially rolled up into multiwall nanoscrolls and retained scroll-like shape after ligand exchange. Folding-unfolding process, however, preserves 2D optical properties.

The optical properties of nanosheets were studied by absorption, photoluminescence and circular dichroism spectroscopy. In the absorption and photoluminescence spectra, well-resolved LH, HH, and SO exciton transitions and a pronounced exciton luminescence band were observed. The exchange of ligands led to a spectral shift of all bands by a value of about 50 nm in the red region. In the spectra of circular dichroism, five pronounced rotational bands were found in the spectral range of 300-500 nm with a half-width of about 20 nm and a high magnitude of rotation with calculated g-factor of  $3 \times 10^{-3}$ . The folding mechanism and its impact on optical properties are discussed.

This work was supported by the Russian Foundation for Basic Research (Nos. 19-03-00481 and 16-29-11694).

**References**

- [1] N. N.Shlenskaya et.al. // *Chem. Mater.* 2017, 29 (2), pp 579–586.
- [2] R. B.Vasiliev et.al. // *Chem. Mater.* 2018, 30 (5), pp 1710–1717.

**LD-I-12****Plasmon-enhanced optical spectroscopies of semiconductor nanostructures**

*A. Milekhin<sup>1</sup>, M. Rahaman<sup>2</sup>, T. Duda<sup>1</sup>, E. Rodyakina<sup>3</sup>, R. Vasiliev<sup>4</sup>, K. Anikin<sup>1</sup>, V. Dzhanan<sup>5</sup>,  
A. Latyshev<sup>3</sup>, D. Zahn<sup>2</sup>*

<sup>1</sup>*A.V. Rzhhanov Institute of Semiconductor Physics, Laboratory of near-field optical spectroscopy and nanosensorics, Novosibirsk, Russian Federation*

<sup>2</sup>*Chemnitz University of Technology, Semiconductor Physics, Chemnitz, Germany*

<sup>3</sup>*A.V. Rzhhanov Institute of Semiconductor Physics, Laboratory of Nanodiagnostics and Nanolithography, Novosibirsk, Russian Federation*

<sup>4</sup>*Moscow State University, Department of Material Science, Moscow, Russian Federation*

<sup>5</sup>*V.E. Lashkaryov Institute of Semiconductor Physics, Department of Optics and Spectroscopy of Semiconductor and Dielectric Materials, Kiev, Ukraine*

The results of a Tip-Enhanced Raman Scattering (TERS) and Surface-Enhanced InfraRed Absorption (SEIRA) study of CdSe nanocrystals (NCs) and CdSe/CdS nanoplatelets (NPLs) on arrays of Au nanodiscs and nanoantennas fabricated using nanolithography are discussed.

Monolayers (MLs) of CdSe NCs with a size of 5-6 nm and sub-MLs of CdSe/CdS NPLs consisting of 1.5 nm CdSe core and 0.6 nm CdS shell were deposited on plasmonic substrates using the Langmuir-Blodgett technology.

TERS by longitudinal optical (LO) and surface optical (SO) phonons in CdSe-based nanostructures placed in the gap between the TERS tip apex and Au nanodiscs was observed. The spatial variation of LO and SO frequencies is explained by the heating induced by the strong local field under localized surface plasmon resonance (LSPR) conditions.

The TERS signal from CdSe NCs on Au nanodisk arrays forms a pattern of ordered rings with a diameter equal or below that of the Au nanodisks dependent on the excitation energy. A superposition of the TERS image on the corresponding AFM topography shows that the centers of the rings and Au nanodisks perfectly coincide. This indicates that the TERS signal strongly depends on the LSPR energy of the coupled system of the tip and the nanodisk and their relative position.

TERS maps for CdSe/CdS NPLs reproducing the size and shape of the NPLs are consistent with AFM images and allowed the phonon spectrum of single NCs and NPLs to be investigated. SEIRA by optical phonons of MLs of CdSe-based nanostructures on Au nanoantennas with structural parameters allowing the coupling of the LSPR and diffraction modes is discussed. The frequency positions of the absorption features evidence that the SO phonons of the NCs are active in the SEIRA spectra.

**Acknowledgements**

The reported study was funded by Volkswagen Foundation and RFBR in the research projects 19-52-12041 and 18-02-00615.

**LD-O-1****Photoluminescence and up-conversion in CdSe quantum dots in liquid-crystal polymer matrix**

*L. Golovan<sup>1</sup>, A. Elopov<sup>1</sup>, V. Zaytsev<sup>1</sup>, S. Zobotnov<sup>1</sup>, D. Zhigunov<sup>2</sup>, O. Karpov<sup>3</sup>, G. Shandryuk<sup>3</sup>, A. Merekalov<sup>3</sup>*

*<sup>1</sup>M.V. Lomonosov Moscow State University, Physics Department, Moscow, Russian Federation*

*<sup>2</sup>Skolkovo Institute of Science & Technology, Center for Photonics and Quantum Materials, Moscow, Russian Federation*

*<sup>3</sup>A.V. Topchiev Institute of Petrochemical Synthesis RAS, Laboratory 21 "Polymer Modification" named after N.A. Platé, Moscow, Russian Federation*

Study of nanocomposites based quantum dots (QD) is of great importance for fabrication of novel media for radiation generation and control. Employment of liquid-crystal polymers (LCP) as a matrix for the QD embedding is very promising since they allow formation of ordered QD arrays and high QD concentration. Measurement of QD-LCP nanocomposite photoluminescence (PL) spectra and PL kinetics is the first stage of study of such nanocomposites.

To reveal an effect of the matrix on carrier recombination in QDs we employed both CdSe and core/shell CdSe/ZnS QD embedded into smectic BA-6PA and amorphous PMBA-6A polymers with various QD mass fractions (up to 60%). QD diameter was 4.1 nm.

PL was excited by picosecond Nd:YAG laser pulses at 532 nm. The PL spectra contain two bands (2.15 and 1.70 eV) corresponding to exciton radiative recombination and radiative recombination in defects (traps) at QD-matrix interface, the latter band intensity increases for CdSe in LCP matrix in comparison with amorphous one and practically disappear in CdSe/ZnS QD nanocomposites. Increase of QD concentration results in PL lifetime decrease for QDs in LCP matrices. Time dependence of the PL signal is well described by sum of two decaying exponents for CdSe QD with decay time of 40-60 and 100-300 ns; the latter one disappears for CdSe/ZnS QDs. Comparison of LCP and amorphous matrix QD nanocomposites evidences faster PL decay and less quantum yield in the latter case. Core/shell QDs exhibit more effective PL and weaker effect of the matrix than CdSe QDs.

Employing femtosecond Cr:forsterite laser pulses (1250 nm, 80 fs, 80 MHz) allowed us to detect both second-harmonic (SH) and up-converted signals. Depending on types of QDs and matrices, the latter spectrum are either two-photon excited PL trap spectrum or anti-Stokes PL coincides with one excited at 532 nm. The up-conversion could be considered as an anti-Stokes PL in the QDs excited by the SH.

In conclusion, PL, SH and up-conversion measurements of CdSe and CdSe/ZnS QDs embedded in the polymer matrices indicate potential use of the LCP for formation of QD nanocomposites allowing effective light generation.

This work was supported by Russian Foundation for Basic Research (grant 18-02-00548), synthesis of QDs and polymer matrices was carried out within the State Program of TIPS RAS.

**LD-O-2****Laser cleaning of historical paper with pulsed and cw radiation**

*I. Balakhnina<sup>1</sup>, N. Brandt<sup>1</sup>, A. Chikishev<sup>1</sup>, Y. Juma<sup>2</sup>*

<sup>1</sup>*Moscow State University, Physical Department and International Laser Center, Moscow, Russian Federation*

<sup>2</sup>*Moscow Chemical Lyceum, Moscow, Russian Federation*

There has been considerable recent interest in the application of laser radiation in restoration of objects of cultural heritage [1,2]. In particular, laser radiation is used for cleaning of paper materials. For example, nanosecond pulsed laser radiation at a wavelength of 532 nm cleans paper surface from dirt or ink better than an eraser does without damaging the base layer [3]. Laser cleaning involves ablation, since the absorption of radiation by particles of dust or ink is significantly greater than that of cellulose fibers.

The results of [4,5] show that nanosecond pulsed laser radiation at a wavelength of 532 nm can be used not only to eliminate surface contaminants, but also bleach paper (i.e., restore original optical properties or decrease discoloration). Such effects also result from laser ablation.

In this work, we demonstrate that the paper ablation is a two-threshold process in which the first and second thresholds correspond to ablation of microparticles contained in paper material and cellulose fibers, respectively.

We also demonstrate bleaching of historical paper under cw irradiation at a wavelength of 532 nm, a laser power of 1 W, and an irradiation spot of 2 mm. The degree of bleaching (decrease in discoloration) is quantitatively determined using the  $L^*a^*b^*$  color coordinates. It is shown that a variation in the  $L^*$  coordinate depends on the exposure time. A significant distinctive feature of paper bleaching under cw irradiation is almost complete absence of degradation of ink on the surface of paper.

Prospects for application of laser ablation in the study and restoration of historical papers are discussed.

**References**

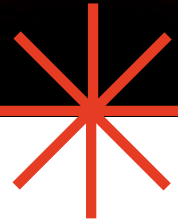
- [1] S. Siano, J. Agresti, I. Cacciari, D. Ciofini, M. Mascalchi, I. Osticioli, A.A. Mencaglia. Laser cleaning in conservation of stone, metal and painted artifacts: state of the art and new insights on the use of the Nd:YAG lasers. *Applied Physics A.*, 106: 419-446, 2012.
- [2] I.A. Grigoreva, V.A. Parfenov, D.S. Prokuratov, A.L. Shakhmin. Laser cleaning of copper in air and nitrogen atmospheres. *Journal of Optical Technology*, 84(1): 1-4, 2017.
- [3] J. Kolar, M. Strlic, D. Muller-Hess, A. Gruber, K. Troschke, S. Pentzien, W. Kautek. Laser Cleaning of Paper using Nd:YAG Laser Running at 532 nm. *Journal of Cultural Heritage*, 4:185, 2003.
- [4] I.A. Balakhnina, N.N. Brandt, A.Yu. Chikishev, N.L. Rebrikova, and Yu. Yurchuk. Laser ablation of paper: Raman identification of products. *Applied Physics A*, 117(4): 1865–1871, 2014.
- [5] I.A. Balakhnina, N.N. Brandt, A.Yu. Chikishev, I.G. Shpachenko, Single-pulse two-threshold laser ablation of historical paper. *Laser Physics Letters*, 15: 065605, 2018.



# ALT'19

**INTERNATIONAL CONFERENCE**

**Advanced Laser Technologies**



**PHOTONICS: FUNDAMENTALS,  
APPLICATIONS AND INTEGRATION**

**Prague, Czech Republic**



---

15-20 September 2019

**PH-I-1****Femtosecond, sub-nm-sensitivity probing of plasmonic near-field dynamics***P. Dombi<sup>1</sup>**<sup>1</sup>Wigner Research Centre for Physics, Ultrafast Nanooptics Group, Budapest, Hungary*

Probing nanooptical near-fields represents a major challenge in plasmonics research. Based on our previous research on plasmonic nanoemitters [1], we have shown that ultrafast photoemission from metal nanostructures induced by femtosecond laser pulses can constitute a highly sensitive tool for plasmonic near-field probing by using simple electron spectroscopic methods [2]. I will show how this technique can provide sub-nm sensitivity by exploiting the electron rescattering mechanism at the nanostructure surface. First applications in the investigation of the coupling of propagating and localized plasmon modes were also demonstrated on nanostructured surfaces [3]. In addition, time-resolved measurements of plasmonic near-field dynamics with unprecedented resolution were also performed, the very recent results of which will also be presented.

**References**

- [1] P. Dombi et al., Nano Lett. 13, 674 (2013).
- [2] P. RÁCZ et al., Nano Lett. 17, 1181 (2017).
- [3] J. Budai et al., Nanoscale 10, 16261 (2018).

**PH-I-2****Linear and nonlinear optical responses of plasmonic metasurface with sub-nm gaps***T. Takeuchi<sup>1</sup>, M. Noda<sup>1</sup>, K. Yabana<sup>1</sup>**<sup>1</sup>University of Tsukuba, Center for Computational Sciences, Tsukuba, Japan*

A plasmonic metasurface in which metallic nano-objects are periodically placed on a plane has attracted substantial attention in terms of its exotic optical characteristics [1]. Although investigations have been devoted mostly to metasurfaces with wavelength or sub-wavelength gap distances between constituent nano-objects, experimental studies have been reported recently for periodic structures with much smaller gap distances, reaching to sub-nm [2]. In isolated systems with a sub-nm gap such as a metallic nanodimer, it has been revealed that optical properties show substantial differences between theoretical descriptions using classical and quantum theories in the linear response regime [3]. The difference becomes remarkable for gap distances less than 0.4 nm [4] where the quantum tunneling across the gap becomes sizable. Furthermore, very recently, nonlinear responses of plasmonic metasurfaces with sub-nm gaps have been attracting attention since large third-order nonlinear susceptibility has been observed [5].

We theoretically and numerically investigate the plasmonic metasurface with sub-nm gaps in both linear and nonlinear response regimes. To take into account quantum mechanical effects in the analysis, we employ time-dependent density functional theory (TDDFT) treating the constituent nano-particles by a jellium model. SALMON (<https://salmon-tddft.jp/>) developed by our group [6] has been used for the numerical calculation. We will show transmission, reflection, and absorption rates of the metasurface for a weak incident field to elucidate the electron transport effect through the sub-nm gaps. We also show third-order harmonic generations to explore effects of the electron transport on their nonlinear optical response.

**References**

- [1] N. Meinzer, W. L. Barnes, and I. R. Hooper, *Nat. Photonics* 8, 889 (2014).
- [2] D. Doyle, N. Charipar, C. Argyropoulos, S. A. Trammell, R. Nita, J. Naciri, A. Piqué, J. B. Herzog, and J. Fontana, *ACS Photonics* 5, 1012 (2017).
- [3] W. Zhu, R. Esteban, A. G. Borisov, J. J. Baumberg, P. Nordlander, H. J. Lezec, J. Aizpurua, and K. B. Crozier, *Nat. Commun.* 7, 11495 (2016).
- [4] K. J. Savage, M. M. Hawkeye, R. Esteban, A. G. Borisov, J. Aizpurua, and J. J. Baumberg, *Nature* 491, 574 (2012).
- [5] L. S. Menezes, L. H. Acioli, M. Maldonado, J. Naciri, N. Charipar, J. Fontana, D. Rativa, C. B. Araújo, and A. S. L. Gomes, *J. Opt. Soc. Am. B* 36, 1485 (2019).
- [6] M. Noda, S. A. Sato, Y. Hirokawa, M. Uemoto, T. Takeuchi, S. Yamada, A. Yamada, Y. Shinohara, M. Yamaguchi, K. Iida, I. Floss, T. Otobe, K.-M. Lee, K. Ishimura, T. Boku, G. F. Bertsch, K. Nobusada, K. Yabana, *Comput. Phys. Comm* 235, 356 (2019).

**PH-I-3****Role of higher-order dispersion in second harmonic generation of ultra-short laser pulses in nonlinear photonic crystals***U. Sapaev<sup>1</sup>**<sup>1</sup>Tashkent State Technical University named after Islam Karimov, Faculty of Electronics and Automation, Tashkent, Uzbekistan*

Frequency doubling is the first nonlinear optical process demonstrated experimentally soon after the creation of lasers [1]. In the first experiment, its efficiency was only a fraction of a percent. Nowadays, the energy of primary emission can under certain conditions be almost fully converted to the second harmonic in quadratic nonlinear crystals as, e.g., in experimental works [2], which demonstrated an almost ~95% efficiency using a "proper" modulation of input-beam spatial distribution. Those works, though, used relatively long (nano-, subpico) laser pulses as primary emission. Of interest today is detailed research into the conversion of shorter laser pulses down to several optical periods.

In spite of numerous nonlinear optical media, which can be used to implement frequency doubling and other types of frequency conversion, of special interest are nonlinear photonic crystals (NPC) (crystals with regular domain structure) [3]. Such crystals do not require traditional phase matching to be realized; it is implemented in them by choosing the nonlinear lattice period for selected wavelengths. Generation of the second harmonic in NPC is the most fully investigated nonlinear optical effect, and it has still not lost its significance. This is due to the following practical circumstances. First, the technology of producing femtosecond (chirped) laser pulses has been well developed to date [4]. (In 2018, the authors of that work were awarded the Nobel Prize in Physics for the "method of generating high-intensity, ultra-short optical pulses".) Second, the NPC fabrication technology has been so well developed to date that NPC with different (periodic, random, aperiodic, chirped etc.) domain configurations can be produced [5]. The theory of optical frequency conversion processes in 2D NPC is also being actively developed [6].

The use of ultra-short laser pulses in frequency conversion using NPC is known to lead to several undesirable effects, which reduce the conversion efficiency. These are, for example, the effects of dispersion and group-velocity difference of the interacting pulses [7]. As the results of previous works show [8], these effects can be compensated for by using NPC with linear chirps. In this case, the thicknesses of NPC layers vary linearly in the direction of waves' interaction. This enables generation of wide spectral-range pulses [9].

Here, the process of the frequency doubling of ultra-short laser pulses in NPC was systematically studied by a numerical method. As far as we are aware, this is the first study when the duration of the incident pulse was of the order of 5 fs. To determine the optimal second harmonic conditions, we analyzed the effects of both the phase modulation of the primary pulse and the spatial linear chirp of NPC. The effect of up to the third order of dispersion in spatially chirped NPC was taken into account.

**References**

- [1] P. Franken, A. Hill, C. Peters, G. Weinreich, *Phys. Rev. Lett.* 3, 118 (1961).
- [2] A. A. Gulamov, E. A. Ibragimov, V. I. Redkorechev, T. Usmanov, *Quantum Electron.*, 10(7), 1305 (1983).
- [3] J. A. Armstrong, N. Bloembergen, D. Ducuing, P. S. Pershan, *Phys. Rev.* 127, 1918 (1962).

- [4] D. Strickland, G. Mourou, *Opt. Commun.* 56, 219 (1985).
- [5] D. S. Hum, M. M. Fejer, *Comptes Rendus Phys.* 8, 180 (2007).
- [6] V. Berger Nonlinear Photonic Crystals *Phys. Rev. Lett.* 81, 4136.
- [7] S. A. Akhmanov, V. A. Vysloukh, A. S. Chirkin, *Optics of Femtosecond Laser Pulses*, Nauka, Moscow (1988).
- [8] M. M. Fejer, G. A. Magel, D. H. Jundt, R. L. Byer, *J. Quant. Electron.* 28, 2631 (1992).
- [9] D. D. Hickstein *et al.* *Optica* 4, 1538 (2017).

**PH-I-4****Strong-field interaction and high-harmonic generation in solids**

*N. Tancogne-Dejean*<sup>1</sup>

<sup>1</sup>*Max Planck Institute for Structure and Dynamics of Matter, Theory, Hamburg, Germany*

Recently the strong-field electron dynamics in solids has received a lot of attention, in particular due to the experimental observation of high-harmonic generation (HHG) in solids. The generation of high-order harmonics from atomic and molecular gases enables the production of high-energy photons and ultrashort isolated pulses and obtaining efficiently similar photon energy from solid-state systems could lead, for instance, to more compact extreme ultraviolet and soft x-ray sources. However, in order to reach this goal, the microscopic mechanisms responsible for the ultrafast electron dynamics need to be understood properly.

The dynamics associated with strong fields implies the manipulation of the electrons on the attosecond time-scale, which could lead to tremendous applications in the emerging fields of strong-field optoelectronics and petahertz electronics.

In this talk, we show that *ab initio* calculations, performed within the framework of real-time time-dependent density functional theory (TDDFT), help unraveling the microscopic mechanisms responsible for strong-field physics in solids and two-dimensional materials. Interesting phenomena are predicted to occur when a strong laser interacts with different type of bulk materials, including correlated magnetic materials, or solids with defects. The predictive power of this approach is demonstrated by directly comparing the simulations results to the experimental data.

**PH-I-5****4D-laser technology in nanocluster physics: macroscopic quantum states in thin films on solid surface (modelling and experiment)**

*S. Arakelian<sup>1</sup>, I. Chestnov<sup>1</sup>, A. Istratov<sup>1</sup>, T. Khudaiberganov<sup>1</sup>, A. Kucherik<sup>1</sup>, S. Kutrovskaya<sup>1</sup>, A. Osipov<sup>1</sup>, D. Buharov<sup>1</sup>, O. Butkovskiy<sup>1</sup>*

*<sup>1</sup>Vladimir State University, Department of Physics and Applied Mathematics, Vladimir, Russian Federation*

1. Laser-induced nanostructures and thin films with controllable topology are depended on the laser pulses duration, and may be associated with the 4D-laser technology fabrication of new structures and materials. In fact, the interaction effects of solid targets with laser pulses of different durations for obtaining of various nanocluster structures can be viewed as the possibility of synthesizing the 4D-objects. The result depends not only on the stationary topological/geometric parameters of the system, but also on the dynamic interactions in the system leading to different final stable structures. This is due to the condition that specific mechanisms of nanostructuring are activated. Therefore, time plays the role of a control parameter responsible for phase transitions, as well as the spatial parameters do when nanostructures of various dimensions arise – from quantum dots (0D) to 3D nanostructures. We completed several laser procedures for obtaining nanostructures and thin films with controllable topology. They occur under development of different nonlinear processes in the system (thermodiffusion, gas-dynamic evaporation in pore-like structures with bubbles, ablation products, ballistic movement of the particles in liquid).

2. The physical properties of nanocluster systems are very sensitive to the form, size and distance/spatial distribution between their components. The fact is well known for any material in general, but to change these parameters and to carry out the stable conditions for the ordinary solid state objects we need to put the objects under extremal conditions (cf.[1]). In contrast, nanocluster structures can be easily modified in necessary way in the femto- nanophotonics laser experiments [2]. In our modeling the original shape of the nanoobject was considered spherical but being transformed by the key parameters: values and numbers of the azimuthal distortion coefficient (in terms of «latitude») and the zenithal distortion coefficient (in terms of «longitude»). The electronic energetic bands of the materials may vary dramatically in the case. The topology peculiarities of the granulated metallic film deposited on dielectric substrates are discussed in clustered metallic structures in path integral approach [3] for both Volt-Ampere characteristics and the optical transmission spectra (cf. [4-6]).

3. In superconductor problem the question is how to fabricate the coupling states for charged particles being responsible for electroconductivity. For a cluster system we discuss some alternative mechanisms of electronic coupling (in equilibrium states), and not via a standard Cooper phonon coupling [1]. In our experiment, we obtained a dramatic enhancement (in several orders) of electro-conductivity due to the variation of topological peculiarities of a nanocluster thin film system (cf. [7]). The process may be interpreted as a non-equilibrium phase transition in topological structure induced by laser radiation [8]. Random temporal and spatial variations in selection topological parameters may result in large variations of such coupling (cf. [9]).

**References**

- [1] Lifshitz E.M., Pitaevsky L.P. (2015) Theoretical Physics. Statistical Physics.Part.2: Theory of Condensate State. Vol. IX. *M.: Fizmatlit* 440.

- [2] Arakelian S.M., Kucherik A.O., Prokoshev V.G., et al.(2015) Introduction to the femtosecond nanophotonics, Fundamental principles and methods of laser diagnostics and control of nanostructured materials. *M.: Logos.* 744.
- [3] Feynmann R.P., Hibbs A.R. (1965) Quantum Mechanics and Path Integrals. *McGraw – Hill Book Company, N.Y.* 384.
- [4] Kavokin A. V., Kutrovskaya S. V., et. al. (2017) The crossover between tunnel and hopping conductivity in granulated films of noble metals. *Superlattices and Microstructures* 111:335-339.
- [5] Kutrovskaya S. V., Arakelian S. M., et. al. (2017) The Synthesis of Hybrid Gold- Silicon Nano Particles in a Liquid. *Scientific Reports* 7:10284.6.
- [6] Kucherik A., Kutrovskaya S., Osipov A., et al. (2019) Nano-antennas based on silicon-gold nanostructures. *Scientific Reports.* V.9. 338 (1-6).
- [7] Arakelian S.M., Kucherik A.O., Kutrovskaya S.V., et al. (2018) Laser-induced nanocluster thin-film systems with controlled topology and composition: the possibility of creating superconducting structures based on new physical principles. *Crystallography Reports.* 63. 7. P.1173-1177
- [8] Arakelian S., Kucherik A., Kutrovskaya S., Kavokin A. New challenges of femto-nanophotonics: basic principles and possible applications. (2019) *Journal of Physics: Conference Series.* V.1164. 012016 (1-7).
- [9] Horsthemke W., Malek Mansour M. (1976) The Influence of External Noise on Non-Equilibrium Phase Transitions. *Zs. Phys. B* 24. 307-313.

**PH-I-6****The laser synthesis of nanostructured carbon for photonics**

*A. Kucherik<sup>1</sup>, A. Osipov<sup>1</sup>, V. Samyshkin<sup>1</sup>, S. Arakelian<sup>1</sup>, M. Portnoi<sup>2</sup>, S. Kutrovskaia<sup>3</sup>*

*<sup>1</sup>Stoletov Vladimir State University, Physics and applied mathematics, Vladimir, Russian Federation*

*<sup>2</sup>University of Exeter, School of Physics, Exeter, United Kingdom*

*<sup>3</sup>Westlake University, Institute of Natural Sciences- Westlake Institute for Advanced Study, Westlake, China*

A regular flat array of ultimate one-dimensional (1D) carbon nanostructures – carbynes (also known as linear acetylenic or polyynes) – allows fully analytical treatment within the nearest-neighbor tight-binding model. A Peierls-type double-period distortion in the direction normal to carbyne chains results in a significant reduction of the band gap of the resulting 2D crystal and even in the band gap collapse for very closely-packed collapse. This effect is opposite to the Peierls distortion band gap opening in the purely 1D case. This system also allows analytic treatment of interband dipole transitions predicting a strong polarization and frequency dependence of the transition matrix elements.

We synthesize elongated linear carbon chains (carbynes) in a colloidal solution. The method based on the formation of carbon threads by laser ablation in a colloid accompanied by the stabilization of resulting linear carbon chains by gold nanoparticles. We deposit the synthesized carbyne threads and study free standing carbyne films with the transmission electron microscopy (TEM). TEM images of the carbon threads with gold nanoparticles attached to their ends demonstrate the straight monoatomic carbon chains with linear parts about 10-24 atoms. We observe the signatures of the polyynes allotrope of carbyne in the photoluminescence and Raman spectra of the solutions. We offer the tight-binding model for calculation the HOMO-LUMO optical transition in finite-length carbon chain. The results of our experiments and theoretical description pave the way to fabrication molecular system on base with controlled and tuned optical properties.

This study was supported by the Ministry of Education and Science of the Russian Federation (state project no. 16.5592.2017/6.7), Russian Foundation for Basic Research grant # 18-32-20006\_mol\_a\_ved. It has been performed with a participation of the Innovative Team of International Center for Polaritonics that is supported by Westlake University (Project No. 041020100118).

**PH-I-7****Laser-induced engineering and characterization of multimodal silicon-based nanoparticles***Y. Ryabchikov*<sup>1,2</sup><sup>1</sup>*HiLASE Centre, Institute of Physics of the Czech Academy of Sciences, Dolní Břežany, Czech Republic*<sup>2</sup>*P.N. Lebedev Physical Institute of the Russian Academy of Sciences, Department of Solid State Physics, Moscow, Russian Federation*

Recent progress in laser technologies provokes comprehensive studies on laser-matter interaction using various materials. One of the most interesting and most important employment of lasers is related to synthesis of new nanomaterials with unique properties for a wide set of applications. Interaction between ultrafast laser radiation and bulk/powder materials in different environments provokes efficient substance removal resulting to formation of nanoparticles with properties depending on experimental conditions [1]. Moreover, it has been shown lately that ultrafast laser irradiation significantly modifies semiconductor nanostructures in the presence of metal forming composite nanoparticles [2,3]. Such a modification reveals unique modalities ensuring biomedical applications of nanocomposites, in particular, molecule detection by means of surface-enhanced Raman scattering [4]. Nevertheless, study of laser-synthesized composite nanostructures is at an early stage and information about their properties and applications as well is still missed in literature.

In this work, different kinds of silicon-based nanostructures have been prepared by pulsed laser ablation synthesis. In order to form nanocomposites, a two-step method has been developed [2,3,5]. Firstly, pure silicon nanoparticles are prepared by laser-induced decomposition of silicon microparticles dispersed in deionized water. Their size distributions are controlled by multiple experimental parameters [1]. The second step – their laser-induced structural modification due to laser-ablation of a gold target immersed in silicon nanoparticle colloidal solution has been carried out.

In results, composite silicon-gold nanoparticles with strong size-dependent properties are formed. Synthesized nanostructures have been investigated by different structural, optical and electronic methods. Their employment for molecule detection using surface-enhanced Raman scattering ability is studied as well compared to initial silicon nanoparticles [4].

**Acknowledgements:**

This research work was financially supported from the European Regional Development Fund and the state budget of the Czech Republic (Project BIATRI: CZ.02.1.01/0.0/0.0/15\_003/0000445), from the Ministry of Education, Youth and Sports (Programs NPU I-Project no. LO1602).

**References**

- [1] Yu.V. Ryabchikov, Size Modification of Optically Active Contamination-Free Silicon Nanoparticles with Paramagnetic Defects by Their Fast Synthesis and Dissolution, *Physica Status Solidi* 216(2), A1800685 (2019).
- [2] Yu.V. Ryabchikov, Facile Laser Synthesis of Multimodal Composite Silicon/Gold Nanoparticles with Variable Chemical Composition, *Journal of Nanoparticle Research*, 21(4), 85 (2019).
- [3] Yu.V. Ryabchikov, A.A. Popov, M. Sentis, V.Yu. Timoshenko and A.V. Kabashin, Structural properties of gold–silicon nanohybrids formed by femtosecond laser ablation in water at different fluences, *Proc. of SPIE* 9737, 97370F–1–6 (2016).

- [4] M. Kögler, Yu.V. Ryabchikov, S. Uusitalo, A. Popov, A. Popov, G. Tselikov, A.-L. Välimaa, A. Al-Kattan, J. Hiltunen, R. Laitinen, P. Neubauer, I. Meglinski, A.V. Kabashin, Bare Laser-Synthesized Au-Based Nanoparticles as Non-Disturbing SERS Probes for Bacteria Identification, *Journal of Biophotonics*, 11(7), e201700225 (2018).
- [5] S. Kutrovskaya, S. Arakelian, A. Kucherik, A. Osipov, A. Evlyukhin, A.V. Kavokin, The synthesis of hybrid gold-silicon nanoparticles in a liquid, *Sci. Rep.*, 7, 10284 (2017).

**PH-I-8****Direct laser writing technique for creating non-enzymatic sensors**

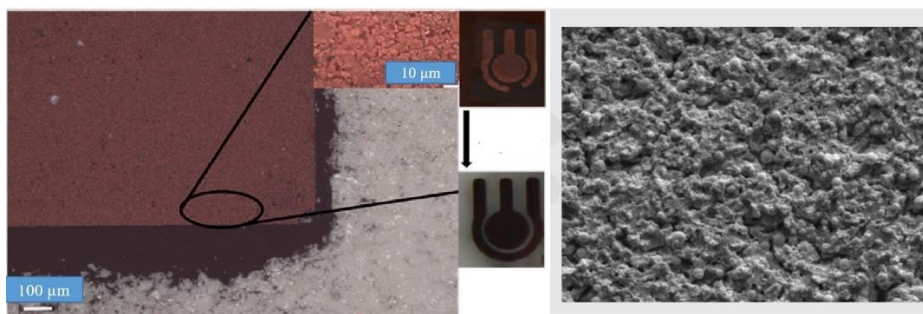
V. Andrianov<sup>1</sup>, E. Khairullina<sup>1</sup>, A. Smikhovskaia<sup>1</sup>, V. Mironov<sup>1</sup>, M. Panov<sup>1</sup>, M. Mizoshiri<sup>2</sup>,  
I. Tumkin<sup>1</sup>

<sup>1</sup>Saint Petersburg State University, Institute of Chemistry, Saint Petersburg, Russian Federation

<sup>2</sup>Nagaoka University of Technology, Dept. of Mechanical Engineering, Nagaoka, Japan

The development of the modern methods for fabrication of new nano- and microcomposite materials is quite important for medicine, science, and industry [1]. In recent years, more and more interest has been paid to the development and production of next-generation sensors, in which electron transfer does not occur through a mediator, but directly to the electrochemically active centers of the surface layer of a sensor material. This allows to significantly increase the analytical signal as well as improve sensitivity and selectivity.

In this work, the metallic and bimetallic electrodes will be fabricated using two methods: Laser-induced Chemical Liquid-phase Deposition of metals from solution (LCLD) [3] and reactive Selective Laser Sintering (SLS) [4]. Both approaches are related to Direct Laser Writing (DLW) techniques, the common feature of which is the localized interaction of laser radiation with the precursor leading to the initiation of a given chemical reaction and subsequent deposition of the required material on the surface of a substrate.



We used ceramic as well as polymeric (flexible) substrates, which are promising for creating flexible devices. The electrochemical measurements showed that metallic and bimetallic microelectrode created by Direct Laser Writing (DLW) techniques significant improvement of the sensor characteristics as compared to that of pure copper and many other analogs. Microelectrodes were used as working electrodes for electrochemical detection of such bioanalysts as glucose, hydrogen peroxide and amino acids.

I.I.T. thanks the Fellowship of President of Russia MK-6153.2018.3. The authors also express their gratitude to the SPbSU Nanotechnology Interdisciplinary Centre, Centre for Optical and Laser Materials Research, Centre for X-ray Diffraction Studies and Chemistry Educational Centre.

**References**

- [1] B.D. Ratner, A.S. Hoffman, F.J. Schoen, J.E. Lemons, Biomaterials Science: An Introduction to Materials in Medicine, third edition, Academic Press, 2012.
- [2] W. Liu, H. Zhang, B. Yang, Z. Li, L. Lei, X. Zhang, A non-enzymatic hydrogen peroxide sensor based on vertical NiO nanosheets supported on the graphite sheet, J. Electroanal. Chem. 749 (2015) 62-67.

- [3] A.V. Smikhovskaia, M.S. Panov, I.I. Tumkin, E.M. Khairullina, S.S. Ermakov, I.A. Balova, M.N. Ryazantsev, V.A. Kochemirovsky, The in situ laser-induced codeposition of copper and different metals for fabrication of microcomposite sensor-active materials, *Anal. Chim. Acta* 1044 (2018) 138–146.
- [4] S. Arakane, M. Mizoshiri, J. Sakurai, S. Hata, Direct writing of three-dimensional Cu-based thermal flow sensors using femtosecond laser-induced reduction of CuO nanoparticles, *J. Micromech. Microeng.* 27 (2017) 055013.

**PH-I-9****Laser optoacoustics of micro- and nanostructures***O. Romanov*<sup>1,2</sup><sup>1</sup>*Belarusian State University, Department of Computer Simulations / Faculty of Physics, Minsk, Belarus*<sup>2</sup>*HiLASE Centre, Institute of Physics of the Czech Academy of Sciences, Dolní Břežany, Czech Republic*

The photoacoustic (optoacoustic) effect is the formation of sound waves due to absorption of the modulated light pulse by irradiated medium. At the present time, the photoacoustic effect is widely used in biomedical studies (optoacoustic tomography), photoacoustic spectroscopy etc. Of particular interest are studies of the interaction of pulsed laser radiation with absorbing micro- and nanostructures. Absorption of pulse energy of the laser beam in materials with variation of the linear dimensions of the absorbent structures ranging from micro- to nanometers allows exciting acoustic oscillations in the frequency range from gigahertz to terahertz. Terahertz frequency acoustic vibrations are of special interest for fundamental research and have numerous potential applications (acoustic imaging of nano-objects, acoustic nanocavities, phononic crystals).

In this work a technique of the numerical simulation of equations of motion of continuous media in the form of Lagrange for a spatially inhomogeneous media (one, two, and three-dimensional micro- and nanostructures) has been developed. This model allows calculating fields of temperature, pressure, density and velocity of the medium depending on the parameters of laser pulses and the characteristics micro- and nanostructures. Examples of implementation of the model are discussed in connection with possible applications in the area of nanophotonics, nanoacoustics, and nanoplasmonics [1-3].

**References**

- [1] N. Khokhlov, G. Knyazev, B. Glavin, Y. Shtykov, O. Romanov, V. Belotelov. Interaction of surface plasmon polaritons and acoustic waves inside an acoustic cavity. // *Optics Letters*, Vol. 42, Issue 18, pp. 3558-3561 (2017).
- [2] Y.K. Shtykov, O.G. Romanov. Modeling of thermomechanical action of femtosecond laser pulses on metallic nanogratings // *Nonlinear Phenomena in Complex Systems*, 2018, Vol.21, No.2, pp.164 – 171.
- [3] V.I. Belotelov, A.N. Kalish, G.A. Knyazev, E.T.T. Nguen, O.G. Romanov, A.L. Tolstik. Optoacoustical transducer based on plasmonic nanoparticles // *Nonlinear Phenomena in Complex Systems*, 2019, V.22, N1, P.55-63.

**PH-I-10****Laser ablation of halide perovskites for nanophotonic applications**

*A.S. Berestennikov<sup>1</sup>, S. Makarov<sup>1</sup>*

*<sup>1</sup>ITMO University, Department of Nanophotonics and Metamaterials, Saint Petersburg, Russian Federation*

Halide-perovskite nanolasers have demonstrated fascinating performance owing to their efficient light emission and low-threshold lasing at room temperature as well as low-cost fabrication. However, being synthesized chemically, controllable fabrication of such nanolasers remains challenging, and it requires template-assisted growth or complicated nanolithography. Here, we review recent achievements for the fabrication of light-emitting nanoparticles and nanolasers by laser ablation of a thin film on glass with femtosecond laser beams [1-3]. The fabricated nanoparticles and nanolasers are made of  $\text{MAPbBr}_x\text{I}_y$  perovskite, which is a popular material in optoelectronics and photovoltaics. High-speed fabrication and reproducibility of nanostructures parameters, as well as precise control of their location on a surface, make it possible to fabricate centimeter-sized arrays of the nanolasers. Our finding is important for direct writing or printing of fully integrated coherent light sources for advanced photonic and optoelectronic circuitry [4].

**References**

- [1] A. Zhizhchenko, et al. “Single-Mode Lasing from Imprinted Halide-Perovskite Microdisks” *ACS Nano* 10.1021/acsnano.8b08948 (2019).
- [2] E. Tiguntseva, et al. “Light-Emitting Halide Perovskite Nanoantennas” *Nano Letters* 18 (2), pp 1185–1190 (2018).
- [3] E.Y. Tiguntseva, et al. “Tunable Hybrid Fano Resonances in Halide Perovskite Nanoparticles” *Nano Letters* 18 (9), 5522-5529 (2018).
- [4] S. Makarov, et al. “Halide-Perovskite Resonant Nanophotonics” *Advanced Optical Materials*, 1800784 (2018).

**PH-O-1****Bruggeman approximation and nanostructures agglomeration two-scale model**

*V. Krasovskii<sup>1</sup>, L. Apresyan<sup>1</sup>, T. Vlasova<sup>1</sup>, S. Rasmagin<sup>1</sup>, V. Kryshob<sup>1</sup>, V. Pustovoy<sup>1</sup>*

*<sup>1</sup>Prokhorov General physics institute, Russian Academy of Sciences, Laser physics, Moscow, Russian Federation*

The Bruggeman approximation [1], also known as the effective medium approximation (EMA), is one of the main heuristic approaches in the photonics of composite materials, making it possible to obtain reasonable estimates for various physical phenomena in randomly inhomogeneous systems without finding exact solutions to the problem (so-called homogenization theory [2]). An important advantage of this approximation is the possibility of describing the occurrence of a percolation threshold, which is absent when using simple forms of perturbation theory [3]. In the literature, several versions of generalizations of this approximation, initially describing isotropic inclusions, were proposed for the case of composites with anisotropic particles [4-6], in which ellipsoids appear instead of spherical particles. Each of them has its own expression for the percolation threshold, and the choice of the optimal model can be different for different specific tasks. When creating composite optical materials, the problem of uniform distribution of fillers in the matrix volume is essential. This problem is especially important in the case of nanocomposites, since nanoparticles often have a pronounced tendency to agglomerate. This paper compares several forms of these generalizations of the EMA, after which one of them is used to construct a two-scale agglomeration model, similar to that proposed in [7]. In this model, the initial filler nanoparticles are divided into two parts: “free” and “agglomerated”, i.e. clot-forming agglomerates. At the same time, to describe both agglomerates and “free” particles, the EMA approximation in the ellipsoid model is used twice, but with different depolarization tensors. As a result, it appears that agglomeration can both increase or decrease the percolation threshold as compared with the case of a completely homogeneous distribution of filler particles. This work was supported by Russian Foundation of Basic Research Grant No 18-02-00786 and Program of RAS presidium I.7P.

**References**

- [1] D.A.G. Bruggema, *Ann. Phys.* (23) 636-664 (1935). DOI: 10.1002/andp.19354160705.
- [2] L.A.Apresyan, *Light & Engineering*, 27 (1) 4-14 (2019). DOI: 10.33383/2018-094.
- [3] Milton G.W. *The Theory of Composites*. Cambridge Univ. Press, 2004.
- [4] Sihvola A. *Electromagnetic Mixing Formulas and Applications*, *Electromagnetic Wave Series 47*, London: IEE Publishing, 1999.
- [5] T. W. Noh, P. H. Song, and A. J. Sievers, *Phys. Rev. B* (44) 5459 -5464 (1991). DOI:10.1103/PhysRevB.44.5459.
- [6] D. Stroud and A. Kazaryan, *Phys. Rev. B* (53) 7076 (1996). DOI: 10.1103/PhysRevB.53.7076.
- [7] Y. Wang, J.W.Shan, G.J.Weng, *J. Appl. Phys.* (118) 065101 (2006). DOI: 10.1063/1.4928293.

**PH-O-2****Photodiodes for detection of IR radiation from WGM lasers**

*E. Kunitsyna<sup>1</sup>, I. Andreev<sup>1</sup>, G. Konovalov<sup>1</sup>, Y. Yakovlev<sup>1</sup>, Y. Lebiadok<sup>2</sup>, M. Ahmetoglu (Afrailov)<sup>3</sup>, B. Kirezli<sup>3</sup>*

<sup>1</sup>*Ioffe Institute, Laboratory of Mid-Infrared Optoelectronics, St. Petersburg, Russian Federation*

<sup>2</sup>*SSPA "Optics- Optoelectronics & Laser Technology"- NAS of Belarus, Optoelectronics Laboratory, Minsk, Belarus*

<sup>3</sup>*Uludag University, Department of Physics, Bursa, Turkey*

Semiconductor disk lasers operating on whispering gallery modes (WGM) in the IR range are of interest for laser-diode spectrometry, medicine, optical ultra-fast computing and switching systems. High Q factor of such lasers allows the use of the materials with low optical gain, thus resulting in a reduced threshold current and room temperature operation.

Detection of 2.0–2.3  $\mu\text{m}$  radiation from WGM lasers is an important task of mid-infrared photonics. For this purpose, cooled (77 K) InSb photodiodes are traditionally used. In this paper, we consider the possibility of applying the uncooled GaInAsSb/GaAlAsSb photodiodes for measuring the emission spectra of WGM-lasers.

The GaInAsSb/GaAlAsSb photodiodes exhibit a spectral sensitivity in the range of 0.9–2.4  $\mu\text{m}$  at room temperature. The monochromatic current sensitivity at the spectrum maximum is 1.1–1.2 A/W, which corresponds to a quantum efficiency of 0.6–0.7 without antireflection coatings. The operating speed of the photodiodes with 2 mm active area diameter at a load  $R = 50 \text{ Ohm}$  does not exceed  $t = 120\text{--}250 \text{ ns}$ . The radiation effect of  $^{60}\text{Co}$  ( $\gamma$ )-ray source with 6 MeV photon energy and  $1.5 \times 10^{11} \text{ gamma/cm}^2$  fluency on the electrical and optical characteristics the photodiodes was investigated.

The emission spectra of the 400  $\mu\text{m}$  half-disk WGM lasers based on quantum-dimensional GaInAsSb/GaAlAsSb heterostructure were studied using a spectrometer with resolution 2  $\text{\AA}$ . The lasers were excited with rectangular electrical pulses. The operating frequencies ranged from 2 to 16 kHz, the pulse duration could vary from 2 to 60  $\mu\text{s}$ . The pump currents were  $I = 140\text{--}250 \text{ mA}$ . As a result, equidistant laser modes were clearly observed on the spectra. The intermode distance of 12  $\text{\AA}$  indicates that the lasers work on the WGM modes of the first order.

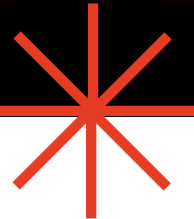
The work was supported by the Russian Foundation for Basic Research (RFBR) under Grant No 18-52-00027 and the Belarusian Republican Foundation for Fundamental Research (BRFFR), project  $\Phi 18\text{P-121}$ .



**ALT'19**

**INTERNATIONAL CONFERENCE**

**Advanced Laser Technologies**



**BIOPHOTONICS**

**Prague, Czech Republic**



---

15-20 September 2019

**B-I-1 (Keynote)****Shedding light on radiotherapy: optical coherence angiography (OCA) to assess tissue functional response to radiation**

A.Vitkin<sup>1</sup>

<sup>1</sup>*University of Toronto / Princess Margaret Cancer Centre, Toronto, Ontario, Canada*

Despite widespread use and tremendous technological and radiobiological advances, radiation therapy as a cancer treatment remains somewhat ‘blind’ – its relative success and outcome are often not known for weeks or months following treatment. Can advanced analysis of in-vivo optical coherence tomography (OCT) images of irradiated animal tumours detect early functional changes induced by radiotherapy? If yes, can these be used to ‘shed light on radiotherapy’ and optimize / personalize its treatment delivery? We address these questions by analyzing OCT temporal and spatial signal statistics (for microvascular and microstructural imaging, respectively). In this talk we will demonstrate the imaging and analysis pipeline, show representative preclinical and clinical results, and discuss implications.

**B-I-2****Translational dynamic optical coherence elastography**

*K. Larin*<sup>1</sup>

<sup>1</sup>*University of Houston, Biomedical Engineering, Houston, USA*

The biomechanical properties of tissues can be dramatically altered by various diseases, such as keratoconus for the cornea of the eye and systemic sclerosis for the skin. Therefore, the ability to measure tissue biomechanical properties could provide critical information for assessing its health and detecting disease etiology as well as monitoring disease progression. Here, I will present pilot results in development of noncontact dynamic optical coherence elastography (OCE) technique to evaluate the biomechanical properties of the cornea and skin of healthy subjects and those affected by diseases.

**B-I-3****Fluorescence lifetime spectroscopy and imaging in medical diagnosis**

L. Marcu<sup>1</sup>

<sup>1</sup>*Department of Biomedical Engineering, University of California at Davis, USA, CA 96516*

This presentation overviews fluorescence lifetime spectroscopy and imaging techniques for label-free in vivo characterization of biological tissues. Numerous studies have shown that tissue autofluorescence properties have the potential to assess biochemical features associated with distinct pathologies in tissue and to distinguish various cancers from normal tissues. However, despite these promising reports, autofluorescence techniques have been sparsely adopted in clinics. Moreover, when adopted they were primarily used for pre-operative diagnosis rather than surgery guidance. This presentation overviews clinically - compatible multispectral fluorescence lifetime imaging (FLIM) techniques developed in our laboratory and their ability to operate as stand-alone tools, integrated in a biopsy needle and in conjunction with the da Vinci surgical robot. We present clinical studies in patients undergoing surgery that demonstrate the potential of these techniques for intraoperative delineation of brain tumors and brain radiation necrosis as well as head and neck cancer including image-guided augmented reality during trans-oral robotic surgery (TORS). Challenges and solutions in the clinical implementation of these techniques are discussed.

**B-I-4****Laser speckle techniques for accessing biological function**

*P. Li<sup>1</sup>, J. Lu<sup>1</sup>, J. Hong<sup>1</sup>, X. Chen<sup>1</sup>*

*<sup>1</sup>Huazhong University of Science and Technology,*

*Wuhan National Laboratory for Optoelectronics, Wuhan, China*

Laser speckle is a phenomenon that will be produced when a coherent light is illuminated to biological tissues. Since the laser speckle is sensitive to the motion and deformation of tissue, laser speckle related techniques are widely attempted to estimate the mechanic and rheological properties of biological tissue, such as blood flow speed, viscosity, elasticity, diffusivity, viability and so on. Moreover, the blood volume and oxygenation can also be obtained by using multiple wavelengths. By combined with the imaging of either endogenous or exogenous fluorescence, we can further access the information of molecule inside the biological tissue. Laser speckle contrast imaging (LSCI) is a full-field, non-contact and low cost optical imaging method for monitoring blood flow and vascular morphology, which is attracting increasing applications in biomedical researches and clinics. Here, the methodology of laser speckle techniques for evaluation of tissue function are discussed, such as the quantitative model for temporal speckle contrast imaging of blood flow, the estimation of viscoelasticity using laser speckle, the imaging processing strategy for the denoising of laser speckle contrast imaging, and the spatial selective regulation of blood flow using wave front engineering and laser speckle. The applications of laser speckle on diagnosis and therapy of skin diseases, burn, and nerve block are also presented.

**B-I-5****Optical micromechanics using laser speckle approaches**

*S. Nadkarni*<sup>1</sup>

<sup>1</sup>*Harvard Medical School, Wellman Center for Photomedicine, Boston, USA*

It is well recognized that disease progression in most pathological conditions such as atherosclerosis, blood disorders, cancer, and orthopedic diseases is accompanied with alterations in the mechanical properties of affected tissues. For instance, the leading cause of death, myocardial infarction (MI) is caused by rupture of mechanically compromised atherosclerotic plaques. In a variety of clotting disorders that result in hyper- and hypo-coagulable states, coagulations defects are associated with changes in blood clot stiffness. In cancer diagnosis, mechanical cues have long been used to detect tumors by sensing tissue stiffness via palpation of the affected site. At the cellular level, altered mechanical properties of the tumor microenvironment have been shown to regulate malignant transformation and cancer cell proliferation independent of biochemical cues. Therefore, the significant evidence on the role of mechanical factors on disease initiation and progression calls for development of novel technologies for biomechanical evaluation of tissue *in situ*.

To meet the need for the mechanical analysis of tissue in its native state, we have developed an optical approach termed, Laser Speckle Rheology (LSR). In LSR, the sample is illuminated with coherent light and time-varying laser speckle patterns are acquired using a high speed CMOS camera. Laser speckle that occurs by the interference of coherent light scattered from the sample, is exquisitely sensitive to the passive Brownian motion of light scattering particles, in turn influenced by the viscoelastic susceptibility of the surrounding medium. We have previously shown, using LSR techniques, that the time scale of speckle intensity fluctuations is highly related with the viscoelastic properties of tissue. In this work, we discuss three opportunities for the application of the LSR technology platform for biomedical research and clinical use. In the first study, we discuss the feasibility of conducting LSR to evaluate the mechanical properties of human coronary plaques via a custom-developed, omni-directional viewing catheter suitable for intracoronary use. A second study demonstrates the utility of the LSR approach in detecting blood coagulation defects in patients by evaluating laser speckle patterns of clotting blood and measuring multiple coagulation parameters using a hand-held, smartphone compatible device. In the third case, we will describe an LSR instrument with improved spatial resolution that measures the mechanical properties of the tumor extracellular matrix and the heterogeneity of the invasive front in human breast carcinoma samples.

**B-I-6****Optical imaging for development and advancement of photodynamic therapy protocols**

*M. Kirillin<sup>1</sup>, D. Kurakina<sup>1</sup>, A. Khilov<sup>1</sup>, A. Orlova<sup>1</sup>, E. Sergeeva<sup>1</sup>, M. Shakhova<sup>2</sup>, A. Mironycheva<sup>3</sup>, A. Malygina<sup>3</sup>, I. Shlivko<sup>3</sup>, N. Orlinskaya<sup>4</sup>*

*<sup>1</sup>Institute of Applied Physics RAS, Laboratory of Biophotonics, Nizhny Novgorod, Russian Federation*

*<sup>2</sup>Privolzhsky Research Medical University, ENT Department, Nizhny Novgorod, Russian Federation*

*<sup>3</sup>Privolzhsky Research Medical University, Skin Diseases Department, Nizhny Novgorod, Russian Federation*

*<sup>4</sup>Privolzhsky Research Medical University, Pathomorphology Department, Nizhny Novgorod, Russian Federation*

Photodynamic therapy (PDT) is a modern treatment technique efficient against a number of tumor and non-tumor pathologies. This technique is based on photoactivation of a photosensitizer (PS) accumulated in the treated area prior to the procedure. Target delivery of PS to the treatment area in combination with proper illumination configuration provides high treatment specificity with low impact to surrounding healthy tissues. Specific optical properties of various PSs provide additional opportunities in configuring PDT protocols. Current paper reports on studies with chlorine-based PSs exhibiting pronounced absorption maxima in the blue and red spectral ranges. Due to spectral dependence of biotissue optical properties employment of different light wavelengths efficiently absorbed by a PS allows to select between superficial and deep action. Development of novel efficient PDT protocols requires for accurate control of a PDT procedure. Optical imaging techniques have high potential in monitoring of a PDT procedure: fluorescence imaging allows to monitor PS accumulation and photobleaching in the course of irradiation, while optical coherence tomography (OCT) with angiographic modality provides structural and functional information about biotissue.

In this paper we report on application of optical imaging techniques for monitoring of PDT performance in both experimental animal studies and clinical practice. The animal study aimed at comparative analysis of anti-tumor PDT protocols with chlorine-based PS employing irradiation with red and blue light and their combination on model CT-26 tumors in mice. The outcomes were verified by a histological inspection. The clinical part of the work reports on development of PDT protocols assisted by optical imaging modalities for treatment of actinic keratosis and basal cell carcinoma. Non-invasive intra-procedural temperature control is proposed as an additional tool for treatment tactics personalization.

The study is supported by Russian Science Foundation (project 17-15-01264).

**B-I-7****Live cell optical microscopy from the millimeter to the nanometer range**

*H. Schneckenburger<sup>1</sup>, V. Richter<sup>1</sup>, P. Weber<sup>1</sup>, M. Wagner<sup>1</sup>*

<sup>1</sup>*Aalen University, Institute of Applied Research, Aalen, Germany*

Optical microscopy is closely related to the Abbe or Rayleigh criterion, giving resolutions around 1  $\mu\text{m}$  for low numeric apertures (e.g. 10 $\times$ /0.30 objective lenses) and about 200 nm for high numeric apertures (e.g. 100 $\times$ /1.40 lenses). Furthermore, optical microscopy provides a depth of focus  $L = n \lambda / A_N^2$  of more than 5  $\mu\text{m}$  for low and around 400 nm for high aperture lenses. This implies that for low aperture and low magnification samples of about 1mm in diameter and 5-10  $\mu\text{m}$  thickness, e.g. cell monolayers, can be easily imaged with a resolution around 1  $\mu\text{m}$ .

If samples are thicker, some sectioning is required, and confocal as well as light sheet techniques have proven to be good standards. Both methods allow for sequential recording of individual layers and for combination in a 3D image. Only in the last 25 years methods have been described with a resolution below the Abbe criterion. They are summarized under the term “super-resolution microscopy“, and include (1) *Stimulated Emission Depletion (STED) Microscopy* where upon optical excitation in a laser scanning microscope the fluorescent spot is confined to 70 nm or less. However, the irradiance exceeds that of a conventional fluorescence microscope considerably, making live-cell microscopy very difficult and requiring essential modifications; (2) *Super-localization microscopy* of single molecules located within a thin illuminated layer of a sample. PALM, STORM and related techniques permit a precision of localization below 20 nm, but again require very high irradiance and exposure times; (3) *Airy Scan* and *Structured Illumination Microscopy (SIM)*, both permitting an increase in resolution by a factor 1.7-2.0 compared to the Abbe criterion. They can be used at moderate light exposure, and appear ideal for live-cell fluorescence microscopy.

The present paper is focused on light sheet microscopy, SIM and their combination [1,2] as well as on *Axial Tomography* [3] permitting a deeper view into 3D cell assemblies and an isotropic resolution around 100 nm. For probing intermolecular distances of 10 nm or less *Förster Resonance Energy Transfer (FRET)* [4] is used in combination with *Total Internal Reflection (TIR)*, e.g. in molecular test systems of pharmaceutical agents.

**References**

- [1] H. Schneckenburger, V. Richter, M. Wagner: “Live-cell optical microscopy with limited light doses”, SPIE Spotlight Series, Vol. SL 42, 2018, 38 pages.
- [2] V. Richter, M. Piper, M. Wagner, H. Schneckenburger: “Increasing Resolution in Live Cell Microscopy by Structured Illumination (SIM)”, *Appl. Sci.* 9 (6) (2019) 1188.
- [3] V. Richter, S. Bruns, T. Bruns, P. Weber, M. Wagner, C. Cremer, H. Schneckenburger: “Axial Tomography in Live Cell Laser Microscopy”, *J. Biomed. Opt.* 22(9) (2017) 91505.
- [4] H. Schneckenburger, P. Weber, M. Wagner, S. Enderle, B. Kalthof, L. Schneider, C. Herzog, J. Weghuber, P. Lanzerstorfer: “Combining TIR and FRET in molecular test systems,“ *Int. J. Mol. Sci.* 20 (2019) 648.

**B-I-8****Guidance for deep brain surgery with optical fibres**

*D. DePaoli<sup>1</sup>, C. Leo<sup>2</sup>, P. Martin<sup>3</sup>, D. Côté<sup>1</sup>*

*<sup>1</sup>CERVO Brain Research Center, Physics, Quebec City, Canada*

*<sup>2</sup>Hospital Enfant Jesus, Neurochirurgie, Quebec City, Canada*

*<sup>3</sup>CERVO Brain Research Center, Neuroscience, Quebec City, Canada*

The clinical outcome of deep brain stimulation (DBS) surgery relies heavily on the implantation accuracy of a chronic stimulating electrode in a small target brain region. Most techniques that have been proposed to precisely target these deep brain regions were designed to map intracerebral electrode trajectory, prior to the chronic electrode placement, sometimes leading to positioning error of the final electrode. Taking advantage of diffuse reflectance spectroscopy and coherent Raman spectroscopy, we developed a new surgical tool that senses proximal brain tissue, through the tip of the chronic electrode, by means of a novel stylet which provides rigidity to DBS leads and houses fiber optics. As a proof of concept, we demonstrate the ability of our non-invasive optical guidance technique to precisely locate the border of the subthalamic nucleus during the implantation of commercially available DBS electrodes in anesthetized parkinsonian monkey. Innovative optical recordings combined to standard microelectrode mapping and detailed post-mortem brain examination allowed us to confirm the precision of optical target detection. We also show the optical technique's ability to detect, in real time, upcoming blood vessels, reducing the risk of hemorrhage during the chronic lead implantation.

**References**

- [1] D. T. DePaoli et al., J. Neurosurgery, 2019.
- [2] D. T. DePaoli, N. Lapointe, Y. Messaddeq, M. Parent, and D. Côté, "Intact primate brain tissue identification using a completely fibered coherent Raman spectroscopy system.," Neurophotonics, vol. 5, no. 3, p. 035005, Jul. 2018.

**B-I-9**

**Non-invasive measurement of cerebral blood flow as a biomarker injury, therapy and recovery**

T. Durduran<sup>1</sup>

<sup>1</sup>*ICFO-The Institute of Photonic Sciences, Medical Optics, Barcelona, Spain*

I will describe more than fifteen years of clinical research on acute ischemic stroke patients using measurements of microvascular cerebral blood flow with diffuse correlation spectroscopy (DCS) as a biomarker of injury, therapy and recovery. I will furthermore provide a vision for the future by going through the recent developments and future, emerging technologies.

**B-I-10****Fiber-based methods for deep brain calcium recording in behaving mice***L. Fu<sup>1,2,3</sup>, Z. Qi<sup>2,3</sup>, X. Li<sup>2,3</sup>**<sup>1</sup>Huazhong University of Science and Technology, wnl0, wuhan, China**<sup>2</sup>Collaborative Innovation Center for Biomedical Engineering, Wuhan National Laboratory for Optoelectronics-Huazhong University of Science and Technology, Wuhan, Hubei 430074, China**<sup>3</sup>Britton Chance Center and MOE Key Laboratory for Biomedical Photonics, School of Engineering Sciences, Huazhong University of Science and Technology, Wuhan, Hubei 430074, China*

Neuronal calcium transients are reflection of neuronal action potential firing. The microscopy should be able to catch the dynamic process of calcium signal transients with a good temporal and spatial resolution for deep brain. Here, we developed a multi-channel fiber photometry system for recording neural activities in several brain areas of an animal or in different animals [1]. With this system, we simultaneously acquired calcium signals from the bilateral barrel cortices of a head-restrained mouse or from the orbitofrontal cortices of three freely moving mice. In addition, a GRIN lens based confocal microscope is also developed to detect the specific cell type calcium signal of deep brain area with single cell resolution [2]. With a 500  $\mu\text{m}$  diameter GRIN lens implanted into the deep brain, approximately hundred neurons can be imaged at 15 frames per second in vivo, which is beyond out of the traditional two-photon microscopy. The activity signals of neurons have been efficiently recorded in orbitofrontal cortices, hippocampus, and striatum nucleus in head-fixed mice with different diameter GRIN lens by this system. Our new results about visual cue-dependent memory circuit for place navigation in hippocampus of mice will be also presented. As spatial coding is an important way for neurons to process information, it will be suitable for researches in deep brain function. In sum, relaying the deep brain calcium signals to the surface with optical fibers is an efficient approach to extend the in vivo optical detection methods. The methods we developed will potentially boost new discoveries in neural circuitry investigations, and finally facilitate the finding of new treatments of psychiatric diseases.

**References**

- [1] V. Emiliani, A.E. Cohen, K. Deisseroth, M. Häusser, “All-Optical Interrogation of Neural Circuits,” *The Journal of Neuroscience* 35(41), 13917–13926 (2015).
- [2] Ghosh KK, Burns LD, Cocker ED, Nimmerjahn A, Ziv Y, Gamal AE, Schnitzer MJ, “Miniaturized integration of a fluorescence microscope,” *Nat Methods* 8(10), 871-8 (2011).

**B-I-11****Plasmonic gap-enhanced Raman tags for biomedical applications***N. Khlebtsov*<sup>1</sup><sup>1</sup>*Institute of Biochemistry and Physiology of Plants and Microorganisms- RAS, Lab of Nanobiotechnology, Saratov, Russian Federation*

Gold and gold/silver layered nanoparticles, in which Raman molecules (RMs) are embedded in a nanometer-sized gap between metal layers (Au@RM@Au, Au@RM@Ag), have great potential in biomedical applications as highly efficient imaging SERS probes [1]. Compared to common SERS tags with outer RMs exciting by plasmonic near field, the embedded RMs of new probes are protected from environmental conditions and subjected to the strongly enhanced internal field in the gap. Another type of efficient SERS tags are the tip functionalized Au(core)@RM@Ag(shell) nanorods (TFNRs) operating in off-resonance mode [2].

In this talk, we summarize our recent efforts in synthesis [3, 4], electromagnetic simulation [5], dip-tissue imaging [2], and lateral flow immunoassay [6] applications of GERTs and tip-functionalized hybrid Au@RM@Ag SERS tags. In the final part of talk we present a reexamination of SERS dependence of Au nanorods (AuNRs) as a function of their aspect ratio and shape morphology. We used the etching method to prepare a set of AuNR colloids of equal number concentrations by keeping the AuNR width and shape morphology while the plasmon resonance was incrementally decreased from 920 to 650 nm through the finely tuned aspect ratio. AuNRs were functionalized with 4-nitrobenzenethiol and SERS spectra of colloids were measured under 785-nm laser excitation. We demonstrate a weak correlation between the plasmonic peak position and the SERS response. This observation contradicts the well-known four-power law for electromagnetic contribution to SERS signal. By contrast to weak plasmonic dependence of the SERS signal from the aspect ratio of AuNRs, the variations in shape morphology of AuNRs lead to strong increase in SERS response. Thus, the rational design of the nanoparticle shape morphology is more important factor towards highest SERS response compared to the on-resonance plasmonic tuning. Further work is needed to explain the discrepancy between the weak dependence of SERS enhancement on the on-resonance conditions and modern theoretical predictions based on classical electromagnetic [5] or quantum-corrected [7] models.

This research was supported by the Russian Scientific Foundation (project no. 18-14-00016) and by RFBR grants nos. 17-02-00075 and 18-52-7803.

**References**

- [1] Jin X., Khlebtsov B.N., Khanadeev V.A., Khlebtsov N.G., Ye J. Rational design of ultra-bright SERS probes with embedded reporters for bioimaging and photothermal therapy. *ACS Appl. Mater. Interfaces*, 2017, 9, 30387-30397.
- [2] Khlebtsov B.N., Bratashov D.N., Khlebtsov N.G. Tip-functionalized Au@Ag nanorods as ultrabright SERS probes for bioimaging in off-resonance mode. *J. Phys. Chem C*, 2018, 122, 17983–17993.
- [3] Khlebtsov B., Khanadeev V., Khlebtsov N. Surface-enhanced Raman scattering inside Au@Ag core/shell nanorods. *Nano Res.* 2016, 9, 2303-2318.
- [4] Khlebtsov B.N., Khlebtsov N.G. Surface morphology of a gold core controls the formation of hollow or bridged nanogaps in plasmonic nanomatryoshkas and their SERS responses. *J. Phys. Chem. C*, 2016, 120, 15385-15394.
- [5] Khlebtsov N.G., Khlebtsov B.N. Optimal design of gold nanomatryoshkas with embedded Raman reporters. *J. Quant. Spectrosc. Radiat. Transfer*, 2017, 190, 89-102.

- [6] Khlebtsov B.N., Bratashov D.N., Byzova N.A., Dzantiev B.B., Khlebtsov N.G. SERS-based lateral flow immunoassay of troponin I using gap-enhanced Raman tags. *Nano Res.*, 2019, 12, 413–420.
- [7] Lin L., Zhang Q., Li X., Qiu M., Jiang X., Jin W., Gu H., Lei D. Y., Ye J. Electron transport across plasmonic molecular nanogaps interrogated with surface-enhanced Raman scattering, *ACS Nano*, 2018, 12, 6492-6503

**B-I-12****Complementary approach to monitoring of photodynamic therapy with target nanoconstructs by fluorescence and optoacoustic imaging**

*I. Turchin<sup>1</sup>, M. Kirillin<sup>1</sup>, D. Kurakina<sup>1</sup>, V. Perekatova<sup>1</sup>, A. Orlova<sup>1</sup>, E. Sergeeva<sup>1</sup>, V. Plekhanov<sup>1</sup>, P. Subochev<sup>1</sup>, S. Mallidi<sup>2</sup>, T. Hasan<sup>2</sup>*

<sup>1</sup>*Institute of Applied Physics of the Russian Academy of Sciences, Radiophysical methods in medicine, Nizhny Novgorod, Russian Federation*

<sup>2</sup>*Massachusetts General Hospital- Harvard Medical School, Wellman Center for Photomedicine, Boston, USA*

We proposed a new complementary approach to monitoring of photodynamic therapy (PDT) of glioblastoma with the use of targeted nanoconstructs containing a photosensitizer (PS) benzoporphyrin derivative (BPD) and IRDye800 dye, antibodies for efficient accumulation of the drug in a tumor, and a chemotherapeutic agent for combined effect on tumor cells. Monitoring of PDT was based on the simultaneous fluorescent and optoacoustic (OA) imaging. The possibilities of a complementary approach were demonstrated in numerical simulations, phantom and *in vivo* studies.

Fluorescence images were simulated by two-step Monte Carlo technique: at first step the distributed fluorescence source is calculated as excitation radiation absorption map; at the second step fluorescence emission is simulated. Monte Carlo simulations combined for OA imaging with k-wave modeling allowed to study the feasibility of the complementary approach.

The optical phantom was designed as a mixture of agar, water, 20% Lipofundin and black ink. The concentrations of the phantom components were chosen to mimic optical properties of mice brain tissue at the excitation and detection wavelengths of both dyes. The liquid phantom was poured into the special cuvette with three transparent plastic tubes filled with IRDye800, BPD and DMSO.

The custom-made fluorescence imaging setup employed in the study included a CCD camera, a filter wheel, and an illumination system adapted for nanoconstruct components (both IRDye800 and BPD dyes). The OA imaging setup employed the concept of dark-field acoustic resolution photoacoustic microscopy, where the scanning OA head is represented by a conical fiber-optic illumination system combined with a spherically focused acoustic detector made of a polyvinylidene difluoride piezo film with a 25  $\mu\text{m}$  thickness. OA experiments were performed at the wavelengths of 690 nm and 785 nm corresponding to the maxima of the optical absorption spectra of BPD and IRDye800 markers.

Fluorescence imaging demonstrated higher contrast as compared to optoacoustic imaging for both components, however, strong light scattering in the surrounding media prevented accurate location of the markers. OA imaging demonstrated the sensitivity to both components enabling depth-resolved detection. Complementary information from fluorescence and OA imaging was shown to be useful in characterizing the drug containing volume. Perspectives of the developed approach in monitoring of a PDT procedure was studied in course of the BPD photobleaching. Fluorescent imaging is sensitive to photobleaching which is a measure of PDT efficiency, and it does not require direct contact with the tissue. Employment of the bimodal approach in monitoring of PS photobleaching indicated its high potential in intraprocedural PDT monitoring.

The work was carried out as part of the RFBR project 17-54-33043 onko-a.

**B-I-13****FDISCO: advanced solvent-based clearing method for imaging whole organs***D. Zhu*<sup>1</sup>*<sup>1</sup>Huazhong University of Science and Technology,  
Wuhan National Laboratory for Optoelectronics, Wuhan, China*

Various optical clearing methods have emerged as powerful tools for deep biological imaging. Organic solvent-based clearing methods, such as three-dimensional imaging of solvent-cleared organs (3DISCO), present the advantages of high clearing efficiency and size reduction for panoptic imaging of large samples such as whole organs, and even whole bodies. However, 3DISCO results in a rapid quenching of endogenous fluorescence, which has impeded its application. Here, we propose an advanced method named FDISCO to overcome this limitation. FDISCO can effectively preserve the fluorescence of various fluorescent probes, and can achieve a long storage time of months while retaining potent clearing capability. We used FDISCO for high-resolution imaging and reconstruction of neuronal and vascular networks. Moreover, FDISCO is compatible with labelling by multiple viruses and enables fine visualization of neurons with weak fluorescence labelling in the whole brain. FDISCO represents an effective alternative to the three-dimensional mapping of whole organs and can be extensively used in biomedical studies.

**References**

- [1] Yisong Qi,† Tingting Yu,† Jianyi Xu, Peng Wan, Yilin Ma, Jingtian Zhu, Yusha Li, Hui Gong, Qingming Luo, Dan Zhu\*, FDISCO: advanced solvent-based clearing method for imaging whole organs, *Science Advances*, 5(1), eaau8355, 2019.

**B-I-14****Integrated effects on skin immersion optical clearing *in vivo***

E. Genina<sup>1,2</sup>, A. Bashkatov<sup>1,2</sup>, V. Tuchin<sup>1,2,3</sup>, V. Zharov<sup>4</sup>

<sup>1</sup>Saratov State University, Optics and Biophotonics, Saratov, Russian Federation

<sup>2</sup>Tomsk State University, Interdisciplinary Laboratory of Biophotonics, Tomsk, Russian Federation

<sup>3</sup>Institute of Precision Mechanics and Control RAS, Laboratory of laser diagnostics of technical and living systems, Saratov, Russian Federation

<sup>4</sup>University of Arkansas for Medical Sciences, Arkansas Nanomedicine Center, Little Rock, USA

The use of optical clearing agents makes it possible to increase the probing depth of non-invasive optical diagnostic methods. However, the protective epidermal barrier of the skin prevents the penetration of hydrophilic immersion liquids into the deeper layers of the skin. The aim of this study is to improve the efficiency of skin optical clearing by increasing the permeability of the epidermis for polyethylene glycol with MW 300 (PEG-300) using different approaches.

We present the results of a comparative analysis of optical immersion clearing of skin in laboratory rats *in vivo* with and without preliminary ablation of epidermis, fraction microablation and/or sonophoresis. Laser ablation and microablation has been implemented using a setup based on a pulsed erbium laser ( $\lambda = 2940$  nm) with different hand-pieces. Sonophoresis has been applied with the following parameters: 1 MHz, 1 W/cm<sup>2</sup>, continuous mode. As an optical clearing agent (OCA) PEG-300 has been used. Basing on optical coherence tomography, we have estimated the scattering coefficient in the process of optical clearing in 2 regions at depths of 50 – 170  $\mu$ m and 150 – 400  $\mu$ m.

The results have shown that both surface and fraction ablation of skin *in vivo* lead to the local edema of the affected region that increases the scattering coefficient. However, the intense evaporation of water from the ablation zone facilitates the optical clearing at the expense of tissue dehydration, particularly in the upper layers. Besides, ablation enhances the transepidermal penetration of OCA. Sonophoresis also provides effective penetration of OCA into dermis. Time dependences of the skin optical clearing efficiency for separate and combined laser irradiation and therapeutic ultrasound action have been obtained.

**B-I-15****OCT and laser speckle imaging for quantification of diffusivity and impact on blood flow of diabetic tissues and organs**

*D.K. Tuchina<sup>1,2,3,4</sup>, P.A. Timoshina<sup>1,2</sup>, V.V. Tuchin<sup>1,2,3,5</sup>*

<sup>1</sup>*Saratov State University, Astrakhanskaya str. 83, 410012 Saratov, Russia*

<sup>2</sup>*Tomsk State University, Lenin's av. 36, 634050 Tomsk, Russia*

<sup>3</sup>*Laboratory of Molecular Imaging, Bach Institute of Biochemistry, Research Center of Biotechnology of the Russian Academy of Sciences, Moscow 119071, Russia*

<sup>4</sup>*Prokhorov General Physics Institute of the Russian Academy of Sciences, 38 Vavilova str., Moscow 119991, Russia*

<sup>5</sup>*Institute of Precision Mechanics and Control RAS, Rabochaya str. 24, 410028 Saratov, Russia*

Diabetes mellitus is a metabolic disease characterized by chronic hyperglycemia accompanied by the disruption of carbohydrate, lipid, and protein metabolism and development of long-term microvascular, macrovascular, and neuropathic disorders, that can be successfully monitored by optical methods [1,2]. This paper presents the results of OCT and speckle imaging studies of tissue pathological transformation associated with protein glycation in animals with model alloxan-induced diabetes. The usage of optical clearing agents (OCAs) as probing molecules for monitoring of tissue diffusivity at protein glycation and blood flow dynamics in the pancreas of animals with induced diabetes have also been analyzed.

Diffuse reflection, total and collimated transmission of ex vivo tissues of rats of the control and diabetic groups were measured by UV-3600 spectrophotometer (Shimadzu, Japan) in a wide spectral range of 350–2500 nm. The difference in optical properties of tissues was observed. Investigation of optical and diffusion properties of diabetic skin in vivo was performed using OCT with the central wavelength of 930 nm and multichannel fiber-optic spectrometer USB4000-Vis-NIR (Ocean Optics, USA) in the spectral range of 500–900 nm during action of glycerol solutions. Glycerol diffusion in diabetic skin was obtained as significantly slower than in the control.

One of the promising techniques for quantification of blood microcirculation is laser speckle contrast imaging (LSCI). The observed in this study significant differences in the response of blood vessels to the action of an OCA in diabetic and control animals could be associated with the differences in the permeability of normal and glycated tissues. The permeability of glycated tissue could vary depending on its structure and composition, as well as on the shape and size of the OCA molecule.

**References**

- [1] D. K. Tuchina and V. V. Tuchin, Optical and structural properties of biological tissues under diabetes mellitus, *Journal of Biomedical Photonics & Engineering* 4 (2) 020201-1-22 (2018).
- [2] O. A. Smolyanskaya, E. N. Lazareva, S. S. Nalegaev, N. V. Petrov, K. I. Zaytsev, P. A. Timoshina, D. K. Tuchina, Ya. G. Toropova, O.V. Korniyushin, A.Yu. Babenko, J.-P. Guillet, V. V. Tuchin, Multimodal optical diagnostics of glycated biological tissues, *Biochemistry (Moscow)* 84, Suppl. 1, S124-S143 (2019).

**B-I-16****Advances in confocal Mueller matrix polarimetry***J. Ramella-Roman<sup>1</sup>, I. Saytashev<sup>2</sup>, S. Sudipta<sup>3</sup>**<sup>1</sup>Florida International University, Biomedical Engineering and Herbert Wertheim College of Medicine, Miami, USA**<sup>2</sup>Florida International University, Herbert Wertheim College of Medicine, Miami, USA**<sup>3</sup>Florida International University, Physics, Miami, USA***Introduction**

Mueller Matrix Polarimetry is a linear modality that has been used extensively in the determination of orientation and retardation of fibrous tissues due to its sensitivity to birefringence. To this day, our understanding of the back reflected polarized signal is limited. We have developed a confocal microscopic system aimed at discriminating the provenance of the polarized signature into a multiscattering environment.

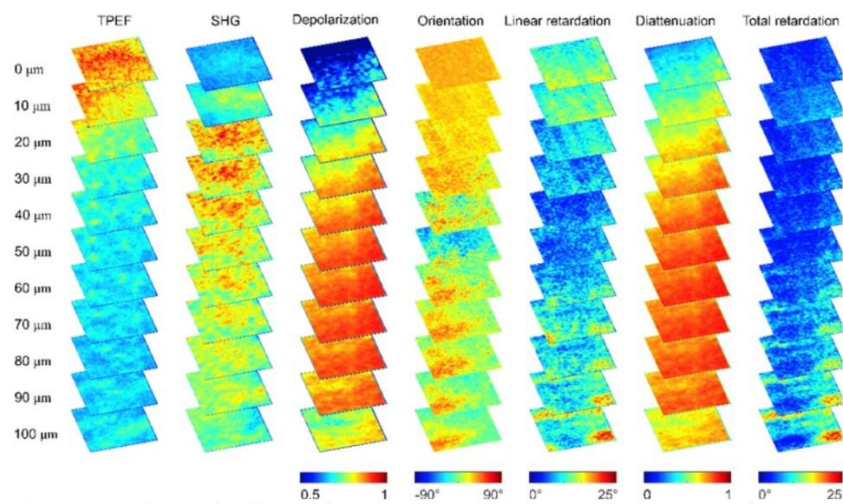
**Methods**

We have developed an instrument that combines two polarization imaging techniques, Muller Matrix reflectance microscopy and Muller Matrix confocal polarimetry, and integrated these modalities into a Nonlinear Microscope (NLM). This system allows for the collection of the total back-reflected Mueller Matrix image as well as depth dependent non-linear and confocal Mueller Matrix images.

The system is based on a pre-compensated femtosecond laser. The reflected light at fundamental wavelength is separated from epi-detected NLM by a short-pass dichroic mirror and directed to CMOS camera placed at the image forming conjugate plane. Dual Liquid Crystal Variable Retarders are used at both illumination and detection to construct the back reflected Mueller Matrix.

**Results/Discussion**

We acquired stacks consisting of 11 images with NLM images as well as depolarization, orientation, linear retardation, diattenuation, and total retardation maps. Polarization properties were assembled in 3D maps with RGB colormap. Typical data is shown in Fig. 1.

**Fig. 1.**

Strong *two-photon* excited fluorescence (TPEF) from epithelial cells of unstained corneas is due to NAD(P)H visualizing intracellular space, however cellular nuclei are represented as low-intensity spots. A change from epithelium to stroma is visualized by transformation of NL signals from TPEF to Second Harmonic Generation (SHG). We observed increase in depolarization and diattenuation, and decrease in linear retardation once the epithelial layer ended. Interestingly, there is a steady increase in retardation past 30  $\mu\text{m}$  depth, which is associated with the presence of collagenous lamellae. Furthermore we observed a significant retardation at epithelial layer obtained by Lu-Chipman decomposition.

### **Conclusions**

We have developed an imaging system that provides depth-resolved TPEF and SHG imaging to achieve 3D reconstruction of cellular and collagen distribution and confocal Mueller Matrix imaging to measure polarization properties and relate it to the total backscattered Mueller Matrix. Our results demonstrate the proof-of-concept depth resolved Mueller Matrix imaging validated by NL microscopy with a great potential in preclinical and clinical use.

**B-I-17****Optical properties of human normal and pathological colorectal tissues from 200 to 1000 nm**

*I. Carneiro<sup>1</sup>, S. Carvalho<sup>1</sup>, R. Henrique<sup>1</sup>, L. Oliveira<sup>2</sup>, V. Tuchin<sup>3</sup>*

<sup>1</sup>*Portuguese Oncology Institute of Porto,*

*Department of Pathology and Cancer Biology and Epigenetics Group-Research Centre, Porto, Portugal*

<sup>2</sup>*Polytechnic of Porto - School of Engineering, Physics Department, Porto, Portugal*

<sup>3</sup>*Saratov state University, Research-Educational Institute of Optics and Biophotonics, Saratov, Russian Federation*

Laser diagnostics and treatment procedures are commonly performed for visible and NIR wavelengths. The UV range is also of interest for clinical procedures, since some tissue chromophores present their absorption bands [1] and emit fluorescence in the UV range [2]. Skin diseases like psoriasis and vitiligo are commonly treated with UV light [3]. The UV range is also of interest due to the optimized refractive index matching that occurs in tissues in this range during optical clearing. Recent studies performed at optical clearing provided the discovery of two new tissue windows in the UV range that might allow the development of new diagnostic or treatment procedures [4], which will need the development of new light sources to work on the UV range. With the objective of evaluating the optical properties of tissues in a wide spectral range, and also to compare between normal and pathological tissues, we have obtained the wavelength dependencies for the optical properties of human normal and pathological colorectal mucosa between 200 and 1000 nm. The obtained results show great similarity to the ones we have previously obtained for the visible-NIR range, but provide greater information, showing the absorption peaks for proteins and DNA in the UV range. Comparing between the data obtained for normal and pathological mucosa, we observe that diseased tissue shows higher protein concentration. The obtained data was almost entirely calculated directly from experimental measurements, with the exception of the reduced scattering coefficient, which was obtained from inverse adding-doubling simulations.

**References**

- [1] M. C. Cheung, J. G. Evans, B. McKenna and D. J. Ehrlich, Deep ultraviolet mapping of intracellular protein and nucleic acid femtograms per pixel, *Cytometry A*, vol. 79, pp. 920-932, (2011).
- [2] I. J. Bigio and J. R. Mourant, Ultraviolet and visible spectroscopies for tissue diagnostics: fluorescence spectroscopy and elastic-scattering spectroscopy, *Phys. Med. Biol.*, vol. 42, pp. 803-814, (1997).
- [3] E. M. Cela, M. L. Paz, J. Leoni and D. H. G. Maglio, *Immunoregulatory Aspects of Immunotherapy* (IntechOpen), Chapter 5, (2018).
- [4] I. Carneiro, S. Carvalho, R. Henrique, L. Oliveira and V. V. Tuchin, Moving tissue spectral window to the deep-UV via optical clearing, *J. Biophotonics*, submitted.

**B-I-18****Laser measurements of erythrocyte aggregation in patients suffering from arterial hypertension**

*A. Lugovtsov<sup>1</sup>, L. Dyachuk<sup>2</sup>, P. Ermolinskiy<sup>3</sup>, A. Maslyanitsina<sup>3</sup>, A. Priezzhev<sup>1</sup>*

*<sup>1</sup>M.V. Lomonosov Moscow State University,*

*Department of Physics and International Laser Center, Moscow, Russian Federation*

*<sup>2</sup>M.V. Lomonosov Moscow State University, Medical Research and Education Center, Moscow, Russian Federation*

*<sup>3</sup>M.V. Lomonosov Moscow State University, Department of Physics, Moscow, Russian Federation*

Erythrocyte reversible aggregation is one of the major phenomena that affect blood microcirculation. Alterations in aggregation properties lead to changing the blood viscosity and, as a consequence, to changes in blood flow through vessels and capillaries. This can lead to significant impairment of blood function, which increases a risk of occurrence of vascular concomitant diseases, and even the mortality especially in the case of cardiovascular pathologies. The erythrocytes aggregation and interaction properties are expected to be impaired in patients with arterial hypertension (AH). Thus, it is necessary to control these parameters during diagnostics and treatment of cardiovascular diseases. In this work, complex studies of the alterations of aggregation parameters of erythrocytes in whole blood samples and of pair interaction of single cells in patients suffering from such a socially significant disease as AH were conducted by laser methods.

The light scattering (laser aggregometry) technique allows for assessing the parameters characterizing the ability of the erythrocytes to reversibly aggregate in large ensembles of the cells. All measurements were performed using the commercially available Rheoscan system (Rheomeditech, Korea). This technique is convenient, fast and relatively simple for in vitro measuring the aggregation properties of erythrocytes. It allows to register the kinetics of the spontaneous aggregation (time dependence of light intensity forward scattered from a sample of whole blood at rest) and shear-induced disaggregation (shear stress dependence of light intensity backscattered from a sample of whole blood under shear flow) of erythrocytes for obtaining the characteristic time of aggregates formation (aggregation rate), aggregation index as well as hydrodynamic strength of aggregates [1].

Home-made double channeled optical tweezers (OT) were used for measuring the aggregation velocity as well as the interaction forces on cellular level [2]. OT are formed by two single-mode Nd:YAG lasers and a water-immersion objective with high numerical aperture. OT allow for freely manipulating the individual cells with a tightly focused laser beam without direct mechanical contact.

In vitro measurements were performed with EDTA-stabilized human blood samples drawn from patients with AH (88 people) and practically healthy volunteers – control (18 people). It was shown that in AH-patients, the aggregation speed of the erythrocytes and forces of the cells interaction are significantly increased relative to those in the control group while the ability of erythrocytes to aggregate in large ensembles is significantly enhanced relative to that in the control group. Basing on the obtained results one can conclude that laser aggregometry and optical trapping and manipulation are appropriate techniques for estimating the blood aggregation properties in whole blood samples and on the level of individual cells.

The work was financially supported by the Russian Foundation for Basic Research grant No. 17-02-01200.

## References

- [1] A.V. Priezzhev, N.N. Firsov, J. Lademann, Light backscattering diagnostics of RBC aggregation in whole blood samples, Chapter 11 in Handbook of Optical Biomedical Diagnostics, Editor V. Tuchin, Washington: SPIE Press, pp. 651 – 674 (2012).
- [2] K. Lee, M. Kinnunen, M.D.Khokhlova, E.V.Lyubin, A.V.Priezzhev, I. Meglinski, A. Fedyanin, Optical tweezers study of red blood cell aggregation and disaggregation in plasma and protein solutions, Journal of Biomedical Optics, vol. 21(3), pp. 035001 (2016).

**B-I-19****Correlations between the blood microrheologic and microcirculation parameters in cardiological patients as determined by laser-optic methods**

*Y. Gurfinkel<sup>1</sup>, A. Priezzhev<sup>2</sup>, A. Lugovtsov<sup>2</sup>, P. Ermolinskiy<sup>2</sup>, L. Dyachuk<sup>3</sup>*

<sup>1</sup>*Lomonosov Moscow State University, Medical Research and Educational Center, MOSCOW, Russian Federation*

<sup>2</sup>*Lomonosov Moscow State University, Department of Physics and International Laser Center, Moscow, Russian Federation*

<sup>3</sup>*Lomonosov Moscow State University, Medical Research and Education Center, Moscow, Russian Federation*

The results of studying the hemorheological properties of the blood from scientific laboratories increasingly translated to cardiology clinics in order to implement them in treating those patients, in particular, who use antiplatelet agents and anticoagulants to improve blood viscosity and reduce the risk of blood clots in the heart cavities.

Recently we compared the blood aggregation parameters (aggregation index, characteristic time of aggregate formation, aggregation force and time) measured *in vitro* by laser aggregometry (LA) and optical trapping (OT) techniques with the parameters of blood rheology measured *in vivo* using vital digital capillaroscopy (VDC) in the nail bed capillaries. Overall 88 patients suffering from the arterial hypertension (AH) and patients with coronary heart disease (CHD) were enrolled in the study.

Our study revealed statistically significant correlation between the numbers of red blood cells (RBC) aggregated in the whole blood sample during the first 10 seconds of spontaneous aggregation *in vitro* and the presence of aggregates in the blood capillaries *in vivo*. Existence of correlation was also shown between the decrease in the average time of RBC aggregation measured *in vitro* and the decrease in the capillary blood-flow velocity (CBV) measured *in vivo*. The most pronounced deterioration in the rheological properties of blood *in vivo* and *in vitro* were found for patients with CHD. Measurements conducted with OT on single RBC in suspension showed statistically significant differences in the aggregation time for patients with AH and CHD ( $p < 0.05$ ) depending on the CBV obtained by the VDC. The aggregation time measured on single RBC with OT depending on and presence or absence of stasis in blood flow detected by VDC revealed no significant differences for the group of hypertensive patients ( $p > 0.05$ ), whereas for the group of patients with CHD, statistically significant differences were obtained ( $p < 0.05$ ).

Our results demonstrate the possibility of using laser aggregometry and optical trapping for estimating the alterations of microrheologic and, consequently, microcirculation parameters. Alterations of RBC aggregation parameters measured *in vitro* can be used to evaluate the alterations of vital capillary blood flow parameters in human body. The earliest detection of microcirculation disorders is the best way to prevent possible complications of cardiovascular diseases and thus provide a well-timed start of treatment.

The Russian Science Foundation supported this study with the grant No. 18-15-00422.

**B-I-20****Lymphedema tissue analysis using optical imaging and machine learning**

*Y. Kistenev<sup>1</sup>, A. Borisov<sup>1</sup>, V. Nikolaev<sup>1</sup>, D. Vrazhnov<sup>1,2</sup>, A. Knyazkova<sup>1</sup>, N. Kryvova<sup>1</sup>, E. Sandykova<sup>3</sup>*

*<sup>1</sup>Tomsk State University, Physics, Tomsk, Russian Federation*

*<sup>2</sup>Institute of Strength Physics and Materials Science of Siberian Branch of the RAS, Tomsk, Russia, Lab. of Phacoacoustics, Tomsk, Russian Federation*

*<sup>3</sup>Siberian State Medical University, Phesics, Tomsk, Russian Federation*

The term "lymphedema" is a kind of fat disorder caused by weak lymph infiltration in a tissue, leading to inflammation, hypertrophy of adipose tissue and fibrosis. The pathophysiology of lipedema is not clearly understood. Lymphedema is divided into primary and secondary. The origin of primary lymphedema mostly connected with genomic abnormality. One of the most important reasons of the secondary lymphedema is complication after cancer surgery or radiotherapy treatment.

There is no cure for lipedema, but there are treatment approaches that allow to slow down the progression. Proper diagnosis and treatment will help prevent complications [1]. Various methods for lymphedema diagnosis are used at the stage of clinical manifestations, which based on extrawater content in a tissue. They include evaluation and physical examination, by assessing volume and shape of the extremities, tissue impedance control in the kHz-MHz range [3].

It should take into account that tissue fibrosis is emerged before clinical manifestations of lymphedema [4]. Methods of optical imaging, such as optical coherent tomography, multi-photon microscopy etc. have spatial resolution of several microns, that is enough for tissue fine structure control.

Evaluation of changing of tissue structure can be based on methods of image analysis and image recognition. The machine learning allows to provide effective image based diagnosis. We plan to discuss most optimal approaches for image segmentation, informative features extraction and predictive model construction, which is suitable for early lymphedema detection.

The work was carried out under partial financial support of the Russian Fund of Basic Research (grant No.17-00-00186, grant No. 18-42-703012).

**References**

- [1] M.Caruana, Lipedema: A Commonly Misdiagnosed Fat Disorder, *Plastic Surgical Nursing*, 38 (4), pp. 149-152 (2018).
- [2] J. E. Tisaire, E.M. Rodrigo, S.Ribeiro et al., Concept Design of a New Portable Medical Device for Lymphedema Monitoring: A EIT Health ClinMed Summer School Project, *Proceedings of the 12th International Joint Conference on Biomedical Engineering Systems and Technologies (BIOSTEC Special Session on Designing Future Health Innovations as Needed)*, pp. 611-620 (2019).
- [3] E.S. Qin, M.J. Bowen, W. F. Chen, Diagnostic accuracy of bioimpedance spectroscopy in patients with lymphedema: A retrospective cohort analysis, *Journal of Plastic, Reconstructive & Aesthetic Surgery*, 71, pp.1041–1050 (2018).
- [4] M. Mihara et al., Pathological steps of cancer-related lymphedema: histological changes in the collecting lymphatic vessels after lymphadenectomy, *PLoS One*. 7(7), e41126 (2012).

**B-I-21****Femtosecond laser micro- and nanotexturing of dental implants: wettability and stem cell behavior**

*T. Itina<sup>1</sup>, X. Sedao<sup>2</sup>, I.S. Omeje<sup>1</sup>, C. Donnet<sup>1</sup>, A. Klos<sup>3</sup>, V. Dumas<sup>3</sup>, A. Guignandon<sup>4</sup>, A. Rave<sup>5</sup>, N. Shchedrina<sup>5</sup>, G. Odintsova<sup>5</sup>*

<sup>1</sup>*LabHC, UMR CNRS 5516/UJM/Univ. Lyon, Optics and Photonics, Saint-Etienne, France*

<sup>2</sup>*LabHC, UMR CNRS 5516/UJM/Univ. Lyon and GIE Manutech-USD, Optics and Photonics, Saint-Etienne, France*

<sup>3</sup>*ENISE, Univ. Lyon, UMR 5513 CNRS, Laboratoire de Tribologie et Dynamique des Systèmes, Saint-Etienne, France*

<sup>4</sup>*Laboratoire SAnté Ingénierie BIOlogie, UJM/Univ. Lyon, Sainbiose, Saint-Etienne, France*

<sup>5</sup>*ITMO University, Megaphotonics, Saint Petersburg, France*

Millions of people experience tooth loss during their life and need dental implants. In addition, implants are often installed earlier in life, so that their durability becomes a very important requirement. One of the ways to increase the durability is to perform surface structuring to increase the integration properties. For this, laser texturing of dental implants has a great advantage and potentially can help to maintain functional implants as long as possible. Particularly, laser-induced combinations of micro- and nano- reliefs alternate cell-surface interactions. A carefully chosen surface topography can literally guide cell behavior. The surface relief definition and laser-based fabrication are still challenging. For the fabrication, femtosecond laser irradiation of titanium-based surfaces is promising since it provides unique possibilities to realize multi-scale textures with high precision.

The choice of optimum surface relief is a key issue. One of the ideas proposed recently is to account for cell size in the fabrication of surface microrelief [1]. As for the nano-relief, herein we propose to use wettability tests for the proper choice. To check these ideas, a combination of cell behavior studies and wettability tests were performed, as described below.

- (i) A series of surface topographies were realized by using femtosecond laser micro- and nanostructuring of Ti alloy surface. Several templates with different size have been used for laser structuring (pits diameters from 50 $\mu\text{m}$  to 150  $\mu\text{m}$ ).
- (ii) Human mesenchymal stem cell cultures (hMSCs) have been then cultivated on structured surfaces. The results reveal that hMSCs preferentially place their nuclei in the smaller pits with a diameter on the order of the cell size. Furthermore, high-resolution laser process helped us to guide hMSCs' interactions with substrates for the development of textured implants with more predictable tissue integrative properties.
- (iii) Wetting tests were performed for several surface reliefs and the results were compared to those of several models (such as Wenzel, Cassie-Baxter, etc.). A considerable change upon ultrasound treatment was observed and explained based on the modeling.

The obtained results can be also helpful in the definition of the proper strategies and improvements for other implants. The reported study was supported by TEXLID project of LABEX MANUTECH-SISE (ANR-10-LABEX-0075), by MANUTECH-SLEGHT (ANR-17-EURE-0026), and by "Formalas" project of PHC KOLMOGOROV operated by Campus France.

**References**

[1] Y. Yu. Karlagina et al., Single step laser-induced fabrication and in vitro verification of the optimum surface topography for cells biointegration, in press.

**B-I-22****Intraoperative diagnosis of human brain gliomas using THz spectroscopy and imaging: a pilot study**

*O. Cherkasova*<sup>1,2</sup>, *A. Gavdush*<sup>2,3</sup>, *N. Chernomyrdin*<sup>2,3</sup>, *S.I. Beshplav*<sup>2,4</sup>, *I. Dolganova*<sup>3,5</sup>,  
*I. Reshetov*<sup>6</sup>, *G. Komandin*<sup>2</sup>, *A. Potapov*<sup>4</sup>, *V. Tuchin*<sup>7,8</sup>, *K. Zaytsev*<sup>2,3</sup>

<sup>1</sup>*Institute of Laser Physics of the Siberian Branch of the Russian Academy of Sciences, Biophysics Laboratory, Novosibirsk, Russian Federation*

<sup>2</sup>*Prokhorov General Physics Institute of the Russian Academy of Sciences, Laboratory of Submillimeter Dielectric Spectroscopy, Moscow, Russian Federation*

<sup>3</sup>*Bauman Moscow State Technical University, Laboratory of Terahertz Technology, Moscow, Russian Federation*

<sup>4</sup>*Burdenko Neurosurgery Institute, Moscow, Russian Federation*

<sup>5</sup>*Institute of Solid State Physics of the Russian Academy of Sciences, Chernogolovka, Russian Federation*

<sup>6</sup>*Institute of Regenerative Medicine, Sechenov First Moscow State Medical University, Moscow, Russian Federation*

<sup>7</sup>*Saratov State University, Department of Optics and Biophotonics, Saratov, Russian Federation*

<sup>8</sup>*Institute of Precision Mechanics and Control of the Russian Academy of Sciences, Saratov, Russian Federation*

Gliomas form the most common type of primary brain tumors [1]. Among the prognostic factor of glioma treatment, achievement of its gross-total resection is a crucial one for reducing the probability of tumor recurrence and increasing the patients' survival. Gliomas usually possess unclear margins, complicating their gross-total resection. Existing methods, applied to differentiate between healthy tissues and gliomas, do not provide satisfactory sensitivity and specificity of diagnosis, especially for low-grade gliomas [2]. Terahertz (THz) spectroscopy and imaging [3] represent promising techniques for the intraoperative neurodiagnosis [4,5]. In this work, we study the THz optical properties of human brain gliomas *ex vivo* featuring WHO grades I to IV, as well as of perifocal regions comprised of intact and edematous tissues [6]. The tissue specimens were characterized using the reflection-mode THz-pulsed spectroscopy and histology. The gelatin embedding of tissues allowed for sustaining their THz response unaltered for several hours, as compared to that of freshly excised tissues. We observed statistical difference between intact tissues and tumors. This allows to objectively uncover strengths of THz technology in the intraoperative diagnosis of human brain tumors.

This work was supported by the Russian Science Foundation (RSF), Project #18–12–00328.

**References**

- [1] Q. Ostrom et al., *Neuro-Oncology* 20(Suppl. 4), iv1–iv86 (2018).
- [2] T. Garzon-Muvdi et al., *Future Oncology* 13(19), 1731 (2017).
- [3] O.A. Smolyanskaya et al., *Progress in Quantum Electronics* 62, 1–77 (2018).
- [4] S.J. Oh et al., *Biomedical Optics Express* 5(8), 2837–2842 (2014).
- [5] Y.B. Ji et al., *Scientific Reports* 6, 36040 (2016).
- [6] A. A. Gavdush et al., *Journal of Biomedical Optics* 24(2), 027001 (2019).

**B-I-23****Triple modality transmission-reflection optoacoustic ultrasound (TROPUS) computed tomography of small animals**

*E. Merčep*<sup>1</sup>, *X.L. Deán-Ben*<sup>2,3</sup>, *D. Razansky*<sup>2,3</sup>

<sup>1</sup>*iThera Medical GmbH, Munich, Germany*

<sup>2</sup>*Faculty of Medicine and Institute of Pharmacology and Toxicology, University of Zurich, Switzerland*

<sup>3</sup>*Institute for Biomedical Engineering and Department of Information Technology and Electrical Engineering, ETH Zurich, Switzerland*

Rapid progress in the development of multispectral optoacoustic tomography techniques has enabled unprecedented insights into biological dynamics and molecular processes in vivo and noninvasively at penetration and spatiotemporal scales not covered by modern optical microscopy methods [2]. Ultrasound imaging provides highly complementary information on elastic and functional tissue properties and further aids in enhancing optoacoustic image quality [2]. We devised the first hybrid transmission-reflection optoacoustic ultrasound (TROPUS) small animal imaging platform that combines optoacoustic tomography with both reflection- and transmission-mode ultrasound computed tomography. The system features full-view cross-sectional tomographic imaging geometry for concomitant noninvasive mapping of the absorbed optical energy, acoustic reflectivity, speed of sound and acoustic attenuation in whole live mice with submillimeter resolution and unrivaled image quality [3]. Graphics processing unit (GPU)-based algorithms employing spatial compounding and bent-ray tracing iterative reconstruction were further developed to attain real-time rendering of ultrasound tomography images in the full ring acquisition geometry. In vivo mouse imaging experiments revealed fine details on the organ parenchyma, vascularization, tissue reflectivity, density and stiffness (Fig. 1).

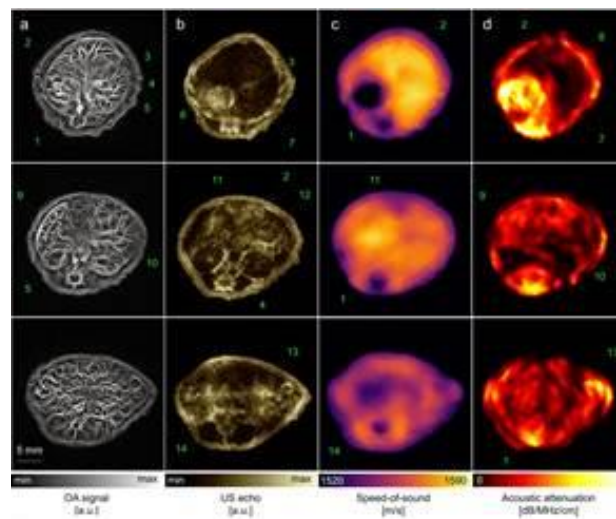


**Fig. 1.** Hybrid transmission-reflection optoacoustic ultrasound (TROPUS) whole-body mouse imaging. (a) Representative cross-sections acquired in the optoacoustic mode. (b) The corresponding reflection-mode ultrasound images. (c), (d) The corresponding transmission-mode ultrasound images showing the distribution of the speed of sound and acoustic attenuation, respectively. Annotations: 1: spinal cord; 2: liver; 3: vena porta; 4: vena cava; 5: aorta; 6: stomach; 7: ribs; 8: skin/fat layer; 9: spleen; 10: right kidney; 11: cecum; 12: pancreas; 13: intestines; 14: muscle.

We further used the speed of sound maps retrieved by the transmission ultrasound tomography to improve optoacoustic reconstructions via two-compartment modeling. The newly developed synergistic multimodal combination offers unmatched capabilities for imaging multiple tissue properties and biomarkers with high resolution, penetration and contrast.

**Acknowledgements:** Financial support is acknowledged from the European Research Council under grant ERC-2015-CoG-682379 and German Research Foundation Grant RA1848/5-1.

## References

- [1] X. L. Deán-Ben, S. Gottschalk, B. McLarney, S. Shoham, D. Razansky. Advanced optoacoustic methods for multi-scale imaging of in vivo dynamics. *Chem Soc Rev* 46, 2158-2198 (2017).
- [2] Merčep E, Burton NC, Claussen J, Razansky D. Whole-body live mouse imaging by hybrid reflection-mode ultrasound and optoacoustic tomography. *Opt Lett* 40, 4643-4646 (2015).
- [3] E. Merčep, J. L. Herraiz, X. L. Deán-Ben, and D. Razansky. Transmission-reflection optoacoustic ultrasound (TROPUS) computed tomography of small animals. *Light Sci Appl* 8, 18 (2019).

**B-I-24****Lasers for skin diagnostics - chromophore mapping and photon path length estimation***J. Spigulis*<sup>1</sup><sup>1</sup>*Institute of Atomic Physics and Spectroscopy, Biophotonics Laboratory, Riga, Latvia*

Recent developments in two laser technologies for in-vivo skin diagnostics will be discussed - multi-laser illumination for snapshot mapping of the main skin chromophores [1], and diffuse reflectance of picosecond laser pulses for determination of photon path lengths in skin structures [2]. A new prototype device enabling simultaneous uniform illumination of skin area by five laser wavelengths (405 nm, 445 nm, 520 nm, 635 nm, 850 nm) is under development and will undergo clinical validation. 405 nm laser line is used for skin autofluorescence excitation, while the spectral line images obtained at illumination by the other four laser wavelengths are exploited for distribution mapping of skin melanin, oxy-hemoglobin, deoxy-hemoglobin and bilirubin. Shape analysis of skin-remitted picosecond laser pulses in the spectral range 520-800 nm provided opportunity to experimentally determine the distributions of photon path lengths in skin at various input-output distances. Knowledge of such distributions helps to improve accuracy and reliability of the skin chromophore maps.

**References**

- [1] J. Spigulis, I. Oshina, A. Berzina, A. Bykov, "Smartphone snapshot mapping of skin chromophores under triple-wavelength laser illumination", *J.Biomed.Opt.*, 22(9), 091508 (2017).
- [2] M. Osis, V. Lukinsone, J. Latvels, I. Kuzmina, U. Rubins, J. Spigulis, "Skin remittance kinetics at the spectral range 550-790 nm", *Quant.Electr.*, 49(1), 2-5 (2019).

**B-O-1****Modeling of a photosensitizer fluorescence response during accumulation and photobleaching in biotissue**

*E. Sergeeva<sup>1</sup>, D. Kurakina<sup>1</sup>, A. Khilov<sup>1</sup>, M. Kirillin<sup>1</sup>*

*<sup>1</sup>Institute of Applied Physics RAS, Laboratory of Biophotonics, Nizhny Novgorod, Russian Federation*

Photosensitizer (PS) fluorescence registration upon its excitation in the course of a photodynamic therapy (PDT) procedure is a novel approach which allows for monitoring the PS distribution in biotissue and to predict the efficiency of PDT. The process of PS penetration and accumulation in biotissue as well as its photobleaching during PDT is accompanied by changes of its fluorescence response. To understand the PS fluorescence dynamics a proper analytical description of light penetration in tissue is required. Most analytical approaches are based on diffusion approximation (DA) of radiative transfer theory while it is not applicable within units of mm from the biotissue boundary. At the same time, this superficial region is the most important in PDT action. We have developed a novel hybrid analytical model of light penetration in biotissues which is valid both at small and large depths. The model is verified by the comparison with the results of Monte Carlo simulations. We have analytically evaluated the dynamics of a PS fluorescence in biotissue during its penetration after topical application. For a specific class of PSs with the two pronounced peaks of absorption spectrum in the red and blue ranges (e.g., chlorin-based PSs) it was demonstrated that due to dispersion of biotissue optical properties the PS penetration depth can be estimated from the ratio of fluorescence signals excited at the two absorption peaks. In the modeling of PS photobleaching during PDT procedure it was shown that red light exposure results in faster decay of fluorescence compared to the exposure in the blue region due to more uniform in-depth distribution of red light compared to blue light. The rate of photobleaching can be estimated by the dynamics of a ratio of fluorescence signals excited at the red peak versus blue peak. Simulated dynamics of the fluorescence signal ratio is in qualitative agreement with the dependencies observed in the course of clinical PDT procedures. The results of the proposed model can assist in understanding the experimentally observed PDT effects.

The study is supported by Russian Science Foundation (project 17-15-01264).

**B-O-2****Optical coherence microscopy combined with optical tweezers for cellular mechanics research**

*M. Sirotin<sup>1</sup>, M. Romodina<sup>1</sup>, E. Lyubin<sup>1</sup>, I. Soboleva<sup>1</sup>, A. Fedyanin<sup>1</sup>*

*<sup>1</sup>Lomonosov Moscow State University, Faculty of Physics, Moscow, Russian Federation*

Today the study of the micromechanical properties of single red blood cells is an urgent task. Deformation and aggregation properties of erythrocytes determine blood rheology in microvessels, so they significantly affect blood microcirculation, causing the occurrence of such pathologies as systemic lupus erythematosus, echinocytosis, as well as various forms of anemia and liver disease [1,2]. In this regard, the development of techniques allowing to determine the micromechanical properties of single living cells under conditions close to natural is of particular interest.

The main methods of studying the mechanics of erythrocytes are following: atomic force microscopy, the method of micropipette aspiration [3], cytometry with an alternating magnetic field [4], and also dynamic light scattering method [5]. However, these methods do not allow non-invasive examination of single living cells.

In our work, we combined two methods of studying micro-objects: optical tweezers and optical coherent microscopy (OCM). Optical tweezers allow us to control objects with submicron accuracy, and the OCM — to detect displacements with an accuracy of 10 nm and build three-dimensional images of the object [6,7].

The main advantage of combining these two methods is the ability to create mechanical excitation on the cell surface with tweezers, simultaneously detect the displacement of the membrane using phase OCM and study the three-dimensional structure of the cell. As a result, it becomes possible to non-invasively study the micromechanics of a living erythrocyte with high accuracy using external excitation with specified parameters.

The developed and assembled setup of optical coherent microscopy combined with optical tweezers allows us to obtain three-dimensional images of single biological cells with a lateral and axial accuracy of 1 micron (Fig. 1(a)); to initiate non-invasive mechanical vibrations of the cell membrane and at the same time to register membrane movement in any point of cell with an accuracy of 10 nm (Fig. 1(b)), which can give comprehensive data about the cell mechanics.

This work was supported by the Russian Foundation for Basic Research (No. 17-08-01716).

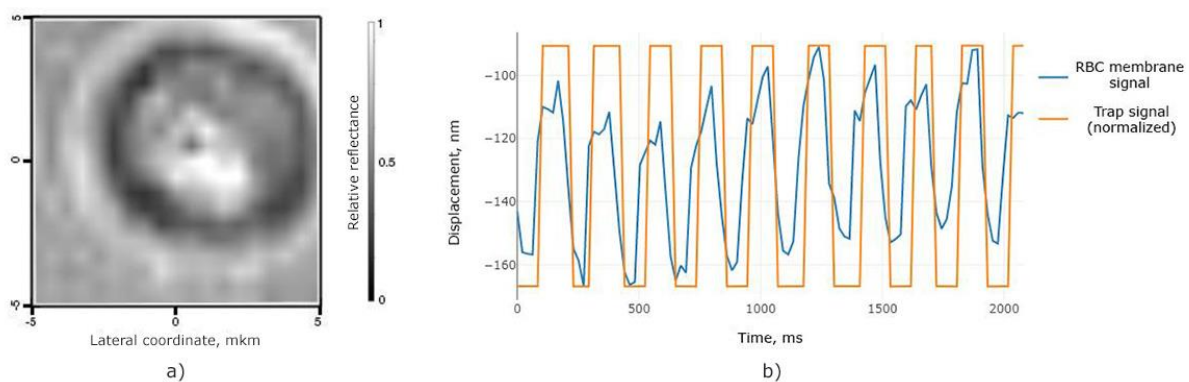


**Fig. 1.** (a) The slice of the three-dimensional image of the erythrocyte obtained by the OCM method. (b) The erythrocyte membrane displacement signal is represented by blue line. Orange line shows schematically the periodic turning optical trap on and off.

## References

- [1] Sokolova I. A., Koshelev V. B., *Technologies of Living Systems* 8 (2011).
- [2] James S. Owen, David J. C. Brown, David S. Harry, and Neil McIntyre, *J. Clin. Invest.* 76, No. 6 (1985).
- [3] Hochmuth R. M., *Journal of Biomechanics* 33 (2003).
- [4] Puig Morales-Marinkovic M., Turner K. T., Butler J. P., Fredberg J. J., Suresh S., *American Journal of Physiology - Cell Physiology* 293 (2007).
- [5] Berdnikov A. V., Semko M. V., Shirokova Yu. A., *Medical devices, systems and complexes* (2004).
- [6] Vasilica Crecea, Benedikt W. Graf, Member, IEEE, Taewoo Kim, Gabriel Popescu, and Stephen A. Boppart, Fellow, IEEE, *IEEE J. Sel. Top. Quantum Electron.* 20, No. 2 (2014).
- [7] Keir C. Neuman and Steven M. Block, *Review of Scientific Instruments* 75, No. 9, p. 2787 (2004).

**B-O-3****Classification of label-free cancerous cells in blood sample during flow based on interferometric phase microscopy (IPM)***N. Nissim<sup>1</sup>, N. Tzvi Shaked<sup>1</sup>**<sup>1</sup>Tel-Aviv University, Biomedical Engineering, Tel-Aviv, Israel*

The initiation and progression of acute diseases such as cancer and immune deficiencies, as well as wound repair and other regenerative processes often depend on the physiology of a small number of highly specialized cells. These cells can be obtained from biopsies including body fluids, such as blood and urine in easily taken routine lab tests [1]. In cell biology and medical research, in targeted diagnostics and in personalized therapeutic interventions, the identification and isolation of intact, disease-associated cell subsets from complex tissues or heterogeneous cell populations is of utmost importance [2].

Various strategies have been developed for the detection of cell types, the most widely used rely on antibody-based capturing of the cells like fluorescence-activated cell sorting (FACS) [3]. However, for many cell types, antigen combinations are missing that would allow for their unambiguous identification. Moreover, the inherent modification of the cell surface chemistry makes label-based approaches incompatible with noninvasive cell processing and, therefore, disqualifies them for usage in many cell therapeutic applications [4].

The refractive index (RI) of the cell interior is related to the optical interaction of the light field with cellular organelles and their chemical composition and, therefore, is easily accessible by optical techniques without affecting the cell physiology. Label-free interferometric phase microscopy (IPM) is able to measure the cell optical thickness profile in sub-nanometer sensitivity [5-8].

We propose an application for the noninvasive and automated cell processing, with high discriminative power on the level of the individual cell. By acquiring holograms of each cell using IPM and achieving its OPD profile, we extract features that highly differentiate cancerous cells from heterogeneous blood sample.

**References**

- [1] Alix-Panabières, C. & Pantel, K. Circulating Tumor Cells: Liquid Biopsy of Cancer. *Clin. Chem.* 59, 110–118 (2013).
- [2] Chen, Y. *et al.* Rare cell isolation and analysis in microfluidics. *Lab. Chip* 14, 626–645 (2014).
- [3] Watanabe, M. *et al.* Multicolor detection of rare tumor cells in blood using a novel flow cytometry-based system. *Cytom. Part J. Int. Soc. Anal. Cytol.* 85, 206–213 (2014).
- [4] Chen, C. L. *et al.* Deep Learning in Label-free Cell Classification. *Sci. Rep.* 6, 21471 (2016).
- [5] Girshovitz, P. & Shaked, N. T. Generalized cell morphological parameters based on interferometric phase microscopy and their application to cell life cycle characterization. *Biomed. Opt. Express* 3, 1757–1773 (2012).
- [6] Haifler, M. *et al.* Interferometric phase microscopy for label-free morphological evaluation of sperm cells. *Fertil. Steril.* 104, 43–47.e2 (2015).
- [7] Balberg, M. *et al.* Localized measurements of physical parameters within human sperm cells obtained with wide-field interferometry. *J. Biophotonics* n/a-n/a (2017). doi:10.1002/jbio.201600186
- [8] Habaza, M. *et al.* Rapid 3D Refractive-Index Imaging of Live Cells in Suspension without Labeling Using Dielectrophoretic Cell Rotation. *Adv. Sci.* n/a-n/a (2016). doi:10.1002/advs.201600205

**B-O-4****One-step phase reconstruction using deep learning in off-axis holography***G. Dardikman-Yoffe<sup>1</sup>, N. Shaked<sup>1</sup>*<sup>1</sup>*Tel Aviv University, Biomedical Engineering, Tel Aviv, Israel*

Phase contrast images supply inherently good contrast for isolated cells *in vitro* without the need for staining, along with valuable information regarding both the internal geometrical structure and the RI distribution of the sample [1]. Digital holography can capture a sample complex wavefront by recording the interference pattern between a sample beam, interacting with the sample, and a reference beam [2]. In off-axis holography [3], one of the interfering beams is slightly tilted relative to the other beam, creating a linear shift that allows separation of the field intensity from the two complex-conjugate wave front terms in the spatial-frequency domain (SFD), and thus reconstruction of the complex wave front from a single hologram. Nevertheless, even upon successful extraction of the wavefront from the SFD, as can be done by cropping one of the cross correlation terms in the SFD [4], the reconstruction of the final phase profile from the recorded wavefront is a complicated task, including five main steps:

- 1) Initial extraction: the initial estimate of the phase is extracted from the wavefront using a simple four-quadrant arctangent function.
- 2) Beam referencing: the phase profile of a sample-free wavefront is subtracted from the initial phase estimate.
- 3) Phase unwrapping: the unwrapped phase is restored from its modulo  $2\pi$  function (where the quotient is unknown); this can be done using a variety of algorithms [5], where a good choice requires certain expertise.
- 4) Linear slope correction: the unwrapped phase is fitted numerically in an iterative process, to find the parasitic tilted plain, such that it can be removed.
- 5) Background noise attenuation: finally, to get a clean image with a completely flat background, various heuristic thresholding and morphological operations have to be applied.

In the past couple of years, the concept of deep learning has emerged as a gold-standard solution to many types of problems in endless fields [6]. Specifically in the field of image processing, deep convolutional neural networks have revolutionized problems ranging from basic classification and segmentation to complex inverse problems in imaging. For the latter case of inverse problems, the residual neural network (ResNet) architecture [7], which adds short-term memory to each layer, has taken the lead due to its ability to force the network to learn new information in every layer beyond what is already encoded in the network. Here, we exploit this concept to train a neural network able to perform steps 2-5 at once, with only the initial estimate of the phase extracted from the sample wavefront as input; this not only eliminates the need to acquire a sample-free wavefront, but also removes the heuristics and inconsistency involved in phase reconstruction, and allows a faster, iteration-free and fully-automated phase reconstruction process.

**References**

- [1] G. Dardikman and N. T. Shaked, "Review on methods of solving the refractive index–thickness coupling problem in digital holographic microscopy of biological cells," *Optics Communications* 422 (2018): 8-16.
- [2] C. M. Vest, *Holographic Interferometry* (Wiley, New York, 1979).

- [3] N. T. Shaked, "Quantitative phase microscopy of biological samples using a portable interferometer," *Opt. Lett.* 37, 2016–2018 (2012).
- [4] P. Girshovitz and N. T. Shaked, "Real-time quantitative phase reconstruction in off-axis digital holography using multiplexing," *Opt. Lett.* 39, 2262–2265 (2014).
- [5] D. C. Ghiglia and M. D. Pritt, *Two-Dimensional Phase Unwrapping: Theory, Algorithms, and Software* (Wiley, 1998).
- [6] Y. LeCun, Y. Bengio, and G. Hinton, "Deep learning," *Nature* 521, 436–444 (2015).
- [7] K. He, X. Zhang, S. Ren, and J. Sun, "Deep residual learning for image recognition," *IEEE Conference on Computer Vision and Pattern Recognition*, 770–778 (2016).

**B-O-5****The new methods for modeling of costal cartilage implants for laryngotracheal defect treatment**

*O. Baum<sup>1</sup>, Y. Alexandrovskaya<sup>1</sup>, V. Svistushkin<sup>2</sup>, E. Sobol<sup>3</sup>*

*<sup>1</sup>Federal Scientific Research Centre 'Crystallography and Photonics' of Russian Academy of Sciences, Institute of Photon Technologies, Troitsk- Moscow, Russian Federation*

*<sup>2</sup>I.M.Sechenov First Moscow State Medical University, Moscow, Russian Federation*

*<sup>3</sup>Arcuo Medical Inc, Arcuo Medical Inc, Incline Village, USA*

Thermo-mechanical effect of laser radiation is a basis for the new methods for modeling of costal cartilage implants of a given shape. In larynx surgery the prospects of the technique are connected with preparation of implants of the proper semicircle -shape. If the final shape of an implant is formed with a surgical scalpel, residual stresses lead to the distortion of the implant. This decreases its survivability after the surgery. Laser-induced stress relaxation in the cartilage implants without disturbing tissue functionality opens new possibilities for implantology.

Studies of the effects of pulsed laser radiation on porcine [1], rabbit [2] and finally, on human [3] cartilages were carried out using a 1.56  $\mu\text{m}$  IR-laser. A theoretical model predicting the laser mode allowed establishing optimal laser setting have been constructed on the basis of thermal-conductivity equation and thermal-stress theory. The location of the maximum laser-induced alteration in the structure of biological tissue was shown using the thermal stress tensor.

The results of this theoretical calculation obtained for porcine and rabbit cartilages showed the possibility of transferring the theoretical approach from the animal cartilage to the isolated human cartilage.

The implantation of the laser-shaped semicircle cartilage during the operation for closing the human laryngotracheal defect has been done. The stability of post operational results has been obtained during 16 months follow-up.

The study was supported by the Russian Foundation for Basic Research (Project No. 18-29-02124).

**References**

[1] O. I. Baum, Yu. M. Alexandrovskaya, V. M. Svistushkin, et.al. *Laser Phys. Lett.*, 16, 035603 (2019).

[2] E. Sobol, O. Baum, Yu. Alexandrovskaya, et.al. *Proc. of SPIE Vol 10039, 100390U-1* (2017).

**B-O-6****Antibacterial silicon-based laser-fabricated nanocoatings**

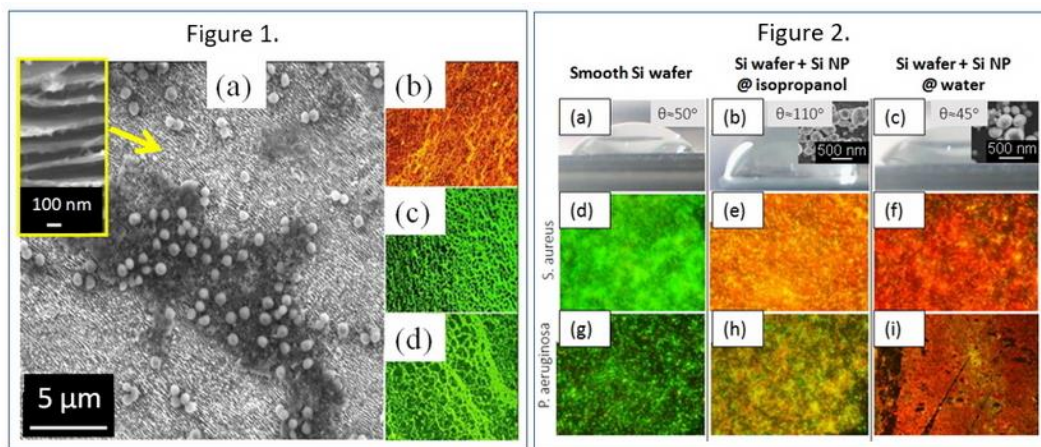
*A. Ionin<sup>1</sup>, S. Kudryashov<sup>1</sup>, A. Nastulyavichus<sup>1</sup>, I. Saraeva<sup>1</sup>, N. Smirnov<sup>1</sup>, A. Rudenko<sup>1</sup>, E. Tolordava<sup>2</sup>, D. Zayarny<sup>1</sup>, S. Gonchukov<sup>3</sup>, Y. Romanova<sup>2</sup>*

<sup>1</sup>*P. N. Lebedev Physics Institute of Russian Academy of Science, Quantum Radiophysics, Moscow, Russian Federation*

<sup>2</sup>*N.F. Gamaleya Federal Research Centre of Epidemiology and Microbiology, Laboratory of gene engineering of pathogenic microorganisms, Moscow, Russian Federation*

<sup>3</sup>*National Research Nuclear University MEPhI Moscow Engineering Physics Institute, Laser Plasma, Moscow, Russian Federation*

Antibacterial coatings were fabricated by laser ablation of silicon in liquid media. Laser radiation (1030 nm, 10 ps, 10  $\mu$ J) was focused on the Si wafer under the 5-mm layer of liquid carbon disulfide (CS<sub>2</sub>) and raster-scanned across the surface. The resulting laser-induced morphology consisted of nanosheets (NS) with high height-to-width ratio, and its antibacterial properties were tested on *S. aureus* strain. Fig.1. demonstrates SEM image of Si NS with *S. aureus* biofilm (a), optical images of bacteria, stained with fluorescent dye (b) – dead and alive on the smooth Si wafer (c) and on the silica glass (d).



The *S. aureus* strain was grown in a nutrient medium and incubated for 24 h at 37°C on the surface of Si NS, smooth Si wafer and silica glass as a control. Their staining with “Live/Dead Biofilm Viability Kit” allowed assuming, that no any biofilm was formed on the Si NS, unlike smooth Si and silica glass. The bacterial death was possibly caused by the mechanical damage of the cell membrane on the sharp edges of Si NS, or its possible chemical activity. Another type of antibacterial coating was fabricated by placing Si nanoparticles (NPs) on a smooth Si wafer. NPs were prepared by laser ablation (1064nm, 120ns, 0.1mJ) of silicon plate under the 3-mm layer of either isopropanol or deionized water. Fig.2. demonstrates angles and optical images of alive (green) and dead (red) bacteria on the surface of smooth Si wafer (a, d, g), wafer with Si NPs, prepared in isopropanol (b, e, h) and in deionized water (c, f, i). The resulting Si NP colloidal solutions were air-dried, and their antibacterial activity and hydrophobic properties were tested using *S. aureus* and *P. aeruginosa*.

The research was supported by the Russian Science Foundation (Project #18-15-00220).

**B-O-7****Laser-induced hydrodynamic effects in urological operation**

*V. Minaev<sup>1</sup>, N. Minaev<sup>2</sup>, V. Yusupov<sup>2</sup>, A. Dymov<sup>3</sup>, N. Sorokin<sup>3</sup>, V. Lekarev<sup>3</sup>, A. Vinarov<sup>3</sup>, L. Rapoport<sup>3</sup>*

<sup>1</sup>*NTO "IRE-Polus", medical applications department, Fryazino, Russian Federation*

<sup>2</sup>*Federal Scientific Research Centre "Crystallography and Photonics" of Russian Academy of Sciences, Institute of Photon Technologies, Moscow, Troitsk, Russian Federation*

<sup>3</sup>*I.M.Sechenov First Moscow State Medical University, Institute of Urology and Reproductive Health, Moscow, Russian Federation*

When laser light with the wavelength of 1.94  $\mu\text{m}$  is used in operations, performed in environment of physiological solution, three types of action on soft tissue are possible.

Contact mode: combination of laser light and heated in place of contact fiber end actions. This mode is followed by the bright shining in contact point, carbonization of biotissue and possible formation of viable fragments of pathological tissue (Fig.1 a).

At remote action the superintensive liquid boiling of near the output end of the fiber leading to formation of a steam-gas macrobubble which do not absorb light - "Mozes effect". If biotissue is in this bubble, then laser light act on it. In this case the area of action is well visualized and carbonization decreases (Fig.1 b).

At the power of laser light near 100 W the two-phase stream consisting of steam-gas microbubbles and heated water is formed at macrobubble distal end. Speed of this stream can exceed 1 m/s and it can cut soft biotissue (the mode of hydrodynamic section). In this mode the area of action is well controlled, there is no carbonization and the probability of emergence of viable fragments (Fig.1 c) is small.

Two last modes with the maximum pulse power of 120 W are effectively used for operations of prostatic hyperplasia enucleation and resections bladder wall with tumour.

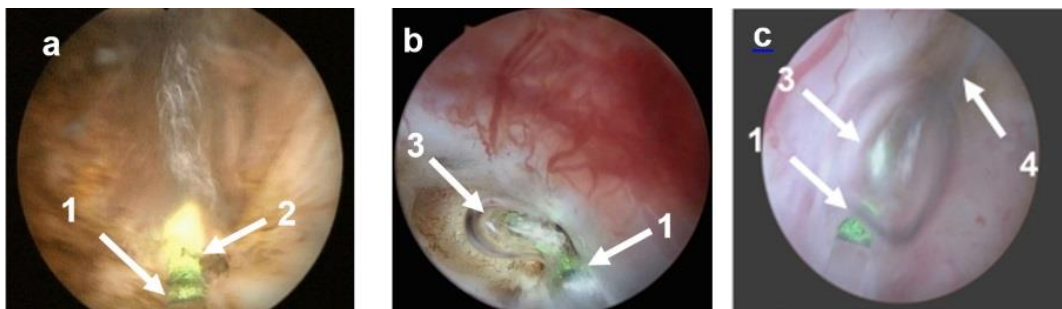


**Fig.1.** Modes: a – contact (CW, 60 W), b - "Mozes effect", c– hydrodynamic section. 1 – the end of the fiber, 2 – the place of contact, 3 – steam-gas macrobubble, 4 – two-phase stream.

**B-O-8****Sapphire shaped crystals as a prospective material platform for novel modalities of medical diagnosis and therapy**

*I. Dolganova*<sup>1,2</sup>, *G. Katyba*<sup>1,3</sup>, *I. Shikunova*<sup>1</sup>, *I. Reshetov*<sup>4</sup>, *M. Schcedrina*<sup>4</sup>, *K. Zaytsev*<sup>2,3</sup>,  
*V. Tuchin*<sup>5,6</sup>, *V. Kurlov*<sup>1</sup>

<sup>1</sup>*Institute of Solid State Physics of the Russian Academy of Sciences, Laboratory of Shaped Crystals, Chernogolovka, Russian Federation*

<sup>2</sup>*Bauman Moscow State Technical University, Laboratory of Terahertz Technology, Moscow, Russian Federation*

<sup>3</sup>*Prokhorov General Physics Institute of the Russian Academy of Sciences, Laboratory of Submillimeter-Wave Dielectric Spectroscopy, Moscow, Russian Federation*

<sup>4</sup>*Sechenov First Moscow State Medical University, Department of Oncology-Radiotherapy and Plastic Surgery, Moscow, Russian Federation*

<sup>5</sup>*Saratov State University, Chair of Optics and Biomedical Physics, Saratov, Russian Federation*

<sup>6</sup>*Institute of Precision Mechanics and Control of the Russian Academy of Sciences, Laboratory of laser diagnostics of technical and living systems, Saratov, Russian Federation*

Sapphire shaped crystals feature a beneficial combination of physical properties, which makes them rather prospective for the development and fabrication of medical instruments for diagnosis, therapy, and surgery [1]. They are nonmagnetic, biocompatible, enable operation in a harsh environment, including biological tissues and liquids, provide exceptional waveguiding properties for electromagnetic radiation of different frequencies delivering to the object, and possess high mechanical strength, thermal conductivity, and high melting point [2]. Applying the unique technology of shaped crystal growth [3], it is possible to manufacture sapphire crystals with internal capillary channels, allowing for combination of several functions in a single medical instrument. Most of the additional functions are optically-based. Thus, sapphire scalpel with internal channels can be used for tissue resection, fluorescent diagnostics, and coagulation [4]; capillary needles can be applied for photodynamic therapy and laser interstitial thermal therapy due to placing of quartz fibres inside them and forming of the needle tips of complex form, which determine a desirable radiation distribution [5]; sapphire neuroprobes enable intraoperative diagnosis, brain tissue aspiration, and coagulation of blood vessels [6]; sapphire applicators for cryosurgery can include quartz fibres in order to optically control the freezing process [7,8]. We demonstrate recent developments and experimental study of such instruments, which open novel horizons in medical approaches for treatment, surgery, and diagnosis.

This work was funded by the Russian Foundation for Basic Research (RFBR), according to the research project # 18-38-20140.

**References**

- [1] G.M. Katyba et al., *Progress in Crystal Growth and Characterization of Materials* 64, 133–151 (2018).
- [2] V.N. Kurlov. Reference Module in Materials Science and Materials Engineering. Ed. by Saleem Hashmi. Oxford: Elsevier, 2016.
- [3] P.I. Antonov, V.N. Kurlov, *Progress in Crystal Growth and Characterization of Materials* 44, 63–122 (2002).
- [4] V.N. Kurlov et al., *Bulletin of the Russian Academy of Sciences: Physics* 73, 1341–1344 (2009).
- [5] I.A. Shikunova et al., *Proceedings of SPIE* 10716, 1071605 (2018).

- [6] I.A. Shikunova et al., *Optics and Spectroscopy* 126, 545–553 (2019).
- [7] I.A. Shikunova et al., *Proceedings of SPIE* 10716, 1071605 (2018).
- [8] E.N. DUBYANSKAYA et al., *Proceedings of SPIE* 10685, 1068529 (2018).

**B-O-9****The OCE-assisted monitoring of slow strains in laser-reshaped cartilage implants***Y. Alexandrovskaya<sup>1,2</sup>, O. Baum<sup>1,2</sup>, V. Zaitsev<sup>1</sup>**<sup>1</sup>Institute of Applied Physics, Russian Academy of Sciences, Nizhny Novgorod, Russian Federation**<sup>2</sup>Federal Scientific Research Centre 'Crystallography and Photonics' of Russian Academy of Sciences, Biophotonics laboratory, Troitsk, Moscow, Russian Federation*

The infrared laser-induced thermal and stress fields are applied to cartilaginous tissue to perform its reshaping and obtain allo- and autoimplants of new stable curvature [1]. In particular, the medical technology for the larynx stenosis treatment using laser-modified semicircle costal cartilage slices has been developed and tested showing positive results on animals and patients [1-3]. The most serious side effects are connected with the spontaneous deformation of the implanted tissue causing its poor engraftment. Thus, rapid and non-destructive monitoring of residual stress in cartilage is of utmost importance to control the quality of the laser-reshaped implants. Here we present a technique of the combined OCT-based elastographic measurement to monitor the velocity of the post-irradiational dilatation of costal cartilage implants. We observe post-reshaping slow strains caused by residual unrelaxed stresses. During the operation an unaided eye cannot distinguish such slow, but potentially dangerous strains accompanying unfolding of the semi-circular implant. High sensitivity of OCT-based strain mapping makes it possible to detect such strains on intervals ~tens of seconds, which bodes well for intraoperational applications. The cumulative strain kinetics for different time intervals after laser irradiation was analyzed. The criteria for laser-induced relaxation of mechanical stresses in cartilage were formulated.

The study was supported by Russian Science Foundation grant 16-15-10274.

**References**

1. O.I. Baum, Yu.M. Alexandrovskaya, V.M. Svistushkin, S.V. Starostina and E.N. Sobol 2019, *Laser Phys. Lett.*, 16, 035603.
2. E. Sobol, O. Baum, Yu. Alexandrovskaya, A. Shekhter, L. Selezneva, V. Svistuskin 2017, *Proc. of SPIE*, 10039, 100390U-1.
3. O.I. Baum, Y.M. Soshnikova, E.N. Sobol et al 2011, *Lasers Surg. Med.*, 43, 511.

**B-O-10****Endovenous laser coagulation using two-micron laser radiation: mathematical modeling and in vivo experiments**

*S. Artemov<sup>1</sup>, A. Belyaev<sup>2</sup>, O. Bushukina<sup>3</sup>, S. Khrushchalina<sup>1</sup>, S. Kostin<sup>2</sup>, A. Lyapin<sup>1</sup>, P. Ryabochkina<sup>1</sup>, A. Taratynova<sup>1</sup>*

*<sup>1</sup>National Research Mordovia State University, Physics and chemistry Institute, Saransk, Russian Federation*

*<sup>2</sup>National Research Mordovia State University, Medicine Institute, Saransk, Russian Federation*

*<sup>3</sup>National Research Mordovia State University, Agriculture Institute, Saransk, Russian Federation*

Endovenous laser coagulation (EVLC) is an effective treatment for varicose veins. This method combines low invasiveness and the almost complete absence of postoperative complications, which reduces the rehabilitation duration compared to, for example, phlebectomy. The occurrence of complications after EVLC is usually associated with thermal damage to perivenous tissues due to the use of high laser power levels (8–20 W for radiation with wavelengths of 810–980 nm [1-3]; 5–15 W for radiation with wavelengths of 1470–1550 nm [2-4]).

The task of identifying the optimal EVLC parameters that provide effective vein coagulation with minimal damage to the surrounding tissues is usually solved by conducting experiments with various parameters. Additional attraction of mathematical modeling methods will allow solving this problem more effectively. Since EVLC is a complex of phenomena, it is rather difficult to take into account the contribution of each of them to the final result, but even taking into account only the main processes allows us to establish the dependence of the procedure effectiveness on the treatment parameters and evaluate its possible complications.

This paper presents the results of an EVLC modeling using radiation of the solid-state laser based on an LiYF<sub>4</sub>:Tm crystal with a wavelength of 1910 nm and a power of 1.5 to 4 W. The calculations were made in the COMSOL Multiphysics® Modeling Environment and were aimed at estimating the temperature distribution in the blood, vein wall and adjacent tissues when exposed to the indicated radiation. We also carried out in-vivo EVLC experiments on the sheep veins using the specified exposure parameters, the effectiveness of which was evaluated on the basis of histological studies, ultrasound studies, and clinical observations of animals during the postoperative period.

Values of the venous wall temperature, assessed as a result of modeling, correspond to the lesions character revealed by histological analysis of vein sections harvested immediately after EVLC and 40 days after it. Wherein, the damage caused by the use of 4 W radiation is irreversible, which ensures successful and permanent occlusion of the vessel. The use of 1.5 W radiation power does not contribute to the formation of a blood clot and leads to the vein wall damage, which is insufficient for vessel coagulation, and may lead to recanalization.

**References**

- [1] MILON Group <http://www.milon.ru/index.phtml?tid=1312>.  
 [2] Sokolov A.L., Liadov K.V., Lutsenko M.M., Lavrenko S.V., Liubimova A.A., Verbitskaya G.O., Minaev V.P. (2009) Endovascular laser ablation with wavelength 1,560 nm for varicose veins. *Angiol Sosud Khir* 15:69–76.

- [3] Malskat W.S.J., Giang G., De Maeseneer M.G.R., Nijsten T.E.C., Van der Bos R.R. (2016) Randomized clinical trial of 940- versus 1470-nm endovenous laser ablation for great saphenous vein incompetence. *Br. J. Surg.* 103:192-198.
- [4] Almeida J., Mackay E., Javier J., Mauriello J., Raines J. (2009) Saphenous laser ablation at 1470 nm targets the vein wall, not blood. *Vasc. Endovas. Surg.* 43:467–472.

**B-O-12****The phenomenon of electromechanical properties of cartilage tissue during cooling and heating from -10°C to 40°C***E. Kasianenko<sup>1</sup>, A. Omelchenko<sup>1</sup>**<sup>1</sup>Federal Scientific Research Centre “Crystallography and photonics” of Russian Academy of Sciences, Institute of Photon Technologies, Moscow, Russian Federation*

Medical operation of laser-induced reshaping cartilage tissue allows achieving a stable form of cartilage. After bending of the form, mechanical stresses arise in the volume of the tissue, which relaxes after the laser impact due to the heating [1]. It is known that the mechanical properties of cartilage tissue are determined by the interaction of the charges of the matrix molecules [2, 3]. The reshaping of cartilage during laser heating is associated with a change in the matrix, as well as the possible transfer of its electrical charges and electrical conductivity of the tissue [4]. To ensure the effectiveness and safety, it is advisable to monitor the physical characteristics of the tissue, which affect the degree of exposure and the moment of switching off the laser.

The purpose of work was to study the kinetics of the activation energy of electric charges generation during repetitively pulsed laser heating of cartilage in a regime close to that used in medical technology. Relaxation of charges during tissue cooling to -10°C and subsequent generation by laser heating were controlled by measuring the electrical conductivity of the tissue.

Measurement of electrical conductivity with the help of direct current allows us to control the electrophysical properties of the tissue: the state of free charges, their mobility and concentration in the matrix. An analysis of the dependences of the conductivity of the articular cartilage and the dynamics of its heating on the time of laser heating showed the temperature dependence of the electrical conductivity of the tissue. The change in conductivity during cooling of cartilage to negative temperatures allowed to draw conclusions about the behaviour of the mobility of free charges in the cartilage matrix. The knowledge of the activation energy of the charge generation process makes it possible to determine and monitor the structural changes in cartilage during laser heating.

These results can be used as the basis for the control and diagnostic system for monitoring changes in the tissue state during laser-induced reshaping of cartilage implants.

The study was supported by the Russian Foundation for Basic Research (Project No. 18-29-02124).

**References**

- [1] Bagratashvili V.N., Sobol E.N., Shekhter A.B. Lasernaya engeneria khrashey. M. FizMatLit 2006 (in Russian).
- [2] Omel'chenko A.I. (2009). Effect of repetitive laser pulses on the electrical conductivity of intervertebral disc tissue. *Quantum Electronics*, 39(3), 279
- [3] Légaré A., Garon M., Guardo R., Savard P., Poole A.R., Buschmann M.D. Detection and analysis of cartilage degeneration by spatially resolved streaming potentials. *J Orthop Res* 2002;20:819e26.
- [4] Sobol E.N., Milner T.E., et al. Laser reshaping and regeneration of cartilage. *Laser Phys. Lett.* 2007, 4, No. 7, p. 488–502.



# ALT'19

**INTERNATIONAL CONFERENCE**

**Advanced Laser Technologies**



## THz PHOTONICS

**Prague, Czech Republic**



15-20 September 2019

**THz-I-1 (Keynote)****Charge carrier transport in nanomaterials probed in the THz range**

*P. Kuzel<sup>1</sup>, H. Nemeč<sup>1</sup>*

*<sup>1</sup>Institute of Physics of the Czech Academy of Sciences, THz spectroscopy group, Prague, Czech Republic*

Terahertz spectroscopy has been used for almost two decades for investigations of nanomaterials, including nanocrystals, nanoparticles, nanowires, nanotubes or 2D crystals. Its great importance stems from the fact that it is a noncontact method and, owing to its high frequency and broadband character, it is capable of characterizing charge transport properties within individual nano-objects but also among them. In addition, probing of photo-initiated ultrafast charge dynamics is possible thanks to the sub-picosecond time resolution. Despite this unprecedented potential, the interpretation of the measured terahertz conductivity spectra in many materials is still intensively debated.

In this contribution we discuss the state of the art of the theoretical formalism and shortly review the most important experimental findings on THz conductivity in semiconductor nanostructures.

**THz-I-2****Time and spectrally resolved gain dynamics in THz quantum cascade lasers***J. Darmo<sup>1</sup>, G. Derntl<sup>1</sup>, D. Theiner<sup>1</sup>, G. Scalari<sup>2</sup>, M. Beck<sup>2</sup>, J. Faist<sup>2</sup>, K. Unterrainer<sup>1</sup>**<sup>1</sup>Photonics Institute, TU Wien, Campus Gusshausstrasse, 1040 Vienna, Austria**<sup>2</sup>Institute of Quantum Electronics, ETH Zürich, Auguste-Piccard-Hof 1, Zurich, 8093, Switzerland*

In this contribution we present our investigations of the gain recovery dynamics of a heterogeneous terahertz quantum cascade laser and their role in the stable operation of a broadband active region. We employ THz-pump/THz-probe time domain spectroscopy (TDS). The measurements reveal a strong coupling between cavity photon field and the carrier transport in the quantum cascades as well as between individual sections of the QCL active region.

A broadband terahertz (THz) gain medium is a basic component for future THz sources. Remarkable progress in this field was achieved using heterogeneous THz quantum cascade heterostructures (QCH), which stacks different quantum cascades. However, the coherent and stable operation of those devices depends crucially on the interaction between the individual stacks. The individual stacks can interact optically due to the overlapping spectral gain curves of the individual stacks and due to the strong feedback from the photon field to the electron transport through the heterostructure. Therefore, the gain profile and its dynamics in the heterogeneous quantum cascade laser (QCL) can differ significantly from a QCL with a standard design.

The investigated heterogeneous THz QCH [1] is composed of three individual stacks centered at 2.3 THz, 2.6 THz and 2.9 THz, respectively. It was fabricated in a double metal waveguide cavity and biased above lasing threshold. We have measured gain recovery times between 34 ps and 50 ps, where the shorter times were measured for low temperature and high bias current [2]. Furthermore, our time domain technique allows also spectrally resolve the gain dynamics and thus to reveal the interactions between the individual sections of the heterogeneous QCH.

We observed that the gain of the low (transition at <2.3 THz) and the high frequency sections (transition at >2.7 THz) recover similarly, while the recovery of the central gain section (transition at 2.3-2.5 THz) exhibits completely different development in time within the first 24 ps after gain perturbation. For longer delay times the three gain sections show the same recovery time for low temperature and high bias current operation and is matching the global GRT values presented in [2]. The abnormal recovery behavior for small pump-probe delay times, we believe, is connected to a re-absorption or an absorption and re-emission process of photons shared by two stacks. The experimental results are compared with a rate equation model and we analyze the connection of the observed interactions to the stability of a heterogeneous THz QCL and discuss the results with respect to a comb formation.

[1] D. Turcinková et al., Appl. Phys. Lett., 99, 191104, 2011.

[2] C. G. Derntl et al., Appl. Phys. Lett., 113, 181102, 2018.

**THz-I-3****THz quantum cascade lasers: Materials evaluation and optimization**H. Detz<sup>1,2</sup><sup>1</sup>*TU Wien, Center for Micro- and Nanostructures, Wien, Austria*<sup>2</sup>*Brno University of Technology, Central European Institute of Technology Brno, Czech Republic*

Intersubband transitions enable compact coherent sources for THz frequencies by circumventing bandgap-related restrictions of conventional diode lasers. While superlattice-based quantum cascade laser (QCL) active regions provide some freedom regarding the selection of quantum well and barrier material, the interplay of beneficial material parameters and technical maturity leads to a complex situation question regarding the optimum material system. In contrast to mid-infrared QCLs, THz devices have been realized mostly based on GaAs/AlGaAs heterostructures due to their technological maturity. A lack of progress regarding the maximum operating temperature (Tmax) led to a search for alternative material combinations. Nevertheless, recent improvements allowed to push Tmax of GaAs/AlGaAs THz QCLs beyond 200 K and enabled thermo-electric cooling as a major step towards system integration [1,2].

The lower effective mass ( $m^*$ ) of InGaAs quantum wells leads to a larger optical gain [3]. The combination with InAlAs barriers, lattice-matched or strain-balanced on InP substrates also reached a high level of maturity. For THz QCL active regions, this material system remains challenging as precise lattice-matching is required over the whole active region thickness, typically around 10 – 15  $\mu\text{m}$ . As a side effect of the higher conduction band offset (CBO), thinner barrier layers are required for emission energies in the THz range, which leads to larger relative thickness errors. Alternatively, GaAsSb was used as barrier material, which leads to slightly thicker and therefore less critical layer thicknesses due to its moderate CBO of 0.36 eV. While the electronic properties are clearly advantageous, the growth of mixed-anion alloys like GaAsSb, particularly including group V switching, still requires optimization [4]. Both InGaAs-based material systems were shown to be interesting candidates for improved future device generations, presently reaching Tmax of 155 K with InAlAs barriers and 142 K using GaAsSb barriers.

Recently, InAs-based THz QCL active regions were studied to exploit the even lower  $m^*$ . Lattice-matched AlAsSb barriers exhibit a CBO of 1.6 eV, which leads to layer thicknesses approaching the single monolayer level, which still need to be grown reproducibly over several  $\mu\text{m}$  active region thickness [3]. While this material combination is clearly not as mature, already first-generation devices were operational. We will review the perspectives of different THz QCL material systems. Though not yet competitive to GaAs-based devices, the potential of the low  $m^*$  heterostructures is underlined by state-of-the-art operational devices. Further improvement of the growth conditions is expected to boost the performance devices based on mixed-anion barriers.

**References:**

- [1] L. Bosco et al., Appl. Phys. Lett. 115, 010601 (2019).
- [2] M.A. Kainz et al., Opt. Express 27, 20688 (2019).
- [3] H. Detz et al., Phys. Stat. Solidi A 216, 1800504 (2019).
- [4] T. Zederbauer et al., APL Mater. 5, 035501 (2017).

**THz-I-4****Advanced control of complex matter by high-field terahertz pulses***F. Giorgianni*<sup>1</sup><sup>1</sup>*Paul Scherrer Institut, Research with Neutrons and Muons, Villigen PSI, Switzerland*

Terahertz interaction with matter has become one of the hottest topics in ultrafast community. Indeed, intense terahertz pulses have recently proved to be a pivotal tool to manipulate and control the properties of complex condensed matter systems with strongly correlated electrons [1]. In these materials, electronic correlations entangled with other degrees of freedom may induce new electronic phases and unconventional physical phenomena such as superconductivity in cuprates, giant magnetoresistance and insulating-to-metal transition (IMT).

Vanadium sesquioxide ( $V_2O_3$ ) is considered as a classical prototype of materials exhibiting IMTs, thus attracting broad attention in fundamental and applied physics. The IMT in  $V_2O_3$  is mainly driven by electronic correlations, described by the Mott physics, concomitant with a lattice distortion [2].

When an IMT is driven by conventional stimuli such as temperature, pressure, fast voltage and deposition of optical energy with near infrared laser, the electronic and lattice contributions could not be adequately disentangled. On the other hand a pure electronic process may open a promising avenue towards the next generation of faster and more energy-efficient electronic devices. Using intense THz pulses, we reveal the emergence of an ultrafast electric-field driven metallization of  $V_2O_3$  by quantum tunneling [3]. We show that strong THz electric field, non-resonant with the phonon modes, are capable to induce a sub-picosecond electronic switching faster than lattice transition. A second example of complex electronic phase control by THz field is the superconductivity. Recent experiments on superconductors have shown that low-energy collective mode can be manipulate by intense THz light pulses through nonlinear processes [4,5].

Intense THz pulse is an effective approach to control complex electronic phases, with promising pathways towards novel nonlinear processes hindered to conventional stimuli.

**References**

- [1] D. Nicoletti, and A. Cavalleri, Nonlinear light-matter interaction at terahertz frequencies, *Advances in Optics and Photonics* 8, 401 (2016).
- [2] M. M. Qazilbash, et al., Electrodynamics of the vanadium oxides VO<sub>2</sub> and V<sub>2</sub>O<sub>3</sub>, *Physical Review B*, 77, 115121 (2008).
- [3] F. Giorgianni, J. Sakai, and S. Lupi, Overcoming the thermal regime for the electric-field driven Mott transition in vanadium sesquioxide, *Nature Communications* 10, 1159 (2019).
- [4] R. Matsunaga, et al. Light-induced collective pseudospin precession resonating with Higgs mode in a superconductor. *Science* 345, 1145 (2014).
- [5] F. Giorgianni, et al. Leggett mode controlled by light pulses. *Nature Physics* 11 (2019).

**THz-I-5****Long wavelength stimulated emission in HgTe/CdHgTe quantum well heterostructures**

*A. Dubinov<sup>1,2</sup>, V. Gavrilenko<sup>1,3</sup>, V. Rumyantsev<sup>1,3</sup>, M. Fadeev<sup>1,4</sup>, V. Utochkin<sup>1</sup>, V. Aleshkin<sup>1,3</sup>, N. Mikhailov<sup>5,6</sup>, S. Morozov<sup>1,2</sup>, Z. Krasilnik<sup>1,2</sup>, C. Sirtori<sup>7</sup>*

<sup>1</sup>*Institute for Physics of Microstructures RAS, Semiconductor physics department, Nizhny Novgorod, Russian Federation*

<sup>2</sup>*Lobachevsky State University, Radiophysics department, Nizhny Novgorod, Russian Federation*

<sup>3</sup>*Lobachevsky State University, Advanced School of General and Applied Physics, Nizhny Novgorod, Russian Federation*

<sup>4</sup>*L2C, UMR CNRS 5221, Montpellier University, Terahertz Spectroscopy Group, Montpellier, France*

<sup>5</sup>*A.V. Rzhanov Institute of Semiconductor Physics, Siberian Branch of Russian Academy of Sciences, Lab #15, Novosibirsk, Russian Federation*

<sup>6</sup>*Novosibirsk State University, Physics department, Novosibirsk, Russian Federation*

<sup>7</sup>*Laboratoire de Physique de l'Ecole Normale Supérieure, Physique Quantique et Dispositifs QUAD, Paris, France*

The development of compact semiconductor far-infrared sources is an important problem of modern physics of semiconductors. Promising candidates are lasers based on HgTe/HgCdTe heterostructures with quantum wells (QWs). HgCdTe has low enough phonon frequencies to enter 5 - 12 THz region, currently unavailable for quantum cascade lasers (QCLs) and allows bandgap tuning down to less than 10 meV (2 THz).

Stimulated emission (SE) under optical pumping was obtained in HgTe/HgCdTe quantum well (QW) heterostructures in the spectral range up to 25  $\mu\text{m}$  for dielectric waveguide and up to 31  $\mu\text{m}$  for “Reststrahlen band mode localization”. It was shown that longer pumping wavelengths provide better performance. Under near-IR pumping ( $\lambda_{\text{exc}} \sim 2.3 \mu\text{m}$ ), we observed quenching of SE from HgTe/CdHgTe QW laser structures as the pumping increased beyond the SE threshold. We attribute this effect to the excessive “heating” of non-equilibrium charge carriers leading to activation of Auger processes (which have a threshold with respect to carrier energy). Switching to mid-IR ( $\lambda_{\text{exc}} \sim 10.6 \mu\text{m}$  using CO<sub>2</sub>-laser) pumping allowed to avoid the SE quenching and resulted into much better output characteristics of the laser structures in the wavelength range from 14 to 20  $\mu\text{m}$ . At shorter wavelengths  $\lambda \sim 10 \mu\text{m}$  the excitation threshold power was shown to be as low as 120 W/cm<sup>2</sup> and the SE was obtained even at CW excitation ( $\lambda_{\text{exc}} \sim 0.9 \mu\text{m}$ ). Under low-power cw QCL pumping ( $\lambda_{\text{exc}} \sim 8 \mu\text{m}$ ) photoluminescence signal was found in HgTe/CdHgTe heterostructures up to 20  $\mu\text{m}$ . These results suggest that it is possible to achieve SE under cw pumping at the wavelengths above 10  $\mu\text{m}$  at higher pumping intensity. HgCdTe heterostructures prove to be a promising candidate for far-IR lasers and optical converters from mid-IR QCLs to far-IR region.

This work was financially supported by the Russian Foundation of the Basic Research (#18-52-16013).

## THz-I-6

### THz gyrotrons and beyond

*A. Fokin<sup>1</sup>, M. Glyavin<sup>1</sup>*

<sup>1</sup>*IAP RAS, Plasma physics and High power electronics, Nizhny Novgorod, Russian Federation*

This report aims to bring together information about the development and the most striking application examples of high frequency (0.3-1.5 THz) gyrotrons [1,2]. The paper describes the main features of terahertz devices. The data about pulsed and CW tubes, working at the in the specified frequency range, are given. These gyrotrons demonstrate (in some specific combinations) extremely low voltage and beam current, narrow frequency spectrum, wide frequency tuning.

The pulsed gyrotron has been used successfully for initiation of localized gas discharges [3]. Such plasma is promising for development of both a point source of multi-charged ions and a source of high-energy ultraviolet (extreme ultraviolet EUV or XUV). CW tubes widely used for the high-resolution molecular spectroscopy and diagnostic of various media. A significant improvement of spectrum quality, due to power growth in contrast with traditional BWO, was obtained and the sensitivity of the radio-acoustic detector was increased about three orders [4]. Simultaneous non-linear excitation of high harmonics during the operation at fundamental one was demonstrated. Such case radiation power at harmonics was several orders lower than in fundamental, but, any way, significantly higher than in solid state and classical vacuum electronic tubes.

Novel schemes of high frequency gyrotrons are analyzed. The electron optics and electrodynamic methods of mode selection for single mode harmonic excitation are presented. The dual electron beam gyrotron demonstrated operation at second harmonic with a frequency about 0.8 THz [5], axis-encircling CW gyrotron realized 0.4 THz operation at the third harmonic [6] and complex cavity gyrotron with phase corrector obtained pulsed 1.2 THz at the second harmonic [7].

### References

- [1] M.Yu. Glyavin, T. Idehara, S.P. Sabchevski. Development of THz gyrotrons at IAP RAS and FIR UF and their applications in physical research and high-power THz technologies. *IEEE Transactions on Terahertz Science and Technology*, 5, 5, 788-797 (2015).
- [2] M. Glyavin, G. Denisov, V. Zapevalov et al. High-power terahertz sources for spectroscopy and material diagnostics *PHYSICS-USPEKHI*, 59, 6, 595-604 (2016).
- [3] A. Sidorov, S. Golubev, S. Razin et al. Gas discharge powered by the focused beam of the high-intensive electromagnetic waves of the terahertz frequency band. *J. Phys. D: Appl. Phys.*, 51, 46, 464002 (2018).
- [4] M.A. Koshelev, A.I. Tsvetkov, M.V. Morozkin et al. Molecular gas spectroscopy using radioacoustic detection and high-power coherent subterahertz radiation sources. *J. Mol. Spectrosc.*, 331, 9–16, (2017).
- [5] T. Idehara, M. Glyavin, A. Kuleshov et al. A Novel THz-Band Double-Beam Gyrotron for High-Field DNP-NMR Spectroscopy, *Rev. Sci. Instrum.*, 88, 094708 (2017).
- [6] I. Bandurkin, V. Bratman, Yu. Kalynov et al. Developments of terahertz large-orbit high harmonic gyrotrons at IAP RAS. Report 4.1, 20th International Vacuum Electronics Conference (IVEC 2019), Busan, Korea, April 29 - May 1, 2019.
- [7] A.V. Savilov, I.V. Bandurkin, M.Yu. Glyavin et al. High-harmonic gyrotrons with irregular microwave systems. 3rd International Conference Terahertz and Microwave Radiation: Generation, Detection and Applications (TERA-2018). Nizhny Novgorod, Russia, October 22 - 25, 2018 EPJ Web of Conferences 195, 01015 (2018).

**THz-I-7****The nonlinearity of the refractive index of optical media in the terahertz spectral range**

*S.A. Kozlov<sup>1</sup>, M.V. Melnik<sup>1</sup>, Zhukova M.O.<sup>1</sup>, O. Vorontosova<sup>1</sup>, S.E. Putilin<sup>1</sup>, A.N. Tsyarkin, Xi-Cheng Zhang<sup>1,2</sup>*

<sup>1</sup>*International Laboratory of Femtosecond Optics and Femtotechnologies, ITMO University, St. Petersburg, 197101, Russia, kozlov@mail.ifmo.ru*

<sup>2</sup>*The Institute of Optics, University of Rochester, Rochester, NY 14627, USA*

Terahertz (THz) frequency range has become an active research area due to its perspective applications. Recent advances in research have brought high intensity broadband sources of THz radiation into play ( $10^{13}$  W/cm<sup>2</sup> or higher) into play [1], that it gets which make it possible to observe nonlinear effects in this spectral range [2]. The most important parameter characterizing the nonlinearity of the material response in the field of intense waves is the coefficient of its nonlinear refractive index  $n_2$ . There is number of different techniques for  $n_2$  estimation. The most widespread is Z-scan [3]. This method was originally designed for strictly monochromatic radiation. However, it is become common in the case of femtosecond pulsed radiation with a broad spectrum [4]. Thus, this approach can be used for broadband THz radiation as well [2, 5].

This work presentation will gives a brief overview on the theory of low-inertia mechanisms of nonlinearity of the polarization response of condensed matter in THz spectral range and then introduce new results, both analytical and experimental, on estimations of  $n_2$  of some liquids and direct measurements of the coefficient of water in this spectral range.

We estimate the nonlinear refractive index coefficient  $n_2$  of optical media through the use of a recent theoretical treatment [6]. This treatment ascribes the THz nonlinearities in media to a vibrational response that is orders of magnitude larger than typical electronic responses. This model assumes that the nature of the nonlinearity of optical media refractive index in THz spectral range is caused by the anharmonicity of molecular vibrations. We find that the predicted value of  $n_2$ , for example, for water in the low-frequency limit is  $n_2 = 5.0 \times 10^{-10}$  cm<sup>2</sup>/W, which is 6 orders of magnitude higher than for the visible and IR ranges. It is interesting that theoretical estimates of the coefficient  $n_2$  of vibrational nature for liquids show that the quadratic nonlinearity of anharmonic vibrations of each molecule determines the main contribution to the cubic nonlinearity of the polarization response of these isotropic media.

We present the direct measurement of water nonlinear refractive index coefficient for the broadband pulsed THz radiation with the conventional Z-scan method technique. Since the Z-scan this method works with plane-parallel samples only, flat water jet was used. The experimental setup for measuring  $n_2$  of a liquid jet was based on TERA-AX source of THz radiation. The THz pulse energy was 400 nJ, the pulse duration was 0.5 ps and the spectrum width was from 0.1 to 2.5 THz. Pulsed THz radiation was focused and collimated by two parabolic mirrors. The spatial size of the THz radiation at the output of the generator was 25.4 mm. Caustic diameter was 1 mm (FWHM) and the radiation intensity of the THz beam  $10^8$  W/cm<sup>2</sup>. Flat water jet was moved along the caustic area using a motorized linear translator. The water jet had a thickness of 0.1 mm and was oriented along the normal to the incident radiation. The jet was obtained using the nozzle which combines the compressed-tube nozzle and two razor blades. The pressure was created by the pump and the hydroaccumulator which reduces the pulsations. The rate of laminar flow was enough for a complete renewal of water in the area of interaction at a laser repetition rate of 1 kHz. For  $n_2$  determination Z-scan curves measured with closed aperture were used. The direct

measurement of the nonlinear refractive index coefficient  $n_2 = 7.0 \times 10^{-10} \text{ cm}^2/\text{W}$  of water in the THz frequency range is shown. These results are consistent with the theoretical estimateions above.

We have discussed the correctness of the known Z-scan method for calculating the nonlinear refractive index coefficient for broadband THz radiation regarding the pulse number of cycles pulses have. We have demonstrated that the error in determining the nonlinear refractive index coefficient is always greater than 70% for true single-cycle pulses. With the increase in the number of oscillations up to three the measurement error shows strong dependence on the sample thickness and can vary from 2% to 90% depending on the chosen parameters. It is demonstrated that the decrease in the sample thickness leads to the reduction of the nonlinear refractive index coefficient determination error, and this error is  $<2\%$  when the ratio between the sample thickness and the pulse longitudinal spatial size is  $\leq 1$ .

The study is funded by RFBR project No. 19-02-00154.

## References

- [1] M. Shalaby, C. Hauri, Nature Communications, 6, 5976 (2015);
- [2] A. Tsyarkin, M. Melnik, M. Zhukova, I. Vorontsova, S. Putilin, S. Kozlov, X. Zhang, et al. Optics express, 27 (8), 10419-10425 (2019);
- [3] M. Sheik-Bahae et al. IEEE journal of quantum electronics, 26 (4), 760-769 (1990);
- [4] X. Zheng et al., Optics Letters, 40 (15), 3480 (2015);
- [5] M. Melnik, et al., Scientific Reports, 9 (1), 9146 (2019);
- [6] K. Dolgaleva et al., D. Materikina, R. Boyd, S. Kozlov, Physical Review A., 92 (2), 023809 (2015).

**THz-I-8****Mapping ultrafast ionization of atoms and clusters with terahertz field driven streak-camera**

*M. Krikunova*<sup>1</sup>

<sup>1</sup>*ELI Beamlines, Institute of Physics Academy of Sciences of the Czech Republic, Dolní Břežany, Czech Republic*

Any target exposed to the focus of the intense extreme ultra-violet (XUV) or X-ray laser beam will be transformed into highly excited non-equilibrium states. Capturing the ultrafast ionization dynamics of a sample is crucial for the understanding of multiphoton and nonlinear X-ray physics phenomena. An experimental access to these ultra-short time scales is very challenging because it requires methods able to look inside of intense ultra-short XUV pulses. We use the terahertz (THz) field driven streak-camera concept to map the complex temporal structure of individual XUV pulses as well as to study multi-electron dynamics in clusters and nano-particles upon illumination by these XUV pulses [1,2].

In the THz-streaking experiment the THz field acts on the free electrons in the continuum. The effect can be understood as an additional momentum acquired by the free electrons in the presence of the oscillating electric field. By changing the time-delay between the ionizing XUV pulse with respect to the THz-streaking field and measuring the electron kinetic energy spectra, a streaking spectrogram is obtained. In the streaking experiment half of the oscillation period of the streaking field has to be shorter than the temporal width of the electron distribution. Therefore, to resolve the electron dynamics that is initiated by the femtosecond XUV pulse, a THz-field is used.

In this contribution we present our recent investigations based on the THz-field driven streak camera concept [1,2]. We discuss the implementation of the THz-radiation for studies of ultra-fast processes at the ELI-Beamlines near Prague, in the Czech Republic - the international user facility that is currently approaching the user-operation. We present the current status of the multi-purpose user end-station (MAC) for experiments in atomic, molecular, and optical sciences and coherent diffractive imaging that is developed for advanced photon science experiments on low density targets (atoms, molecules, clusters, nano-particles and aerosols) in a broad range of the electromagnetic spectrum from THz to XUV [3].

**References**

- [1] T. Oelze et al, *Sci. Rep.*, 7, 40736 (2017).
- [2] T. Oelze et al, *Phys. Rev. A*, 99, 043423 (2019).
- [3] E. Klimešová et al, *Sci. Rep.* 9, 8851 (2019).

**THz-I-9****Generation of the second harmonic of optical radiation in the presence of a strong terahertz field***A. Stepanov<sup>1</sup>**<sup>1</sup>Institute of Applied Physics, Nizhny Novgorod, Russian Federation*

The generation of the second harmonic of optical radiation (SHG) is a non-linear process widely used, in particular, for the diagnosis of various media, especially their surfaces and boundaries [1]. In centrosymmetric media, SHG is forbidden in the dipole approximation and therefore very weak. The application of an additional DC or low frequency field to the SHG process leads to the removal of the restriction and allows the use of SHG for diagnostic purposes, etc. In this paper, we will present the results of the study of the generation of the second harmonic (SH) in various materials, using the powerful short-pulse terahertz radiation as an auxiliary field. THz pulses were generated in a nonlinear LiNbO<sub>3</sub> crystal when it was irradiated with femtosecond laser radiation in intensity tilt front scheme. Then they were focused on the sample using an off-axis parabolas; the maximum field at the focus reached 300 kV / cm. A portion of the femtosecond laser pulse was also focused on the sample. Registration of SH was carried out using a photomultiplier with a photon counting system. Semiconductor materials Si, InAs, and GaP were used as samples. In part of the experiments, studies were carried out with samples of single-layer graphene. SHG studies were also carried out in gaseous media (air, Ar, He).

In the experiments, the dependences of the SH on the azimuthal angle of crystalline semiconductor samples, the signals of the second harmonic with different combinations of polarizations involved in the generation of SH were recorded. A phenomenological theory of SHG in crystalline semiconductors was developed. For graphene, a theory has been developed that links the generation of SH with the “field” broadening of interband resonance in the region of production of electron-hole pairs in k-space, resulting in the appearance of anisotropy of the electric dipole response [2].

**References**

- [1] Aktsipetrov O.A., Baranova I.M., Evtukhov K.N. Nonlinear optic of silicon and silicon nanostructures. M. Fizmatlit, 2012 (in Russian).
- [2] M. Tokman, S. Bodrov, Y. Sergeev, A. Korytin, I. Oladyshkin, Y. Wang, A. Belyanin, and A. Stepanov. Second harmonic generation in graphene dressed by a strong terahertz field, Phys. Rev. B 99, 155411 (2019).

**THz-I-10****On the way to generation and application of extremely high field THz pulses**

*J. Hebling<sup>1,2,3</sup>, T. György<sup>1</sup>, Nugraha P. S.<sup>2,3</sup>, L. Pálfalvi<sup>1</sup>, A. András Fülöp<sup>2,3</sup>, Krizsán G.<sup>1,3</sup>, L. Tokodi<sup>1</sup>, Z. Tibai<sup>1</sup>, G. Almási<sup>1,3</sup>*

<sup>1</sup>*Institute of Physics, University of Pécs, Ifjúság ú. 6. Pécs 7624, Hungary*

<sup>2</sup>*MTA-PTE High-Field Terahertz Research Group, Ifjúság ú. 6, Pécs 7624, Hungary*

<sup>3</sup>*Szentágotthai Research Centre, University of Pécs, Ifjúság ú. 20, Pécs 7624, Hungary*

Acceleration of electrons [1] and protons [2], and generation of single-cycle attosecond pulses [3] are promising applications of very intense terahertz (THz) pulses. One of the most effective ways to generate high energy near single-cycle THz pulses is the optical rectification of tilted-pulse-front (TPF) pump pulses in LiNbO<sub>3</sub> (LN) crystal [4]. Using this technique, the energy of the generated THz pulses was increased by six orders of magnitude reaching the mJ level in the last decade [5]. However, the energy scalability is limited by the imaging errors and the large angular dispersion connected to the needed large tilt angle. Furthermore, the prism shape of the LN has significant influence on the quality of the generated beam shape. To reduce the effect of angular dispersion, a modified version of the TPF THz generation was demonstrated by replacing the optical grating to a stair-step echelon [6]. A high THz generation efficiency was achieved, but this echelon setup still requires a prism-shaped nonlinear crystal with the same wedge angle as in the conventional setup. Recently, we proposed [7] and demonstrated [8] a hybrid-type setup (Fig. 1), which is a combination of the conventional scheme, containing diffraction optics and imaging, and a nonlinear material with an echelon profile created on its entrance surface (nonlinear echelon slab, NLES). Contrary to all the LN setups used so far, a plane parallel nonlinear crystal can be used. Because of the plan-parallel structure and the reduced tilt angle, the beam quality is perfect, contrary to the beam generated by conventional TPF setup (see Fig. 2a,b).

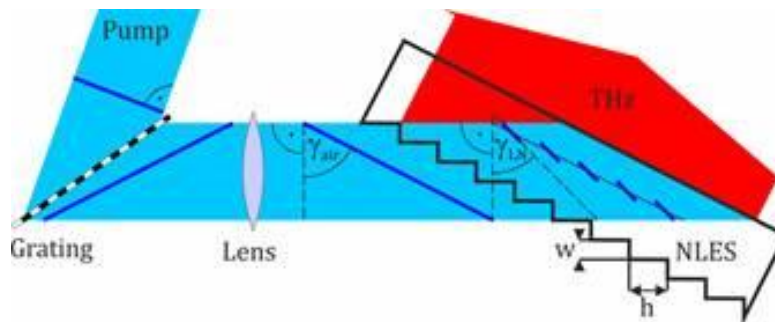


**Fig. 1.** Scheme of the proposed and demonstrated nonlinear echelon slab (NLES) hybrid THz source.

To overcome the drawbacks of imaging errors, we proposed an imaging-free NLES setup [9]. In this case not the plane parallel NLES results uniform THz beam shapes, instead one with a small wedge angle (8.6°). The efficiency exceeds that of the conventional setup and plane parallel NLES (Fig. 2c).

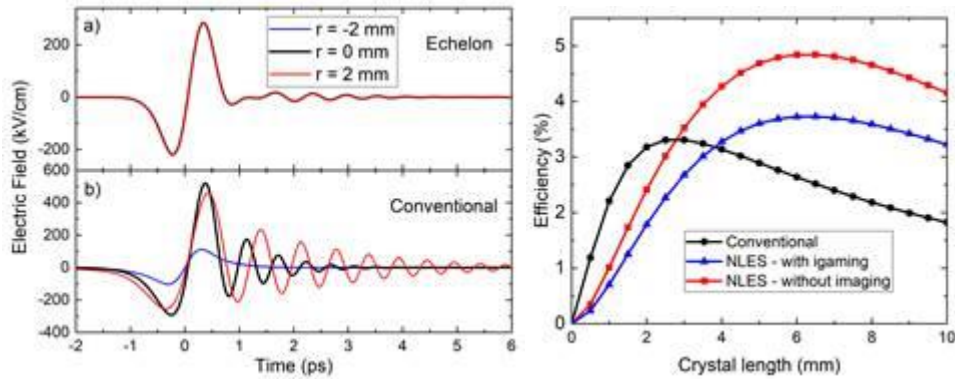


**Fig. 2.** Calculated THz pulse waveforms at different position across the THz beam for a LN-based plan parallel NLES (a) and a prism (b). Optical to THz generation efficiency of the conventional setup, the plane parallel NLES (with imaging) and the imaging-free NLES setup. (c).

Using NLES setups, the generated THz pulse energy is perfectly scalable to 10s of mJ level simply by increasing the pump beam diameter, in contrast to the conventional, prism-based setup. According to our calculations generation of multicycle THz pulses is also possible with high efficiency by NLES if the pump pulse is intensity-modulated.

**Funding:** European Union, co-financed by the European Social Fund Grant (EFOP-3.6.1.-2016-00004).

## References

- [1] A. Fallahi, M. Fakhari, A. Yahaghi, M. Arrieta, and F. X. Kärtner, "Short electron bunch generation using single-cycle ultrafast electron guns," *Physical Review Accelerators and Beams* **19**, 081302 (2016).
- [2] L. Pálfalvi, J. A. Fülöp, G. Tóth, and J. Hebling, "Evanescent-wave proton postaccelerator driven by intense THz pulse," *Physical Review Special Topics - Accelerators and Beams* **17**, 031301 (2014).
- [3] Gy. Tóth, Z. Tibai, A. Sharma, J. A. Fülöp, and J. Hebling, "Single-cycle attosecond pulse by Thomson backscattering of terahertz pulses," *J. Opt. Soc. Am. B* **35**, A103-A109 (2018).
- [4] J. Hebling, G. Almási, I. Z. Kozma, and J. Kuhl, "Velocity matching by pulse front tilting for large-area THz-pulse generation," *Opt. Express* **10**, 1161-1166 (2002).
- [5] J. A. Fülöp, Z. Ollmann, C. Lombosi, C. Skrobol, S. Klingebiel, L. Pálfalvi, F. Krausz, S. Karsch, and J. Hebling, "Efficient generation of THz pulses with 0.4 mJ energy".
- [6] B. K. Ofori-Okai, P. Sivarajah, W. R. Huang, and K. A. Nelson, "THz generation using a reflective stair-step echelon," *Opt. Express* **24**, 5057-5068 (2016).
- [7] L. Pálfalvi, Gy. Tóth, L. Tokodi, Zs. Márton, J. A. Fülöp, G. Almási, and J. Hebling, "Numerical investigation of a scalable setup for efficient terahertz generation using a segmented tilted-pulse-front excitation," *Opt. Express* **25**, 29560-29573 (2017).
- [8] P. S. Nugraha, G. Krizsán, Cs. Lombosi, L. Pálfalvi, Gy. Tóth, G. Almási, J. A. Fülöp, and J. Hebling, "Demonstration of a Tilted-Pulse-Front Pumped Plane-Parallel Slab Terahertz Source," accepted in *Opt. Lett.*
- [9] Gy. Tóth, L. Pálfalvi, J. A. Fülöp, G. Krizsán, N. H. Matlis, G. Almási, and J. Hebling, "Numerical investigation of imaging-free terahertz generation setup using segmented tilted-pulse-front excitation," accepted in *Opt. Express*.

**THz-I-11****Consistent description of the THz radiation generation in gases**

*S. Stremoukhov*<sup>1,2</sup>

<sup>1</sup>*NRC "Kurchatov Institute", Moscow, Russian Federation*

<sup>2</sup>*Lomonosov Moscow State University, Faculty of Physics, Moscow, Russian Federation*

The recent results of investigations on the THz radiation generation in two-color laser field interacting with extended gas media are presented. Basing on the non-perturbative quantum-mechanical description of the THz radiation generated by a single atom and the extended gas model based on the obtained quantum-mechanical information about the amplitudes and phases of the THz radiation projections on the orthogonal axes and effects of propagation of the laser field radiation [1,2] we have numerically investigated the influence of the laser field parameters and the parameters of the gas on the spectral, integral, polarization and spatial characteristics of the generated radiation. Different schemes of the two-color laser field organizations have been investigated during the current study. The effects of the quasi-phase matching in extended gas have been discussed. Methods on the control over the efficiency and polarization characteristics are presented.

**References**

- [1] S. Yu. Stremoukhov, A. V. Andreev, "Spatial variations of the intensity of THz radiation emitted by extended media in two-color laser fields", *Laser Physics Letters*, V. 12, p. 015402 (2015).
- [2] S. Stremoukhov, A. Andreev, "Quantum-mechanical fingerprints in generation of elliptical terahertz radiation by extended media interacting with two-color laser field", *Journal of the Optical Society of America B: Optical Physics*, V. 34(2), pp. 232-237 (2017).

**THz-I-12****Terahertz spectroscopy of spin-phonon excitations in multiferroics**

*F. Kadlec<sup>1</sup>, S. Kamba<sup>1</sup>, C. Kadlec<sup>1</sup>, J. Vít<sup>1</sup>, V. Goian<sup>1</sup>*

*<sup>1</sup>Institute of Physics- Czech Academy of Sciences, Dielectrics, Praha 8, Czech Republic*

Magnetoelectric multiferroics are crystals where ferromagnetic and ferroelectric orders occur simultaneously. In many cases, interactions between the two orders are observed, which makes these materials attractive not only because of their fundamental properties but also in view of potential applications, such as memory elements, magnetic sensors or components for spintronics. Such coupling is, in general, observed on both static and dynamic scales. In the THz range, the dynamic coupling manifests itself often by characteristic excitations, so-called electromagnons, which can be viewed as periodic oscillations of both atomic positions and spin orientations. The talk will introduce examples of multiferroic systems featuring electromagnons, results of their measurements in external magnetic field and discuss their main properties.

**THz-I-13****Sub-wavelength-resolution terahertz imaging of soft biological tissues**

*K. Zaytsev<sup>1</sup>, N. Chernomyrdin<sup>1</sup>, I. Dolganova<sup>2</sup>, G. Katyba<sup>2</sup>, I. Spektor<sup>1</sup>, V. Karasik<sup>3</sup>, I. Reshetov<sup>4</sup>, V. Tuchin<sup>5</sup>*

<sup>1</sup>*Prokhorov General Physics Institute of the Russian Academy of Sciences, Laboratory of Submillimeter Dielectric Spectroscopy, Moscow, Russian Federation*

<sup>2</sup>*Institute of Solid State Physics of the Russian Academy of Sciences, Laboratory of Shaped Crystals, Chernogolovka, Russian Federation*

<sup>3</sup>*Bauman Moscow State Technical University, Research and Educational Center of Photonics, Moscow, Russian Federation*

<sup>4</sup>*Sechenov First Moscow State Medical University, Department of Plastic Surgery, Moscow, Russian Federation*

<sup>5</sup>*Saratov State University, Department of Optics and Biophotonics, Saratov, Russian Federation*

Terahertz (THz) biophotonics attracts considerable interest as a promising tool for diagnosis of malignancies with different nosology and localization [1]. Nevertheless, majority of modern THz spectroscopy and imaging modalities rely on lens- and mirror-based optical systems, which obey the Abbe diffraction limit and provide the spatial resolution of  $>\lambda$ ;  $\lambda$  is electromagnetic wavelength [2]. The resolution of several hundreds of microns, or even of several millimeters, strongly limits capabilities of THz technology in malignancy diagnosis, pushing further developments into the realm of sub-wavelength-resolution THz imaging [1]. In our work, we developed a method of THz solid immersion microscopy for continuous-wave reflection-mode imaging of soft biological tissues with a sub-wavelength spatial resolution [3–5]. In order to achieve strong reduction in the dimensions of beam caustic, an electromagnetic wave is focused into the evanescent field volume behind a medium with a high refractive index. We have experimentally demonstrated a  $0.15\lambda$ -resolution of the proposed imaging modality at  $\lambda = 500 \mu\text{m}$ . The proposed technique does not involve any sub-wavelength near-field probes and diaphragms, thus, providing high energy throughout. We have applied the developed method for the THz imaging of various soft biological tissues: a plant leaf blade, cell spheroids, tissues of the breast *ex vivo*, human brain gliomas *ex vivo* and glioma models from rats *ex vivo* [4–6]. The observed results justify capabilities of the proposed THz imaging modality in biology and medicine.

This work was supported by the Russian Science Foundation, Project # 17-79-20346.

**References**

- [1] O.A. Smolyanskaya et al., *Progress in Quantum Electronics* 62, 1–77 (2018).
- [2] N.V. Chernomyrdin et al., *Review of Scientific Instruments* 88(1), 014703 (2017).
- [3] N.V. Chernomyrdin et al., *Applied Physics Letters* 110(22), 221109 (2017).
- [4] N.V. Chernomyrdin et al., *Applied Physics Letters* 113(11), 111102 (2018).
- [5] N.V. Chernomyrdin et al., *Optics & Spectroscopy* 126(5), 644–651 (2019).
- [6] A.A. Gavdush et al., *Journal of Biomedical Optics* 24(2), 027001 (2019).

**THz-I-14****Radiation sources based on semiconductor devices for multichannel THz-IR spectroscopy**

*V. Vaks<sup>1</sup>, V. Anvertev<sup>1</sup>, M. Chernyaeva<sup>1</sup>, E. Domracheva<sup>1</sup>, S. Pripolzin<sup>1</sup>*

*<sup>1</sup>Institute for Physics of Microstructures RAS, Terahertz spectrometry, Nizhny Novgorod, Russian Federation*

Actual problems in the gas analysis are associated with developing the methods of analysis of multicomponent gas mixtures for various applications.

The special consideration is given to improving the sensitivity of spectroscopic analysis owing combining the terahertz spectral approach with IR quantum cascade lasers (QCL).

The main problem of high precise spectroscopy is development of high-stable tunable coherent radiation sources. The modern spectroscopic requirements to THz radiation sources are frequency stabilization with accuracy  $\sim 10^{-8}$  -  $10^{-10}$  from carrier frequency, high spectral purity and smooth tuning of frequency in wide frequency range.

The development of semiconductor technology will open the new horizon in realization of the radiation sources and detectors for terahertz spectroscopy. Developing the semiconductor devices being combined radiation sources for different frequency ranges may be a new direction of devices design.

The review of modern semiconductor radiation sources of THz and IR ranges is presented.

QCLs operating in continuous and pulse modes are used for IR range. The various approaches to IR QCL frequency stabilization (superheterodyne method, Pound–Drever–Hall method, stabilization at the frequency of gas absorption line) were considered.

The development of THz emitters based on QCL up to 3-4 THz is presented. The possibility of frequency multiplying the frequency of QCL for the developing the inaccessible part of THz range over 5 THz is considered. The multiplier based on semiconductor superlattices (SL) operated from 0.1 to 10 THz will be used.

Elaboration of new semiconductor radiation sources allow developing the multichannel THz-IR nonstationary spectroscopy for fast qualitative and quantitative analysis of some substances, which can be important for various applications. Such substances are, e.g., metabolites concerned with cancer disease for its early diagnostics.

The authors acknowledge the support from Presidium RAS Program No. 5: "Photonic technologies in probing inhomogeneous media and biological objects"

**THz-I-15****Terahertz continuous wave systems for sensing applications**

*I.M. Lee<sup>1</sup>, E.S. Lee<sup>1</sup>, H.S. Kim<sup>1</sup>, D.W. Park<sup>1</sup>, M.G. Kim<sup>1</sup>, K. Moon<sup>1</sup>, D.H. Choi<sup>1</sup>, J.H. Shin<sup>1</sup>, K.H. Park<sup>1</sup>*

*<sup>1</sup>ETRI Electronics and Telecommunications Research Institute, Terahertz Research Section, Daejeon, Korea Republic of*

The industrial understandings and the interests on the potential of the terahertz (THz) technologies have grown greatly and now many industrial researchers and engineers are actively searching the proper THz technologies or systems as a novel technological solution that can resolve their practical problems in the industrial fields.

As a research group in a government-funded research institute, we have experienced lots of industrial requests from variety of industrial fields. Among the variety of technical problems or issues that they want to find out that if our THz technology can resolve the problems and provide a breaking-throughs over their real-industrial troubles, some are in their progress to soon be applied to a mass-production process as a non-destructive testing (NDT) technology, and some are still under the development for the realizations of small, compact, and cost-effective systems.

For the industrially - available terahertz technologies, we have developed THz continuous wave (CW) technologies from materials to the application systems [1-6]. Our in-house developed THz technologies and systems start to show the usefulness and possibilities of terahertz waves to the industrial applications. For an example, our proto-type for a CW THz system for inspecting a mass-production process of a car manufacturing company have shown its feasibility as a stand-off sensing and imaging instrument to find human errors that are hard to find with other technologies.

Our vision in the THz technologies are over a wide range of fields including imaging, spectroscopy, and next generation of wireless telecommunications and we have been struggled to developing practical technologies in all these fields.

In the presentation, to provide an illustrative introduction to our progresses in the applications of THz technologies to the industrial fields, our recent research and development results on the key components and systems will be presented. We believe that our devices - DML as a compact, broadband beating light source, nano-electrode-photomixer as a high-power THz emitter, and UTC-PD photomixer as a highly-efficient THz generator, and SBD as a sensitive broadband THz detector – and the THz CW systems based on these would be the key components for developing industrial THz applications.

**References**

- [1] N. Kim, et al., *Laser Phys. Lett.* 10, 085805 (2013).
- [2] E. S. Lee, et al., *J. Lightwave Tech.* 36, 274 (2018).
- [3] E. S. Lee, et al., *ETRI J.* 4, 665 (2016).
- [4] S.-P. Han, et al., *Opt. Express*, 22, 28977 (2014).
- [5] K. Moon, et al., *Appl. Phys. Lett.*, 112, 031102 (2018).
- [6] E. S. Lee, et al., *SPIE Photonics West*, 10917-12 Invited, (2019).

**THz-O-1****THz emission spectra produced by filamentation of single-color IR and UV laser pulses**

*A. Ionin<sup>1</sup>, O. Kosareva<sup>1,2</sup>, Y. Mityagin<sup>3</sup>, D. Mokrousova<sup>1</sup>, N. Panov<sup>1,2</sup>, G. Rizaev<sup>1</sup>, S. Savinov<sup>3</sup>, L. Seleznev<sup>1</sup>, D. Shipilo<sup>1,2</sup>*

<sup>1</sup>*P. N. Lebedev Physical Institute of the Russian Academy of Sciences, Division of Quantum Radiophysics, Moscow, Russian Federation*

<sup>2</sup>*Lomonosov Moscow State University, Faculty of Physics and International Laser Center, Moscow, Russian Federation*

<sup>3</sup>*P. N. Lebedev Physical Institute of the Russian Academy of Sciences, Division of Solid State Physics, Moscow, Russian Federation*

We report on the observation of THz radiation spectra emitted by a single-color infrared (IR) and ultraviolet (UV) filaments. We use Ti: sapphire laser system pulse at the central wavelength of 740 nm and the third harmonic at 248 nm. The pulse duration is about 90 fs. The laser pulse is focused by the lens with the focal length of 7 cm. The THz radiation is directed to the Fourier interferometer and registered by superconducting NbN hot-electron bolometer. For both wavelengths the terahertz radiation is emitted into the cones. The maximum terahertz signal for the IR filament is stronger than for the UV one by more than an order of magnitude. Observed terahertz radiation spectra are shown in Figs. 1a and 1b for the IR and UV filaments, respectively.

In both IR and UV pulse cases, the spectra on the optical axis (angle is equal to zero) have their longer wavelength components enhanced as compared with the spectra of the pulses propagating in the off-axis direction. These off-axis spectra are similar to each other. At all the directions studied the terahertz radiation spectra for IR pulses are spread towards 5-6 THz in contrast to the spectra of the UV pulse which extend towards ~2.5 THz only.

Possible explanation to this phenomenon is that the IR filament is characterized by the higher intensity and plasma density as well as the smaller transverse size as compared to the UV filament. This results in the higher transverse gradient of intensity and plasma density in the IR filament. Therefore, the ponderomotive electron acceleration and photo current in the IR filament are higher than in the UV one. Consequently, the IR filament should deliver higher THz signal and larger spectral broadening than the UV filament. This is in agreement with our experimental observation.

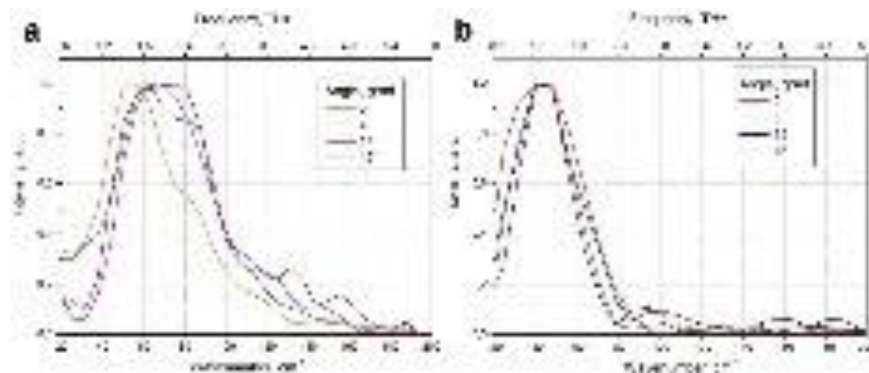


**Fig. 1.** Terahertz radiation spectra formed in the IR (a) and UV (b) filament observed under different angles.

**THz-O-2****Properties of backward terahertz emission from two-color laser induced microplasma**

*A. Ushakov*<sup>1</sup>, *P. Chizhov*<sup>1</sup>, *N. Panov*<sup>2</sup>, *S. Daniil*<sup>2</sup>, *V. Bukin*<sup>1</sup>, *A. Savel'ev*<sup>2</sup>, *O. Kosareva*<sup>2</sup>,  
*S. Garnov*<sup>1</sup>

<sup>1</sup>*Prokhorov General Physics Institute of the Russian Academy of Sciences, Oscillation, Moscow, Russian Federation*

<sup>2</sup>*Lomonosov Moscow State University, Physics, Moscow, Russian Federation*

Femtosecond laser induced plasma in gas media is one of the key sources of terahertz (THz) radiation for different applications [1]. To reach a high power THz pulses in these sources two-color femtosecond pulses (basically consist of fundamental wave and its second harmonic) are typically used [2]. One of the main research directions for these sources is investigation of output angular distribution of THz emission in terms of focusing regime of two-color pump pulses [3]. A special interest is connected with tight focusing regime, which leads to forming of a subwavelength plasma channel (so-called “microplasma”) [4]. For these sources output angular distribution of THz emission is broad, and there is some part of THz emission that can spread from induced by two-color pulses microplasma in opposite direction to propagation of two-color pump (so-called “backward” THz emission) , that has been demonstrated experimentally [5].

In this work we study experimentally the properties of “backward” THz emission from microplasma induced by two-color femtosecond laser pulses: waveform, spectrum and energy. By the controlled reflection of the propagated in forward direction THz emission, we observe “backward” and “forward” THz emissions in the same waveform and thus evidenced of the existence of “backward” THz emission. The comparative spectral analysis of “backward” and “forward” THz emission is demonstrated. A shift of maximum in low-frequency region for “backward” THz emission in comparison with “forward” one is observed. Measurements of the energy of “backward” and “forward” THz emissions provide its ratio to be ~5.5% in terms of two-color pump energies in region 1.2-2 mJ. All of these results are in good agreement with numerical simulations in the framework of interferometric model [6].

**References**

- [1] X.-C. Zhang, J. Xu, Introduction to THz Wave Photonics, Springer (2010).
- [2] D. J. Cook, R. M. Hochstrasser, Opt. Lett. 25 (18), 1210 (2000).
- [3] A. A. Ushakov, P. A. Chizhov, V. A. Andreeva, N. A. Panov, D. E. Shipilo, M. Matoba, N. Nemoto, N. Kanda, K. Konishi, V. V. Bukin, M. Kuwata-Gonokami, O. G. Kosareva, S. V. Garnov, and A. B. Savel'ev, Opt. Express 26 (14), 18202–18213 (2018).
- [4] A. P. Shkurinov, A. S. Sinko, P. M. Solyankin, A. V. Borodin, M. N. Esaulkov, V. V. Annenkov, I. A. Kotelnikov, I. V. Timofeev, X. C. Zhang, Phys. Rev. E 95 (4), 043209 (2017). [5]. A. A. Ushakov, M. Matoba, N. Nemoto, N. Kanda, K. Konishi, P. A. Chizhov, N. A. Panov, D. E. Shipilo, V. V. Bukin, M. Kuwata-Gonokami, J. Yumoto, O. G. Kosareva, S. V. Garnov, and A. B. Savel'ev, JETP Lett. 106 (11), 706–708 (2017).
- [6] N. A. Panov, O. G. Kosareva, V. A. Andreeva, A. B. Savel'ev, D. S. Uryupina, R. V. Volkov, V. A. Makarov, and A. P. Shkurinov, JETP Lett. 93 (11), 638–641 (2011).

**THz-O-3****Control of terahertz emission from long two-color filaments**

*P. Chizhov<sup>1</sup>, A. Ushakov<sup>1</sup>, V. Bukin<sup>1</sup>, S. Garnov<sup>1</sup>*

*<sup>1</sup>Prokhorov General Physics Institute of the Russian Academy of Sciences,  
Oscillations department, Moscow, Russian Federation*

Terahertz generation in gas plasma created by two-color femtosecond laser pulses is attracting a lot of attention due to ability of high-energy laser pumping and broad spectrum of generated radiation [1]. However, this scheme is sensitive to mutual phase shift between harmonics [2]. For long filaments this phase difference is changing along the plasma channel leading to an off-axis peak in spatial THz distribution [3] and to possibility of waveform control by initial phase mismatch adjustment between harmonics [4].

We investigate experimentally THz generation in two-color femtosecond filaments with lengths up to 100 mm. For such lengths a strong influence of phase walk-off between harmonics along the plasma channel on terahertz emission is observed. It is demonstrated the possibility of THz pulse waveform and power control by simultaneous use of adjustment of the initial phase shift between harmonics and screening of a part of the THz radiation with a metallic iris diaphragm. We also demonstrate the spectral filtering by use of  $\pi$ -retarder screens for a distinct THz frequency or by use of axicon PTFE-lenses.

**References**

- [1] X.-C. Zhang, A. Shkurinov, Y. Zhang, *Nature Photonics* 11 (1), 16 (2017).
- [2] M. Kress, T. Löffler, S. Eden, M. Thomson and H. Roskos, *Opt. Lett.* 29 (10), 1120 (2004).
- [3] Y. S. You, T. I. Oh, and K. Y. Kim, *Phys. Rev. Lett.* 109 (18), 183902 (2012).
- [4] Z. Zhang, Y. Chen, M. Chen, Z. Zhang, J. Yu, Z. Sheng and J. Zhang, *Phys. Rev. Lett.* 117 (24), 243901 (2016).

**THz-O-4****High-power far-IR generation from seeded KTP off-axis THz parametric oscillator***Y.C. Huang<sup>1</sup>, M.H. Wu<sup>1</sup>, W.C. Tsai<sup>1</sup>, Y.C. Chiu<sup>1</sup>**<sup>1</sup>NTHU, ipt, Hsinchu, Taiwan Province of China*

In the far-infrared spectrum between 20 and 60  $\mu\text{m}$ , the free-electron laser (FEL) is the only wavelength-tunable coherent radiation source capable of generating kilowatt to megawatt peak powers with a linewidth of the order of 1%. Here, we report the detection of  $>70$  kW radiation power at about 52  $\mu\text{m}$  in a  $<94$  ps pulse width from a  $\text{KTiOPO}_4$  (KTP) off-axis terahertz (THz) parametric oscillator at room temperature, when pumping it with 11.9 mJ energy in a 450 ps pulse from a single-frequency Nd:YAG laser and seeding it with a 14  $\mu\text{J}$ , 40-GHz-linewidth Stokes pulse from a synchronously pumped KTP parametric generator. When limiting the radiation to a linewidth of  $\sim 8 \times 10^{-4}$ , we measured  $>45$  kW radiation power for the far-infrared radiation. With 63% coupling efficiency of the silicon prism atop the KTP crystal, the measured  $>70$  and  $>45$  kW far-infrared radiation correspond to  $>111$  and  $>71$  kW powers extracted from the KTP crystal of the seeded off-axis THz parametric oscillator. The radiation source accomplished in this work has great potential to become a tabletop and economical alternative for the bulky and expensive far-infrared FELs in national facilities.

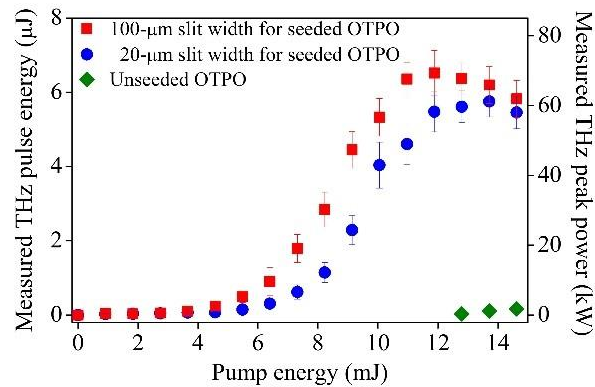


**Fig. 1.** Measured peak power and energy of THz-wave radiation as a function of pump energy for the OTPO.

**THz-O-5****Reconfigurable terahertz optics made of thin films with phase transition***P. Solyankin<sup>1</sup>, A. Shkurinov<sup>2</sup>, B. Knyazev<sup>3</sup>, O. Kameshkov<sup>3</sup>**<sup>1</sup>ILIT RAS – Branch of the FSRC «Crystallography and Photonics» RAS, -, Shatura, Russian Federation**<sup>2</sup>Lomonosov Moscow State University, Faculty of Physics and International Laser Center, Moscow, Russian Federation**<sup>3</sup>Budker Institute of Nuclear Physics of the Siberian Branch of RAS, n/a, Novosibirsk, Russian Federation*

Recent progress in terahertz (THz) sources development, such as quantum cascade lasers (QCL), significantly increases the availability of the THz photonics for practical applications. To minimize the cost and the size of optical components for such systems one can utilize diffractive optics. Moreover, such components can be made reconfigurable, that is hard to achieve with usual optics.

In this work we present two types of optical components for 3.1 and 3.7 THz QCL radiation: switching focusers based on Fresnel zone plates and beamsplitters based on gratings. These structures were made by etching of thin (100-450 nm) films of vanadium dioxide (VO<sub>2</sub>) on sapphire substrates. Due to the phase transition, VO<sub>2</sub> film can significantly change its transparency for the THz radiation under heating above 68°C or under optical irradiation [1]. In low-temperature transparent state film does not affect on incident THz beam, while in opaque high-temperature state Fresnel lenses or gratings are formed.

We made switching focusers with  $F = 50$  mm and 100 mm, each structure contained 7 rings (see Fig. 1). With the help of microbolometer camera we were able to measure intensity distributions near the focal point of our structures and compare it with numerical simulations. We

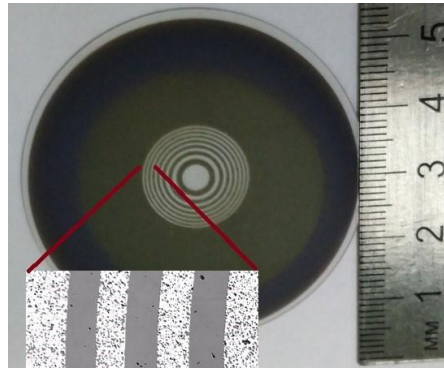


**Fig.1.** Example of the fabricated device.

achieved up to 38 times contrast in the focal spot between two states of the film. Power efficiency and focal spot size at different frequencies were measured. 3-way beamsplitter with 1:6:1 ratio was demonstrated, intensity contrast in 1-st order maximum between two phase states was as high as 68. For more details, one can see our work [2].

This work was partially supported by the Russian Foundation for Basic Research under project no. 16-29-11800 ofi-m. Work was partially supported by the Ministry of Science and Higher Education within the State assignment of the FSRC "Crystallography and Photonics" RAS.

**References**

- [1] Cocker, T. L., Titova, L. V., Fourmaux, S., Holloway, G., Bandulet, H. C., Brassard, D., Kieffer, J.-C., El Khakani, M. A., Hegmann, F. A. Phase diagram of the ultrafast photoinduced insulator-metal transition in vanadium dioxide // *Physical Review B* 2012, V. 85 No. 15, P. 155120.
- [2] Solyankin, P. M., Esaulkov, M. N., Chernykh, I. A., Kulikov, I. V., Zhanaveskin, M. L., Kaul, A. R., Makarevich, A.M., Sharovarov, D.I., Kameshkov, O.E., Knyazev, B.A., Shkurinov, A. P. (2018). Terahertz Switching Focuser Based on Thin Film Vanadium Dioxide Zone Plate. *Journal of Infrared, Millimeter, and Terahertz Waves*, 39(12), 1203-1210.

**THz-O-6****Study of the spectrum of bound water in 0.07-2.6 THz range**

*M. Konnikova*<sup>1</sup>, *M. Nazarov*<sup>2</sup>, *O. Cherkasova*<sup>3,4</sup>, *A. Shkurinov*<sup>1,5</sup>

<sup>1</sup>*M.V.Lomonosov Moscow State University, Department of Physics and International Laser Center, Moscow, Russian Federation*

<sup>2</sup>*Kurchatov Institute National Research Center, Photonics and additive technologies, Moscow, Russian Federation*

<sup>3</sup>*Institute of Laser Physics of SB RAS, Biophysics Laboratory, Novosibirsk, Russian Federation*

<sup>4</sup>*Tomsk State University, laboratory of Biophotonics, Tomsk, Russian Federation*

<sup>5</sup>*FSRC «Crystallography and Photonics» RAS, Crystallography and Photonics, Shatura, Russian Federation*

Water plays a huge role in the functioning of biological systems and can be classified as a bulk and bound water [1]. Strongly or weakly bound water, as well as free (unbound) water, makes valuable but different contribution to the THz response of biological objects. The reason for the change in the THz response in biological samples is the transition of part of water from free to bound state and back. To interpret the results, we need to know precisely spectrum of bound water. Our measurements were performed using two THz-TDS spectrometers described previously [2, 3]. We measured the THz spectra of dry and wet glucose pressed into tablets. Then we added some water to these tablets and again measured the THz spectra. Water concentrations in glucose were varied from 0% to 30% (v/v). THz signal of free water starts to appear after 14-16% v/v water concentrations in glucose. Till 30% water concentrations glucose, free water and crystals coexists in this mixture, even phonon resonances are detectable. In THz absorption spectra we can recognize the contribution both free water (by strong dispersion below 0.2 THz) as well as glucose crystals with its own phonon spectra above 1.4 THz. We obtained the absorption of bound water and confirmed that it is an order of magnitude less than that of free water.

This study was funded by RFBR projects № 17-00-00275 (17-00-00270) and 18-52-00040 (in data processing part), by the Ministry of Science within the State assignment FSRC «Crystallography and Photonics» RAS in part of equipment.

**References**

- [1] O.A. Smolyanskaya et al., Progress in Quantum Electronics vol. 62, pp. 1–77, 2018.
- [2] M.M. Nazarov et al., Quantum Electronics, vol. 46(6), pp. 488-495, 2016.
- [3] M.M. Nazarov et al, J Infrared Mill.Terah.Waves, vol. 39, pp. 840-853, 2018.

**THz-O-7****Terahertz response of silicon surface with nanoscale gold particles**

*A. Sinko<sup>1,2</sup>, K. Moldosanov<sup>3</sup>, P. Solyankin<sup>2</sup>, I. Ozheredov<sup>1,2</sup>, A. Shkurinov<sup>1,2</sup>*

<sup>1</sup>*MSU, Faculty of Physics, Moscow, Russian Federation*

<sup>2</sup>*ILIT RAS — Branch of FSRC “Crystallography and Photonics” RAS, n/a, Shatura, Russian Federation*

<sup>3</sup>*Kyrgyz Russian Slavic University, Department of Natural and Technical Sciences, Bishkek, Kyrgyzstan*

The spectra of terahertz generation from the surface of silicon crystals with different types of conductivity upon excitation by femtosecond laser pulses at different temperatures were experimentally recorded. Comparison of the characteristic spectral features with the energy structure of the impurity levels of silicon makes it possible to identify the type of sample conductivity. A comparison is made with the results obtained at cryogenic temperatures in the case of deposition of gold nanoparticles on the surface of a semiconductor (Fig. 1). The spectral features obtained after the deposition of nanoparticles are considered in the model of terahertz re-radiation as a result of their two-phonon absorption.

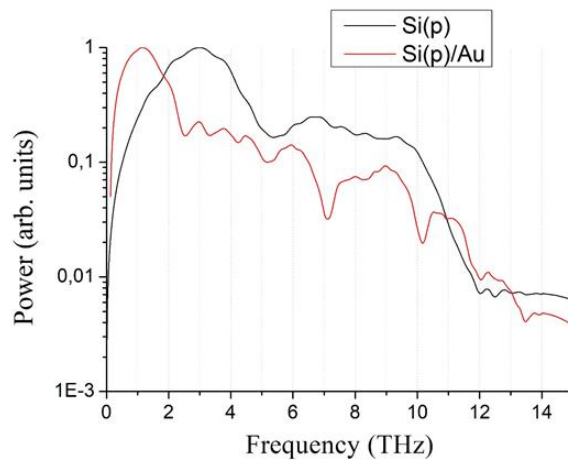


**Fig. 1.** THz emission spectra from the surface of p-type silicon in the case of a clean surface and in the case of nanoparticle deposition.

**THz-O-8****Angular distribution of THz radiation from clustered plasma and enhancing of THz emission intensity**

*N. Kuzechkin<sup>1,2</sup>, A. Balakin<sup>1,2</sup>, M. Dzhidzhoev<sup>1</sup>, V. Gordienko<sup>1</sup>, I. Ivanov<sup>1</sup>, T. Semenov<sup>3</sup>, A. Shkurinov<sup>1,2</sup>*

*<sup>1</sup>Lomonosov Moscow State University, Faculty of Physics & International Laser Centre, Moscow, Russian Federation*

*<sup>2</sup>Russian Academy of Sciences, Institute on Laser and Information Technologies, Branch of the FSRC “Crystallography and Photonics”, Shatura, Russian Federation*

*<sup>3</sup>Russian Academy of Sciences, FSRC “Crystallography and Photonics”, Moscow, Russian Federation*

Interaction of intense laser pulses with the gas-cluster targets results in fairly efficient generation of terahertz radiation. Some studies of such generation were carried out in several experimental and theoretical works [1] - [5]. However the current state of the problem of THz generation in clustered plasma indicates the necessity of further studies for obtaining complete and detailed theoretical interpretation of the experimental effects presented in [1] - [4] and for enhancement of optical to THz conversion efficiency. For example, in [5], it was concluded on the basis of theoretical analysis, that low-frequency radiation from clustered plasma can acquire dipole character under certain conditions of cluster excitation, in contrast with quadrupole radiation observed in [1],[2],[4].

In this work we present the results of experimental studies of the generation of THz radiation during the interaction of intense laser pulses with cluster beams. The basic scheme of the experimental setup is described in detail in our previous paper [3], and for the present study this setup was supplemented by the special module to provide a possibility of measurement of the angular distribution of THz radiation power. Femtosecond laser radiation was focused on the cluster targets differing in size, concentration and internal atomic density of clusters constituting them. We used argon and freon (CF<sub>2</sub>Cl<sub>2</sub>) cluster beams. Parameters of the cluster beams were calculated by numerical simulation and indirectly confirmed in the experiment of Rayleigh scattering measurement. The effect of the polarization state of the laser pulse on the THz emission was studied. Under various experimental conditions, we performed measurements of the angular distribution of the THz radiation power in the horizontal plane. We have found that under certain conditions the polarization state of the exciting laser pulse can influence the efficiency of the generation of THz radiation, which was not observed in previous studies.

Figure 1 demonstrates the effect of laser polarization on THz emission from freon clusters. Also we observed that the THz radiation power from argon clusters at a distance of 13.5 mm below the nozzle edge is rather more than at a distance 1.5 mm away. The results of our numerical simulation has demonstrated that ratio between argon monomers, small and large clusters fractions significantly different at these two positions. We made an attempt of theoretical explanation of the phenomena described above.

This study was supported by RFBR Grant № 17-02-01217.

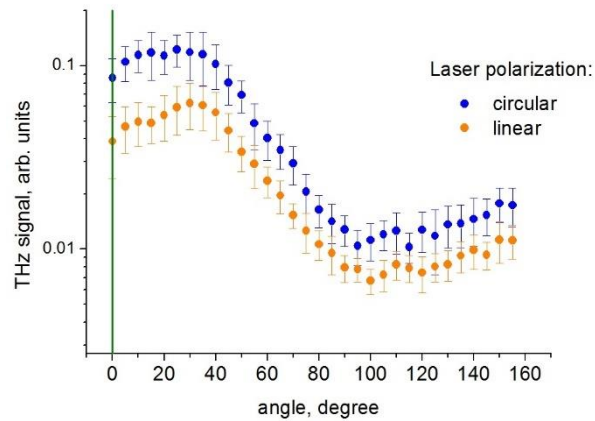


Fig. 1.

## References

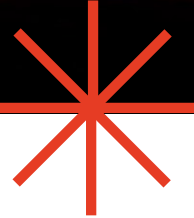
- [1] T. Nagashima, H. Hirayama, K. Shibuya, M. Hangyo, M. Hashida, S. Tokita, and S. Sakabe. Terahertz pulse radiation from argon clusters irradiated with intense femtosecond laser pulses. *Opt. Exp.* 17, 8907 (2009).
- [2] F. Jahangiri, M. Hashida, T. Nagashima, S. Tokita, M. Hangyo, and S. Sakabe. Intense terahertz emission from atomic cluster plasma produced by intense femtosecond laser pulses. *Appl. Phys. Lett.* 99, 261503 (2011).
- [3] A.V. Balakin, M.S. Dzhidzhoev, V.M. Gordienko, M.N. Esaulkov, I.A. Zhvaniya, K.A. Ivanov, I.A. Kotelnikov, N.A. Kuzechkin, I.A. Ozheredov, V.Y. Panchenko, A.B. Savel'ev, M.B. Smirnov, P.M. Solyankin, A.P. Shkurinov. Interaction of High-Intensity Femtosecond Radiation With Gas Cluster Beam: Effect of Pulse Duration on Joint Terahertz and X-Ray Emission. *IEEE Trans. Terahertz Sci. Technol.* 7, 79 (2017).
- [4] F. Jahangiri, M. Hashida, S. Tokita, T. Nagashima, M. Hangyo, and S. Sakabe. Enhancing the energy of terahertz radiation from plasma produced by intense femtosecond laser pulses. *Appl. Phys. Lett.* 102, 191106 (2013).
- [5] A.A. Frolov. Dipole Mechanism Generation of Terahertz Waves under Laser–Cluster Interaction. *Plasma Phys. Rep.* 44, 40 (2018).



# ALT'19

**INTERNATIONAL CONFERENCE**

**Advanced Laser Technologies**



## HiLASE Workshop

**Prague, Czech Republic**



---

15-20 September 2019

**HiLASE-I-1****Two-dimensional material printing via blister-based laser-induced forward-transfer**

*N. Goodfriend<sup>1</sup>, A.V. Bulgakov<sup>1</sup>, N.M. Bulgakova<sup>1</sup>, E.E.B. Campbell<sup>2</sup>, O. Nerushev<sup>2</sup>, T. Mocek<sup>1</sup>, R. Kitaura<sup>3</sup>, T. Hotta<sup>3</sup>*

<sup>1</sup>*HiLASE, Centre, Institute of Physics of the Czech Academy of Sciences, Dolní Břežany, Czech Republic*

<sup>2</sup>*University of Edinburgh, School of Chemistry, Edinburgh, United Kingdom*

<sup>3</sup>*Nagoya University, Department of Chemistry, Nagoya, Japan*

Fundamental research of two dimensional materials such as graphene and transition metal dichalcogenides (TMDs) is demonstrating their potential for opto-electronics with specific focus on stacked heterostructures [1]. However, positioning of the nanomaterials in a clean and rapidly reproducible method is yet to be established. The issue of contamination, structural damage, induced stress regions, and precise placement is slowing the advancement of this field. The work presented will focus on the recent advancement of blister-based laser-induced forward-transfer (BB LIFT) as a non-contact or chemical approach to the transfer of these nano-materials.

The mechanism utilises a femtosecond laser to cause confined ablation at the interface of a transparent material and opaque metal film. The ablated material causes the rapid expansion of the metal film into a blister which ejects the surface material in a comparatively linear fashion, enabling its use as a printing technique. BB LIFT has been shown to gently desorb nanostructures from the scale of 150 nm [2] to fragile molecules which heat or laser irradiation would otherwise cause structural changes to the molecule [3]. It has also been demonstrated that two-dimensional materials can be transferred without inducing structural damage as determined by AFM and Raman spectroscopy of the TMDs MoS<sub>2</sub> and MoSe<sub>2</sub>. Figure 1 displays some examples of MoSe<sub>2</sub> transferred from a ~250 nm titanium surface irradiated by a 120 fs 800 nm laser pulse over a distance of 2 mm. The presented work will focus on the advancements in this technique, expanding the array of transferred two-dimensional materials as well as working towards rapid generation of hetero-structures.

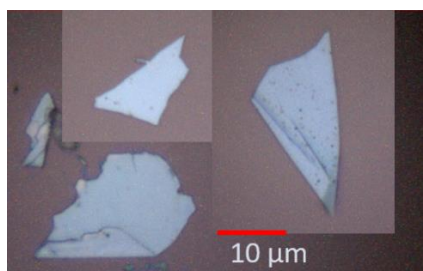


**Fig. 1.**

**References**

- [1] P. Miró, M. Audiffred, and T. Heine, "An atlas of two-dimensional materials," *Chem. Soc. Rev.* 43, 6537 (2014).
- [2] A. V. Bulgakov, N. Goodfriend, O. Nerushev, N. M. Bulgakova, S. V. Starinskiy, Y. G. Shukhov, and E. E. B. Campbell, "Laser-induced transfer of nanoparticles for gas-phase analysis," *J. Opt. Soc. Am. B* 31, C15 (2014).
- [3] N. T. Goodfriend, S. Y. Heng, O. A. Nerushev, A. V. Gromov, A. V. Bulgakov, M. Okada, R. Kitaura, J. H. Warner, H. Shinohara, and E. E. B. Campbell, "Blister-based-laser-induced-forward-transfer: A non-contact, dry laser-based transfer method for nanomaterials," *Nanotechnology* 28, 384301 (2018).

**HiLASE-I-2****Numerical study of thermal dynamics and stress build-up in laser-induced periodic surface structures formation on metals and dielectrics**

*Y. Levy<sup>1</sup>, E.L. Gurevich<sup>2</sup>, N.M. Bulgakova<sup>1</sup>*

*<sup>1</sup>HiLASE Centre, Institute of Physics of the Czech Academy of Sciences, Dolní Břežany, Czech Republic*

*<sup>2</sup>Ruhr-Universität Bochum, Applied Laser Technologies, Bochum, Germany*

Laser-induced periodic surface structures (LIPSS) are believed to originate from a periodic deposition of laser energy, resulting from the interference between electromagnetic surface waves and the laser pulse itself [1]. From this periodic absorption of the laser light to the final morphology of LIPSS, different pathways of relaxation of the absorbed energy are conceivable that results in relocation of material with creation of periodic surface relief [2]. In this study, we wish to shed light on possible routes leading to the LIPSS formation.

The dynamics of temperature have been investigated numerically for the cases of irradiation of different materials by ultrashort linearly-polarized laser pulses with estimation of stress build-up. For this aim, a two-dimensional numerical code based on the two-temperature model has been developed. A modulation is introduced in the laser pulse spatial profile to reproduce the inhomogeneous deposition of energy [3] and the amplitude of the subsequent temperature modulation is followed at the surface of gold and fused silica. Change in optical properties during the laser pulse action are considered via the Drude model. In gold, dynamic optical response is conditioned by swift variation of the collision frequencies of electrons upon their heating while, in fused silica, charge-carriers excitation dynamics is simulated using the rate equation and the carrier density introduced into the optical model.

It has been found that perturbations of the temperature profile can remain substantial for several hundreds of picoseconds in the molten phase of gold in spite of its relatively high thermal conductivity. Change in optical properties also shows a significant effect on the dynamics of temperature modulation under the irradiation regimes above the material modification threshold. The thermal stresses, which can develop in the surface region of the irradiated materials, have been evaluated for our particular irradiation configuration.

**References**

- [1] J.E. Sipe et al., Laser-induced periodic surface structure. I. Theory, Phys. Rev. B 27, 1141 (1983).
- [2] S. Maragkaki et al., Wavelength dependence of picosecond laser-induced periodic surface structures on copper, Appl. Surf. Sci., 417, 88 (2017).
- [3] Y. Levy et al., Relaxation dynamics of femtosecond-laser-induced temperature modulation on the surfaces of metals and semiconductors, Appl. Surf. Sci. 374, 157 (2016).

**HiLASE-I-3****Nonlinear excitation of solids and transient band gap dynamics upon femtosecond laser irradiation of semiconductors: insights from first principles simulations**

*T. Derrien*<sup>1,2</sup>, *N. Tancogne-Dejean*<sup>2</sup>, *V. Zhukov*<sup>1,3,4</sup>, *H. Appel*<sup>2</sup>, *A. Rubio*<sup>2</sup>, *N.M. Bulgakova*<sup>1</sup>  
<sup>1</sup>*HiLASE Centre, Institute of Physics of the Czech Academy of Sciences, Dolní Břežany, Czech Republic*

<sup>2</sup>*Max Planck Institute for Structure and Dynamics of Matter, Theory Department, Hamburg, Germany*

<sup>3</sup>*Novosibirsk State Technical University, Physical-Technical Faculty, Novosibirsk, Russian Federation*

<sup>4</sup>*Institute of Computational Technologies, Siberian Branch of the RAS, Novosibirsk, Russian Federation*

The irradiation of bandgap materials by intense and ultrashort laser pulses leads to the excitation of numerous quantum and macroscopic phenomena [1-3]. To describe a wide variety of physical and chemical processes, both first-principle theories and phenomenological descriptions are of importance [4]. In particular, time-dependent density functional theory (TDDFT) is an efficient first-principle method to predict the excitation dynamics of electrons in laser-irradiated bandgap materials.

In this work, the transient excitation of silicon was studied by extensive TDDFT simulations. The density of conduction band electrons, the total electronic current and the electronic energy were calculated for a wide range laser intensities and for different laser wavelengths. The approach has enabled to achieve a detailed description of the transition from the multiphoton to the tunneling regime of photoionization, characterized by a decrease of a number of photons required for excitation of valence electrons to the conduction bands. The associated nonlinear absorption rates were calculated as a function of laser intensity for several wavelengths. It was found that, at high laser intensities, the density of the excited conduction electrons saturates to the number of electrons initially present in the valence band while, after saturation, free electrons continue to absorb laser energy. The dependence of the free-electron energy on wavelength has peaks, which shift with increasing the laser field strength.

To explain these effects, the dynamics of the electron energy levels in the laser field was studied using a Floquet Hamiltonian, which describes the influence of the laser field on the electronic bands. At low laser intensities, the replicas of the electronic bands are found to locate at energies shifted in comparison to the ground state that is explained by the interaction between the electronic bands. When intensity is increasing, the replicas can cross, manifesting the transient closure of the band gap. This effect is related to the electron tunneling and can be described by the dynamic Floquet-Stark metallization [5-7].

As a whole, this work provides quantitative information that is of high importance for the improvements of theories describing excitation, metallization and damage of laser-irradiated bandgap materials, an important step for gaining more control over ultrashort laser processing of semiconductors and dielectrics.

**References**

- [1] Shugaev, M. V. et al., *MRS Bulletin*, 41, 960(2016).
- [2] Bulgakova, N. M. et al., *Appl. Phys. A*, 81, 345 (2005).

- [3] van Driel, H. M. *Phys. Rev. B*, 35, 8166 (1987).
- [4] Derrien, T. J.-Y. and Bulgakova N. M., in *preparation*.
- [5] Kwon, O. et *al.*, *Sci. Rep.*, 6, 21272 (2016).
- [6] Durach, M.; Rusina, A.; Kling, M. F. & Stockman, M. I. *Phys. Rev. Lett.*, 107, 086602 (2011).
- [7] Schiffrin, A. et *al.*, *Nature*, 493, 70 (2012).

**HiLASE-I-4****Qualification of laser optics for high-power LIDAR space missions**

*N. Bartels<sup>1</sup>, P. Allenspacher<sup>1</sup>, W. Riede<sup>1</sup>*

*<sup>1</sup>DLR, Institute of Technical Physics, Stuttgart, Germany*

Space environment presents unique challenges for the operation of optics and optical coatings as part of laser systems.

This talk summarizes the test technology status for qualifying single component laser optics for space applications and lessons learned from these tests. Tests involve the measurement of laser-induced damage thresholds (LIDT) according to the S-on-1 test procedure detailed in ISO 21254-2 [1] as well as raster scans to test large surface areas.

Another topic is the investigation of laser-induced molecular contamination (LIMC), which can degrade optical components and furthermore dramatically lower the LIDT. We recently developed an ISO technical report [2] describing the systematic measurement of LIMC. Methods to prevent and clean laser-induced deposits are also presented.

Finally, the degradation of non-linear optical crystals due to ionizing radiation (space radiation) and methods for ground-based testing are discussed.

**References**

- [1] ISO 21254 (all parts), Lasers and laser-related equipment - Test methods for laser-induced damage threshold [2] ISO/TR 20811:2017(E), Optics and photonics - Lasers and laser-related equipment – Laser-induced molecular contamination.
- [2] ISO/TR 20811:2017(E), Optics and photonics - Lasers and laser-related equipment - Laser-induced molecular contamination.

**HiLASE-I-5****Laser-induced damage threshold - coating materials and pulse durations**

*H. Kessler<sup>1</sup>*

*<sup>1</sup>Manx Precision Optics Ltd., Sales, Ballasalla, Isle of Man, United Kingdom*

Among the many factors having an influence on the laser-induced damage threshold (LIDT) of optical components are the coating materials used for the optical coating and the pulse duration. In the ns-pulse regime it is relatively easy to scale the LIDT for different pulse durations, but once pulses get shorter than 1 ns, the scaling 'laws' work less and less reliably and the coating material properties themselves become and more and more decisive and LIDT-limiting factor.

The talk will explore the LIDT characteristics and scaling laws for various pulse durations and explore the influence of the coating materials while suggesting solutions on how to maximise the LIDT of optical coatings given the natural restrictions imposed by the available coating materials.

**HiLASE-I-6****A summary on the limitations in measuring a well-defined laser-induced damage threshold**

*I. Balasa<sup>1</sup>, S. Paschel<sup>1</sup>, L. Jensen<sup>1</sup>*

*<sup>1</sup>Laser Zentrum Hannover e.V., Laser Components, Hannover, Germany*

Energy density, power density and linear power density are physical quantities representing the laser-induced damage threshold and are intended to define a confidence level in optical components for the application. As long as the relevant qualification parameters match the application conditions, this works well and is standardized by ISO-21254. If this is not the case, scaling laws and boundary values are documented in comprehensive literature: Mostly known the pulse duration scaling in the short pulse duration regime, the indication of the linear power density for long pulses and large optical components, limitations to the applied laser beam diameter concerning defect distributions, or the repetition frequency scaling of the damage threshold. The diversity of the individual constraints is a result of more than 50 years of intensive and interdisciplinary research in the field of laser-induced damage in optical materials.

**HiLASE-I-7****Process monitoring for metal additive manufacturing by Laser Metal Deposition**

*C. Prieto<sup>1</sup>, M. Diez<sup>1</sup>, S. Carracelas<sup>1</sup>, C. Gonzalez<sup>2</sup>, P. Rey<sup>1</sup>, J. Arias<sup>1</sup>*

*<sup>1</sup>AIMEN, Advanced Manufacturing, O Porriño, Spain*

*<sup>2</sup>AIMEN, Robotics & Control, O Porriño, Spain*

Among Additive manufacturing, Direct Energy Deposition processes, and particularly Laser Metal Deposition (LMD) that build up parts by melting and fusing material as it is being deposited, are showing a growing interest in the industry. They have strong capabilities to build large-sized components, even over non-flat surfaces and with fast building rates comparing to other AM processes. However, work remains for LMD to reach the status of a full production-ready technology for AM applications. An overview on the state of the art of the process monitoring and control solutions and approaches that are being develop to ensure LMD-AM process qualification and good part quality is introduced.

In the context of the european project Integradde, a novel and integrated solution based on data analysis of MWIR coaxial high-speed imaging features and main parameters involved during LMD-p processes is being developed. The developed framework and software tools allow the 3D visualization and reconstruction of thermal features spatially resolved during LMD build-up. In this work, we present the correlation of experimental build information obtained from different stainless steel built parts by LMD with quality parameters measured by DT and NDT. Thus, we investigate and analyse the influence of process parameters and path planning strategies on part quality results, mechanical properties, microstructure and formation of defects.

**Acknowledgements**

This work is carried out under FoF-04-2018 project on the topic "Pilot lines on metal additive manufacturing" <http://www.integraddeproject.eu>. This project has received funding from the European Union's Horizon 2020 research and innovation program under grant agreement No 820776.

**HiLASE-I-8 (Keynote)****High speed Laser Induced Forward Transfer for flexible electronics applications***I. Zergioti<sup>1</sup>**<sup>1</sup>National Technical University of Athens, Physics Department, Athens, Greece*

Over the past decade, printed electronics technology has evolved and is now used in applications such as flexible screens, intelligent labels and packaging. Among the printing techniques, Laser-induced forward transfer (LIFT) technique is capable of printing electrical circuits quite inexpensively and quickly. At the same time, this technique is environmentally friendly and has no restrictions in terms of viscosity. In this work we highlight the newest trends of LIFT manufacturing for the development of a variety of components with electronic, optoelectronic and sensing functionality such as RFID antennas, RF transmission lines, organic thin-film transistors, metallic interconnects, circuits defects repairing and chemical sensors.

Novel printing methods, such as non-contact and “direct-write” printing techniques, represent a class of emerging technologies over the past decade, with respect to micro patterning of electronic circuitry. Laser-induced forward transfer technique in particular, has been widely investigated, because it is relatively fast, environmentally friendly and has no restrictions in terms of viscosity. In this work, we employ a high-speed imaging set up in order to investigate the liquid jet's propagation formed during the printing procedure. Different Ag nanoparticle inks are studied and compared, over a wide range of viscosities and two different cases of surface tension. The initial phases of the spreading process are largely influenced by the impact speed, the jet diameter just before impact and the break time during the wetting phase, the rheological properties of the ink, especially surface tension, combined with the wetting properties of the receiver substrate will determine the final spreading and shape of the printed droplet. Following the printing process analysis, a systematic experimental and theoretical investigation of the laser sintering was conducted on printed micro-patterns comprising Ag and Cu viscous nanoparticle inks. The main goal of this investigation is the determination of the optimal processing parameters for the fabrication of highly conductive Ag and Cu patterns on polymeric substrates with current applications in organic and large area electronics.

In this work we highlight the newest trends of LIFT manufacturing for the development of a variety of components with electronic, optoelectronic and sensing functionality such as RFID antennas, RF transmission lines, organic thin-film transistors, metallic interconnects, circuits defects repairing and chemical sensors.

**HiLASE-I-9****Modeling of femtosecond laser induced out of equilibrium electron transport in metals**

*S. Coudert<sup>1</sup>, G. Duchateau<sup>1</sup>, P. Lalanne<sup>2</sup>, S. Dilhaire<sup>3</sup>*

*<sup>1</sup>CELIA- Universite de Bordeaux, ifcia, Talence, France*

*<sup>2</sup>LP2N-Universite de Bordeaux, plasmonics, Talence, France*

*<sup>3</sup>LOMA - Universite de Bordeaux, Laser, Talence, France*

Plasmonic devices enables to manipulate light at extremely narrow space scales, down to tenth of the optical free wavelength of light, and even less. Applications of such devices include the enhanced Raman spectroscopy, sensing, and photonic nanoswitches. These developments lead to the emergence of new field of investigation: managing hot electrons production and transport which promise further significant advantages as unprecedented efficiency for water photocatalysis and photovoltaic devices for example. It is thus crucial to understand the field induced electron dynamics at short time and space scales.

Such conditions are fulfilled by irradiating a nanometric film by femtosecond laser pulses. In that case, the heated volume can be significantly smaller than the electron mean free path, and the averaged electronic relaxation time is of the order of the pulse duration. More precisely, for a laser wavelength in the visible range, the photon energy is much larger than the electron temperature, leading to an electron energy distribution far from the equilibrated Fermi-Dirac statistics on the shortest timescales. The so-called hot electrons then may lead to an energy transport departing from the standard diffusive (Fourier) behavior.

To model the laser induced out of equilibrium electron transport in metals, we have developed an approach relying on the resolution of the kinetic Boltzmann equation which provides the evolution of the electron energy distribution in time and in one dimension of space. This approach is based on a decomposition of the distribution function on a Legendre polynomial basis set, making the numerical scheme efficient. The results show that the out of equilibrium energy distribution affects the energy transport, highlighting a non-trivial behavior due to the simultaneous contribution of both diffusive and ballistic electronic transport. The numerical results are compared to data obtained with a pump-probe thermo-reflectance setup. The results are in a good agreement, validating the present theoretical development.

## HiLASE-I-10

### Nano-ablation by femtosecond laser-metal interactions

*S. Sakabe*<sup>1,2</sup>, *M. Hashida*<sup>1,2</sup>, *S. Inoue*<sup>1,2</sup>

<sup>1</sup>*Kyoto University,*

*Institute for Chemical Research- Advanced Research Center for Beam Science, Uji- Kyoto, Japan*

<sup>2</sup>*Kyoto University, Graduate School of Science- Department of Physics, Kyoto, Japan*

Lasers are widely used in the industry as modern processing tools for drilling, cutting, fluting, grooving, peening, and so on. All the processing is based on laser ablation. Major processing has been done with rather long pulse lasers (several tens picoseconds to microsecond pulse duration, here simply we call it “nanosecond laser”), and the physics of nanosecond laser ablation has been abundantly studied to be understood well by thermohydrodynamics and laser plasma physics. Recent significant developments of femtosecond laser technologies are opening new aspects in the laser-matter interactions and their applications. In the femtosecond laser interaction with matter, we are observing distinguishing phenomena, which are never seen in nanosecond laser interactions. For femtosecond laser ablation, extremely small amount of ablation less than some nanometer depth is observed even with rather small laser fluence, resulting in discriminative morphology on the matter surface. We name it “nanometer-ablation (simply, nano-ablation)”.

In this presentation, first comparing of laser fluence dependence of ablation rate for femtosecond laser with that for nanosecond laser, the term of nano-ablation is defined with the classification of laser fluence into three (high, middle and low) and distinguish features of femtosecond laser ablation for metals are overviewed. Femtosecond laser nano-ablation is discussed from three aspects, those are, (i) ablation rate, (ii) ion emission, and (iii) surface morphology. Multiple thresholds seen in laser fluence dependence on ablation rate can be interpreted by multiphoton processes and optical field ionization [1]. Ions emitted from the ablation process in low fluence are not distributed in the energy spectrum of Maxwell Boltzmann but in that of Coulomb explosion of nano particles [2]. Laser induced periodic surface structure, so-called LIPSS, is seen in middle fluence [3]. From the observed phenomena, laser produced surface plasma seems to play an important role in LIPSS formation [4]. Even in low fluence nano structure can be seen, but is not LIPSS. We have interpreted it to be formed by aggregation of nano particles in the laser-induced near field around some initial nano hollow and cracks [5].

Finally, potential of nano-ablation with femtosecond lasers to some applications are introduced.

### References

- [1] M. Hashida, *et al.*, Physical Review B 81, 115442(2010); Y. Miyasaka *et al.*, Applied Physics Letters 106, 013101 (2015).
- [2] Y. Miyasaka, *et al.*, Physical Review B 86, 075431 (2012).
- [3] S. Sakabe *et al.*, Physical Review B 79, 033409(2009), (ERATA) 91, 159902(E) (2015); K. Okamuro, *et al.*, Physical Review B 82, 165417 (2010); M. Hashida, *et al.*, Physics Letters 102, 174106 (2013).
- [4] M. Hashida, *et al.*, Applied Physics A 122, 484 (2016); K. Takenaka, *et al.*, Applied Surface Science 478, 882 (2019).
- [5] M. Shimizu, *et al.*, Applied Physics Letters 103, 174106 (2013).

**HiLASE-I-11****Laser ablation mass spectrometry for in-vivo detection of cancer: the SPIDERMASS project**

*C. Focsa*<sup>1</sup>, *M. Ziskind*<sup>1</sup>, *B. Fatou*<sup>2</sup>, *I. Fournier*<sup>3</sup>, *M. Salzet*<sup>3</sup>

<sup>1</sup>*University of Lille, PhLAM, Physics of Lasers, Atoms and Molecules, Villeneuve d Ascq, France*

<sup>2</sup>*Harvard Medical School, Boston Children's Hospital, Boston, USA*

<sup>3</sup>*University of Lille, PRISM - Proteomics- Inflammatory Response- Mass Spectrometry, Villeneuve d Ascq, France*

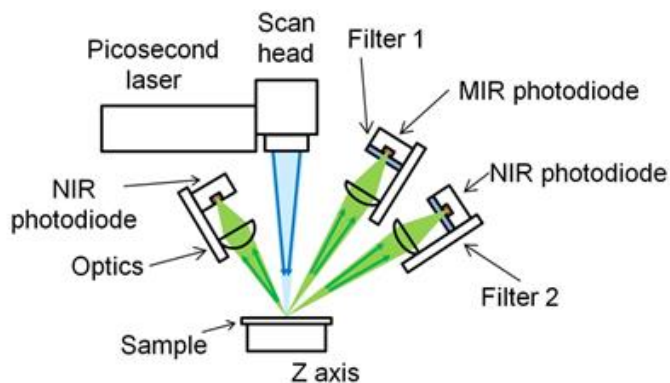
Laser micro-sampling is a promising tool for ambient pressure imaging of biological material by mass spectrometry (MS). Conventional approaches use laser energy coupling into the analyzed sample through electronic (UV, VIS) or vibrational (IR) channels [1,2]. We have recently developed a new instrument (called SpiderMass [3,4]) for in vivo and real-time MS molecular analysis using a laser microprobe operating under ambient conditions through resonant IR excitation of endogenous water molecules. In our prototype, a fibered IR Optical Parametric Oscillator (OPO) is tuned at 2.94  $\mu\text{m}$  to excite the most intense vibrational band (O-H stretching mode) of water, which acts as a natural matrix leading (through a MALDI mechanism) to the generation of ions that can be transported over a few meters to a MS instrument. The molecular patterns (metabolites, lipids and proteins) thus retrieved [5] are specific to cell phenotypes and benign versus cancer regions can easily be differentiated in order to define the tumor resection margins and to assess the cancer stage. A first assessment of the prototype performances was recently performed in a veterinary surgical room on dog sarcoma [6]. SpiderMass was also successfully demonstrated in other fields, like analysis of human skin, real-time drug metabolism pharmacokinetic (DMPK) analysis, or food safety [7].

**References**

- [1] B. Fatou, M. Wisztorski, C. Focsa, M. Salzet, M. Ziskind, I. Fournier, *Substrate-Mediated Laser Ablation under Ambient Conditions for Spatially-Resolved Tissue Proteomics*, Sci. Rep. 5 (2015) 18135
- [2] T. Maulouet, B. Fatou, C. Focsa, M. Salzet, I. Fournier, M. Ziskind, *Optimizing the substrate-mediated laser ablation of biological tissues: Quest for the best substrate material*, Appl. Surf. Sci. 473 (2019) 486
- [3] Salzet, M., Fournier, I., Focsa, C., Ziskind, M., Fatou, B., and Wisztorski, M. (2019). *Device for real-time in vivo molecular analysis*. In (US Patent 10,254,275 B2).
- [4] B. Fatou, Ph. Saudemont, E. Leblanc, D. Vinatier, V. Mesdag, M. Wisztorski, C. Focsa, M. Salzet, M. Ziskind, I. Fournier, *In vivo Real-Time Mass Spectrometry for Guided Surgery Application*, Sci. Rep. 6 (2019) 25919
- [5] B. Fatou, M. Ziskind, P. Saudemont, J. Quanico, C. Focsa, M. Salzet, I. Fournier, *Remote Atmospheric Pressure Infrared Matrix-Assisted Laser Desorption-Ionization Mass Spectrometry of Proteins*, Mol. Cell. Proteomics 17 (2018) 1637
- [6] Ph. Saudemont, J. Quanico, Y.-M. Robin, A. Baud, J. Balog, B. Fatou, D. Tierny, Q. Pascal, K. Minier, M. Pottier, C. Focsa, M. Ziskind, Z. Takats, M. Salzet, I. Fournier, *Real-time molecular diagnosis of tumors using water-assisted laser desorption/ionization mass spectrometry technology*, Cancer Cell 34 (2018) 840
- [7] B. Fatou, P. Saudemont, P. Duhamel, M. Ziskind, C. Focsa, M. Salzet, I. Fournier, *Real time and in vivo pharmaceutical and environmental studies with the SpiderMass instrument*, J. Biotechnol. 281 (2018) 61

**HiLASE-I-12****High speed laser surface texturing and time-resolved temperature measurement***J. Martan<sup>1</sup>, D. Moskal<sup>1</sup>, M. Kučera<sup>1</sup>, L. Prokešová<sup>1</sup>, M. Honner<sup>1</sup>**<sup>1</sup>University of West Bohemia, New Technologies - Research Centre, Plzen, Czech Republic*

Laser micromachining using high power ultrashort pulsed lasers is the scientific field of intensive developments in last years. Although the process is so called “cold ablation”, for high power lasers, thermal effects occur and can cause degradation of material or surface topography. An innovative laser surface texturing (LST) method was developed to enable high processing speeds and low thermal effects at the same time. It is called shifted LST method [1]. In order to be able to characterize the heat accumulation in material in pulse laser processes, a measurement system was developed for time resolved temperature measurements in nanosecond time scale. It is based on high speed infrared detectors (Fig. 1). The system was first used to characterize laser marking of stainless steel by a nanosecond laser [2]. It was found that for shorter pulse duration the temperature rises over the melting temperature and causes melting and decrease of corrosion resistance. After that, the system was used to evaluate heat accumulation in laser surface texturing by different methods, including the shifted LST. For the used 14 W average power picosecond laser system, the heat accumulation was detected for very low scanning speeds ( $< 0.05$  m/s) for all pulse energies in machining of lines and for certain scanning strategies in laser surface texturing

**Fig. 1.**

of dimples. The shifted LST method proved to be a reliable method for precision surface texturing at high scanning and processing speeds. The fast temperature measurement system can be used as a tool for technology developers for comparing different scanning strategies and material removal approaches and for choosing the right strategy for the desired application. This will be mainly important for kW class pulsed lasers.

The work has been supported by the Ministry of Education, Youth and Sports of the Czech Republic (OP RDI program, CENTEM project, no. CZ.1.05/2.1.00/03.0088, co-funded by the ERDF) and ERDF ("LABIR-PAV / Pre-application research of infrared technologies" project, No. CZ.02.1.01/0.0/0.0/18\_069/0010018).

**References**

- [1] J. Martan, D. Moskal, M. Kučera, Laser surface texturing with shifted method — Functional surfaces at high speed, *J. Laser Appl.* 022507 (2019) 1–9.
- [2] M. Kučera, J. Martan, A. Franc, Time-resolved temperature measurement during laser marking of stainless steel, *Int. J. Heat Mass Transf.* 125 (2018) 1061–1068.

**HiLASE-I-13****Femtosecond laser inscription of fiber Bragg gratings for laser and sensing applications**

*A. Dostovalov<sup>1,2</sup>, A. Wolf<sup>1,2</sup>, E. Evmenova<sup>1</sup>, M. Skvortsov<sup>1,2</sup>, S. Abdullina<sup>1</sup>, K. Bronnikov<sup>1,2</sup>, S. Yakushin<sup>2</sup>, A. Kuznetsov<sup>1</sup>, S. Kablukov<sup>1</sup>, S. Babin<sup>1,2</sup>*

<sup>1</sup>*Institute of Automation and Electrometry SB RAS, Fiber optics lab, Novosibirsk, Russian Federation*

<sup>2</sup>*Novosibirsk State University, The Department of Physics, Novosibirsk, Russian Federation*

The possibility of a local refractive index change in transparent materials by femtosecond laser pulses has opened up new possibilities for creating fiber Bragg gratings (FBGs) for laser and sensing applications. In particular, it expanded the operating temperature (due to the use of sapphire fibers) and strain range (due to inscription without removing the protective coating) in comparison with FBGs inscribed by UV radiation. In case of FBG inscription for fiber lasers, the flexibility of femtosecond laser writing technology made it possible to create new configurations of fiber laser cavities, in particular, to inscribe FBGs in active optical fibers that are non-photosensitive for UV radiation.

The results of FBG inscription by femtosecond laser radiation to create single-frequency DFB fiber lasers generating radiation in spectral ranges of 1.55  $\mu\text{m}$  (erbium)[1,2] and 2  $\mu\text{m}$  (thulium, holmium) with a spectral linewidth of the order of 10 kHz will be presented. In addition, the results of FBG writing in multimode fiber for the selection of transverse modes in Raman fiber laser will be presented [3]. In this case, due to the precise positioning of the FBG in the multimode fiber cross section, it is possible to select certain transverse modes efficiently, which in the case of fundamental mode selection results in an improvement in output beam quality ( $M^2 = 1.2$ ). In addition, the technology of refractive index modification by fs laser pulses allows selective inscription of FBGs in multicore optical fibers that is an actual task for various applications. One of them is sensing systems, including structural-health monitoring, robotics and minimally invasive surgery, where the 3D shape estimation of manipulator is required for accurate and reliable control of the manipulator movement inside the patient's body. The results of FBG arrays inscription in various types of 7 cores fibers, with straight and twisted side cores, to be presented [4]. 2D and 3D shape reconstructions based on these fiber sensors and sources of reconstruction errors will be discussed.

This work was supported by Russian Science Foundation (Grant 18-72-00139).

**References**

- [1] M. I. Skvortsov, A. A. Wolf, A. V. Dostovalov, A. A. Vlasov, V. A. Akulov, and S. A. Babin, "Distributed feedback fiber laser based on a fiber Bragg grating inscribed using the femtosecond point-by-point technique," *Laser Phys. Lett.* 15, 035103 (2018).
- [2] A. Wolf, A. Dostovalov, M. Skvortsov, K. Raspopin, A. Parygin, and S. Babin, "Femtosecond-pulse inscription of fiber Bragg gratings with single or multiple phase-shifts in the structure," *Opt. Laser Technol.* 101, 202–207 (2018).
- [3] E. A. Evmenova, A. G. Kuznetsov, I. N. Nemov, A. A. Wolf, A. V. Dostovalov, S. I. Kablukov, and S. A. Babin, "2Nd-Order Random Lasing in a Multimode Diode-Pumped Graded-Index Fiber," *Sci. Rep.* 8, 17495 (2018).
- [4] A. Wolf, A. Dostovalov, K. Bronnikov, and S. Babin, "Arrays of fiber Bragg gratings selectively inscribed in different cores of 7-core spun optical fiber by IR femtosecond laser pulses," *Opt. Express* 27, 13978–13990 (2019).

**HiLASE-I-14**  
**High power mid-IR DPSSLs**

*J. Hein<sup>1</sup>, J. Körner<sup>1</sup>, J. Reiter<sup>2</sup>, M. Kaluza<sup>1</sup>*

*<sup>1</sup>Friedrich-Schiller University Jena, Institute for Optics and Quantum Electronics, Jena, Germany*

*<sup>2</sup>Helmholtz-Institute Jena, Relativistic Laser Physics, Jena, Germany*

High intensity and therefore high energy laser pulses at mid-infrared wavelengths increasingly attracting high attention. A couple of laser plasma interaction research fields like ion acceleration or laser wake field acceleration as well as the production of secondary radiation sources that range from high harmonics to the THz will benefit from the wavelength scaling of important plasma parameters. Even if the diffraction limited spot size will increase with the longer laser wavelength, larger volumes and interaction length can compensate for the lower intensity. Since most high power lasers worldwide, particularly high energy diode pumped amplifiers, are operating in the near infrared range, costly frequency conversion is required to get the desired pulses at longer wavelength. A considerable advantage could be expected by building diode pumped lasers that directly generate short pulses at such wavelengths with increased repetition rates. Some potential pathways with the prospect to even generate ultra-short pulses in the mid-infrared range based on long known materials and readily available laser diode technology are discussed.

**HiLASE-I-15****Highly efficient frequency conversion scalable from 10 J at 10 Hz to 100 J 10 Hz using DPSSL laser technology**

*J. Phillips<sup>1</sup>, S. Banerjee<sup>1</sup>, P. Mason<sup>1</sup>, K. Ertel<sup>1</sup>, M. Divoky<sup>2</sup>, J. Pilar<sup>2</sup>, A. Lucianetti<sup>2</sup>,  
M. De Vido<sup>1</sup>, T. Butcher<sup>1</sup>, Ch. Edwards<sup>1</sup>*

<sup>1</sup>*STFC, Central Laser Facility, Chilton, Didcot, United Kingdom*

<sup>2</sup>*HiLASE Centre, Institute of Physics of the Czech Academy of Sciences, Dolní Břežany, Czech Republic*

High energy (100 J- level) and high average power (1kW) nanosecond diode pumped solid-state laser (DPSSL) systems operating at near-IR, are required for new scientific applications like material processing, advanced imaging and high energy density (HED) experiments. To increase the functionality of these near-IR DPSSL systems, efficient and stable frequency conversion to visible light is a pivotal step towards development of ultra-short (fs) amplifier via OPCPA or Ti:Sapphire pumping. Recently, we have successfully demonstrated a 100J-scale (beam size 75 mm square) DPSSL based on cryogenic gas cooled, multi-slab ceramic Yb:YAG amplifier technology. DiPOLE100 / “BiVOJ” has been operated at 10 Hz with pulse energy of 105 J and pulse duration of 10 ns with an optical-to-optical conversion efficiency of 22.5%<sup>1</sup>. Owing to the limited availability of large aperture non-linear optical crystals<sup>2</sup>, we have used a scaled-down approach with the 10J and 100J outputs, respectively. The 100J output beam is 75 mm square and we reduce this beam to 50 mm square. For the 10 J output we reduce the beam from 22 mm to 14 mm square. We also present the design of 10 J and 100 J frequency conversion stages where the 10 J has been implemented on the “Bivoj” laser at HiLASE as part of the “HiLASE Centre of Excellence” Widespread Teaming project, where it will be used for experiments including damage testing of optics and laser shock peening We describe frequency conversion for second harmonic from the fundamental for 60% conversion efficiency at 5.6J input. We also show results for frequency conversion to third harmonic at 60% conversion efficiency for the same input. The second harmonic RMS is 0.84% at 3.58 J at SHG with 60% efficiency for 1.8 hours measured at HiLASE. We also describe at setup for 100 J for frequency conversion at CLF using the DiPOLE100.

The authors gratefully acknowledge funding for this work from the H2020 Widespread Teaming action and the Czech Ministry of Science.

**References**

- [1] P. Mason, M. Divoky, K. Ertel, J. Pillar, T. Butcher, M. Hanus, S. Banerjee, J. Phillips, J. Smith, Mariastefania De Vido, A. Lucianetti, C. Hernandez-Gomez, T. Mocek and J. Collier *Optica* Vol 4, No. 4, 438 (2017).
- [2] J. P Phillips, S. Banerjee, M. Fitton, T. Davenne, J. Smith, K. Ertel, P. Mason, T. Butcher, Mariastefania, J. Greenhaulgh, C. Edwards, C. Hernandez-Gomez and J. Collier, *Optics Express*, 24, 19682, (2016).

**HiLASE-I-16****Unstable cavity lasers for compact short pulse high energy lasers**

*J. Hein<sup>1</sup>, J. Körner<sup>1</sup>, M.C. Kaluza<sup>1</sup>, D. Rostohar<sup>2</sup>, A. Lucianetti<sup>2</sup>, T. Mocek<sup>2</sup>, S. Zulic<sup>2</sup>*

*<sup>1</sup>Friedrich-Schiller University Jena, Institute of Optics and Quantum Electronics, Jena, Germany*

*<sup>2</sup>HiLASE Centre, Institute of Physics of the Czech Academy of Sciences, Dolní Břežany, Czech Republic*

Nowadays, most diode pumped high energy class laser amplifiers follow the so called master oscillator power amplifier scheme. Here, an oscillator generates a rather low energetic pulse that is then further amplified stepwise by a chain of amplifiers. Though this concept is capable of delivering high energy pulses with very flexible pulse parameters, the complexity of such systems is a major drawback if it comes to robustness, size and economics.

We will present an alternative approach based on a novel unstable cavity design with intrinsic gain modulation that allows the generation of nanosecond pulses with more than 1 J output energy directly from a laser cavity with a top-hat shaped output beam distribution. The novel design reduces the minimum gain needed in such cavity compared to the state of the art unstable cavity layout using graded reflectivity mirrors and therefore can be combining this design with lower gain material like high efficient ytterbium doped gain media. Furthermore, our approach allows operating such cavity with zero output coupling, while still establishing a top-hat shaped intra cavity intensity distribution. Due to this the operation in a cavity dump mode or as regenerative amplifier is possible as well.

With a prototype system we demonstrated the operability of this design. The system is based on cryogenically cooled Yb:YAG ceramic and allows to generate an output energy of >1 J in a hexagonal top-hat beam. The system is very compact (approx. 80x60cm<sup>2</sup>) and also achieves a very high conversion efficiency of more than 30% from installed pump power to output energy.

**HiLASE-I-17****Quarter century development of laser shock peening and expansion of applications with novel palmtop lasers***Y. Sano*<sup>1</sup><sup>1</sup>*Institute for Molecular Science, Division of Research Innovation and Collaboration, Okazaki, Japan*

Compressive residual stress (RS) in the near surface layer of metallic materials has favourable effects to prolong fatigue life and reduce stress corrosion cracking (SCC) susceptibility [1,2]. Laser shock peening (LSP) is known as an effective tool to introduce compressive RS by irradiating intense laser pulses to the surface of materials covered with water for confining laser-induced plasma [3]. LSP has been applied to jet engine fan blades to prolong their service lives since 1990's [4]. However, the application of LSP is limited mainly to production in factories because the laser system was huge and sensitive to surrounding conditions, consequently it is not convenient for field operation.

To cope with this situation, we reduced the pulse energy down to 10 mJ, one to three orders of magnitude smaller than that of the usual LSP conditions, and applied to HT780 (780 MPa grade structural steel) base material and the welded joints [5]. Compressive RS was built on surface by LSP with 10 mJ pulse energy. Fatigue test results showed that LSP with 10 mJ significantly prolonged fatigue life and has the almost same effect as LSP with 200 mJ pulse energy (Fig. 1). Then, we started developing ultra-compact palmtop laser oscillators with pulse energy of 20 mJ [5] and completed a prototype together with a battery-driven power supply. The laser oscillators can be easily handled by a multi-axes robotic arm (Fig. 2), which could realize actual applications of LSP to the maintenance of aged infrastructure such as bridges in the field. The effects of LSP with low energy laser pulses on RS and fatigue properties, the status of the palmtop laser development and concept to apply LSP to infrastructure will be presented.

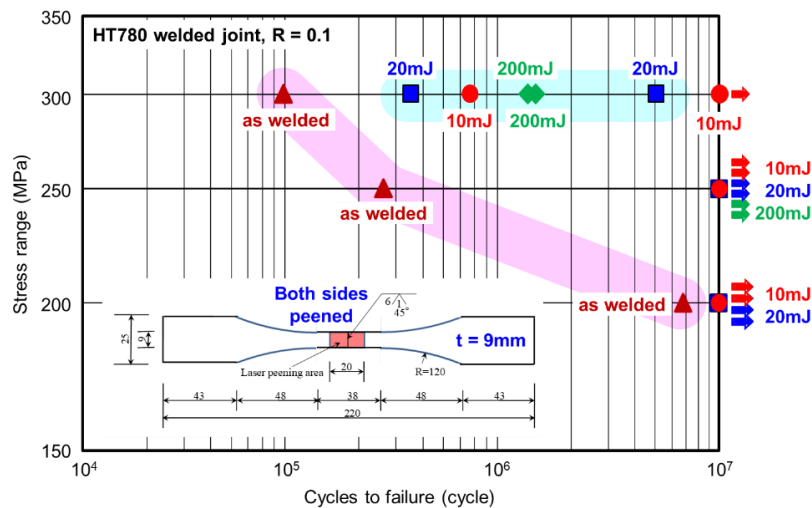


**Fig.1.** Fatigue test results of as-welded and LSPed HT780 joints.

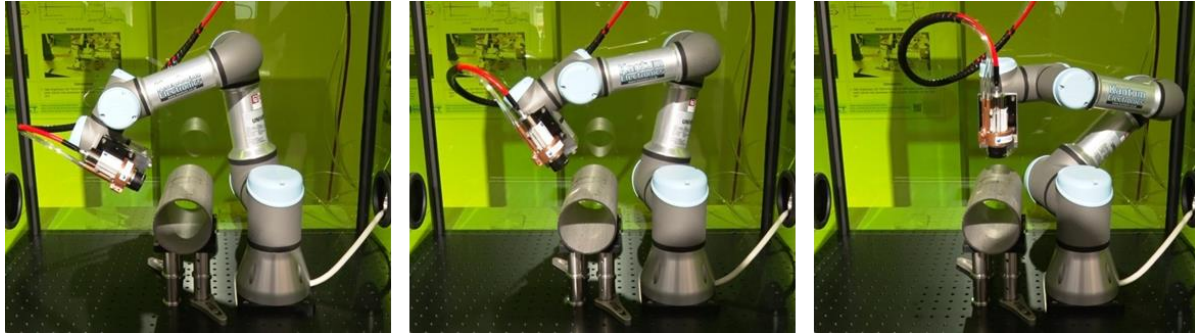


**Fig. 2.** A palmtop laser oscillator driven by a robotic arm.

## References

- [1] Y. Sano, M. Obata, T. Kubo, N. Mukai, M. Yoda, K. Masaki and Y. Ochi: Retardation of Crack Initiation and Growth in Austenitic Stainless Steels by Laser Peening without Protective Coating, *Mater. Sci. Eng. A*, vol. 417 (2006) 334-340.
- [2] Y. Sano, M. Kimura, K. Sato, M. Obata, A. Sudo, Y. Hamamoto, S. Shima, Y. Ichikawa, H. Yamazaki, M. Naruse, S. Hida, T. Watanabe and Y. Oono: *Proceedings of the Eighth International Conference on Nuclear Engineering (ICONE-8)*, Baltimore, 2000 (paper no.: ICONE-8441).
- [3] Y. Sano, N. Mukai, K. Okazaki and M. Obata: *Nucl. Instrum. Meth. Phys. Res. B*, vol. 121 (1997) 432-436.
- [4] D.W. See, J.L. Dulaney, A.H. Clauer and R.D. Tenaglia: The Air Force Manufacturing Technology Laser Peening Initiative, *Surface Eng.*, vol. 18 (2002) 32-36.
- [5] <https://www.youtube.com/watch?v=nMsOkkEPK5I>.

**HiLASE-I-18****Microstructural issues of materials properties after laser shock peening**

*V. Vasudevan*<sup>1</sup>

<sup>1</sup>*University of Cincinnati, Mechanical and Materials Engineering, Cincinnati, USA*

This talk will mainly focus on the nature of the gradient microstructure generated by laser shock peening (LSP) of metals with and without an ablative coating. The characteristics of the near-surface microstructures that can result as studied by EBSD/OIM, XRD and TEM, including dislocation and crystallite structures, texture, strain-induced martensite, surface oxides, nanostructures, etc, their dependence on the process variables and thermal stability will be described with examples from a variety of alloys such as IN718, IN718+, Ti-6Al-4V, Ti6242, alloy 600, 304 stainless steel, Al 7075 and Al 5083. Local property changes measured by nanoindentation, microhardness and micropillar compression tests will be reported. The results showing the relationship between process parameters and the near-surface microstructure and thermal stability of both, mechanical properties, including hardening and fatigue, corrosion and stress corrosion cracking behavior, will be presented and discussed.

**HiLASE-I-19****Laser peen forming of large scale specimen with complex shape***M. Luo<sup>1</sup>, Y. Hu<sup>1</sup>**<sup>1</sup>Shanghai Jiao Tong University, Mechanical Engineering, Shanghai, China*

Laser peen forming (LPF) is now emerging as a viable means for the shaping of large scale panels. Complex shaping of large scale panel after laser peen forming is very challenge due to its high flexible process to form by a large amount of laser shocks. The aim of this study is to develop an effective way to complete efficient process planning of LPF for complex shape forming. The eigen-moment is defined to describe the deformation behaviour of metal plates under LPF, which can provide an efficient way to analyse the bending shape under different process parameters. And the distributed eigen-moment in the panel is prescribed as an PDE-constrained optimization problem to achieve the process planning of complex shaping. A complex shape with saddle geometry is used as a typical case to demonstrate this method with experiments. The experiments conducted with the planned parameters can produce an expected shape to match the objective geometry. Besides, a flexible 3D scanning facility is developed for LPF of large-scale panels. A brief introduction of this system will be given. And a few cases for LPF of large scale panel will also be provided.

**HiLASE-I-20****Mechanisms of residual stress generation using Laser Shock Peening**

*N. Smyth<sup>1</sup>, M. Leering<sup>1</sup>, M. Fitzpatrick<sup>1</sup>*

*<sup>1</sup>Coventry University, Faculty of Engineering- Environment & Computing, Coventry, United Kingdom*

Laser Shock Peening (LSP) is an advanced surface treatment used to introduce beneficial compressive residual stress in metallic structures. These residual stresses can significantly enhance fatigue performance thus extend the service life and increase the damage tolerance of safety critical components and structures. Therefore, LSP can provide major cost and safety benefits when applied correctly. However, this complex process can have the opposite effect when poor process parameters are selected or if tensile balancing stresses are not considered.

Laser peening requires preselection of a number of processing parameters each having an influence on the induced residual stress field. With the advancements in laser technology, the ‘Bivoj’ laser system at HiLASE is one of the most versatile and customisable systems available to carry out LSP activities. We conducted an experimental investigation in which the most significant processing parameters, namely laser energy, pulse duration and spot size, were independently varied to characterise their effect on the formation of residual stresses in aerospace aluminium. The resultant residual stress fields were measured using incremental hole drilling method.

Using the unique capabilities of the Bivoj system, we have been able to purely study the effects of the laser pulse temporal profile on the formation of residual stresses. In the past, similar studies would have to be carried out over many laser systems. By using a single system experimental error and laser variation between sources have been reduced. The distribution of laser intensity and the manner in which energy is supplied to the target surface has been seen to greatly affect the outcome of the processing. The temporal profile was varied from classical LSP shapes such as a Gaussian and flat top to double peaked profiles. The constructive interference of the propagating stress waves created by the two pulse peaks can lead to high magnitude and deeper introduced residual stresses. The peak intensity and full width half maximum have been kept constant across all profiles, as shown in the normalised intensity plots in figure 1. In parallel with experimental programme is a series of mechanistic finite element simulations of the pulse and material interaction.

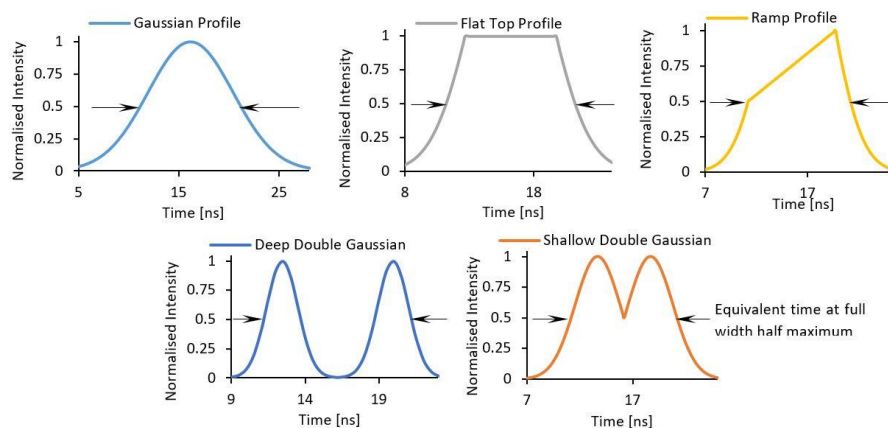


**Fig. 1.** Normalised Laser Shock Peening temporal profile.

**HiLASE-O-1****Effect of phase shift, polarisation vector orientation and incident angle shift on multiple beam interference pattern.**

*D. Jochcová<sup>1,2</sup>, J. Kaufman<sup>1,2</sup>, P. Hauschwitz<sup>1,2</sup>, J. Vanda<sup>1</sup>, J. Brajer<sup>1</sup>, D. Rostohar<sup>1</sup>, T. Mocek<sup>1</sup>*

*<sup>1</sup>HiLASE Centre, Institute of Physics of the Czech Academy of Sciences, Dolní Břežany, Czech Republic*

*<sup>2</sup>Czech Technical University in Prague, Faculty of Nuclear Sciences and Physical Engineering, Prague, Czech Republic*

Nanostructuring and microstructuring approaches such as Electron Beam Litography or Nanoimprint Litography, frequently used in microelectronics manufacturing, require considerable amount of time. In order to reduce processing time, laser patterning methods based on interference of multiple beams have been developed. Within one laser pulse, significant part of an irradiated area on a sample surface is patterned with desired micro or submicrostructures. Nowadays, interference patterning is not limited just to periodic lines and dots. Controlling of number of interfering beams, orientation of polarisation vectors, relative phase shift and incident angle of beams allows to customize an intensity distribution in an interference field even more. Simulations of various interference patterns were generated and some of them were observed via CCD.

**HiLASE-O-2****Two-step nanosecond laser processing for dual-scale micro- and nanostructure fabrication of superhydrophobic stainless steel surface.**

*P. Hauschwitz<sup>1,2</sup>, J. Radhakrishnan<sup>1</sup>, R. Bicistova<sup>1</sup>, D. Jochcova<sup>1,2</sup>, J. Brajer<sup>1</sup>, D. Rostohar<sup>1</sup>, T. Mocek<sup>1</sup>*

*<sup>1</sup>HiLASE Centre, Institute of Physics of the Czech Academy of Sciences, Dolní Břežany, Czech Republic*

*<sup>2</sup>Czech Technical University in Prague, Faculty of Nuclear Sciences and Physical Engineering, Prague, Czech Republic*

Growing demand for superhydrophobic surfaces in recent years is associated with many attractive science and engineering applications including self-cleaning, anti-icing and anti-corrosive behaviours. Stainless steel type AISI 304L is one of the most versatile and widely used engineering material in industries. Inspired by the “lotus effect” dual scale nano/microstructures have been fabricated by direct laser writing method with nanosecond laser source using two ablation regime. Primarily, microstructures were fabricated with a tightly focused beam in strong ablation regime and subsequently in soft ablation regime to create nano-scale structures by a defocused laser beam. However, the formation of a metal oxide layer on the top of the geometries of freshly prepared laser patterned metal surface causes hydrophilic behaviour. The hydrophilic to superhydrophobic transformation takes several days or weeks by the ageing technique in atmospheric condition unless the laser-patterned surface is covered with non-polar elements with some chemical techniques. In this study, the transition time has been drastically reduced to a few hours by high vacuum processing technique by accelerating the chemisorption process. Wetting properties with respect to laser processing parameters and surface morphology are examined and found to be consistent for large droplet volumes.

## HiLASE-O-3 100 W industrial thin disk regenerative amplifier

*H. Zhou<sup>1</sup>, M. Chyla<sup>1</sup>, J. Horacek<sup>1</sup>, P. Crha<sup>1</sup>, J. Mužík<sup>1</sup>, O. Novák<sup>1</sup>, M. Smrž<sup>1</sup>, T. Mocek<sup>1</sup>*  
*<sup>1</sup>HiLASE Centre, Institute of Physics of the Czech Academy of Sciences, Dolní Břežany, Czech Republic*

High-power ultrafast laser with high repetition rate has been applied in various scientific and industrial fields, such as laser shock peening (LSP), laser micromachining, Mid-IR generation and laser welding. we report on an industrial grade picosecond Yb:YAG thin-disk regenerative amplifier of TRL 6 level for wavelength conversion, Mid-IR generation and various industrial applications. It is a new generation of several years operated Perla C100 laser developed at HiLASE Centre. The laser provides a stable output at repetition rate of 50 kHz with average power of 100 W and <2 ps pulse duration. The thermal effect of the thindisk is one of the main issues affecting the system stability. In order to reduce the quantum defect in the gain medium, the Zero Phono Line (ZPL) pumping approach was applied. By directly pumping the disk at 969 nm wavelength to the upper level of Yb:YAG, a highly stable fundamental mode operation was achieved. The front-end was based on PM fiber components in order to obtain stable and reliable seed source. Three stages of amplification, including two stages of amplification with single cladding gain fiber and one stage of amplification with double cladding gain fiber, are designed to stretch and amplify the seed pulses from 150 fs, 50 MHz and ~200 mW with 10 nm spectral bandwidth to 500 ps, 1 MHz and 1 W with 3 nm spectral bandwidth. The front-end can be upgraded by a 4-pass rod amplifier in order to obtain higher seed power. The seed beam from the fiber amplifier can be amplified up to 9W output power after passing the rod-type gain media (2%-doped Yb:YAG) 4 times. The 4-pass scheme of the rod amplifier can provide high stability, high amplification efficiency and good beam quality of  $M^2 < 1.17$ . The average power stability of 0.7% of regenerative amplifier is supported by stable operation of the front-end with relatively high seed energy. A Chirped Volume Bragg Grating (CVBG) is used as a robust and compact pulse compressor for high power picosecond pulses. Benefiting from the high dispersion, 2 mJ at 50 kHz laser pulses are compressed bellow 2 ps. Cavity stabilization, beam pointing stabilization systems and pulse picker are integrated into the control system of the laser which together with a robust, thermally stabilized housing provides the stability necessary for realization of the various industrial goals. The pulse-on-demand capability of the laser allows the user to control each individual pulse. Benefiting from the modular design concept, this laser can be used for wavelength conversion and Mid-IR generation modules also developed at HiLASE Centre.

**HiLASE-O-4****Single-shot laser beam parameters measurement for near infrared laser beams***S. Nagisetty<sup>1</sup>, T. Miura<sup>1</sup>, M. Chyla<sup>1</sup>, M. Smrž<sup>1</sup>, T. Mocek<sup>1</sup>**<sup>1</sup>HiLASE Centre, Institute of Physics of the Czech Academy of Sciences, Dolní Břežany, Czech Republic*

High power lasers are increasingly used in wide range of material processing and are valuable tools in manufacturing processes [1-3]. Monitoring the laser beam parameters including focused spot size and focal plane location throughout the manufacturing process provides the data needed to evaluate performance and real-time optimize the processes to maintain accuracy. With most beam parameter monitoring systems, the laser beam is not available for processing during the measurement. Moreover, in some cases the measured beam parameters can differ from those during processing. Ideally, a simultaneous measurement of the beam during processing is desired. An important parameter for laser material processing is the beam quality. Additionally, high power lasers cause thermally induced stress on processing optics and results in focal plane shifting [4]. This implies a necessity to monitor the laser beam parameters frequently during processing application. According to ISO 11146,  $M^2$  is obtained by measuring the second moment laser beam widths in at least 10 positions along the beam propagation path [5]. Despite its experimental simplicity, this standard scanning method needs movable parts to scan and measure intensity distributions along the beam propagation and still is time consuming. Hence, this standard method is not suitable for real time monitoring and characterizing the fast dynamics of the laser system.

In this paper, we present simple and fast single-shot method for measuring the  $M^2$  by using photosensitive glass plate, imaging lens and CMOS camera without any moving parts. Photosensitive glass is made of highly transparent material containing nano-sized crystals that effectively converts near-infrared laser beams to visible fluorescence at 550 nm by up-conversion process. When the near-infrared laser beam focused into the cross-sectional direction of photosensitive glass plate instead of perpendicular direction, the visible fluorescence of the glass plate indicates the focusing property of the input beam. Then the visualized beam propagation in the glass is imaged precisely using a high-resolution imaging system and the high number of beam widths around beam waist can be measured. We measured  $M^2$  value of fiber coupled diode laser in two configurations and the results are in excellent agreement compared to standard method. In addition we present the real-time monitoring of focus shift using this technique.

**References**

- [1] M. Smrž, et al. "Advances in High-Power, Ultrashort Pulse DPSSL Technologies at HiLASE," *Appl. Sci.* 7, 1016 (2017).
- [2] C. Wandera, A. Salminen, F. O. Olsen, and V. Kujanpää, "Cutting of stainless steel with fiber and disk laser," 404, 404 (2018).
- [3] I. C. A. Roat and D. Petre, "Industrial Application of High Power Diode Pumped Solid State Laser for Welding Technology," 6 (n.d.).
- [4] F. Abt, A. Heß, and F. Dausinger, "Focusing of high power single mode laser beams," 202, 202 (2018).
- [5] ISO, "Lasers and laser-related equipment — Test methods for laser beam widths, divergence angles and beam propagation ratios — Part 2: General astigmatic beams," *Iso 11146-2 2005*, 15 (2002).

**HiLASE-O-5****Effect of laser shock peening on the microstructure, residual stress, hardness, and fatigue behavior of additive manufactured CoCrMo alloy**

*M. Kattoura<sup>1</sup>, B.T. Donkor<sup>1</sup>, J. Song<sup>1</sup>, J. Kaufman<sup>2</sup>, S.R. Mannava<sup>1</sup>, V.K. Vasudevan<sup>1</sup>*

*<sup>1</sup>University of Cincinnati, Mechanical and Materials Engineering, Cincinnati, USA*

*<sup>2</sup>HiLASE, Centre, Institute of Physics of the Czech Academy of Sciences, Dolní Břežany, Czech Republic*

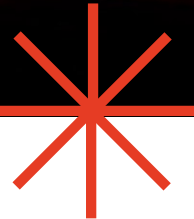
Laser Shock Peening (LSP) is a process where high energy nanosecond laser pulses are used to modify surface characteristics of treated materials. In this work, the effects of LSP on the microstructure, residual stress, hardness and fatigue behaviour of Additive Manufactured (AM) CoCrMo Alloy was investigated. The CoCrMo alloys is commonly utilized in biomedical industry due to its high wear-resistance and biocompatibility. It is used in manufacturing of medical tools, various artificial joints including dental partial bridge work, hips and knee implants. Three processing parameters were studied to optimize the laser peening process: 1) sacrificial layer: black vinyl tape versus aluminum tape, 2) shift between two peening layers, and 3) laser wavelength: infrared laser (1064 nm) versus its second harmonic (532 nm). In all studied laser peening conditions, laser peening induced a Strain-Induced Martensitic Transformation (SIMT) shifting the initially FCC structure to HCP+FCC structure at the surface. The initially high tensile residual stresses created by the AM process were converted to high compressive stresses that protect the material against different type of metal failures. The laser peened samples showed increase in the yield strength by around 15%, the surface hardness was increased roughly by 15% and the fatigue life was improved 10x to 15x when compared to the unpeened samples.



# ALT'19

**INTERNATIONAL CONFERENCE**

**Advanced Laser Technologies**



## Posters

**Prague, Czech Republic**



---

15-20 September 2019

**LM-PS-1****Numerical simulations of energy relaxation in molybdenum thin films upon irradiation by femtosecond and picosecond laser pulses***K. Hlinomaz<sup>1,2</sup>, Y. Levy<sup>1</sup>, T.J.Y. Derrien<sup>1</sup>, N.M. Bulgakova<sup>1</sup>**<sup>1</sup>HiLASE Centre, Institute of Physics of the Czech Academy of Sciences, Dolní Břežany, Czech Republic**<sup>2</sup>Faculty of Nuclear Sciences and Physical Engineering, Czech Technical University in Prague, Department of Physical Electronics, Praha, Czech Republic*

Laser processing of thin films can be employed in electronic component manufacturing and in photovoltaics [1]. However, the control of the process remains delicate due to the high number of phenomena that are taking place in the film. These are dependent on the film thickness, on the choice of substrate, and on the laser wavelength, energy and pulse duration. In addition, several modifications mechanisms can play a role in the modification of the film and/or of the substrate via oxidation [2], melting, ablation via phase explosion [3, 4] or spallation [5]. As a result, both optical and thermal phenomena are contributing to dynamics of the energy absorption, an interplay that can be addressed by numerical modeling. In particular, subtle effects such as transient change of optical properties, rapid electron excitation, thickness-dependent electron-phonon collision rate [6], and stress generation can induce important macroscopic consequences. In view of achieving a better control of laser modification of thin films, more efforts are required in the development of theoretical and numerical descriptions.

In this work, we investigate the energy absorption and subsequent melting of a thin film of molybdenum in contact with a substrate via numerical simulations. The role of the fused silica (resp. soda-lime glass) substrates was investigated for irradiation using short laser pulses of 200 fs (resp. 10 ps) duration. For this purpose a numerical code based on two-temperature model (TTM) was developed. After ensuring the energy conservation of the numerical solver, melting threshold fluences were computed and compared with experimental data on femtosecond and picosecond irradiation [7, 8]. The numerical results well repeated the experimental literature, and enable the possibility to perform further predictions. In addition, the applicability of the thin-film reflectivity model to the case of metals will be discussed.

**References**

- [1] J. Bovatsek et al., *Thin Solid Films* 518, 2897-2904 (2010).
- [2] A. V. Dostovalov et al., *Appl. Surf. Sci.* 491, 650-658 (2019).
- [3] N. M. Bulgakova, A. V. Bulgakov, *Appl. Phys. A*, 73, 199-208 (2001).
- [4] M. V. Shugaev et al., in *Advances in the Application of Lasers in Materials Science*, Springer, 274, 107-148 (2018).
- [5] C. Wu, L. V. Zhigilei, *Appl. Phys. A*, 114, 11-32 (2014).
- [6] K. Sokolowski-Tinten et al., *New J. Phys.* 17, 113047 (2015).
- [7] S.-S. Wellershoff et al., *Appl. Phys. A* 69, S99-S107 (1999).
- [8] M. Domke et al, *Phys. Proc.* 56, 1007-1014 (2014).

**LM-PS-2****Ultrashort laser heating and ablation by one and two pulses of donut-like spatial form**

*A. Fedotov<sup>1,3</sup>, Y. Okru<sup>2</sup>, Y. Tsitavets<sup>3</sup>, I. Gnilitzky<sup>4</sup>*

<sup>1</sup>*HiLASE Centre, Institute of Physics of the Czech Academy of Sciences, Dolní Břežany, Czech Republic*

<sup>2</sup>*Belarusian State University, Energy Physics, Minsk, Belarus*

<sup>3</sup>*Belarusian State University, Computer Modelling, Minsk, Belarus*

<sup>4</sup>*University of Modena and Reggio Emilia, Department of Engineering Sciences and Methods, Modena, Italy*

We have investigated the process of metal melting and ablation caused by femtosecond laser pulses of high intensity by means of numerical experiment. We have used finite element model implemented in COMSOL Multiphysics for the simulation in the framework of two-temperature model (separate electronic and lattice temperatures and heat conduction). We have considered temperature dependent transport coefficients and phase transitions possibility as well. During the study we developed COMSOL 3-dimensional transient model for gold that allows us to model the laser heating and melting in metals, induced by ultrafast laser pulses both of gaussian and non-gaussian spatial form. We have studied the temperature dynamics and ablation characteristics from the number of pulses (single or pair) and the form (gaussian or donut-like) (Figure).

It was revealed that the heat energy deposited from a single or double pulsed beam of a donut form (pulse duration  $\tau_p = 100$  fs, beam radius  $R = 10$   $\mu\text{m}$ ) preserve the volume right under beam center of symmetry unheated for the time comparable to  $10\tau_p$ . The temperature under the center of symmetry of the incident pulse varies slightly, and it has been established that at a depth of 20 nm below the surface there is a collapsing thermal region. This feature of the propagation of the temperature field is of interest for the study of nanostructured surfaces and other relevant applications.

We achieve the highest ablation depth for the pair of pulses irradiation when the second pulses is launched while the melting front reaches a maximum. If the second pulse is launched when temperature increase cause by the first pulse is highest, the ablation depth associated with evaporation will be lower. This is due to a change in the absorption coefficient  $\kappa$ , which decreases with increasing temperature.

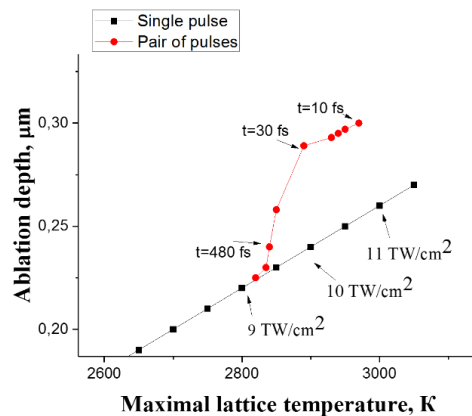


**Fig. 1.** Maximal ablation depth achieved in system vs. maximal lattice temperature for different intensity of incident pulses

## References

- [1] Venkatakrishnan, K. Femtosecond pulsed laser ablation of thin gold film / K. Venkatakrishnan, B. Tan, B.K.A. Ngoi // *Opt. Laser Technol.* – 2002. – Vol. 34, № 3. – P. 199-202.
- [2] Hopkins, P.E. Effects of electron scattering at metal-nonmetal interfaces on electron-phonon equilibration in gold films / P.E. Hopkins, J.L. Kassebaum, P.M. Norris // *J. Appl. Phys.* – 2009. – Vol. 105, № 2. – P. 023710.
- [3] Rethfeld B. Ultrafast dynamics of nonequilibrium electrons in metals under femtosecond laser irradiation / B. Rethfeld [et al.] // *Phys. Rev. B.* – 2002. – Vol. 65, № 21.

**LM-PS-3****Investigation of dynamics of plasmon resonance conditions at the interface of an aqueous solution of copper phthalocyanine - Ag film**

*M. Kononov<sup>1</sup>, V. Pustovoy<sup>1</sup>, V. Svetikov<sup>1</sup>*

*<sup>1</sup>Prokhorov General Physics Institute of the Russian Academy of Sciences, Laser Physics, Moscow, Russian Federation*

Devices and sensors based on the principles of surface plasmon resonance (SPR) are currently widely used for research and practical purposes [1].

Such devices are widely used for measuring the optical constants of materials, as well as as sensors of low concentrations (up to 10-12 M). The study of the properties of low concentration solutions has recently attracted increasing attention of researchers. In particular, the influence of ultra-low concentrations of substances on biological objects, including animal and human organisms, can be reflected in the biological response both at the molecular-cellular and at the level of a living organism as a whole [2].

In the previous work, we applied SPR to study the dependence of the SPR excitation parameters on the concentration of solutions [3]. In those experiments the SPR parameters showed nonmonotonic dependence upon the concentration in the range from 1 to 12 of 100-fold dilution of a copper phthalocyanine solution ( $C_{32}H_{16}CuN_8$ ) with an initial concentration of 0.001M. Further studies and the construction of an adequate model of the physical state of the interface under the conditions of extremely low concentrations of active substances were required to explain the results. Such a task is relevant both for experimental physics and for understanding many fundamental phenomena in pharmaceuticals and medicine.

In this work, to study aqueous solutions of copper phthalocyanine ( $10^{-6}$  -  $10^{-12}$  M), a measurement scheme based on the use of a fixed laser wavelength (632.8 nm) was chosen. In this case, the excitation parameters are determined from the dependence of the reflected radiation intensity upon the angle of incidence on the studied interface of different phases. Such an excitation scheme provides the highest sensitivity of the method. The accuracy of the measurements of the investigated phase is  $10^{-7}$  units of refractive index [4-6].

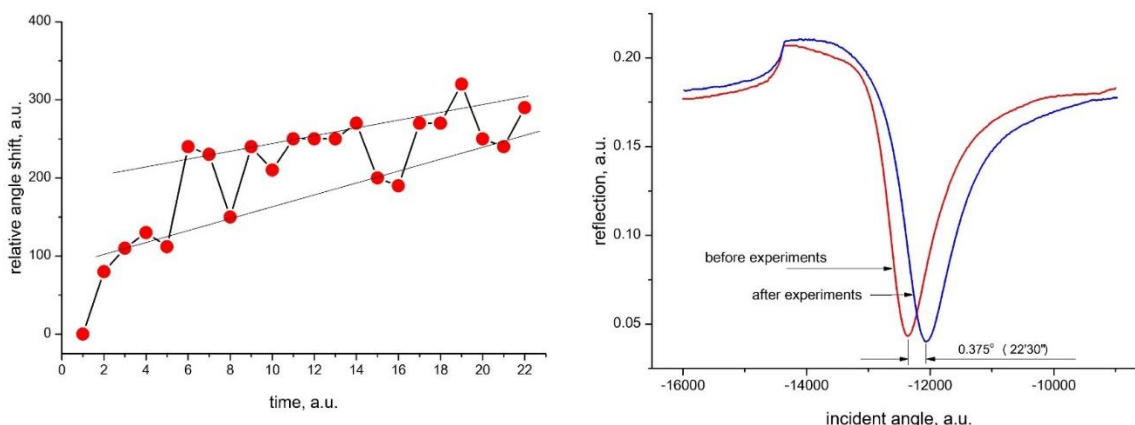


**Fig.1.** Reflection angle upon the time of measurements.

**Fig. 2.** Reflection curve upon the incident angle on the measurement interface.

The obtained data showed a monotonic change in the resonance conditions in the first 4-5 measurement cycles (Fig. 1). Further measurements showed the dynamic state of the surface at

which the SPR excitation condition varied within a certain range of values (fig. 1). The values of the SPR parameters during the measurements indicate an irreversible change in the resonance conditions (fig.2), which indicates the stable nature of the modification of the studied interface. In general, the method makes it possible to measure aqueous solutions of active substances of ultra-low concentrations (10<sup>-12</sup> M).

## References

- [1] Maier S.A. Plasmonics: Fundamentals and Applications // Springer Science+Business Media, 2007.
- [2] Epstein O. The spatial homeostasis hypothesis // Symmetry. – 2018. – Vol.10(4). – 103. doi:10.3390/sym10040103.
- [3] Kononov M.A., Pustovoy V.I., Svetikov V.V., Timoshenkov A.S., Solovjev V.S. Plasmonic spectroscopy of the water solutions of the copper phthalocyanine adsorbed on silver surface // Proceedings of the 2018 IEEE Conference of Russian Young Researchers in Electrical and Electronic Engineering, 2018. p. 1989-1991.
- [4] Kononov M.A., Khakamova N.P., Pustovoy V.I., Svetikov V.V. Investigation of the adsorption of copper phthalocyanine from aqueous solutions on the metal surface by the plasmon resonance method // The 26th International Conference on Advanced Laser Technologies. – Tarragona, Spain. – September 09-14, 2018. – P.LD-P-9.
- [5] Vinogradov S.V., Kononov M.A., Pustovoi V.I., Svetikov V.V. Plasmonic spectroscopy of the water solutions of the copper phthalocyanine adsorbed on a silver surface // Applied physics. 2017. Vol. 1. p. 69-73.
- [6] Vinogradov S.V., Kononov M. A., Kononov V. M., Savransky V.V. // Bulletin of the Lebedev physics institute . 42, (1), 30, (2015).

**LM-PS-4****Study of the dynamics of measuring plasmon resonance conditions at the water-film Ag-AgC-C interface.***M. Kononov<sup>1</sup>, V. Pustovoy<sup>1</sup>, V. Svetikov<sup>1</sup>**<sup>1</sup>Prokhorov General Physics Institute of the Russian Academy of Sciences, laser physics, Moscow, Russian Federation*

Modern technological operations in microelectronics, integrated photonics, and also in modern biomedical research require precision measurements of the geometric and dielectric parameters of molecules adsorbed onto the metal surface from aqueous solutions.

We used the technique of excitation of surface plasmon resonance (SPR, Fig.1) in our work to determine these parameters.

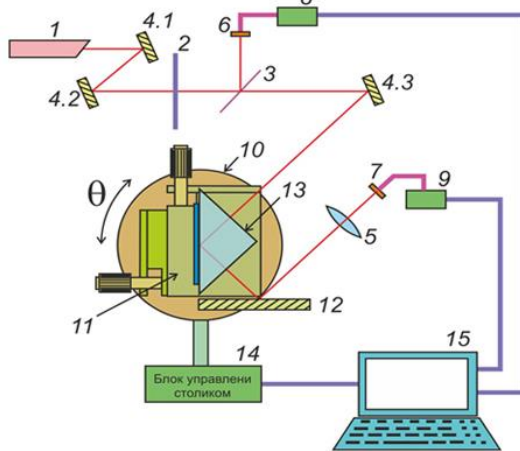


Fig.1 Experimental setup.

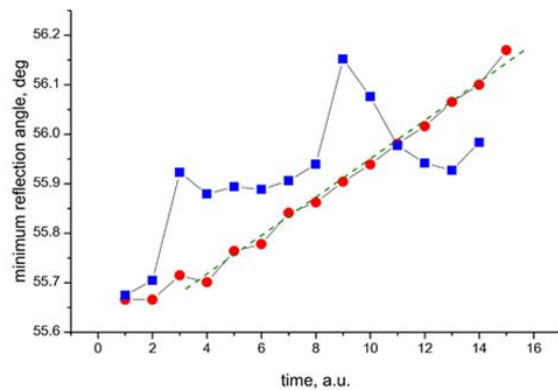


Fig.2 – The dependencies of the minimum reflection angle upon the time (red p.– closed cell; blue – open cell).

The interactions of water dipoles on the surface of a silver film doped with carbon atoms has been investigated in the work. The interaction of water with the metal surface was studied under conditions of continuous metal stay in the aquatic environment in the regime of periodic water change and in the regime of periodic water change with short-term contact of the metal surface with air. The change in the parameters of the SPR excitation had a character close to linear (Fig. 2, curve 1) in the regime of constant dwelling of metal in water. For the mode of periodic contact of metal with air, the dependence of the reflection minimum angle was complex (Fig. 2, curve 2). This dependence indicates the complex dynamics of the processes occurring on the metal surface in the mode of periodic metal contact with air. In particular, this may be due to the reorientation of water molecules and the dynamics of the destruction of the network of hydrogen bonds.

**References**

- [1] Kononov M.A., Pustovoy V.I., Svetikov V.V., Timoshenkov A.S., Solovjev V.S. Plasmonic spectroscopy of the water solutions of the copper phthalocyanine adsorbed on silver surface // In: Proceedings of the 2018 IEEE Conference of Russian Young Researchers in Electrical and Electronic Engineering, ElConRus 2018 2018. p. 1989-1991.
- [2] Vinogradov S.V., Kononov M.A., Pustovoy V.I., Svetikov V.V. Plasmonic spectroscopy of the water solutions of the copper phthalocyanine adsorbed on a silver surface //Appl. Phys. 2017. Vol. 1. p. 69-73.

**LM-PS-5****Study of the dynamics of plasmon resonance conditions at the water-film Ag interface**

*M. Kononov<sup>1</sup>, V. Pustovoy<sup>2</sup>, V. Svetikov<sup>1</sup>*

*<sup>1</sup>Prokhorov General Physics Institute of the Russian Academy of Sciences, laser physics, Moscow, Russian Federation*

*<sup>2</sup>Prokhorov General Physics Institute of the Russian Academy of Sciences, Laser Physics, Moscow, Russian Federation*

In this work, we studied the conditions for the excitation of surface plasmon resonance (SPR) at the interface of a silver film-deionized water. The interaction of water with metals is of interest to scientific groups working in various branches of science and engaged in the creation of sensory systems.

The particular interest is the mechanism of interaction of dipoles of water molecules with a metal surface, which characterizes the adsorption interaction. The relevance of this topic is largely due to the demand for optical sensor devices in biology and medicine.

We used the method of SPR excitation on a glass prism in according to the Kretschman geometry in our studies. The experiments were conducted in the scheme of a closed cell with a constant flow of water. A feature of this scheme is the lack of contact of the metal surface with air. The main detection element is the prism with a refractive index of  $n = 1.75$ , has been covered by a silver film with a thickness of 54 nm on the hypotenuse surface [1,2].

We investigated the dynamics of changes of the SPR conditions on the time without changing (updating) the aquatic environment. It was shown that the plasmon resonance conditions at the metal-water interface does not remain stationary, but varies monotonically on time. Such behavior of resonance conditions is associated with a change in the density of the electronic states of a metal surface. This leads to a change in the distribution density of water molecules on the surface with the formation of an ordered structure that repeats the crystallographic symmetry of the metal.

**References**

- [1] Plasmonic spectroscopy of the water solutions of the copper phthalocyanine adsorbed on silver surface// Proceedings of the 2018 IEEE Conference of Russian Young Researchers in Electrical and Electronic Engineering, ElConRus 2018 2018. p. 1989-1991.
- [2] Vinogradov S.V.,Kononov M.A.,Pustovoi V.I.,Svetikov V.V. Plasmonic spectroscopy of the water solutions of the copper phthalocyanine adsorbed on a silver surface //Appl. Phys. 2017. Vol. 1. p. 69-73.

**LM-PS-6****An analysis of the nonequilibrium ionization of silicon vapor under the influence of pulsed laser radiation**

*O. Koroleva<sup>1</sup>, V. Mazhukin<sup>1</sup>, A. Mazhukin<sup>1</sup>, E. Bykovskaya<sup>1</sup>*

*<sup>1</sup>Keldysh Institute of Applied Mathematics of Russian Academy of Sciences KIAM RAS, Mathematical Modelling, Moscow, Russian Federation*

The development of numerous applications such as laser processing and surface structuring of materials, pulsed laser deposition (PLD) [1], laser-induced breakdown spectroscopy (LIBS) [2], and the production of nanomaterials make the study of the fundamental aspects of the theory of laser processes relevant.

The process of laser irradiation with matter combines a number of problems, such as energy release into the medium, its heating, phase transformations, ionization, accompanied by gas-dynamic phenomena in the evaporated substance and the resulting plasma. Plasma development is closely related to the processes of nonequilibrium kinetics, and the transfer of laser and intrinsic radiation in a line-like and continuous spectrum. Despite years of research, the kinetics of the emergence and development of plasma near the irradiated surface of a solid, the dynamics of the formation of a plasma plume have not yet been fully investigated [3].

Optical destruction of evaporated material near the surface of a solid target is a combination of processes that lead to a qualitative change in the gaseous medium of its properties. The medium changes from a state of partially ionized gas, completely transparent to the incident radiation, to a state of complete ionization, which absorbs laser radiation intensively. Therefore, optical breakdown, which constitutes the initial stage of the rapid formation of a laser plasma, is the subject of special attention and thorough research.

In the present work, optical breakdown in silicon vapor under the influence of laser radiation in the wavelength range  $\lambda = 0.8 \div 1.06 \mu\text{m}$  is considered. The study of the mechanisms of optical breakdown of silicon vapor, their interaction and change leads to the need to consider the kinetics of population of multilevel systems, the quantitative description of which requires the construction of appropriate kinetic models. To study the conditions and characteristics of optical breakdown, a complete collision-radiation model has been developed that describes the kinetics of nonequilibrium ionization of silicon atoms and ions by laser radiation. The model takes into account not only collisional-radiative transitions, but also the main photoionization-recombination processes. Accounting for the energy balance of the electronic and atomic-ion subsystems allows the model to be used to describe the optical breakdown in a wide frequency range. The development of a nonequilibrium plasma in the radiation field of an infrared laser is analyzed.

**Acknowledgements:**

The work was funded by the Russian Foundation for Basic Research grant No. 19-07-01001.

**References**

- [1] R. Eason (ed.) *Pulsed Laser Deposition of Thin Films* (Wiley, Hoboken, 2007).
- [2] D.A. Cremers, L.J. Radziemski, *Handbook of Laser-Induced Breakdown Spectroscopy* (Wiley, New York, 2006).
- [3] V.I. Mazhukin, V.V. Nossov, I. Smurov, G. Flamant. Analysis of nonequilibrium phenomena during interaction of laser radiation with metal vapors. *Surveys on Mathematics for Industry*, 2001, 10 (1), 45-82.

**LM-PS-7****Mathematical modeling of dynamic metal fragmentation with ultrashort laser pulses**

*V. Mazhukin<sup>1</sup>, A. Shapranov<sup>1</sup>, M. Demin<sup>1</sup>, A. Aleksashkina<sup>1</sup>*

*<sup>1</sup>Keldysh Institute of Applied Mathematics of Russian Academy of Sciences KIAM RAS, Mathematical Modelling, Moscow, Russian Federation*

In the fs-ps-second range of laser irradiation of a metal target (Al), 2 high-speed PLA mechanisms [1] were investigated: separation and spallation. Both mechanisms are realized with the direct action of ultrashort (fs, ps) laser pulses on the surface, which provide large negative pressure values in the spallation zone. The expansion of the cavity and the departure of the surface layer of the material occurs due to inertial forces.

The simulation results showed:

- a) The separation is a stage of dynamic fragmentation of the liquid phase closely related to the process of homogeneous melting, which takes place under conditions of strong overheating ( $T_{\max} \sim 1.4 T_m$ ) of the near-surface region of the solid phase [2]. Removal of material occurs in the form of periodically repeating bursts of liquid metal, forming a cloud of small droplets on the side of the irradiated surface.
- b) In the spallation, the solid-state metal fragments are removed from the back side of the target (Al). The mechanism of destruction in this case is determined by compression pulses, which, when reflected from the free surface, create tensile stresses that can lead to breaks (spalling) from the back surface. Solid fragmentation is promoted by the nucleation of a liquid phase (melting) near the back surface, the conditions for the occurrence of which are greatly facilitated by tensile stresses.

**Acknowledgements:**

The work was funded by the Russian Foundation for Basic Research grant No. 19-07-01001.

**References**

- [1] V.I. Mazhukin, M.M. Demin, A.V. Shapranov. High-speed laser ablation of metal with pico-and subpicosecond pulses. *Appl. Sur. Sci.*, 2014, 302, 6-102.
- [2] V.I. Mazhukin, A.V. Shapranov, A.V. Mazhukin, O.N. Koroleva. Mathematical formulation of a kinetic version of Stefan problem for heterogeneous melting/crystallization of metals. *Mathematica Montisnigri*, 2016, vol. 36, pp. 58-77.

**LM-PS-8****Femtosecond and picosecond laser-induced damage thresholds of semiconductors in air and water**

M. Stehlík<sup>1,2</sup>, C. Liberatore<sup>1</sup>, I. Mirza<sup>1</sup>, N.M. Bulgakova<sup>1,3</sup>, A.V. Bulgakov<sup>1,3</sup>

<sup>1</sup>*HiLASE Centre, Institute of Physics of the Czech Academy of Sciences, Dolní Břežany, Czech Republic*

<sup>2</sup>*Faculty of Nuclear Sciences and Physical Engineering, Czech Technical University in Prague, Praha, Czech Republic*

<sup>3</sup>*Kuteteladze Institute of Thermophysics, Siberian Branch of RAS, Novosibirsk, Russian Federation*

Nanoparticle synthesis and micro-/nanostructure generation can be achieved by an efficient and versatile method of pulsed laser ablation in liquids (PLAL). PLAL is based on a simple experimental arrangement but its theoretical description is difficult and still involves many unanswered questions. Theoretical models of the laser ablation process work usually with a damage threshold (DT) parameter which is precisely defined and can be accurately measured. Surprisingly, published experimental results on the DTs in liquids are contradictory when compared to results of the DTs in air. Explanations of the influence of the ambient environment are based on different physical mechanisms such as light scattering [1], heat transfer to liquid, reflectivity [2] or vapor pressure. Here, we provide results of a systematic study of the DTs of semiconductors (Si, Ge) irradiated by near infrared (1030 nm) laser pulses in water. The experiments were done with the targets irradiated by fs (260 fs) and ps (7 ps) laser pulses in single-shot and multi-shot regimes. The DT results in water are compared to ones in air which were obtained under the same irradiation multi-shot regimes. The discussion of DT results takes into account the influence of pulse duration, accumulation effects in the multi-shot irradiation regimes, and nonlinear effects during ultrashort laser pulse propagation in water.

**References**

- [1] S. V. Starinskiy, Y. G. Shukhov, A. V. Bulgakov, Laser-induced damage thresholds of gold, silver and their alloys in air and water, *Appl. Surf. Sci.* 396, 1765 (2017).
- [2] H. Liu, F. Chen, X. Wang, Q. Yang, H. Bian, J. Si, X. Hou, Influence of liquid environments on femtosecond laser ablation of silicon, *Thin Solid Films.* 518, 5188 (2010).

**LM-PS-9****Role of adsorbed water in fs laser nanoablation of diamond**

*V. Gololobov<sup>1</sup>, V. Kononenko<sup>1</sup>, V. Konov<sup>1</sup>*

<sup>1</sup>*Prokhorov General Physics Institute of the Russian Academy of Sciences,  
Natural Sciences Center, Moscow, Russian Federation*

Earlier (see, e.g. [1, 2]) we have shown that laser nanoablation of diamond requires oxygen-containing gas environment (atmospheric or rare air).

For better understanding of chemical processes that govern laser nanoablation, in the present work we measured nanoablation rates at different air pressures in the range from 1 atm down to  $10^{-7}$  torr. Polished monocrystalline CVD diamond samples were irradiated by multiple 100 fs pulses (repetition frequency 1 kHz) with wavelength  $\lambda = 400$  nm and fluence  $3 \text{ J/cm}^2$ . It was found that quite unexpectedly the ablation rate dependence on air pressure is non-monotonous (Fig.1).

Almost equal values of rates in air and at pressure  $10^{-7}$  torr as well as 20-fold increase near  $10^{-5}$  torr are explained by competition of the two phenomena. The first is reaction of weakly bonded surface carbon atoms with oxygen which rate grows linearly with oxygen pressure and results in diamond etching. The second is adsorbed water layer formation in air that prevents penetration of oxygen molecules to the sample surface. The thickness and homogeneity of such layers drops with air pressure decrease and at lower pressures their shielding influence on surface oxidation becomes less pronounced.

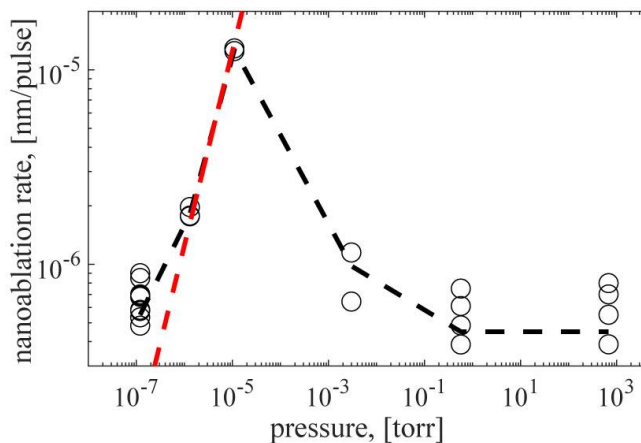


**Fig. 1.** Diamond surface nanoablation rate versus atmospheric pressure.

**References**

- [1] Kononenko, V. V., Gololobov, V. M., Komlenok, M. S., Konov, V. I., "Nonlinear photooxidation of diamond surface exposed to femtosecond laser pulses." *Laser Physics Letters* 2015, 12(9): 5.
- [2.] Kononenko, V. V., Vlasov, I. I., Gololobov, V. M., Kononenko, T. V., Semenov, T. A., Khomich, A. A., Shershulin, V. A., Krivobok, V. S., Konov, V. I., "Nitrogen-vacancy defects in diamond produced by femtosecond laser nanoablation technique." *Applied Physics Letters* 2017, 111(8): 4.

**LM-PS-10****Multi-octave blue shift of femtosecond mid-IR light bullet**

*A. E. Dormidonov<sup>1</sup>, V. Kandidov<sup>2</sup>, S. Chekalin<sup>3</sup>, V. Kompanets<sup>3</sup>*

*<sup>1</sup>VNIIA, Research Center for Pulse Technique, Moscow, Russian Federation*

*<sup>2</sup>Moscow Lomonosov State University, Physics Department, Moscow, Russian Federation*

*<sup>3</sup>Institute of Spectroscopy RAS, Laser Spectroscopy, Moscow, Russian Federation*

Light bullet (LB) is a wave packet, which is extremely compressed in space and time during a process of nonlinear optical self-interaction of femtosecond laser pulse in the anomalous group velocity dispersion (AGVD) regime. The LB is a stable self-organized formation, which does not depend on the wide range of the input pulse parameters. Its peak intensity reaches  $10^{13}$ – $10^{14}$  W/cm<sup>2</sup>, duration is less than two optical cycles and diameter is about several wavelengths. LB is a broadband source of the supercontinuum (SC) and moves in the medium at the velocity close to the group velocity  $v_g$  of the initial pulse. The main feature of the SC spectrum of a Mid-IR LB is the appearance of a narrow isolated anti-Stokes wing (ASW), which is located in the visible region of the SC.

In this work, we study analytically and experimentally the general characteristics of the formation of the ASW in the LB SC spectrum in process of the filamentation of femtosecond laser pulse in AGVD regime in fluorides and selenides. It is established that the material dispersion of the medium determines the location of ASW in the visible region of SC for filamentation of pulses at wavelengths from the near and middle infrared range in different transparent dielectrics.

**LM-PS-11****Surface treatment by nanosecond laser for diffusion welding**

*S. Mikolutskiy<sup>1</sup>, T. Malinskiy<sup>2</sup>, V. Yamshchikov<sup>3</sup>, Y. Khomich<sup>2</sup>*

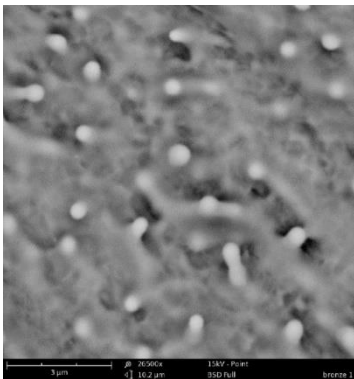
*<sup>1</sup>Institute for Electrophysics and Electric Power RAS, Laboratory 5, Saint Petersburg, Russian Federation*

*<sup>2</sup>Institute for Electrophysics and Electric Power RAS, Laboratory 3, Saint Petersburg, Russian Federation*

*<sup>3</sup>Institute for Electrophysics and Electric Power RAS, Branch of Institute for Electrophysics and Electric Power RAS, Saint Petersburg, Russian Federation*

Improving the quality of the compound in diffusion welding of homogeneous and dissimilar metals is possible due to the formation of ordered, micron and submicron surface structures on the welded surfaces with given geometry parameters. These structures directionally change the physicochemical properties of the surface. Structured micro and nanorelief significantly increases the contact area, which should lead to an increase in the structural strength and reliability of the welded joint, in particular, improvement of temporary resistance and relative elongation, as well as lowering the temperature of the diffusion welding process are take place.

In this work we study the possibility of changing the adhesive properties of metals and alloys by micro- and nanostructuring their surface when exposed to nanosecond laser pulses (Nd:YAG laser) with a radiation wavelength of 355 nm. The formation of submicron structures in the form of spheres with a diameter of about 500 nm, which are located on the tops of conical legs up to 1  $\mu\text{m}$  in height (Fig. 1), was revealed on the surface of CuCrZr-bronze samples [1]. The formation of such structures is observed at laser pulse energy densities from 0.6 to 1.2  $\text{J}/\text{cm}^2$ , and the number of spherical structures per unit area increases with increasing laser pulse energy density. It was also found that the number of such structures per unit area increases with a decrease in the scanning speed of the laser beam on the surface and correlates with the surface concentration of chromium according to analysis of the elemental composition.



Laser treatment of zirconium bronze samples and stainless steel, their diffusion welding and subsequent static tensile tests revealed an increase in the temporal resistance of the welded joint compared to untreated samples. Investigation of this effect may lead to a noticeable improvement in the quality of welded joints of dissimilar materials [2].

**Fig. 1.** SEM image of bronze surface irradiated by scanning beam of Nd:YAG-laser.

**References**

- [1] Yu.A. Vashukov, S.F. Demichev, V.D. Elenev, T.V. Malinskiy, S.I. Mikolutskiy, Yu.V. Khomich, V.A. Yamshchikov. Laser processing of metal alloys for diffusion welding. *Applied Physics*. 2019. No. 1. P. 82.
- [2] Yu.A. Zheleznov, T.V. MalinskyYu.V. KhomichV.A. Yamshchikov. The Effect of a Scanning Nanosecond Laser Pulse Beam on the Microtopography of Ceramic  $\text{Al}_2\text{O}_3$  Coatings. *Inorganic Materials: Applied Research*. 2018. V. 9. P. 460.

**LM-PS-12****Electron dynamic near silicon surface irradiated by ultrashort laser pulse**

*D. Polyakov<sup>1</sup>, E. Yakovlev<sup>1</sup>*

*<sup>1</sup>ITMO University, Faculty of Laser Photonics and Optoelectronics, Saint-Peterburg, Russian Federation*

The problem of electron emission from solid surfaces induced by the action of ultrashort laser pulses has attracted the attention of researchers since the seventies of the last century. One can point out on several phenomena that can be associated with ultrafast electron emission: «Coulomb explosion» [1], creation of dynamic waveguide related with the depletion of surface layers of semiconductor by electrons [2]. However, the role of electron emission in the general picture of the interaction of femtosecond laser pulses with solids remains unclear despite a significant amount of experimental and theoretical work. One of the main problems of the existing theoretical descriptions of electron emission from semiconductor or dielectric materials is neglecting the influence of self-consistent electrical field on electron transport near solid/vacuum interface (space charge effect).

In this work we present a theoretical model that takes into account the influence of space charge effects on ultrafast electron dynamics near solid/vacuum interface. In the framework of presented model the possibility of related with emission phenomena (such as «Coulomb explosion», creation of dynamic waveguide) were analyzed for silicon. In addition, we make suggestion that the time-depending dipole moment induced by the emission separation of charges should lead to the generation of electromagnetic radiation from the terahertz frequency range. The properties of such radiation were investigated.

This work was supported by RFBR Grant #18-32-00839.

**References**

- [1] N.M. Bulgakova, R. Stoian, A. Rosenfeld, I.V. Hertel, E.E.B. Campbell. Phys. Rev. B 69 (2004) 054102.
- [2] G.A. Martsinovskii, G.D. Shandybina, D.S. Smirnov, S.V. Zobotnov, L.A. Golovan, V.Yu. Timoshenko, P.K. Kashkarov. Opt. Spectrosc. 105 (2008) 67.

**LM-PS-13****Fabrication of samarium nanoparticles by femtosecond laser ablation in liquid**

*E. Popova-Kuznetsova<sup>1</sup>, A. Popov<sup>1</sup>, G. Tikhonovsky<sup>1</sup>, S. Klimentov<sup>1</sup>, V. Duflot<sup>2</sup>,  
I. Zvestovskaya<sup>1</sup>, A. Kabashin<sup>1,3</sup>*

*<sup>1</sup>MEPhI- Institute of Engineering Physics for Biomedicine PhysBio, Bio-nanophotonics  
Laboratory, Moscow, Russian Federation*

*<sup>2</sup>Scientific-Research Physical Chemistry Institute, Branch of the L. Ya Karpov, Obninsk,  
Russian Federation*

*<sup>3</sup>Aix Marseille University- CNRS, LP3 laboratory, Marseille, France*

Nuclear nanomedicine provides unique opportunities to treat tumors due to its targeting ability, good loading capacity and enhanced retention. This field of science has become increasingly important over the last decades, promising an attractive and powerful alternative to conventional chemotherapy. However, synthesis of radioactive agents in nanoscale is rather challenging. Here, we have chosen a different way. First, we produce nanomaterials and only after that “activate” them into radioactive form. Our approach is based on synthesis of enriched Sm-152 oxide nanoparticles by femtosecond laser ablation in liquids. We have shown that it is possible to produce 100 nm nanoparticles with different shape fractions. Moreover, application of additional laser fragmentation step allows one to finely tune nanoparticles size between 5 and 20 nm.

**LM-PS-14****Hydrodynamic modelling and simulations of collisional shockwaves in gas targets for the optimisation of collisionless shock acceleration of ions**

*S. Passalidis<sup>1,2</sup>, O. Ettliger<sup>2</sup>, G. Hicks<sup>2</sup>, N. Dover<sup>2,3</sup>, Z. Najmudin<sup>2</sup>, E.P. Benis<sup>4</sup>, E. Kaselouris<sup>1</sup>, N.A. Papadogiannis<sup>1</sup>, M. Tatarakis<sup>1</sup>, V. Dimitriou<sup>1</sup>*

<sup>1</sup>*Hellenic Mediterranean University, Institute of Plasma Physics & Lasers, Rethymno, Greece*

<sup>2</sup>*Imperial College, The John Adams Institute - The Blackett Laboratory, London, United Kingdom*

<sup>3</sup>*National Institutes for Quantum and Radiological Science and Technology (KPSI-QST), Kansai Photon Science Institute, Kyoto, Japan*

<sup>4</sup>*University of Ioannina, Department of Physics, Ioannina, Greece*

A study on hydrodynamic modelling and simulations of collisional shockwaves in gaseous targets towards the optimisation of collisionless shock acceleration (CSA) of ions is performed. The models developed correspond to the specifications required for experiments with the CO<sub>2</sub> laser at the Accelerator Test Facility (ATF) at Brookhaven National Laboratory (BNL) as well as to the Vulcan Petawatt system at Rutherford Appleton Laboratory (RAL). In both cases, a laser prepulse is simulated to interact with hydrogen gas targets. The energy is deposited in five different areas across the gas jet, having values in the range of 0.1 mJ to 100 mJ for BNL and 5 mJ to 1 J for RAL, respectively. It is demonstrated that by controlling the pulse energy, the deposition area and the backing pressure, a blast wave suitable for generating nearly monoenergetic accelerated ion beams can be formed. Depending on the energy absorbed and the deposition area, an optimal temporal window may be determined for the acceleration considering both the necessary overdense state of plasma and the required short scale-lengths for monoenergetic ion beam production.

**HiLASE-PS-1****Development of 2  $\mu\text{m}$  fiber front-end for Ho:YAG thin disk amplifier**

*J. Huynh<sup>1,2</sup>, J. Černohorská<sup>1,2</sup>, M. Písařík<sup>1</sup>, P. Peterka<sup>3</sup>, M. Smrž<sup>1</sup>, T. Mocek<sup>1</sup>*

*<sup>1</sup>HiLASE Centre, Institute of Physics of the Czech Academy of Sciences, Dolní Břežany, Czech Republic*

*<sup>2</sup>Czech Technical University in Prague- Faculty of Nuclear Sciences and Physical Engineering, Department of Physical Electronics, Praha, Czech Republic*

*<sup>3</sup>Institute of Photonics and Electronics ASCR- v.v.i, Fiber lasers and non-linear optics, Praha, Czech Republic*

Over the past years mid-infrared lasers have attracted considerable technological and scientific interests. 2  $\mu\text{m}$  sources can be used in various applications such as: remote sensing [1], free space communication [2], LIDAR [3], material processing of polymers [4], medicine and surgery [5], or pump sources for mid-IR OPA [6].

In this paper we present development of 2  $\mu\text{m}$  fiber front-end for Ho: YAG thin disk amplifier with average power >10 W. The front-end consists of passively mode-locked soliton holmium fiber ring oscillator followed by thulium/holmium-fiber tandem amplifier. Self-starting holmium fiber oscillator work in soliton operation at 23 MHz repetition rate, 15 mW of output average power and 1 ps output pulse duration.

Progress and current status of 2  $\mu\text{m}$  laser system (PERLA D) at HiLASE centre will be presented.

**References**

- [1] Upendra N. Singh, Brian M. Walsh, Jirong Yu, Mulugeta Petros, Michael J. Kavaya, Tamer F. Refaat, and Norman P. Barnes, "Twenty years of Tm:Ho:YLF and LuLiF laser development for global wind and carbon dioxide active remote sensing," *Opt. Mater. Express* 5, 827-837 (2015).
- [2] Petros, M., Refaat T.F., Singh U.N., Yu J., Antill C., Remus R., Taylor B.D., Wong T.-H., Reithmaier, K., Lee J., Ismail S., Davis K.J., "Development of an advanced Two-Micron triple-pulse IPDA lidar for carbon dioxide and water vapor measurements," *EPJ Web Conf.* 176 01009 (2018) DOI: 10.1051/epjconf/201817601009.
- [3] Orr, B. J. (2017). Infrared LIDAR Applications in Atmospheric Monitoring. In *Encyclopedia of Analytical Chemistry*, R. A. Meyers (Ed.). doi:10.1002/9780470027318.a0711.pub2.
- [4] Ilya Mingareev, Fabian Weirauch, Alexander Olowinsky, Lawrence Shah, Pankaj Kadwani, Martin Richardson, Welding of polymers using a 2 $\mu\text{m}$  thulium fiber laser, *Optics & Laser Technology*, Volume 44, Issue 7, 2012, Pages 2095-2099, ISSN 0030-3992, <https://doi.org/10.1016/j.optlastec.2012.03.020>.
- [5] Kang, H. W., Lee, H. , Teichman, J. M., Oh, J. , Kim, J. and Welch, A. J. (2006), Dependence of calculus retropulsion on pulse duration during HO:YAG laser lithotripsy. *Lasers Surg. Med.*, 38: 762-772. doi:10.1002/lsm.20376.
- [6] D. Sanchez, M. Hemmer, M. Baudisch, S. L. Cousin, K. Zawilski, P. Schunemann, O. Chalus, C. Simon-Boisson, and J. Biegert, "7  $\mu\text{m}$ , ultrafast, sub-millijoule-level mid-infrared optical parametric chirped pulse amplifier pumped at 2  $\mu\text{m}$ ," *Optica* 3, 147-150 (2016).

## **HiLASE-PS-2**

### **Robotic arm HMI for laser shock peening applications**

*M. Böhm<sup>1,2</sup>, J. Kaufman<sup>1</sup>, J. Brajer<sup>1</sup>, T. Mocek<sup>1</sup>*

*<sup>1</sup>HiLASE Centre, Institute of Physics of the Czech Academy of Sciences, Dolní Břežany, Czech Republic*

*<sup>2</sup>Faculty of Nuclear Sciences and Physical Engineering, Czech Technical University in Prague, Prague, Czech Republic*

The HiLASE centre is equipped with a Laser shock peening (LSP) station. LSP is a surface enhancing technique and it is used to prolong the fatigue life of metallic materials. Part of the station is an industrial robotic arm used to handle the processed parts. Learning to program an industrial robotic arm using a tech pendant has a steep learning curve and requires special training. In order to facilitate the utilisation of the LSP station at the HiLASE centre for untrained operators, a human-machine interface (HMI) for the station's industrial robotic arm is being developed. This project aims to determine what type of HMI is the most suitable for the given application and to implement this solution. A computer based HMI is chosen as most suitable for the LSP station, because it is low-cost and flexible. The HMI in question uses a commercially available Online programming software to connect to the robot controller. Online programming allows executing the movements on the real robot at the same time as it is being simulated. The software is shipped with Application programming interfaces (APIs) for various industrial robotic arm controllers. The actual Graphical User Interface (GUI) of the HMI is created using a high-level programming language. The HMI allows the operator to control the main LSP parameters, namely the spot size, spot overlap and the size and number of the patches. Additionally, the operator can choose between different peening strategies, which can affect the final results. The HMI for the LSP station has been developed and in the future will make it necessarily for the operator to control the peening process more precisely.

### HiLASE-PS-3

#### Method in vacuum to align and bond precision opto-mechanical components required for space applications

S. Priya<sup>1</sup>, P. Ribes Pleguezuelo<sup>1</sup>, T. Bolz<sup>1</sup>, S. Wendt<sup>1</sup>, M. Mohaupt<sup>1</sup>, E. Beckert<sup>1</sup>, E. Wille<sup>2</sup>,  
M. Bavdaz<sup>2</sup>, A. Tünnermann<sup>1</sup>

<sup>1</sup>Fraunhofer Institute for Applied Optics and Precision Engineering IOF, Precision Engineering, Jena, Germany

<sup>2</sup>European Space Agency - ESA/ESTEC, Optics, Noordwijk, Netherlands

The assembling of space optical devices working in X-ray or UV-optic regimes can only be validated in similar to working vacuum conditions. The intention of the work is to develop an in vacuum assembling technique able to align and robustly bond optical components required for space missions.

In order to prove the concept, we adapted the laser soldering technique Solderjet Bumping to be operational in vacuum conditions. This low-stress soldering technique has been previously used to assemble optical space devices, but has never before been implemented under vacuum conditions. Finite-Element-Method (FEM) analysis, assembling campaigns in air and in vacuum conditions and mechanical and thermal environmental tests in final assemblies are being carried out to prove that the laser assembling technique can provide a solution for the assemble of future space telescopes or similar opto-mechanical setups required for space missions.

Moreover, the vacuum alignment and bonding solder technique of test samples is compared to the application of space qualified epoxies.

**Keywords:** Solderjet Bumping, space optics, Laser based soldering, X-ray and UV telescopes.

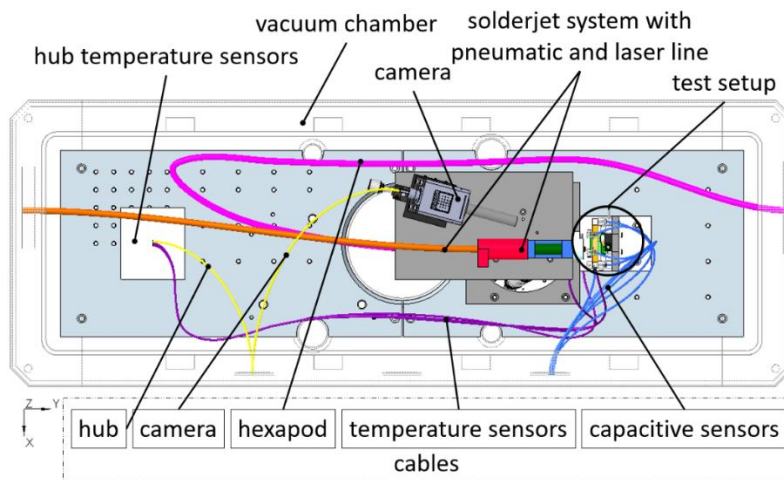


**Fig. 1.** Schematic of the laser soldering technique Solderjet Bumping, mounted inside a vacuum chamber where thanks to a hexapod device, we are able to bond test samples (10<sup>-5</sup> mbar vacuum regime).

**PH-PS-1****Nanoscale profilometry based on spectrally resolved white-light interferometry**

*I. Likhachev<sup>1</sup>, V. Pustovoy<sup>2</sup>*

*<sup>1</sup>General Physics Institute, Laser Physics, Moscow, Russian Federation*

*<sup>2</sup>General Physics Institute, Laser Physics Department, Moscow, Russian Federation*

Based on the method of Spectrally Resolved White-Light Interferometry (SRWLI), an all optical technique for measuring the surface profiles is proposed. The distinguishing features of the technique are the following:

- the possibility of high-precision absolute distance measurement (not only its variation); no need to calibrate before starting measurements;
- a large dynamic range of measurements;
- insensitivity of the measurement result to smooth changes in the spectrum of the radiation source, its drift, and optical power level;
- the possibility of carrying out remote measurements performed by selecting the required length of fiber;
- insensitivity of the measuring probe to electromagnetic interference;
- small system size determined by the use of fiber optic components.

The XY accuracy of the mechanical stage position is about 1 nm, but in practice the XY accuracy was limited by the light beam width which amounted to about 10 micrometer. The vertical (Z) position of the sample can be controlled with accuracy of 1 nm. All the XYZ coordinates measurements require about 300 ms of time.

**References**

- [1] I. G. Likhachev, V. I. Pustovoy, V. V. Svetikov, and V. I. Krasovskii, Monitoring two-coordinate positioning by means of optical spectral coding, *Journ. of Optical Technology*, 2018, Vol. 85, Issue 12, pp. 255-258.
- [2] I. G. Likhachev, V. I. Pustovoy, V. V. Svetikov, Optical spectral encoding for nanopositioning, *The 18th International Conference on Laser Optics ICLO-2018, St. Petersburg, Russia, 4-8 June, 2018.*

**PH-PS-2****Luminescent temperature control of up-conversion nanoparticles**

V. Kochubey<sup>1,2</sup>, A. Pravdin<sup>1</sup>, Y. Konukhova<sup>1</sup>, A. Skaptsov<sup>1</sup>, E. Sagaidachnaya<sup>1</sup>, I. Yanina<sup>1,2</sup>,  
N. Kazadaeva<sup>1</sup>, A. Doronkina<sup>1</sup>, V. Tuchin<sup>1,2,3</sup>, E. Genina

<sup>1</sup>Saratov State University, Physical, Saratov, Russian Federation

<sup>2</sup>Tomsk State University, Interdisciplinary Laboratory of Biophotonics, Tomsk,  
Russian Federation

<sup>3</sup>Institute of Precision Mechanics and Control RAS, Laboratory of Laser Diagnostics of  
Technical and Living Systems, Saratov, Russian Federation

The photoluminescence spectra of NaYF<sub>4</sub><sup>3+</sup>Er<sup>3+</sup> upconversion nanoparticles, located under a tissue layer, were recorded in a wide temperature range. It is shown that the determination of temperature of the nanoparticles from the photoluminescence spectra, an error occurs associated with the distortion of the spectrum due to light scattering in the sample. Thus, we have shown that the absorption and scattering of NP photoluminescence in a sample distorts the NP temperature data obtained from their luminescence characteristics. Distortion occurs even in the case of weakly absorbing and dissipating adipose tissue with a thickness of ~ 0.1 mm. A correction algorithm has been developed to reduce this error. The algorithm developed for the correction of data is able to obtain the temperature of upconversion nanoparticles.

**LP-PS-1****Determination of surface modification and nonlinear absorption thresholds of silicon using mid-infrared ultrashort laser pulses**

*J. Sládek<sup>1,2</sup>, I. Mirza<sup>1</sup>, A.V. Bulgakov<sup>1,3</sup>, Y. Levy<sup>1</sup>, W. Marine<sup>1</sup>, B. Csanaková<sup>1,4</sup>, L. Roškot<sup>1,4</sup>, O. Novák<sup>1</sup>, N.M. Bulgakova<sup>1</sup>, M. Smrž<sup>1</sup>*

<sup>1</sup>*HiLASE Centre, Institute of Physics of the Czech Academy of Sciences, Dolní Břežany, Czech Republic*

<sup>2</sup>*Faculty of Nuclear Sciences and Physical Engineering- Czech Technical University in Prague, Department of Solid State Engineering, Prague, Czech Republic*

<sup>3</sup>*S.S. Kutateladze Institute of Thermophysics SB RAS, Novosibirsk, Russian Federation*

<sup>4</sup>*Faculty of Nuclear Sciences and Physical Engineering- Czech Technical University in Prague, Department of Physical Electronics, Prague, Czech Republic*

During last decades, there has been a growing interest in surface and volumetric modification of semiconductor materials using ultrashort laser pulses for application in microelectronics, optoelectronics and photovoltaics [1, 2]. The action of conventional near-IR ultrashort laser pulses on silicon and germanium is limited to surface modification, since these semiconductors are opaque in this spectral region. Experiments have been performed to demonstrate that, by tightly focusing mid-IR ultrashort laser pulses [3, 4] inside Si, local nonlinear optical absorption can be initiated [5, 6]. The laser-generated free carrier density leads to optical breakdown and can potentially induce volumetric structural modification. However, laser beam focusing inside the material bulk is accompanied by processes connected to nonlinear beam propagation, such as the Kerr effect and light scattering by free electron plasma, which overlap with nonlinear absorption. For obtaining knowledge on absorption nonlinearity of semiconductor materials at a certain wavelength, it is essential to study absorption behavior by placing a precise focal spot on the material surface, to determine the intensities corresponding to surface modification threshold and to derive the absorption order. In this work, we have performed a systematic study of surface modification and nonlinear absorption of Si using 1.6 and 3.2  $\mu\text{m}$ , few ps long laser pulses. The transmission signal was measured as a function of pulse intensity using a light collection setup. The correlation results between surface modification and multiphoton excitation in semiconductor materials will be presented and discussed.

**References**

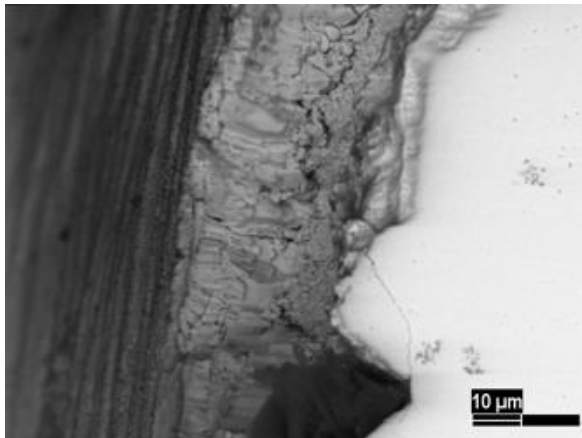
- [1] C. Wu, C.H. Crouch, L. Zhao, et al., *Appl. Phys. Lett.* 78 (2001) 1850–1852.
- [2] M.T. Winkler, D. Recht, M. Sher, A.J. Said, E. Mazur, M.J. Aziz, *Phys. Rev. Lett.* 106 (2011) 178701.
- [3] M. Vyvlečka, O. Novák, M. Smrž, T. Mocek, *Appl. Opt.* 57, (2018) 8412-8417.
- [4] B. Csanaková, O. Novák, L. Roškot, J. Mužík, H. Jelínková, M. Smrž, T. Mocek, " *Proc. SPIE* 11033, (2019) 110330J.
- [5] D. Grojo, S. Leyder, P. Delaporte, W. Marine, M. Sentis, O. Utéza, *Phys. Rev. B* 88 (2013), 195135.
- [6] S. Leyder, D. Grojo, P. Delaporte, W. Marine, M. Sentis, O. Utéza, *Appl. Surf. Sci.* 278 (2013) 13–18.

**LP-PS-2****High removal rate laser machining of zirconia with nanosecond pulsed laser**

*D. Panov<sup>1</sup>, V.N. Perovskiy<sup>1</sup>, D.V. Ushakov<sup>1</sup>, A.S. Schekin<sup>1</sup>, E.D. Ishkinyaev<sup>1</sup>*

*<sup>1</sup>National Research Nuclear University MEPhI, Department of Laser Physics, Moscow, Russian Federation*

Different ceramics has a lot of application in prosthetics. One of them is zirconia. This ceramic has an outstanding mechanic, thermal and optical properties [1]. This key factors made zirconia a widespread material in dentistry, especially in a prosthesis. Still, most dental prostheses are manufactured with conventional techniques like milling. However, nowadays, new ways of production dental prosthesis are developing. One of the most perspectives is laser machining. In prevues works, we considered the possibility of the technique with different laser sources [2]. It is



known, that nanosecond pulsed lasers are usable and low-cost laser sources. It can be used as the main source for laser machining of the prosthesis. In spite of this, the problem of low removal rate and structural changing under laser radiation exist. In this work, ways of obtaining the highest removal rate with low structural changing are considered. To obtain the highest removal rate, dependence removal rate, surface roughness on parameters of laser radiation and scanning system was studied. Structural changing of zirconia under laser processing is studied. HAZ ratio from laser flense was obtained.

**References**

- [1] D. V. Ganin, S. I. Mikolutskiy, V. N. Tokarev, V. Yu. Khomich, V. A. Shmakov, V. A. Yamshchikov, “Formation of micron and submicron structures on a zirconium oxide surface exposed to nanosecond laser radiation”, *Kvantovaya Elektronika*, 44:4 (2014).
- [2] D. V. Panov, *et al* 2019 *J. Phys.: Conf. Ser.* 1238 012028.

**LP-PS-3****Hydrophobic surfaces obtained with nanosecond pulsed laser on stainless steel and dependence on its parameters**

*D. Panov<sup>1</sup>, V.N. Petrovskiy<sup>1</sup>, A.S. Schekin<sup>1</sup>, M.P. Pashalov<sup>1</sup>, E.D. Ishkinaev<sup>1</sup>*

*<sup>1</sup>National Research Nuclear University MEPhI, Department of Laser Physics, Moscow, Russian Federation*

Superhydrophobic surfaces are surfaces with contact angle higher than 120°. Hydrophobic surfaces have a lot of applications in technology, biology and medicine. Such surfaces can be obtained by laser surface patterning through creating roughness on the surface. At some such technique was observed [1,2]. As radiation source usually uses lasers with short and ultrashort pulse duration. Recently a number of researches have been published, which consider nanosecond pulse lasers as a radiation source for creating hydrophobic surfaces. Usage of nanosecond lasers can decrease cost and rise proliferation of the technique.



In this work, manufacturing of hydrophobic and superhydrophobic surfaces on stainless steel was considered. Dependence of contact angle and different parameters of laser radiation and scanning system is considered. Influence of spatial characteristics on contact angle is studied. Hydrophobic and superhydrophobic surfaces are obtained. However, usage of only the lasers without any other tools occurs a problem with contact angle time dependence. It is necessary to find the best set

of parameters to reduce this problem.

**References**

- [1] A. Y. Vorobyev, Chunlei Guo, Multifunctional surfaces produced by femtosecond laser pulses, *Journal of Applied Physics* 2015 117:3.
- [2] Ta, Duong; Dunn, Andrew; J. Wasley, Thomas; Li, Ji; Kay, Robert; Stringer, Jonathan; Smith, Patrick; Esenturk, Emre; Connaughton, Colm; D. Shephard, Jonathan. (2016) Laser textured superhydrophobic surfaces and their applications for homogeneous spot deposition, *Appl. Surf. Sci.*

**LP-PS-4****Laser synthesis of the LiCoO<sub>2</sub> thin films***L. Parshina<sup>1</sup>, O. Novodvorsky<sup>1</sup>, O. Khramova<sup>1</sup>**<sup>1</sup>ILIT RAS – Branch of the FSRC «Crystallography and Photonics» RAS, Laboratory of nanostructures and thin films, Shatura, Russian Federation*

The LiCoO<sub>2</sub> solid-state thin-film electrolytes are ideal candidates for the fabrication of all-solid-state electrochromic devices and thin-film batteries [1, 2]. The use of the solid-state electrolyte in an electrochromic device will greatly simplify the fabrication technique, reduce the coloration time and ensure functioning at lower temperatures, which will increase the durability and reliability of the device [3]. Currently, investigations of the LiCoO<sub>2</sub> solid-state thin-film electrolytes are making in order to improve their ionic conductivity and optical transparency.

The LiCoO<sub>2</sub> thin films on the *c* - sapphire and high-conductive silicon substrates were produced at the substrate temperature of 25 to 500 °C by the pulsed laser deposition. The film synthesis was from the LiCoO<sub>2</sub>: Li<sub>2</sub>O ceramic targets. The targets were produced from the LiCoO<sub>2</sub> and Li<sub>2</sub>O powders by pressing and annealing at the temperature of 1200 °C for two hours. The Li<sub>2</sub>O concentration in the target was 5 %. Ablation of the targets was performed by the excimer KrF-laser radiation with the wavelength of 248 nm at the energy density on the target of at least 3 J/cm<sup>2</sup> and the oxygen pressure of 100 mtorr in the vacuum chamber during the film growth. The optical, electrical properties and the surface morphology of the produced films with the thickness of 20–40 nm were investigated depending on the type and the substrate temperature. By the AFM and SEM methods it was established that the films produced on both types of the substrate at room temperature had a granular surface structure. The size of the granules was several hundred nanometers. It was found that with an increase in the substrate temperature during the growth of the LiCoO<sub>2</sub> film, its surface roughness decreased to 10 nm for the film produced at 500 °C on the *c*-sapphire substrate. The study of the transmission spectra of the LiCoO<sub>2</sub> films produced on the *c*-sapphire substrate showed that with a change in the substrate temperature from 25 to 500 °C, the transparency of the films increased by 30 % in the whole of the spectral range under study. It was established that the LiCoO<sub>2</sub> films produced on the *c*-sapphire substrate, regardless of its temperature, were dielectrics. The LiCoO<sub>2</sub> films deposited at room temperature on the silicon substrates with the resistivity of 1·10<sup>-3</sup> Ohm·cm became highly conductive with the resistivity of about 2.5·10<sup>-7</sup> Ohm·cm.

This work was supported by the Ministry of Science and Higher Education within the State assignment FSRC «Crystallography and Photonics» RAS in part of «the thin films synthesis» and the Russian Foundation for Basic Research (Project № 19-29-03032, 17-07-00615, 16-29-05385) in part of «analysis of the thin films».

**References**

- [1] A. Yano et al., Journal of The Electrochemical Society, 165, A3221 (2018).
- [2] Sh.-Ch. Wang et al., Thin Solid Films, 520, 1454 (2011).
- [3] K. J. Patel et al., J. Solid State Electrochem., 21, 337 (2017).

## LP-PS-5 Laser-assisted deposition of carbon nanocomposites

*G. Shafeev<sup>1</sup>, I. Rakov<sup>1</sup>, N. Melnik<sup>2</sup>*

<sup>1</sup>*Prokhorov General Physics Institute of RAS, Wave Research Center, Moscow, Russian Federation*

<sup>2</sup>*Lebedev Physical Institute, Solid state physics, Moscow, Russian Federation*

Carbon nanocomposites deposition under toluene irradiation through transparent glass by nanosecond infrared laser radiation was experimentally investigated. The dependence of deposited films thickness on the laser pulse duration and absorbed energy amount is revealed. Previously it was shown the process of laser-assisted deposition diamond-like films (DLF) from hydrocarbons by copper vapor laser. However, authors didn't study laser parameters effect on the morphology and size of obtained films and used laser source didn't allow synthesized nanocomposites with thickness of more than 100 nm [1]. The atomic force microscope, scanning electron microscope, modulation interference microscope and Raman spectroscopy are employed to characterize the deposited films. The average film thickness on a glass substrate increases with the number of laser pulses. Raman spectra (Fig.1) analysis confirms the presence of significant amount  $sp^3$  fraction and some  $sp^2$  fraction. According to the literature [2, 3] peak position in the region of  $1350\text{ cm}^{-1}$  is characteristic of nanodiamonds.

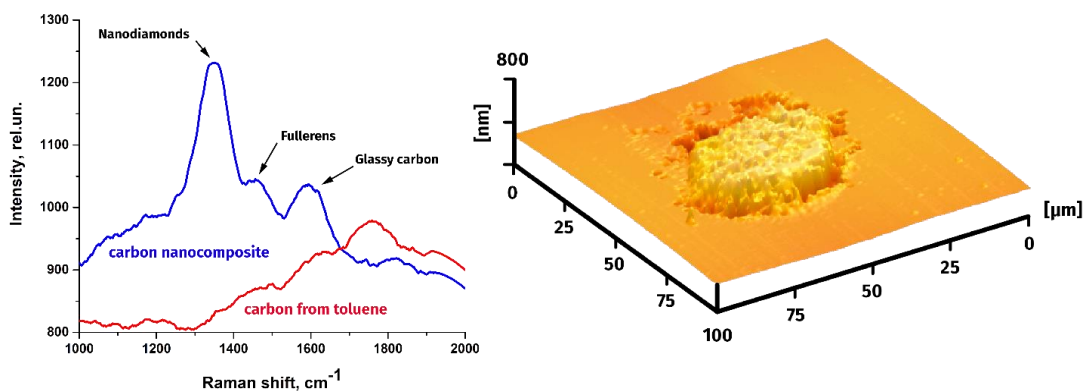


Fig. 1.

The work was partially supported by RFBR grant 18-32-01044 mol\_a.

### References

- [1] Simakin A. V., Shafeev G.A., Loubnin E.N. Laser deposition of diamond-like films from liquid aromatic hydrocarbons // *Appl. Surf. Sci.*, 2000, 154(4) 405–410.
- [2] Mermoux M.*et al.* Raman spectroscopy study of detonation nanodiamond // *Diamond and Related Materials*, 2018, 87, 248–260.
- [3] Robertson J. Diamond-like amorphous carbon // *Mater. Sci. Eng. R Reports*, 2002.

**LP-PS-6****Modeling of laser crystallization of thin amorphous layers of silicon under experimental conditions of cw laser irradiation**

*J. Beránek<sup>1</sup>, O. Aktas<sup>2</sup>, S. MacFarquhar<sup>2</sup>, Y. Franz<sup>2</sup>, S. Mailis<sup>3</sup>, N. M. Bulgakova<sup>1</sup>,  
A. C. Peacock<sup>2</sup>*

*<sup>1</sup>HiLASE Centre, Institute of Physics of the Czech Academy of Sciences, Dolní Břežany, Czech Republic*

*<sup>2</sup>Optoelectronic Research Centre, University of Southampton, Southampton, United Kingdom*

*<sup>3</sup>Skolkovo Institute of Science and Technology, Center for Photonics and Quantum Materials, Skolkovo, Russian Federation*

Unique electrical and optical properties of crystalline silicon and silicon-based materials are of fundamental importance for applications in electronics, photovoltaics and communications. These materials have shaped the technical progress in many fields in recent decades. One of dynamically developing areas is silicon photonics [1], where nanoscale waveguides are finding use in components ranging from passive interconnects to active modulators and emitters. Such structures can be fabricated on various kinds of substrates and integrated with other electronic and optical components. However, the current methods used for producing high-quality crystalline silicon typically require high temperatures, which places important restrictions on device integration and miniaturization. On the other hand, amorphous silicon (a-Si) is relatively easy to deposit on various substrates at relatively low temperatures, but with inferior optical and electronic properties.

A solution to this problem is to fabricate high quality crystalline silicon waveguides and components by laser crystallizing deposited a-Si structures. Here we report our numerical investigations of laser processing of amorphous silicon waveguides for the experimental conditions with using a continuous wave (cw) argon ion laser. It was shown experimentally [1] that it is possible to obtain high optical quality poly-silicon waveguides by laser annealing of amorphous silicon films via heating to a temperature sufficient to melt the material but to avoid its noticeable evaporation that is consistent with our modelling and interpretation of the physical processes for the case of silicon optical fibers [2].

In this work, we report on the modelling of another waveguide geometry for exploring the temperature evolution of a-Si irradiated by cw laser at 488 nm wavelength. Physical modelling of laser-matter interaction provides an important insight for laser microfabrication as the processes of laser energy absorption, heat transfer and cooling during fabrication create specific conditions that affect the grain formation and growth and, therefore, influence the quality of final structure [3]. It allows to better understand the process of silicon crystallization in different regimes and can help to overcome drawbacks in production of high-quality silicon structures. To model thermodynamic changes in each particular case, it is necessary to develop a numerical code operating with high temporal and spatial resolutions, which is tailored to specific 2D and 3D geometries.

In our modeling, the irradiated samples represent the stripes of amorphous silicon with width of 1–2  $\mu\text{m}$  and thickness of 400 nm located on a glass substrate that are used in experiments. For this aims, we apply a finite-difference implicit scheme with splitting by the coordinates that provides high stability at reasonable simulation times and good energy conservation. The dynamics of laser heating in melting of a-Si in such geometry will be analysed with deriving the time of complete melting and the heat transferred to the glass substrate.

## References

- [1] Yohann Franz et al. Laser “Annealing of Low Temperature Deposited Silicon Waveguides”, Conference on Lasers and Electro-Optics (CLEO), OSA Technical Digest (online) (Optical Society of America, 2017), paper SM3K.4.
- [2] N. Healy et al., “Extreme electronic bandgap modification in laser-crystallized silicon optical fibres”, *Nat. Mater.* 13, 1122-1127 (2014).
- [3] N. H. Nickel, “Laser Crystallization of Silicon – Fundamentals to Devices”, Chapter 1 (Academic Press, 2003).

**LP-PS-7****Novel polymers for selective laser sintering: a new approach to 3D printing**

*S. Minaeva<sup>1</sup>, M. Syachina<sup>1</sup>, A. Mironov<sup>1</sup>, N. Minaev<sup>1</sup>, E. Krumins<sup>2</sup>, S. Howdle<sup>2</sup>, V. Popov<sup>1</sup>*

*<sup>1</sup>Institute of Photon Technologies of Federal Scientific Research Centre “Crystallography and Photonics” of Russian Academy of Sciences, Laboratory of Supercritical Fluid Technologies, Moscow, Russian Federation*

*<sup>2</sup>University of Nottingham, School of Chemistry, Nottingham, United Kingdom*

New polymeric powder materials with specific dyes coating and particle sizes varied from 0,5 to 30,0  $\mu\text{m}$  for selective laser sintering (SLS) have been developed. Supercritical carbon dioxide was used as a processing medium for polyamide (PA) and ultrafine polymethylmetacrylate (PMMA) particles coating. This allows both coloring of the particles and SLS products from them for decorative purposes, as well as give an absorption properties to particles at a desirable wavelength (the polymer itself may have low absorption for this wavelength) for carrying out the process of surface-selective laser sintering SSLS.

Based on PA particles with the orange coating the structures were obtained by SSLS with 405 nm laser (Fig. 1). Laser beam-delivery optical system based on X-Y galvanoscanner and focusing microobjective has been developed for guidance and scanning laser radiation at a wavelength of 405 nm along the working surface of the polymer powder layers.

Ultrafine PMMA powders with given microparticles distribution in sizes (mean diameters - 0.5 to 3  $\mu\text{m}$ ) have been produced by dispersion polymerization in supercritical carbon dioxide. Experimental fine mechanical system to form homogeneous thin (ca. 20  $\mu\text{m}$ ) layers of PMMA powders has been developed. Sintered polymer structures based on PMMA particles with addition of carbon black nanoparticles with a spatial resolution up to 30  $\mu\text{m}$  were fabricated. Similar structures from PMMA particles with blue coating were produced by SSLS technique using 405 nm laser (Fig. 2).

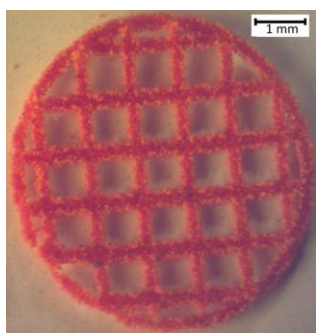


**Fig. 1.** The structure based on PA particles with the orange coating

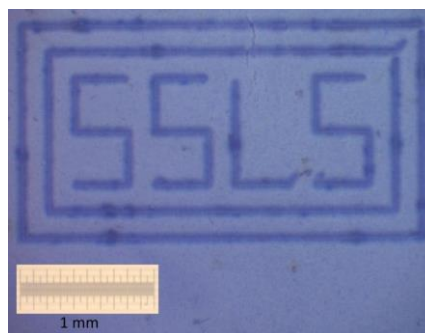


**Fig. 2.** The structure based on PMMA particles with the blue coating

This work was supported by the Ministry of Science and Higher Education within the State assignment FSRC «Crystallography and Photonics» RAS in part of SSLS process development and Russian Foundation of Basic Research (Project No. 17-53-10014 KO\_a) in part of PMMA microparticles synthesis and characterization.

**LP-PS-8****Photocatalytic activity of  $\text{TiO}_x\text{N}_y$  nanostructures prepared by pulsed laser ablation in water**

*A.M. Mezzasalma<sup>1</sup>, S. Spadaro<sup>1</sup>, F. Barreca<sup>1</sup>, F. Neri<sup>1</sup>, E. Fazio<sup>1</sup>*

*<sup>1</sup>Università di Messina,*

*Dipartimento di Scienze Matematiche e Informatiche- Scienze Fisiche e Scienze della Terra, Messina, Italy*

$\text{TiO}_2$  is extensively studied in view of photocatalytic applications thanks to its low cost, long lifetime of electron/hole pairs and high oxidizing power of photogenerated holes. However, the large bandgap of  $\text{TiO}_2$  (3.2 eV for anatase and 3 eV for rutile) limits its good photocatalytic activity to a small fraction of solar energy radiation (UV light) [1]. According to theoretical results [2], the extension into visible range should be obtained by synthesizing N-doped  $\text{TiO}_2$  or titanium oxynitride ( $\text{TiO}_x\text{N}_y$ ). However, for large scale usage, it is crucial to synthesize  $\text{TiO}_x\text{N}_y$  photocatalysts characterized by improved performance surface properties and high chemical and physical stability in order to obtain a significant catalytic activity upon UV and visible light.

In this work,  $\text{TiO}_{2-x}\text{N}_x$  nanocolloids, chemically and morphologically stable, were prepared by ablating in water  $\text{TiO}_{2-x}\text{N}_x$  pressed powders as well as pristine TiN and  $\text{TiO}_2$  targets. A combination of analytical techniques including X-ray photoelectron spectroscopy (XPS), Raman spectroscopy, scanning/transmission electron microscopies (SEM/STEM) and conventional optical techniques have been used to study structural and morphological properties of the nanocomposite. The samples were composed of nearly spherical nanoparticles with a size below 40 nm and tuned surface chemical bonding configurations. Under UV irradiation, all the produced nanostructures show a photo-catalytic activity towards the methylene blue dye molecule.

**References**

[1] S. Filice, J. of Col. and Inter. Sci. 489, (2017).

[2] R. Asahi et al., Science 293, 269 (2001).

**LP-PS-9****Review of experimental results of laser shock processing in Al 6061-T6 samples in the last 15 years in Mexico**

*G. Gomez-Rosas<sup>1</sup>, C. Rubio-González<sup>2</sup>, M.Á. Santana-Aranda<sup>1</sup>, J.G. Quiñones-Galván<sup>1</sup>, G. Garcia-Torales<sup>3</sup>, V. Granados-Alejo<sup>2</sup>, E. Castañeda<sup>4</sup>, C.A. Reynoso-García<sup>4</sup>, S. Hereñú<sup>5</sup>, J.L. Ocaña-Moreno<sup>6</sup>*

<sup>1</sup>*Centro Universitario de Ciencia Exactas e Ingenierías- Universidad de Guadalajara, Departamento de Física, Guadalajara, Mexico*

<sup>2</sup>*Centro de Ingeniería y Desarrollo Industrial, Departamento de Investigación, Querétaro, Mexico*

<sup>3</sup>*Centro Universitario de Ciencia Exactas e Ingenierías- Universidad de Guadalajara, Departamento de Electrónica, Guadalajara, Mexico*

<sup>4</sup>*Centro Universitario de Ciencia Exactas e Ingenierías- Universidad de Guadalajara, Departamento de Ingeniería Mecánica Eléctrica, Guadalajara, Mexico*

<sup>5</sup>*Instituto de Física del Rosario, Instituto de Física, Rosario, Argentina*

<sup>6</sup>*Centro Laser UPM- Universidad Politécnica de Madrid, Centro Laser UPM, Madrid, Spain*

Laser Shock Processing (LSP) is a technique for strengthening of metals, by inducing a compressive residual stress [1,2]. In this work, we present a review of experimental results obtained by our research group on the laser shock processing of Al 6061-T6, during the last 15 years. A convergent lens is used to deliver a high energy laser pulse, produced by a Q-switched Nd:YAG laser, on the surface of aluminum 6061-T6 specimens. Fatigue crack growth and fracture [1], high level compressive residual stresses [2], characterization of the shock wave [3], the effect of pulse density on the residual stress distribution, and other experimental results are presented [4].

**References**

- [1] C. Rubio-Gonzalez, *et al.* “Effect of laser shock processing on fatigue crack growth and fracture toughness of 6061-T6 aluminum alloy”. *Material Science and Engineering*, 386, 291-295. 2004.
- [2] G. Gomez-Rosas, *et al.* “High level compressive residual stresses produced in aluminium alloys by laser shock processing”, *Applied Surface Science* 252, 883-887, 2005.
- [3] R. Gonzalez-Romero *et al.* “Piezoresistive method for a laser induced shock wave detection on solids” *Proceeding of SPIE* 10403, 2017.
- [4] V. Granados-Alejo *et al.* “Influence of laser peening on fatigue crack initiation of notched aluminium plates”. *Structural Engineering and Mechanics* 62, 739-748, 2017.

**LP-PS-10****Simplified model for estimations of threshold fluences for laser melting and evaporation of nanoparticles**

*V. Pustovalov<sup>1</sup>, A. Chumakov<sup>2</sup>*

<sup>1</sup>*Belarusian National Technical University, Polytechnical Institute, Minsk, Belarus*

<sup>2</sup>*Institute of physics of NAS Belarus, centre of plasma, Minsk, Belarus*

Action of laser radiation pulses on nanoparticles leads to the initiation of different processes, for example, melting or evaporation of nanoparticle, and so on [1-4]. Many of these processes have thermal nature and threshold character. It means the initiation of these processes is realized under the achievement of some fixed threshold values of nanoparticle temperatures under the action of laser pulses with threshold radiation parameters. Theoretical investigations and estimations of laser threshold fluencies are carried out for melting and evaporation of solid spherical nanoparticles by laser pulses in a liquid media.

A new analytical methodology of general interest is presented for the explanation and determination of threshold parameters of various processes of laser-nanoparticles interaction. A simplified model for estimation of laser threshold fluence for melting  $E_M$  and evaporation  $E_{EV}$  of solid (metal) nanoparticles has been developed. The temporal dependencies [5] of nanoparticle temperature are used for estimations of threshold laser fluencies.

$$T_0 = T_\infty + IK_{abs}r_0[1 - \exp(-t/\tau_0)]/4k_\infty$$

The characteristic time  $\tau_0$  is determined by  $\tau_0 = c_0\rho_0r_0^2/3k_\infty$ ,  $c_0$ ,  $\rho_0$  are the heat capacity and density of nanoparticle material accordingly,  $I$  - laser intensity,  $K_{abs}$  - efficiency factor of absorption of laser radiation with wavelength  $\lambda$  by spherical nanoparticles with radius  $r_0$  [6,7],  $t$  - time,  $k_\infty$  is the heat conduction coefficient of surrounding medium (water).

The dependencies of threshold fluencies on pulse durations, laser wavelengths and nanoparticle radii are established and discussed. The model has been validated through direct comparison with the results of laser experiments with nano, pico- and femtosecond lasers and mutual agreement of these results. Comparison of some predicted values of the threshold laser fluencies for melting and evaporation of gold spherical nanoparticle in water with experimental data is given. Estimation of maximal nanoparticle temperature at the end of laser action can provide the determination of realized processes under laser action on nanoparticles and necessary validation of experimental data.

Explanation of the existence of minimal values of  $E_M$ ,  $E_{EV}$  at  $r_0 \sim 20-40$  nm for various laser wavelengths has been given. It is significant, that the values of  $E_M$ ,  $E_{EV}$  don't depend on pulse durations  $t_p$ , that much less than characteristic time of  $\tau_0$ ,  $t_p \ll \tau_0$ . These model and results can be used for the precise processes of nanoparticles treatment and applications in various laser technologies. This model is used analytical equations and can be applied for different experimental conditions.

The knowledge of optimum range of fluence can be translated to the requirements for a laser and nanoparticles parameters. The precise determination or estimations of threshold parameters is very important for the success of laser-nanoparticle applications in different fields of nanoscience and nanotechnology

## References

- [1] R. Cavicchi, D. Meier, C. Presser, V. Prabhu, S. Guha, Single laser pulse effects on suspended Au-nanoparticle size distributions and morphology, *J. Phys. Chem. C*, vol. 117, pp. 10866-10875 (2013).
- [2] O. Warshavski, L. Minai, G. Bisker, D. Yelin, Effect of single femtosecond pulses on gold nanoparticles. *J. Phys. Chem. C*, vol.115, pp. 3910-3917 (2011).
- [3] A. Fales, W. Vogt, J. Pfefer, I. Ilev, Quantitative evaluation of nanosecond pulsed laser-induced photomodification of plasmonic gold nanoparticles, *Scientific reports*, vol. 7, 15704 (2017).
- [4] S. Inasawa, M. Sugiyama, Y. Yamaguchi, Bimodal size distribution of gold Nanoparticles under picoseconds laser pulses. *J. Phys. Chem. B*, vol. 109, pp. 9404-9410 (2005).
- [5] V.K. Pustovalov, Light-to-heat conversion and heating of single nanoparticles, their assemblies, and surrounding medium under laser pulses. Review. *RSC Advances*, vol. 6, pp. 81266 – 81289 (2016).
- [6] L. Astafyeva, V. Pustovalov, W. Fritzsche, Characterization of plasmonic and thermo-optical parameters of spherical metallic nanoparticles, *Nano-Structures & Nano-Objects*, vol. 12, pp. 57–67 (2017).
- [7] V.K. Pustovalov, A.N. Chumakov, Optical characteristics of metallic Nanoparticles during melting by laser radiation. *J. Appl. Spectroscopy*, vol. 84, pp. 71-75 (2017).

## LP-PS-11

### Simulation of hole drilling in glass using ultrashort pulse laser in consideration of heat accumulation

C. Wei<sup>1</sup>, Y. Ito<sup>1</sup>, R. Shinomoto<sup>1</sup>, K. Nagato<sup>1</sup>, N. Sugita<sup>1</sup>

<sup>1</sup>The University of Tokyo, School of Engineering- Department of Mechanical Engineering, Tokyo, Japan

The micro processing of glass is crucial in various fields such as manufacturing of packages for integrated circuits [1] as well as microfluidic biochips [2]. Ultrashort pulse laser is considered an effective method for micro processing of glass. The shapes of holes drilled by ultrashort pulse laser highly depend on the processing conditions, indicating the importance of constructing simulations for shape prediction. A simulation of ultrashort pulse laser processing of glass utilizing the combination of beam propagation method and rate equation of electron density was developed, showing high shape-prediction accuracy [3]. However, in the simulation, electron density is considered as the only criterion of material removal: where the electron density is higher than the threshold, material in this region is removed. Consequently, heat accumulation between pulses is overlooked, resulting in impossibility to predict the shapes of holes drilled with high repetition rate. This study aims to develop a simulation of ultrashort pulse laser drilling of glass, where heat accumulation between pulses is taken into account, so that the dependency of repetition rate can be estimated.

In this study, in addition to electron density, temperature is considered as another criterion of material removal. Material in the region, where the temperature rises over boiling point, is removed. To calculate the temperature increase caused by each pulse, we assume the entire energy of ionized electrons is transferred to phonons. Thermal diffusion between pulses is calculated with heat equation. Consequentially, additional material removal can be calculated with criterion aforementioned. There are two parameters which affect the temperature calculation. Therefore, experiments of hole drilling with ultrashort pulse laser under high environmental temperature are conducted to determine both parameters.

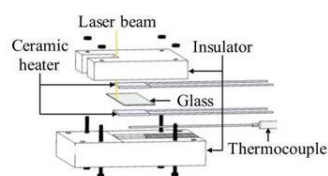


Fig. 1 Experimental setup

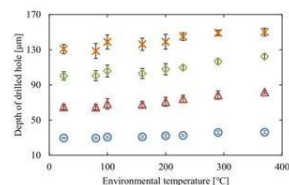


Fig. 2 Dependence of hole depth on environmental temperature.

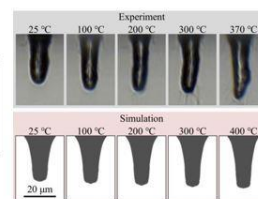


Fig. 3 Comparison of drilled holes between experiment and simulation.

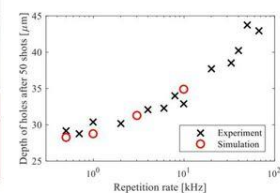


Fig. 4 Dependence of hole depth on repetition rate.

The experimental setup is shown in Fig.1. Before the start of the experiments, a glass piece was placed between two ceramic heaters, which were placed between two pieces of thermal insulation material. During the experiments, the glass piece was drilled by ultrashort pulse laser. In the meantime, environmental temperature was monitored with thermocouples and a thermographic camera. The glass pieces used in the experiments is made of non-alkaline glass. Yb: KWG laser with pulse duration 228 fs, wavelength 514 nm, repetition rate 1 kHz was used in the experiments. As a result of the experiments (Fig.2), increase in depth of holes was observed with the increase in environmental temperature. This increase in depth is attributed to the additional evaporation of the material caused by high environmental temperature. Two parameters aforementioned were

calculated based on the results of experiments, enabling the simulation to correspond to the experimental results (Fig.3). Using the developed simulation, high shape-prediction accuracy was achieved, as confirmed in the comparison of simulations and experimental results under high repetition rates (Fig.4).

## References

- [1] L. Brusberg, H. Schroder, M. Topper, and H. Reichl, "Photonic System-in-Package technologies using thin glass substrates," in *2009 11th Electronics Packaging Technology Conference*, pp. 930–935, 2009.
- [2] Y. Bellouard, A. Said, M. Dugan, and P. Bado, "Fabrication of high-aspect ratio, micro-fluidic channels and tunnels using femtosecond laser pulses and chemical etching," *Opt. Express*, vol. 12, no. 10, p. 2120, 2004.
- [3] Sun, M., et al.: Numerical analysis of laser ablation and damage in glass with multiple picosecond laser pulses, *Opt. Express*, 21-7,(2013), 7858.

**LP-PS-12****Surgical elimination of deformations of the facial skeleton using the method of computer virtual planning and laser stereolithography technology**

*S. Cherebylo<sup>1</sup>, V. Vnuk<sup>1</sup>, E. Ippolitov<sup>1</sup>, M. Markov<sup>1</sup>, S. Kamaev<sup>1</sup>, M. Novikov<sup>1</sup>, P. Mitroshenkov<sup>2</sup>*

*<sup>1</sup>ILIT RAS – Branch of the FSRC “Crystallography and Photonics” of RAS, laboratory of laser synthesis of bulk products, Shatura, Russian Federation*

*<sup>2</sup>FSBI “Clinical hospital №1” administrative Department of the President of Russian Federation, maxillofacial surgery, Moscow, Russian Federation*

This paper deals with the application of computer virtual modeling and 3d printing technology in the surgical removal of maxillofacial deformities.

Modern medicine has achieved great success in reconstructive surgeries [1], but the treatment of patients with complex defects and asymmetric facial deformities is still an urgent problem. The application of computer simulation and laser stereolithography allows to pre-plan in detail the course of the surgical intervention to reduce the time to perform the surgery to improve its quality, and as a result to short the rehabilitation period of the patient. Defects of the midface are formed as a result of acquired or congenital genesis, and the problem of their elimination is associated with a complex relief of the facial area [2]. One of the most common injuries is the area of the zygomatic-ocular complex. To restore the anatomy of damaged bone structures, a virtual three-dimensional reconstruction of the bone defect model is required. Using of the stereolithographic models of as reconstructive implants mold so and skull for find fitting is most advisable method [3].



**Fig. 1.** Model made by Laser stereolithography

This work was supported by the Ministry of Science and Higher Education within the State assignment FSRC « Crystallography and Photonics» RAS in pat «making models», Russian Foundation For Basic Research (RFBR) (Project № 18-29-03238) in pat «software product and a composite material».

**References**

- [1] Mitroshenkov P. Reconstructive surgery of total and subtotal defects of the upper, middle and lower zones of the facial skeleton. 2010. 416 P.
- [2] Cherebylo S.A., A.V. Evseev, P.N. Mitroshenkov. Application of laser stereolithography in reconstructive maxillofacial surgeons [Electronic resource] / 2005. URL: [http://nuclphys.sinp.msu.ru/school/s09/09\\_40.pdf](http://nuclphys.sinp.msu.ru/school/s09/09_40.pdf)
- [3] Stuchilov V.A., Nikitin A.A., Evseev A.V. Clinical aspects of the use of laser stereolithography in the surgical treatment of injuries of the midface / Clinical dentistry. 2001. -№3.- p. 54-57.

**LP-PS-13****Deposition of oxide nanostructures by nanosecond laser ablation of silicon in oxygen-containing background gas**

*A. Rodionov<sup>1,2</sup>, S. Starinskiy<sup>1,2</sup>, Y. Shukhov<sup>2</sup>, A. Bulgakov<sup>2,3</sup>, E. Maksimovskiy<sup>4</sup>, V. Sulyaeva<sup>4</sup>*

*<sup>1</sup>Novosibirsk State University, physical department, Novosibirsk, Russian Federation*

*<sup>2</sup>Institute of Thermophysics, Sb RAS, Novosibirsk, Russian Federation*

*<sup>3</sup>HiLASE Centre, Institute of Physics of the Czech Academy of Sciences, Dolní Břežany, Czech Republic*

*<sup>4</sup>Institute of Inorganic Chemistry, Sb RAS, Novosibirsk, Russian Federation*

Silicon and silicon-based nanostructures are widely used in field of creation protective and insulate coatings, photovoltaic and development new optical elements. One of the promising methods for the synthesis of silicon nanostructures is pulsed laser ablation. Today, the question about the interaction of ablation products and background environment has not been studied enough. In this work, we studied the composition of thin films synthesized by ablation of silicon in background argon, oxygen, air and their mixture at various pressures. Irradiation was carried out by the Nd:YAG laser with a wavelength of 532 nm and a pulse duration of 8 ns. SEM analysis showed that the films obtained at identical background pressure, but different oxygen concentrations, have a similar morphology. The oxidation state of the films was determined by using FTIR, EDX, XPS analysis methods. The results obtained using various techniques are in good agreement with each other. The oxidation state of the films increase with increase in the pressure of background Ar-O<sub>2</sub> mixture from 20 to 60 Pa, at a constant oxygen partial pressure 0.5 Pa. The films is uniformly oxidized at a background mixture of argon and oxygen with pressure of 60 Pa, regardless of oxygen content in range 2-100%. We assume that this is due to a change in the type of interaction between the gas and laser plume. Also observed uneven spatial oxidation of films. We assume that the uneven oxidation of the film is associated with the heterogeneous oxidation of the laser plume. As a result, oxygen-rich regions are formed on the substrate.

This work was financed by the partial support of a grant of the President of Russian Federation (MK-2404.2019.8, samples obtaining). The study of samples properties was carried out under state contract with IT SB RAS (AAAA-A17-117022850025-1).

**LP-PS-14****Compressed laser-induced  $\mu$ -plasma (CL $\mu$ P) for fused silica structuring: ps vs ns**

*V. V. Koval<sup>1</sup>, V.S. Rymkevich<sup>1</sup>, A. A. Samohvalov<sup>1</sup>, V. Veiko<sup>1</sup>*

<sup>1</sup>*ITMO University, Saint Petersburg, Russia*

Glass microstructuring by CL $\mu$ P is a very promising method for different applications upon making any micro-analytic systems as well as microoptical and diffractive elements [1,2]. In our method plasma extension is limited by the close contact between a glass plate and a highly absorbing target, so it's compressed (Fig.1a). Such plasma induced by  $\sim 50$  ns pulses of Yb: fiber laser have  $\sim 1.5$   $\mu$ s lifetime and becomes q-CW with repetition rate in the range of  $\sim 100$  kHz. Fused silica microstructuring under these conditions require multipulse processing mode, because an etching rate is rather small and is about 20 – 50 nm/pulse with fluences  $\sim 6$  J/cm<sup>2</sup> ( $1.3 \cdot 10^8$  W/cm<sup>2</sup>). These regimes can be useful for precision DOE fabrication, but high depth relief on fused silica is not available. Also, a width of craters in multipulse regimes are higher than a laser beam spot size. In order to minimize plasma plume volume and to achieve higher etching rates it's suggested to use laser radiation of picosecond pulse duration range. For fluences in the range below  $\sim 6$  J/cm<sup>2</sup> ( $2 \cdot 10^{11}$  W/cm<sup>2</sup> for 30 ps) the etching rate is up to 700 nm/pulse and a crater width is smaller than a laser beam spot, that can be caused by plasma-focusing effects. For higher fluences higher etching rates are possible, but in this case strong nonlinear effects define relief formation processes. However, high peak fluences in CL $\mu$ P are limited by laser-induced damage threshold of the free fused silica surface, that in the case of 30 ps pulses is measured to be  $\sim 12$  J/cm<sup>2</sup>.

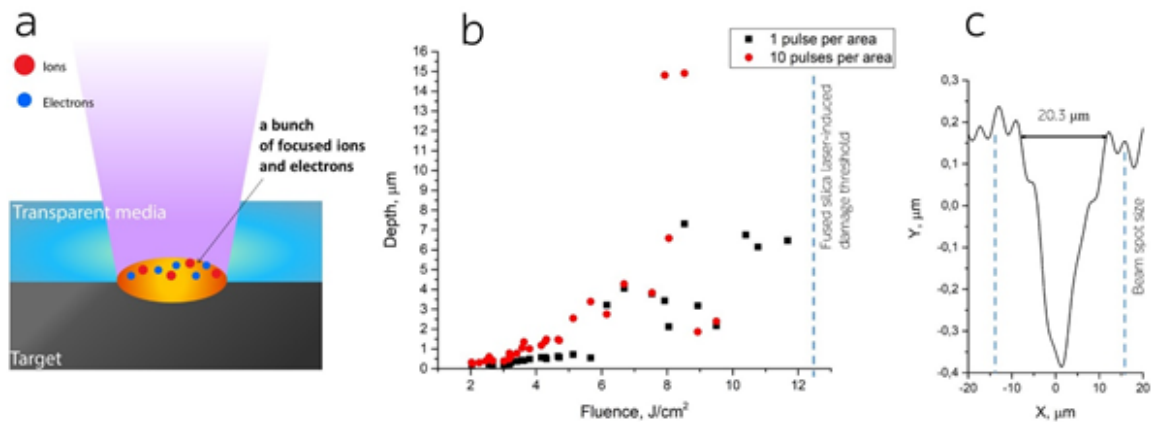


**Fig. 1.** Schematic of CL $\mu$ P processes (a), dependence of relief depth on laser fluence for 30 ps pulses (b), profile of single pulse crater (c).

The reported study was financially supported by the Ministry of Education and Science of the Russian Federation, research agreement No. 14.587.21.0037 (RFMEFI58717X0037).

**References**

- [1] Veiko, V. P., Volkov, S. A., Zakoldaev, R. A., Sergeev, M. M., Samokhvalov, A. A., Kostyuk, G. K., & Milyaev, K. A. (2017) Laser-induced microplasma as a tool for microstructuring transparent media. *Quantum Electronics*, 47(9), 842.
- [2] Kostyuk, G. K., Zakoldaev, R. A., Koval, V. V., Sergeev, M. M., & Rymkevich, V. S. (2017). Laser microplasma as a tool to fabricate phase grating applied for laser beam splitting. *Optics and Lasers in Engineering*, 92, 63-69.

## LP-PS-15

### Laser printing of silver screen printing inks

*P. Sopena<sup>1</sup>, J.M. Fernández-Pradas<sup>1</sup>, P. Serra<sup>1</sup>*

*<sup>1</sup>Universitat de Barcelona, Applied Physics Department, Barcelona, Spain*

Laser-induced forward transfer (LIFT) is a widely extended direct-write printing technique, being able to deposit from biological solutions to inorganic inks. In LIFT a very thin layer of material is spread on a donor substrate which is placed facing a receiver substrate. Then, through the action of a laser pulse focused on the donor film a bubble is created inside the ink, which expansion and further collapse leads to the formation of a jet that propels forward till it reaches the receiver, leading to liquid deposition. Finally, the jet breaks up and a voxel is thus printed. By the successive repetition of this process along the donor film multiple droplets and complex patterns can be reproduced.

The use of LIFT is especially interesting for printed electronic applications. Since there is no nozzle, unlike its major competitor, inkjet printing, there are almost no constraints on the rheological properties of the ink. Thus, extending the range of printable inks from low to high viscosity and from small to large particle size. For instance, this is relevant in the case of conductive inks because screen printing inks can be deposited. The high solid content of these inks allows obtaining very low sheet resistances usable for conductive pads. Since these inks are non-printable using inkjet printing due to nozzle-clogging, we propose LIFT for such task.

In this work we investigate the LIFT of silver screen printing inks for producing highly conductive pads. We determine the optimum working conditions for obtaining conductive continuous lines with the lowest sheet resistance by varying the laser pulse energy, repetition rate and donor-receiver gap. Finally, as a proof-of-concept of the technique, we print a high-frequency passive component that performs accordingly to the designed layout.

**LS-PS-1****Cation-deficient sodium-gadolinium molybdates: structure, modeling, energy transformation**

*E. Zharikov<sup>1</sup>, K. Subbotin<sup>1</sup>, V. Dudnikova<sup>2</sup>, D. Lis<sup>1</sup>, A. Titov<sup>1</sup>*

*<sup>1</sup>Prokhorov General Physics Institute RAS, Laser Crystals, Moscow, Russian Federation*

*<sup>2</sup>Lomonosov Moscow State University, Geology Faculty, Moscow, Russian Federation*

Sodium–gadolinium molybdate (NGM) is representative of a large family of compounds crystallized into the scheelite  $\text{CaWO}_4$  structure (tetragonal syngony, space group  $I4_1/a$ ) with a statistical distribution of sodium and gadolinium ions at calcium sites.  $\text{Ca}^{2+}$  in prototype powellite  $\text{CaMoO}_4$  replaced for  $\text{Na}^+$  and  $\text{Gd}^{3+}$  in NGM. Scheelite-like NGM has a cation-deficient structure and, according to its nominal composition, contains up to 1/7 unoccupied cation sites. General formula for charge compositions is  $\text{Na}_x\text{Gd}_{(2-x)/3(1-2x)/3}\text{MoO}_4$ , with  $x$  value varied from 0,2 to 0,6. The average amount of vacancies in crystals grown by Czochralski technique is about 0.07 f.u., which is equal to 7 % of empty cation sites in the sublattice.

The simulation was performed by the method of interatomic potentials using the GULP 4.0.1 code (General Utility Lattice Program), which is based on minimizing the energy of the crystal structure. Atomistic simulation considered two kinds of cation sites distribution: the statistical distribution of sodium, gadolinium, and unoccupied cation positions in the  $I4_1/a$  structure and their partial ordering. As a result of the simulation, structural characteristics of NGM agreed well with the known experimental data. In addition, a number of important elastic and thermodynamic properties of these compounds are predicted.

NGM single crystal is a promising laser host. It provides the broad and strong luminescence bands of  $\text{Ln}^{3+}$  dopants, appropriate for femtosecond laser pulses generation in mode-locked regime as well as for tunable lasing. NGM doped by different rare earths are also promising phosphors for use in white light-emitting diodes, optical displays, and as scintillators, photocatalysts, etc.

Yb-doped scheelite-like NGM is the efficient down-converter, enhancing the efficiency of crystalline silicon photovoltaic cells ( $E_g = 1,14$  eV). The efficient excitation of  $1 \mu\text{m}$   $\text{Yb}^{3+}$  emission by ‘soft’ UV light (260-400 nm) occurs due to quantum cutting. It runs via donor-acceptor interaction: donor optical centers absorb the UV quanta and non-radiatively transfer the excited state energy to a doubled number of acceptors via the mechanism of cooperative down-conversion. Then the acceptor emits the energy as the secondary quanta. Ytterbium ions are the acceptor in these crystals, while the structure of donors is not known so far. The possible donor nature is discussed.

This work has been supported by Russian Scientific Fund (grant # 18-12-00517)

**LS-PS-2****Verdet constant of rare-earth-sesquioxide-based magneto-active ceramics**

*D. Vojna*<sup>1,2</sup>, *O. Slezák*<sup>1</sup>, *R. Yasuhara*<sup>3</sup>, *H. Furuse*<sup>4</sup>, *A. Lucianetti*<sup>1</sup>, *T. Mocek*<sup>1</sup>

<sup>1</sup>*HiLASE Centre, Institute of Physics of the Czech Academy of Sciences, Dolní Břežany, Czech Republic*

<sup>2</sup>*Faculty of Nuclear Sciences and Physical Engineering- Czech Technical University in Prague, Department of Physical Electronics, Prague, Czech Republic*

<sup>3</sup>*National Institute for Fusion Science- National Institutes of Natural Sciences, High-Temperature Plasma Physics Research Division, Toki, Japan*

<sup>4</sup>*Kitami Institute of Technology, Department of Material Science and Engineering, Kitami, Japan*

Faraday devices (FDs) represent one of the fundamental components used in laser systems, for instance, in the multi-pass amplification schemes, regenerative amplifiers or for optical isolation of unwanted back-reflections from one part of the laser system to another. An indispensable part of these devices is a piece of magneto-active material, in which the Faraday rotation is induced by applying the magnetic field.

Most recently, a lot of scientific attention is dedicated to the investigation of rare-earth sesquioxides (RE<sub>2</sub>O<sub>3</sub>, RE – Tb [1-3], Dy [4,5], and Ho [6,7]) ceramics materials. The reason is that these compounds contain a high concentration of magnetically active RE<sup>3+</sup> ions and, hence, it is possible to reduce the length of the needed magneto-optical elements in the FDs. Such a reduction is extremely beneficial for mitigation of the thermal effects arising in the high-power FDs.

We report on comprehensive experimental characterization of the Verdet constant of Dy-based and Ho-based RE-sesquioxide ceramics samples in a broad spectral range from 0.6 to 2.3 μm. These results are valuable for a proper design of 1 – 2 μm high-power FDs.

**References**

- [1] I. L. Snetkov et al., *Wavelength dependence of Verdet constant of Tb<sup>3+</sup>:Y<sub>2</sub>O<sub>3</sub> ceramics*, Appl. Phys. Lett. 108, 161905 (2016).
- [2] A. Ikesue et al., *Polycrystalline (Tb<sub>x</sub>Y<sub>1-x</sub>)<sub>2</sub>O<sub>3</sub> Faraday rotator*, Opt. Lett. 42, 4399-4401, (2017).
- [3] A. Ikesue et al., *Total Performance of Magneto-Optical Ceramics with a Bixbyite Structure*, Materials 12(3), 421, (2019).
- [4] J. R. Morales et al., *Magneto-optical Faraday effect in nanocrystalline oxides*, J. Appl. Phys. 109(9), 093110, (2011).
- [5] I. L. Snetkov et al., *Magneto-optical Faraday effect in dysprosium oxide (Dy<sub>2</sub>O<sub>3</sub>) based ceramics obtained by vacuum sintering*, Opt. Lett. 43(16), 4041-4044 (2018).
- [6] H. Furuse et al., *Magneto-optical characteristics of holmium oxide (Ho<sub>2</sub>O<sub>3</sub>) ceramics*, Opt. Mater. Express 7, 827-833, (2017).
- [7] D. Vojna et al., *Faraday effect measurements of holmium oxide (Ho<sub>2</sub>O<sub>3</sub>) ceramics-based magneto-optical materials*, High Power Laser Science and Engineering 6, (2018).

**LS-PS-3****Structural features and optical properties of  $\text{Ca}_3(\text{VO}_4)_2:\text{Mn}$  laser crystals**

*L. Ivleva<sup>1</sup>, I. Voronina<sup>1</sup>, E. Dunaeva<sup>1</sup>, M. Doroshenko<sup>1</sup>, A. Papashvili<sup>1</sup>*

*<sup>1</sup>Prokhorov General Physics Institute of the Russian Academy of Sciences,  
Laser Materials and Technology Research Center at GPI, Moscow, Russian Federation*

The undoped calcium orthovanadate  $\text{Ca}_3(\text{VO}_4)_2$  with whitlockite-type structure has been investigated earlier for high-temperature ferroelectricity ( $T_c=1383$  K), second-harmonic generation, and stimulated Raman ( $\Omega R=854$   $\text{cm}^{-1}$ ) scattering,  $\text{Ca}_3(\text{VO}_4)_2:\text{Tm}^{3+}$  was suggested as crystalline medium for 2- $\mu\text{m}$  lasers.

In this paper, the functional properties (fluorescent, laser) were studied in their connection with the fundamental characteristics (composition and structure) and depending on the background (composition of the initial charge, the method of introducing activators, growth conditions and post-processing) of  $\text{Ca}_3(\text{VO}_4)_2$  doped with manganese ions. Doped  $\text{Ca}_3(\text{VO}_4)_2$  crystals were grown by Czochralski method. Dopant ions were introduced into the melt in form of oxide ( $\text{Mn}_2\text{O}_3$ ). Another method of activator introducing is diffusion annealing in special mixture. In this case maximal concentration of Mn ions in  $\text{Ca}_3(\text{VO}_4)_2$  was achieved. Absorption spectra measured at low (77K) and room temperature have shown characteristic absorption lines of  $\text{Mn}^{5+}$  ions peaking around 700 nm. Selective excitation into the absorption band at low (15K) temperature allowed to observe three different  $\text{Mn}^{5+}$  ions fluorescence spectra. Two narrow fluorescence spectra were to be quite similar in shape with small difference in position of 1176 nm and 1190 nm. Fluorescence lifetime measured for these two fluorescence maxima have shown about twice difference: 500 ms at 1176 nm and 260 ms at 1190 nm respectively and can be attributed to different  $\text{Mn}^{5+}$  electronic transitions. Additional broadband fluorescence of some new type of  $\text{Mn}^{5+}$  ions optical centers (FWHM of about 1000 nm at 15 K) was observed in  $\text{Ca}_3(\text{VO}_4)_2:\text{Mn}^{5+}$  crystal for longer 768 nm excitation. This type of  $\text{Mn}^{5+}$  optical centers is characterized by much shorter fluorescence lifetime of 100 ms at 15 K and was not reported previously. Much broader fluorescence line of these optical centers allows to obtain oscillation wavelength tuning in the range of 1150-1500 nm which can be interesting for laser applications.

**LS-PS-4****Laser operation of a novel Ho:GdYAP crystal under 1948-nm Tm-fiber laser pumping**

*K. Pierpoint*<sup>1</sup>, *W. Chen*<sup>1,2</sup>, *Y. Zhao*<sup>1</sup>, *K. Scholle*<sup>3</sup>, *S. Lamrini*<sup>4</sup>, *P. Zang*<sup>5</sup>, *Z. Chen*<sup>5</sup>, *X. Mateos*<sup>6</sup>,  
*U. Griebner*<sup>7</sup>, *V. Petrov*<sup>1</sup>

<sup>1</sup>*Max-Born-Institute, Ultrafast Lasers and Nonlinear Optics, Berlin, Germany*

<sup>2</sup>*Fujian Institute of Research on the Structure of Matter- Chinese Academy of Sciences, Crystal and Laser department, Fuzhou, China*

<sup>3</sup>*Futronics Laser GmbH, Research, Göttingen, Germany*

<sup>4</sup>*LISA Laser Products GmbH, Laser research, Katlenburg-Lindau, Germany*

<sup>5</sup>*Jinan University, Department of Optoelectronic Engineering, Guangzhou, China*

<sup>6</sup>*Universitat Rovira i Virgili, Department of Physical and Inorganic Chemistry, Tarragona, Spain*

<sup>7</sup>*Max-Born-Institute, Solid State Light Sources, Berlin, Germany*

Passive REAlO<sub>3</sub> (RE=Y, Gd, Lu) orthorhombic perovskites are attractive for development of efficient rare-earth (RE=Nd, Yb, Tm, etc.) doped solid-state lasers due to their natural birefringence, good thermo-mechanical characteristics and low phonon energy. A novel 1% Ho<sup>3+</sup>-doped GdYAP (Gd:Y=1:9) crystal, a solid-solution of YAlO<sub>3</sub> and GdAlO<sub>3</sub>, was grown in the present work by the Czochralski technique. The inhomogeneous spectral broadening of the absorption and emission bands of the dopant ion due to the compositional disorder in such mixed hosts is favorable for resonant in-band pumping of the <sup>5</sup>I<sub>8</sub>-<sup>5</sup>I<sub>7</sub> Ho transition and ultrashort pulse generation by mode-locking. Here we study for the first time continuous-wave laser operation of the new Ho:GdYAP crystal pumped into one of its absorption peaks by a 1948-nm Tm-fiber laser.

The 3-mm thick, uncoated *a*-cut Ho:GdYAP sample was first studied in a hemispherical cavity with a 100-mm radius-of-curvature output coupler (OC). A maximum slope efficiency of 60% with respect to the double-pass absorbed pump power was obtained for OC transmission T<sub>OC</sub>=10%; the maximum output power reached 2.8 W at an absorbed pump power of 6.3 W. The wavelength was ~2117 nm and the polarization was parallel to the *b*-axis. In a short (~5 mm) plane-parallel cavity, an output power of 3.9 W was reached at an absorbed pump power of 8.5 W with a slope efficiency of 48% (T<sub>OC</sub> = 3%). In this set-up the output wavelength was ~2118 and 2124 nm for T<sub>OC</sub> = 3% and 1%, respectively.

## LS-PS-5

Diode pumped cryogenic Tm:Y<sub>2</sub>O<sub>3</sub> ceramic laser

*F. Yue<sup>1</sup>, V. Jambunathan<sup>1</sup>, S. Paul David<sup>1</sup>, X. Mateos<sup>2</sup>, M. Aguiló<sup>2</sup>, F. Díaz<sup>2</sup>, J. Sulc<sup>3</sup>,  
A. Lucianetti<sup>1</sup>, T. Mocek<sup>1</sup>*

<sup>1</sup>*HiLASE Centre, Institute of Physics of the Czech Academy of Sciences, Dolní Břežany, Czech Republic*

<sup>2</sup>*Física i Cristal·lografia de Materials i Nanomaterials FiCMA-FiCNA, Universitat Rovira i Virgili, Tarragona, Spain*

<sup>3</sup>*Faculty of Nuclear Sciences and Phys. Eng., Czech Technical University in Prague, Prague, Czech Republic*

Compact high average and peak power (HAPP) lasers emitting around two-micron have broad applications in various areas, such as laser induced damage threshold (LIDT) measurements, polymer material processing, debris removal from space, etc [1]. To achieve laser in two-micron region, Tm doped yttrium oxide (Tm:Y<sub>2</sub>O<sub>3</sub>) is a promising active media. The advantage of Tm ion is that it can be excited by commercial available AlGaAs laser diodes around 793 nm, and it also has two-to-one cross-relaxation process, which leads to much higher slope efficiency than the quantum defect limited value [2]. The host material, Y<sub>2</sub>O<sub>3</sub> has very high thermal conductivity, a relatively low maximum phonon energy and sufficiently broad emission when doped with rare earth ions [3]. However, this material suffers from reabsorption losses due to quasi-three level system at room temperature and other parasitic process such as excited state absorption (ESA) and energy-transfer upconversion (ETU), which limit the power scaling and beam quality of laser. To mitigate these issues, cooling the active medium down to cryogenic temperatures is the proper solution. Here in this work, we studied the laser potentialities of this material at cryogenic temperature using Volume Bragg stabilized (VBG) diode laser emitting at 793 nm.

Cryogenic continuous wave laser operation is realized using a “L” shaped cavity with 3 at.% Tm:Y<sub>2</sub>O<sub>3</sub> ceramic sample. Two parameters are varied: output coupler transmission (T<sub>oc</sub> = 5, 9, 15, 20 and 30%) and sample temperature (80 – 180 K in step of 20 K), as shown in Fig. 1 (a) and (b), respectively. A maximum output power of 6.4 W is achieved at sample temperature of 80 K and T<sub>oc</sub> = 30%, corresponding to a slope efficiency of 32.2%. The inset of Fig. 1 (b) shows a very high quality Gaussian beam profile obtained for incident power of 15 W.

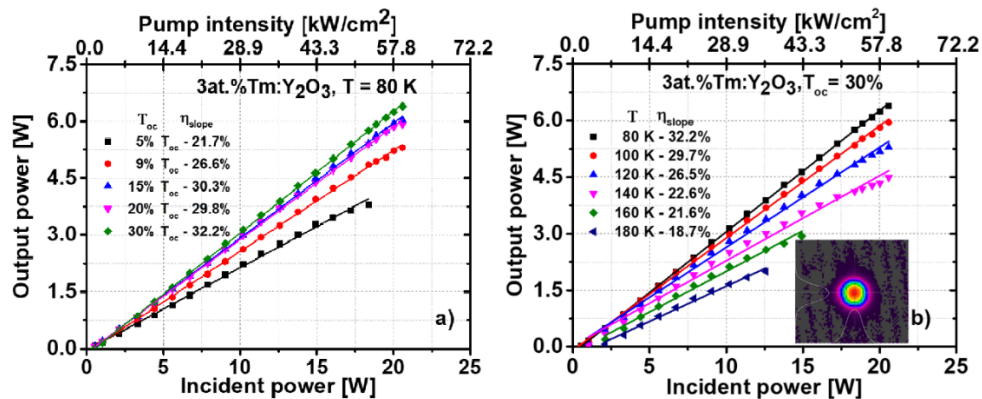


**Fig. 1.** Incident/output characteristics of 3 at.% Tm:Y<sub>2</sub>O<sub>3</sub> ceramic pumped by 793 nm VBG diode (a) for various output couplers with sample temperature of 80 K and (b) for various sample temperatures with T<sub>oc</sub> = 30%. Inset: Far field beam Gaussian profile under pump power of 15 W.

## References

- [1] K. Scholle, P. Fuhrberg, P. Koopmann, and S. Lamrini, "2  $\mu\text{m}$  Laser Sources and Their Possible Applications," in B. Pal (Ed.), "Frontiers in Guided Wave Optics and Optoelectronics," Ch. 21, INTECH Open Access Publisher, Rijeka (2010).
- [2] A. Godard, "Infrared (2–12  $\mu\text{m}$ ) solid-state laser sources: a review," *Comptes Rendus Physique*, vol. 8, issue 10, 1100-1128, (2007).
- [3] C. Kraenkel, "Rare-Earth-Doped Sesquioxides for Diode-Pumped High-Power Lasers in the 1-, 2-, and 3- $\mu\text{m}$  Spectral Range," in *IEEE Journal of Selected Topics in Quantum Electronics*, vol. 21, no. 1, pp. 250-262 (2015).

**LS-PS-6****Radiation hardness of Nd:GdVO<sub>4</sub> laser crystal**

*Y. Kalachev<sup>1</sup>, S. Kutovoi<sup>1</sup>, Y. Zavartsev<sup>1</sup>, A. Zagumennyi<sup>1</sup>, V. Mikhailov<sup>1</sup>, I. Shcherbakov<sup>1</sup>, M. Ashurov<sup>2</sup>, S. Ismailov<sup>2</sup>, K. Saidakhmedov<sup>2</sup>*

<sup>1</sup>*Prokhorov General Physics Institute of the Russian Academy of Sciences, Laser crystals, Moscow, Russian Federation*

<sup>2</sup>*Institute of Nuclear Physics of the Academy of Sciences of Uzbekistan, Nuclear Physics, Ulugbek, Uzbekistan*

In our previous work the radiation hardness of Yb:LaSc<sub>3</sub>(BO<sub>3</sub>)<sub>4</sub> and Yb:LuYSiO<sub>5</sub> laser crystals was studied [1]. Now we studied radiation hardness of Nd:GdVO<sub>4</sub> crystal by comparing transmissions spectra of laser crystal before and after irradiation using <sup>60</sup>Co source. The radiation hardness of undoped GdVO<sub>4</sub> crystal was studied as well. Direct laser experiments were performed. Induced absorption of undoped GdVO<sub>4</sub> crystal was reduced with increasing of time delay after exposition. Crystal absorption at lasing wavelength 1,063 um was reduced from 0.016 cm<sup>-1</sup> to 0.003 cm<sup>-1</sup> in 90 minutes. The 0.5% Nd: Nd:GdVO<sub>4</sub> crystal did not relax to initial absorbance after one week of aging. Its residual absorbance at lasing wavelength was 0.05 cm<sup>-1</sup>.

Laser with  $\gamma$  - irradiated Nd:GdVO<sub>4</sub> crystal demonstrated slope efficiency of ~ 30% at lasing wavelength 1,063 um in spite of the presence of relatively weak crystal staining. Laser output power reach 800 mW at pumping power 4 W. (Fig.1).

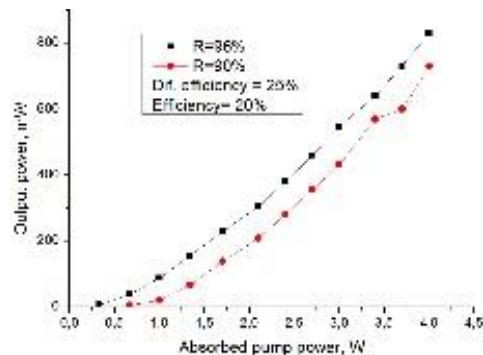


**Fig. 1.**

This means that this crystal can be considered as radiation-resistant at absorbed dose levels up to 10 Mrad, with subsequent cooling of more than 1 day.

This study was supported by the Federal Agency for Scientific Organizations (Contract 0024-2018-0016) and the Presidium of the Russian Academy of Sciences (Programs I.56 and I.7)

**References**

- [1] Radiation Resistance of Yb:LaSc<sub>3</sub>(BO<sub>3</sub>)<sub>4</sub> and Yb:LuYSiO<sub>5</sub> Laser Crystals V. I. Vlasov, Yu. D. Zavartsev, M. V. Zavertyaev, A. I. Zagumennyi, Yu. L. Kalachev, V.A.Kozlov, S. A. Kutovoi, V. A. Mikhailov, and I. A. Shcherbakov. Physics of Wave Phenomena, 2018, Vol. 26, No. 4, pp. 1–5.

**LS-PS-7****Influence of electron and proton irradiations on the optical characterizations of  $\text{La}_3\text{Ga}_{5.5}\text{Ta}_{0.5}\text{O}_{14}$  and  $\text{Ca}_3\text{TaGa}_3\text{Si}_2\text{O}_{14}$** 

*N. Kozlova*<sup>1</sup>, *E. Zabelina*<sup>1</sup>, *O. Buzanov*<sup>2</sup>, *A. Kozlova*<sup>1</sup>, *P. Lagov*<sup>3</sup>, *Y. Pavlov*<sup>4</sup>, *V. Stolbunov*<sup>5</sup>

<sup>1</sup>*NUST MISiS, Laboratory "Single crystals and stock on their base", Moscow, Russian Federation*

<sup>2</sup>*Fomos-Materials, Fomos-Materials, Moscow, Russian Federation*

<sup>3</sup>*NUST MISiS, Department of semiconductor electronics, Moscow, Russian Federation*

<sup>4</sup>*A.N. Frumkin Institute of Physical Chemistry and Electrochemistry Russian Academy of Sciences, A.N. Frumkin Institute of Physical Chemistry and Electrochemistry Russian Academy of Sciences, Moscow, Russian Federation*

<sup>5</sup>*Institute of Theoretical and Experimental Physics, Institute of Theoretical and Experimental Physics, Moscow, Russian Federation*

The irradiation response of  $\text{La}_3\text{Ga}_{5.5}\text{Ta}_{0.5}\text{O}_{14}$  (LGT) and  $\text{Ca}_3\text{TaGa}_3\text{Si}_2\text{O}_{14}$  (CTGS) crystals is poorly investigated and necessary for the study of their defect structure. Study of defects structure and its formation in multicomponent oxide single-crystal dielectric materials is the nontrivial task. The anisotropy of complicated structures with non-cubic lattice leads to various phenomena, e.g. dichroism. Absorption spectra in near UV and visible regions are sensitive to the point defects and their associations in crystal structure. Each absorption band on the spectra is associated with specific type or group of point defects. For LGT and CTGS three absorption bands are observed at  $\lambda \sim 290$  nm, at  $\lambda \sim 360$  nm and  $\lambda \sim (460-480)$ . According to [1] the absorption band at  $\lambda \sim (460-480)$  nm is identified with oxygen defects and F-centers ( $\text{Vo}^{++}$ ,  $2e^-$ ). The origin of two other bands is still not clear. The study of the irradiation effects on ion structures is a productive method for investigation of the origin of the defect structure and mechanisms of its formation. Here, we present the results of our study of LGT and CTGS optical properties under electron and proton irradiations. All investigated samples were cut from crystals grown in JSC "Fomos-Materials" Co. using Czochralski method in iridium crucibles. **Electron irradiation** was performed at the Center of Physical Measurements Investigations of IPCE RAS using the linear accelerator (energy 6 MeV, flux  $4 \cdot 10^{12} \text{ cm}^{-2} \cdot \text{s}^{-1}$ , fluences up to  $1,2 \cdot 10^{16} \text{ cm}^{-2}$ ). **Proton irradiation** was performed on linear accelerator I-2 at the Center of Collective Use "Kamiks" of ITEP (energy 20 MeV, flux  $1 \cdot 10^{11} \text{ cm}^{-2} \cdot \text{s}^{-1}$ , fluence  $1 \cdot 10^{14} \text{ cm}^{-2}$ ). **Optical properties** of samples were measured using UV-Vis-NIR spectrophotometer "Cary-5000" (Agilent Technologies) at non-polarized light taking into account the dichroism (with sample rotation by  $90^\circ$  around the light direction). After irradiation, all samples changed color, become more colored with a grayish tint. Irradiation both with protons and electrons leads to increase of absorption in all investigated wave-length region. The most significant effects are observed in the region of (250-450) nm. The greatest increase in absorption in the region of (250-500) nm is observed after the electron irradiation fluence of  $4 \cdot 10^{15} \text{ cm}^{-2}$ . The subsequent increase of fluence did not lead to the further increase of absorption.

**References**

- [1] N. Kozlova, O. Buzanov, E. Zabelina et.al. Study of the origin of the defects in  $\text{La}_3\text{Ga}_{5.5}\text{Ta}_{0.5}\text{O}_{14}$  single crystals // *Optical Materials* 91 (2019) 482–487.

**LS-PS-8****High-quality factor crystalline silicon WGM microresonators for near and mid-IR wavelengths**

*I. Bilenko<sup>1,2</sup>, A. Shitikov<sup>1,2</sup>, T. Tebeneva<sup>3</sup>, O. Benderov<sup>3</sup>, A. Rodin<sup>3</sup>, N. Kondratiev<sup>1</sup>, V. Lobanov<sup>1</sup>, A. Voloshin<sup>1</sup>*

<sup>1</sup>*Russian Quantum Center, coherent microoptics and radiophotonics, Moscow, Russian Federation*

<sup>2</sup>*Lomonosov Moscow State University, Physics, Moscow, Russian Federation*

<sup>3</sup>*MIPT, Laboratory of applied infrared spectroscopy, Dolgoprudny, Russian Federation*

In the past decades, optical whispering gallery mode (WGM) resonators with high-quality factor Q become powerful tools in a wide range of applications in optics, photonics, and radiophotonics. Different materials and production techniques are used for the WGMs preparation. Silicon is a major semiconductor material for modern microelectronic, so samples of high purity and homogeneity are easily available. However, interest to silicon WGMs was limited because it is not transparent for the visible wavelengths and exhibit strong free electron and two-photon absorption (FEA and TPA) on the 1.5  $\mu\text{m}$  telecom wavelengths.

In our previous work, we experimentally demonstrated ultrahigh Q above  $10^9$  at 1.5  $\mu\text{m}$  - two orders of magnitude higher than ever achieved before [1]. It became possible due to the application of undoped material with very low residual conductivity resulting in negligible FEA and polishing technique that prevents excess surface absorption. Measurements were made using low incident power in order to work below TPA limitations.

In present work, we report results of a different kind of the material comparison made on the 1.5  $\mu\text{m}$  telecom wavelengths and also first successful attempts to observe high-quality resonances at wavelengths below 2  $\mu\text{m}$  – band where TPA in pure silicon is depressed.

All measurements were made by means of the tunable semiconductor lasers. We used original semispherical coupler for the WGM excitation. Diameters of the resonators vary from 2.4 to 2.6 mm, curvature radii – from 0.5 to 1 mm. A large number of modes (fundamental and non-fundamental) were observed and characterized for each sample.

We observe a correlation between the achievable value of Q and the conductivity of the materials. As far as a bulk absorption evaluated from the conductivity and proved experimentally for our samples is too low to affect the Q, we regard these results as evidence of a new surface absorption mechanism to be investigated.

Also, we managed to resolve WGM resonances linewidth corresponded to  $Q > 10^7$  at 2.3  $\mu\text{m}$  wavelength (see Fig.1) limited by our present measurement technique. It is planned to continue material characterization, to apply the ringdown method of Q measurement on 2.3  $\mu\text{m}$  and to expand the measurements to longer wavelengths.

Summarizing, we demonstrated that the silicon high-Q WGM resonators can be effectively used both in near and mid-IR wavelength. The last ones are of great importance as, unlike other materials used for WGM resonators namely,  $\text{CaF}_2$  and  $\text{MgF}_2$ , silicon has low bulk absorption at mid-IR along with very high Kerr nonlinearity. This opens the possibility to use it for Kerr comb sources [2], laser stabilization for heterodyne radiometry [3] and optics to/from THz frequency converters [4].

This work was supported by the Russian Science Foundation (project 17-12-01095).

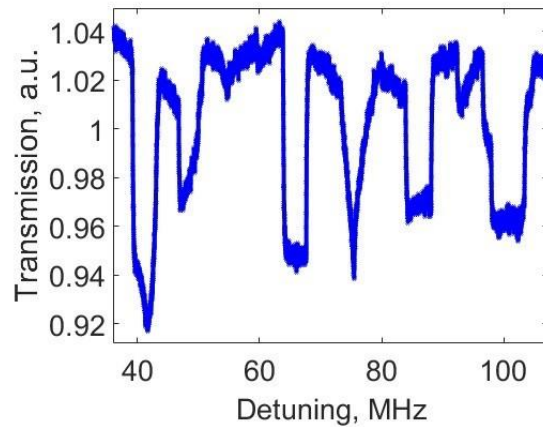


**Fig. 1.**

## References

- [1] A. E. Shitikov, I. A. Bilenko, N. M. Kondratiev, V. E. Lobanov, A. Markosyan, and M. L. Gorodetsky, "Billion Q-factor in silicon WGM resonators," *Optica* 5, 1525 (2018).
- [2] N. G. Pavlov, S. Koptyaev, G. V. Lihachev, A. S. Voloshin, A. S. Gorodnitskiy, M. V. Ryabko, S. V. Polonsky, and M. L. Gorodetsky, "Narrow-linewidth lasing and soliton Kerr microcombs with ordinary laser diodes," *Nat. Photon.* 12, 694 (2018).
- [3] A. Rodin, A. Klimchuk, A. Nadezhdinskiy, D. Churbanov and M. Spiridonov, "High resolution heterodyne spectroscopy of the atmospheric methane NIR absorption", *Opt. Exp.*, Vol. 22, Issue 11, pp. 13825-13834 (2014).
- [4] A. B. Matsko, D. V. Strekalov, and N. Yu. "Sensitivity of terahertz photonic receivers," *Phys. Rev. A* 77, 043812 (2008).

**LS-PS-9****Growth and polarization-resolved spectroscopy of monoclinic Yb<sup>3+</sup>:ZnWO<sub>4</sub> crystals**

*D. Lis*<sup>1</sup>, *P. Loiko*<sup>2</sup>, *K. Subbotin*<sup>1</sup>, *E. Zharikov*<sup>1</sup>, *A. Titov*<sup>1</sup>, *J.M. Serres*<sup>3</sup>, *M. Aguiló*<sup>3</sup>, *F. Díaz*<sup>3</sup>,  
*X. Mateos*<sup>3</sup>

<sup>1</sup>*Prokhorov General Physics Institute of the Russian Academy of Sciences,  
Laser Materials and Technology Research Center at GPI, Moscow, Russian Federation*

<sup>2</sup>*ITMO University, Department of Optical Physics and Modern Natural Science, St. Petersburg,  
Russian Federation*

<sup>3</sup>*Universitat Rovira i Virgili, Física i Cristallografia de Materials i Nanomaterials, Tarragona,  
Spain*

Monoclinic wolframite-type mon tungstate crystals M<sup>2+</sup>WO<sub>4</sub> (where M = Mg, Zn, Mn, Ni, etc.) are the promising laser hosts for doping with trivalent rare-earth ions (RE<sup>3+</sup>). They possess good thermo-mechanical properties, strong Raman activity and provide broad and strong absorption and emission bands for the RE<sup>3+</sup> ions with polarized light. Recently efficient laser operation in the near-infrared was demonstrated at RE<sup>3+</sup>-doped MgWO<sub>4</sub> crystals. In the present work, we report on Czochralski (Cz) growth, structure, vibronic properties and polarized room- and low-temperature spectroscopic studies of an Yb<sup>3+</sup>-doped zinc mon tungstate crystal. ZnWO<sub>4</sub>:5 at.% Yb<sup>3+</sup>:5 at.% Li<sup>+</sup>: crystal (nominal composition) was grown by the Cz method along the [100] direction from melt in air from a platinum–rhodium crucible. Pulling rate was 1 mm/h, rotation rate 6 rpm. After growth the crystal was cooled to 300K with the speed of 8 K/h. The initial charge was prepared from a mixture of ZnO, WO<sub>3</sub>, Yb<sub>2</sub>O<sub>3</sub> and Li<sub>2</sub>CO<sub>3</sub> of high purity grade. Lithium ions were added to ensure the charge compensation. The solid-phase powder synthesis of the preliminarily carefully mixed charge was performed at 900°C for 12 h. The structure (monoclinic, sp. gr. C<sub>2h</sub> - P2/c) and the phase purity of the crystals were confirmed by X-ray diffraction. The crystals exhibited a cleavage along the (010) plane. Polarized Raman spectra were measured for the crystal. The most intense Raman band is at ~904 cm<sup>-1</sup>. ZnWO<sub>4</sub> is an optically biaxial crystal: only one of the optical indicatrix axes (X) coincides with the 2-fold axis (**b**) and the other two ones (Y and Z) are located in the **a-c** plane. The Yb<sup>3+</sup>,Li:ZnWO<sub>4</sub> crystals for the spectroscopic studies were oriented in the frame of the optical indicatrix. Absorption and luminescence spectra of Yb<sup>3+</sup> ions corresponding to the <sup>2</sup>F<sub>7/2</sub> ↔ <sup>2</sup>F<sub>5/2</sub> transition were measured for light polarizations **E** || X, Y, Z. The spectra are strongly polarized. The maximum stimulated-emission cross-section is 2.82×10<sup>-20</sup> cm<sup>2</sup> at 1055.5 nm for light polarization **E** || X and the emission bandwidth is ~12 nm. The lifetime of Yb<sup>3+</sup> ions is 367 μs; the luminescence decay is single-exponential. The Stark splitting is resolved using low-temperature (6 K) spectroscopy. The Yb<sup>3+</sup>:ZnWO<sub>4</sub> crystal is promising for CW and mode-locked lasers at ~1 μm.

**LS-PS-10****Domain kinetics and periodical poling in Rb:KTiOPO<sub>4</sub> and KTiOAsO<sub>4</sub> single crystals for laser light frequency conversion**

*M. Chuvakova*<sup>1</sup>, *A. Akhmatkhanov*<sup>1</sup>, *A. Esin*<sup>1</sup>, *I. Kipenko*<sup>1</sup>, *V. Shur*<sup>1</sup>, *A. Boyko*<sup>2</sup>, *D. Kolker*<sup>2</sup>

<sup>1</sup>*Ural Federal University, Institute of Natural Sciences and Mathematics, Ekaterinburg, Russian Federation*

<sup>2</sup>*Novosibirsk State University, Research Laboratory of Quantum Optics Technology, Novosibirsk, Russian Federation*

Potassium titanyl phosphate Rb:KTiOPO<sub>4</sub> (RKTP) and KTiOAsO<sub>4</sub> (KTA) single crystals with periodical ferroelectric domain structures are one of the promising materials for nonlinear optical applications [1]. Despite the crucial importance of the *in situ* visualization of domain structure kinetics for creation of high quality periodical domain gratings, there are only a few works concerning RKTP and KTA.

We present the results of *in situ* visualization of domain kinetics in RKTP and KTA with the time resolution down to 12.5 μs and simultaneous recording of the switching current data. The wide range of wall velocities with two orders of magnitude difference was observed for switching in a uniform electric field [2]. The kinetic maps allowed analyzing the spatial distribution of wall motion velocities and classifying the walls by velocity ranges. The distinguished slow, fast, and superfast types of domain walls differed by their orientation. It was shown that the fast and slow domain walls provided the smooth input to the switching current, whereas the short-lived superfast walls resulted in short current peaks. The mobility and the threshold fields for all types of domain walls were estimated [3]. The revealed increase in the wall velocity with deviation from low-index crystallographic planes for slow and fast walls was considered in terms of determined step generation and anisotropic kink motion. The domain kinetics and switching fields were compared in RKTP and KTA. It was shown that the more pronounced input of slow domain walls in KTA results in formation of narrow stripe domains important for periodical poling.

The periodical domain structure with period of 40 μm was created in RKTP single crystals for OPO generation at 2.4 μm using the 1.053 μm pulsed pump with 16 ns duration at 4 KHz. The single resonance double-pass optical scheme was used. The threshold power 850 mW and threshold energy 210 μJ were obtained.

The obtained knowledge is very important for further development of domain engineering in crystals of KTP family required for creation of high power, reliable, and effective coherent light sources.

**References**

- [1] V. Ya. Shur, E. V. Pelegova, A. R. Akhmatkhanov, and I. S. Baturin, "Periodically Poled Crystals of KTP Family: A Review," *Ferroelectrics* 496, 49–69 (2016).
- [2] V. Ya. Shur, E. M. Vaskina, E. V. Pelegova, M. A. Chuvakova, A. R. Akhmatkhanov, O. V. Kizko, M. Ivanov, and A. L. Kholkin, "Domain wall orientation and domain shape in KTiOPO<sub>4</sub> crystals," *Appl. Phys. Lett.* 109, 132901 (2016).
- [3] V. Ya. Shur, A. A. Esin, M. A. Alam, and A. R. Akhmatkhanov, "Superfast domain walls in KTP single crystals," *Appl. Phys. Lett.* 111, 152907 (2017).

**LS-PS-11****A kW-level small core diameter fiber pump system for Nd:YAG lasers**

*V. Mitrokhin<sup>1</sup>, A. Dormidonov<sup>1</sup>, A. Savvin<sup>1</sup>*

*<sup>1</sup>Dukhov Automatics Research Institute- Federal State Unitary Enterprise- VNIIA, R&P Center of Pulse Technique, Moscow, Russian Federation*

The end-pump for laser systems, especially in case of using fiber pump sources, opens up a lot of unique possibilities for physics, engineering and biomedical applications, where Nd:YAG lasers are the most widely used [1]. Foremost, end-pumping increases the lasing efficiency and improves the generation spatial quality. Secondly, there is not necessity to make an optical pump system around the active media and, as a result, very compact solutions can be designed for oscillators [2]. Another consequence of using end-pumping with fiber pump sources is the possibility of constructing distributed systems for using in applications like laser ignition [3], in this case a pumping system as the most expensive element of the laser is placed out from the area of interaction with combustible substances, which excludes its damage.

In this work, we demonstrate the high-intensity fiber light source for pumping Nd:YAG lasers. It is based on possibility of using Nd:YAG crystal absorption peak near 532 nm for pumping. Designed fiber pump laser source is formed with Nd:YAG laser operating in free-oscillation mode with intracavity frequency doubling and the fiber light transportation system with a small core diameter fiber. Our designed fiber system had output power after 10 meters fiber with core diameter 100  $\mu\text{m}$  over than 1 kW.

**References**

- [1] M. Lackner, “Lasers in Chemistry: Probing and Influencing Matter” Wiley-VCH, Weinheim, (2008).
- [2] H. Kofler, et. al. “Experimental development of a monolithic passively Q-switched diode-pumped Nd:YAG laser” Eur. Phys. J. D 58, 209 (2010).
- [3] P. Nicolaie, et. al. “Composite, all-ceramics, high-peak power Nd:YAG/Cr:YAG monolithic micro-laser with multiple-beam output for engine ignition” Optics Express. 19(10): 9378 (2011).

**LS-PS-12****Synchronously pumped crystalline Raman lasers with combined frequency shift**

*S. Smetanin<sup>1</sup>, M. Frank<sup>2</sup>, M. Jelínek<sup>2</sup>, D. Vyhlídal<sup>2</sup>, V. Shukshin<sup>1</sup>, L. Ivleva<sup>1</sup>, E. Dunaeva<sup>1</sup>, I. Voronina<sup>1</sup>, P. Zverev<sup>1</sup>, V. Kubeček<sup>2</sup>*

*<sup>1</sup>Prokhorov General Physics Institute of the Russian Academy of Sciences,  
Department of Laser Materials and Photonics, Moscow, Russian Federation*

*<sup>2</sup>Czech Technical University, Faculty of Nuclear Sciences and Physical Engineering, Prague 1,  
Czech Republic*

Comparative investigation of characteristics of spontaneous and stimulated Raman scattering (SRS) in different crystals with tetragonal scheelite- and zircon-type structure at both high and low frequency anionic group vibrations is presented. It has been found that among these crystals, the SrMoO<sub>4</sub>, SrWO<sub>4</sub>, and GdVO<sub>4</sub> crystals are the most perspective for SRS generation on both stretching and bending modes of internal anionic group vibrations with the strongest SRS pulse shortening under picosecond synchronous laser pumping because of not only highly intense stretching Raman mode for efficient primary extracavity long-shifted SRS conversion, but also the most broadened bending Raman mode for the strongest SRS pulse shortening down to the inverse linewidth of the broadened bending Raman mode ( $\sim 1$  ps) at secondary intracavity short-shifted SRS conversion. The strongest 42-fold pump pulse shortening down to 860 fs at the 1228-nm Stokes component with the combined ( $882\text{ cm}^{-1} + 382\text{ cm}^{-1}$ ) Raman shift in the extracavity GdVO<sub>4</sub> Raman laser with synchronous pumping by the 1063-nm, 36-ps, 150-MHz Nd:GdVO<sub>4</sub> laser has been demonstrated. Highly efficient operation of the synchronously pumped ultrafast Raman lasers based on BaWO<sub>4</sub> (conversion up to 69 %), SrWO<sub>4</sub> (conversion up to 45 %), and GdVO<sub>4</sub> (conversion up to 50 %) Raman-active crystals has been achieved.

**LS-PS-13****Stimulated Brillouin scattering phase conjugate mirror (SBS-PCM) using purified liquid medium for high average input***S. Cha<sup>1</sup>, H.J. Kong<sup>1</sup>**<sup>1</sup>KAIST, Department of Physics, Daejeon, Republic of Korea*

To achieve a laser inertial fusion energy, the laser fusion driver should operate at high repetition rate more than 10 Hz [1] and produce more than 100 kJ per one module [2]. One of the most promising techniques to make such laser system is coherent beam combining using stimulated Brillouin scattering phase conjugate mirror (SBS-PCM) [2]. The SBS-PCM has simple structure which consists of a cell and a feedback mirror, and it is good to compensate wavefront aberration by its phase conjugate property. Its feasibility was demonstrated in 2010 at the low power of 1 W [3], and the demonstration at the high power of 100 W class is on the progress.

One of the remaining issues to develop the SBS-PCM for the high energetic and high repetitive laser is the thermal issue in the SBS-PCM cell. At the high average input power of 100 W class with the high repetition rate over 1 kHz, the thermal load of the SBS liquid medium becomes a serious problem [4]. With high input power and a high repetition rate, the absorbed laser beam changes the refractive index of the SBS medium, defocuses the laser beam, and makes the convection or boiling in the liquid. This effect reduces the focal spot intensity of the input laser beam and degrades the SBS reflectivity in a liquid medium. If there are impurities in the SBS liquid media, this effect will become severe.

To resolve this issue, the authors chose HT-270 liquid as the SBS medium and are purifying the medium. The HT-270 liquid has the boiling temperature of 270°C and the high viscosity of 11.7 cSt, which is expected to make small convection. To test the medium, Kumgang laser system will be utilized [5]. The result will be shown in the conference.

**References**

- [1] W. J. Hogan, et al., Energy from Inertial Fusion (International Atomic Energy Agency, Vienna, 1995), Chap. 3.
- [2] H. J. Kong, S. Park, S. Cha, and M. Kalal, *Opt. Mater. (Amst)*. 35, 807–811 (2013).
- [3] J. S. Shin, S. Park, H. J. Kong, and J. W. Yoon, *Appl. Phys. Lett.* 96, 3–5 (2010).
- [4] M. Nakatsuka, H. Yoshida, Y. Fujimoto, K. Fujioka, and H. Fujita, *JKPS* 43, 607-615 (2003).
- [5] H. J. Kong, S. Park, S. Cha, H. Ahn, H. Lee, J. Oh, B. J. Lee, S. Choi, and J. S. Kim, *High Power Laser Sci. Eng.* 3, e1 (2015).

**LS-PS-14****Generation and properties of dissipative Kerr solitons in optical microresonators with backscattering**

*V. Lobanov<sup>1</sup>, N. Kondratiev<sup>1</sup>, D. Skryabin<sup>1,2</sup>*

*<sup>1</sup>Russian Quantum Center, Group of Coherent Microoptics and Radiophotonics, Skolkovo, Russian Federation*

*<sup>2</sup>University of Bath, Department of Physics, Bath, United Kingdom*

During the last decade generation of optical frequency combs in optical microresonators has been studied extensively and has been demonstrated in different settings [1,2]. Great attention has been paid to the coherent frequency combs associated with the dissipative Kerr solitons (DKS). Conventionally, narrow-linewidth laser sources have been used for microresonator pumping and frequency comb generation. Recently, it was shown that one may use laser diode, single-frequency or even multi-mode, for this purpose [3,4]. Such approach becomes feasible due to the effect of the self-injection locking of a laser diode to a high-Q microresonator [5,6]. Self-injection locking uses resonant Rayleigh scattering on internal and surface inhomogeneities when a fraction of incoming radiation in resonance with the frequency of selected microresonator mode reflects back to the laser providing fast optical feedback. It may result in a significant reduction of laser linewidth. Besides that, such narrow-linewidth laser source may be used as a pump for the generation of DKS that was demonstrated experimentally. However, to date there is no adequate theory describing nonlinear effects in optical microresonators in the self-injection locking regime. As a first step to uncover the physics of soliton generation in this regime it is necessary to describe the backward wave influence on it.

In our work, we derive a model from the first principles taking linear forward to backward wave coupling and nonlinear cross-action into account and got the system of two coupled LLE-like equations. Further it was shown that if microresonator finesse is large enough such equations may be simplified and rewritten in a coordinate system rotating with the angular frequency equal to microresonator FSR. Due to the opposite directions of rotation cross-action terms depend not on the local but on the averaged intensity. Using derived equations, we studied the process of soliton generation by means of conventional frequency scan approach. It was found that soliton generation is possible if linear coupling coefficient is less than some critical value. In that case one may observe the sequence of sech-shaped pulses in the forward and backward waves. If coupling coefficient exceeds this critical value the transition from a chaotic regime to cw state was observed. However, it was found that solitons may exist at high values of the coupling coefficient. It was revealed that soliton existence domain is defined by both coupling coefficient and pump detuning value. Higher values of coupling coefficient require higher values of detuning for soliton existence. Interestingly, since nonlinear cross-coupling is defined by the averaged intensity existence domains for states with different number of solitons are not the same. It was revealed that decreasing the detuning leads to the transition from multi-soliton to single-soliton regime.

This work was supported by Russian Science Foundation (Project 17-12-01413).

**References**

- [1] T.J. Kippenberg, et al., “Dissipative Kerr solitons in optical microresonators,” *Science*. 361(6402), eaan8083 (2018).

- [2] A.L. Gaeta, M. Lipson, T.J. Kippenberg, "Photonic-chip-based frequency combs," *Nat. Photon.* 13, 158–169 (2019).
- [3] N.G. Pavlov, et al., "Narrow-linewidth lasing and soliton Kerr microcombs with ordinary laser diodes," *Nat. Photon.* 12, 694–698 (2018).
- [4] A.S. Raja, et al., "Electrically pumped photonic integrated soliton microcomb," *Nat. Comm.* 10, 680 (2019).
- [5] N.M. Kondratiev, et al., "Self-injection locking of a laser diode to a high-Q WGM microresonator," *Opt. Express* 25, 28167-28178 (2017).
- [6] R.R. Galiev, et al., "Spectrum collapse, narrow linewidth, and Bogatov effect in diode lasers locked to high-Q optical microresonators," *Opt. Express* 26, 30509-30522 (2018).

**LD-PS-1****Using of laser irradiation for the diagnosis of polar state in dielectrics**

*O. Sergeeva<sup>1</sup>, A. Solnyshkin<sup>1</sup>, I. Pronin<sup>2</sup>, S. Sharofidinov<sup>3</sup>, S. Kukushkin<sup>4</sup>*

<sup>1</sup>*Tver State University, Department of Condensed Matter Physics, Tver, Russian Federation*

<sup>2</sup>*Ioffe Institute, Department of Dielectrics and Semiconductors, Saint-Petersburg, Russian Federation*

<sup>3</sup>*Ioffe Institute, Center of Nanoheterostructures, Saint-Petersburg, Russian Federation*

<sup>4</sup>*Institute of Problems of Mechanical Engineering RAS, Laboratory of Phase Transitions, Saint-Petersburg, Russian Federation*

Coherent monochromatic laser radiation has a small divergence of beam and constant power. Therefore, a laser is a convenient source of thermal radiation to characterize the polar state in pyroelectric materials. In this paper, the study results of the dynamic pyroelectric effect in thin films of linear pyroelectric of aluminum nitride (AlN) are presented. The AlN thin films epitaxially grown on silicon substrates oriented in the directions  $\langle 111 \rangle$ ,  $\langle 110 \rangle$  and  $\langle 100 \rangle$ . Buffer nanolayer of silicon carbide (SiC) is between the silicon substrate and the AlN film [1]. Pyroelectric properties were studied by the dynamic method of non-destructive testing of a polarized state using laser radiation modulated by rectangular shape pulses. The laser light belongs to the near-IR region ( $\lambda = 980$  nm). The bipolar shape of the electrical response, as well as its frequency dependence, may indicate a pyroelectric nature and, therefore, the existence of a polarized state (Fig. 1).

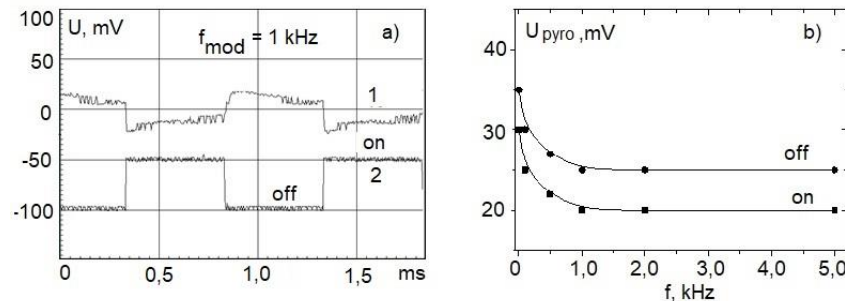


**Fig. 1.** The forms of the modulated heat flow (curve 2) and electrical response (curve 1) (a) and its frequency dependence (b) of AlN films epitaxial expressed on 111-oriented SiC / Si substrates.

The calculation showed that the values of pyroelectric coefficient  $p$  and figure of merit  $p/\epsilon$  ( $\epsilon$  is dielectric permittivity, for AlN  $\sim 9$ ) were the highest for the films grown on substrates oriented in the  $\langle 111 \rangle$ -direction (Table.1).

Table 1.

Films of aluminum nitride	$p$ , $10^{-9}$ C/cm <sup>2</sup> K	$p/\epsilon$ , $10^{-9}$ C/cm <sup>2</sup> K
AlN/SiC/Si(100)	0,9	0,01
AlN/SiC/Si(110)	0,9	0,01
AlN/SiC/Si(111)	2,0	0,22

AlN/SiC/Si(111) films with wide temperature range of the polar state existence and the high value of the figure of merit are promising structures for electronic devices based on the pyroelectric effect.

**References**

[1] Kukushkin S.A. and Osipov A.V. J Appl Phys. 113, 4909 (2013).

**LD-PS-2****Nonlinear optical diagnostics of perovskite thin films of lead zirconate titanate**

*I. Pronin<sup>1</sup>, A. Elshin<sup>2</sup>, E. Mishina<sup>2</sup>, O. Sergeeva<sup>3</sup>, E. Kaptelov<sup>1</sup>, S. Senkevich<sup>4</sup>, D. Kiselev<sup>5</sup>*

*<sup>1</sup>Ioffe Institute, Physics of Dielectrics and Semiconductors, Saint-Petersburg, Russian Federation*

*<sup>2</sup>MIREA - Russian Technological University, Department of Nanoelectronics, Moscow, Russian Federation*

*<sup>3</sup>Tver State University, Department of Condensed Matter Physics, Tver, Russian Federation*

*<sup>4</sup>Ioffe Institute, Department of Physics of Dielectrics and Semiconductors, Saint-Petersburg, Russian Federation*

*<sup>5</sup>National University of Science and Technology, Department of Materials Science, Semiconductors and Dielectrics, Moscow, Russian Federation*

Using nonlinear optical microscopy (femtosecond laser, Avesta-Project,  $\lambda = 800$  nm), atomic force microscopy (Nterga, NT MDT), and dynamic response to modulated laser irradiation (laser module CLM,  $\lambda = 800$  nm) we studied the microstructure, piezoelectric and pyroelectric responses of the perovskite thin films of  $\text{Pb}(\text{Zr},\text{Ti})\text{O}_3$  solid solutions deposited by radio-frequency magnetron sputtering at different distances ( $d = 30\text{-}70$  mm) from the target to the substrate.

Changing the distance allows ones to finely (within 2-3%) vary the composition of the solid solution (elemental ratio Zr/Ti) and optimize the electromechanical parameters of thin films [1].

It was found that the signal of the second optical harmonic (SHG) varies greatly: at large distances ( $d = 60\text{-}70$  mm), the average signal was significantly lower than at the others. In individual perovskite islands, an inhomogeneous distribution of the SHG signal was detected, including signal amplification at the perovskite/pyrochlore boundary, which may be associated with relaxation of mechanical stresses (picture 1). The paper discusses the relationship between the SHG signal, the microstructure, and the polar properties of thin films.

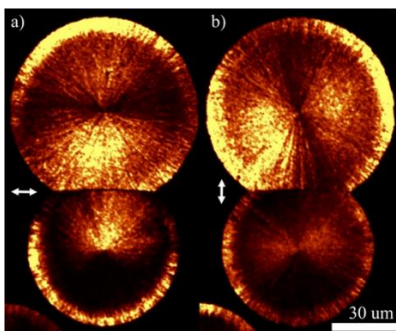


**Fig. 1.** Nonlinear optical images of two spherulitic perovskite islands for different directions of polarization of the laser radiation.

**References**

- [1] Pronin V.P., Dolgintsev D.M., Osipov V.V., Pronin I.P., Senkevich S.V. and Kaptelov E.Yu. IOP Conf. Series: Materials Science and Engineering, 387, 012063 (2018).

**LD-PS-3****Laser-induced modifications of optical properties in molybdenum disulfide covered by bismuth telluride**

*H. Rho<sup>1</sup>, T. Lee<sup>1</sup>, J.H. Ahn<sup>2</sup>*

*<sup>1</sup>Chonbuk National University, Department of Physics, Jeonju, Korea Republic of*

*<sup>2</sup>Korea Maritime and Ocean University, Department of Electronic Material Engineering, Busan, Korea Republic of*

Two-dimensional (2D) van der Waals heterostructures have attracted a great deal of attention due to their potential applications for novel 2D photonic and electronic nanodevices. Here, we report the effect of laser irradiation on the optical phonons and excitons in monolayer molybdenum disulfide (MoS<sub>2</sub>) covered by topological insulator bismuth telluride (Bi<sub>2</sub>Te<sub>3</sub>).

The Bi<sub>2</sub>Te<sub>3</sub>/MoS<sub>2</sub> heterostructure was grown using chemical vapor deposition. When the incident laser power was weak, scattered signals from the monolayer MoS<sub>2</sub> underneath the Bi<sub>2</sub>Te<sub>3</sub> film were not detected owing to the strong absorption of incident laser light by Bi<sub>2</sub>Te<sub>3</sub>. However, when the Bi<sub>2</sub>Te<sub>3</sub> film was exposed to a moderate excitation laser power, the optical phonons of the MoS<sub>2</sub> layer were detected at 384 and 405 cm<sup>-1</sup>, corresponding to the in-plane  $E_{2g}^1$  and the out-of-plane  $A_{1g}$  phonon modes, respectively. To investigate the effect of the laser irradiation on the Bi<sub>2</sub>Te<sub>3</sub>/MoS<sub>2</sub> heterostructure in detail, a sample surface was scanned using visible laser light with a moderate power. Interestingly, the color of the scanned region was changed, indicating that a structural change was occurred in the Bi<sub>2</sub>Te<sub>3</sub> film under laser irradiation. Excitation laser-power dependent Raman measurements showed that the  $A_{1g}$  phonon was varied in energy with increasing the laser power while the  $E_{2g}^1$  phonon did not show any variation in its energy, suggesting that a charge density in MoS<sub>2</sub> was changed. Furthermore, laser-power dependent photoluminescence measurements showed also a variation in the A exciton peak energy. The correlated photoluminescence and Raman scattering results suggested that charge transfer occurred in the vertically stacked Bi<sub>2</sub>Te<sub>3</sub>/MoS<sub>2</sub> heterostructure.

**Acknowledgment:** This research was supported by the Basic Science Research Program through the National Research Foundation of Korea (NRF) funded by the Ministry of Education (Grant No. 2016R1D1A1B03935270).

**LD-PS-4****Affect of phthalocyanine lutetium on the optical properties of silicon carbide nanoparticles**

*V. Krasovskii<sup>1</sup>, S. Rasmagin<sup>1</sup>, L. Apresyan<sup>1</sup>, T. Vlasova<sup>1</sup>, V. Pustovoy<sup>1</sup>*

<sup>1</sup>*Prokhorov General physics institute of RAS, Laser Physics, Moscow, Russian Federation*

Silicon carbide is widely used in electronic devices operating at high temperatures, in the high frequency range, or at high power [1]. In addition to a deep study of bulk monocrystalline silicon carbide, more and more research is being conducted into the properties of silicon carbide nanoparticles (nSiC), which may reveal new applications of silicon carbide (SiC). In this work, we studied the optical properties (namely, absorption spectra) of an nSiC solution surrounded by lutetium diphthalocyanine (LuPc<sub>2</sub>) molecules in order to determine the mutual influence on their properties and the possible use of the nSiC + LuPc<sub>2</sub> solution as components of the Gretzel cell. Control and mixed solutions of nSiC + LuPc<sub>2</sub> in tetrahydrofuran (THF) solvent were prepared: 1 - LuPc<sub>2</sub> + THF 2 ml, 2 - LuPc<sub>2</sub> + THF 1.5 ml + nSiC + THF 0.5 ml, 3 - LuPc<sub>2</sub> + THF 1 ml + nSiC + THF 1 ml, 4 - LuPc<sub>2</sub> + THF 0.5 ml + nSiC + THF 1.5 ml and 5 - nSiC + THF 2 ml. The size of nanoparticles of silicon carbide was about 20 nm. The absorption spectra of these solutions are obtained, see Fig.1. Analyzing Fig.1, the following peak were detected:  $\lambda_m = 656$  nm (Q-band) Lu LuPc<sub>2</sub>,  $\lambda_m = 340$  nm (B-band) LuPc<sub>2</sub> and  $\lambda_m = 366$  nm for nSiC [2]. For nanoparticles of silicon carbide, the band gap is 3.38 eV, which corresponds to the 2H-SiC polytype.

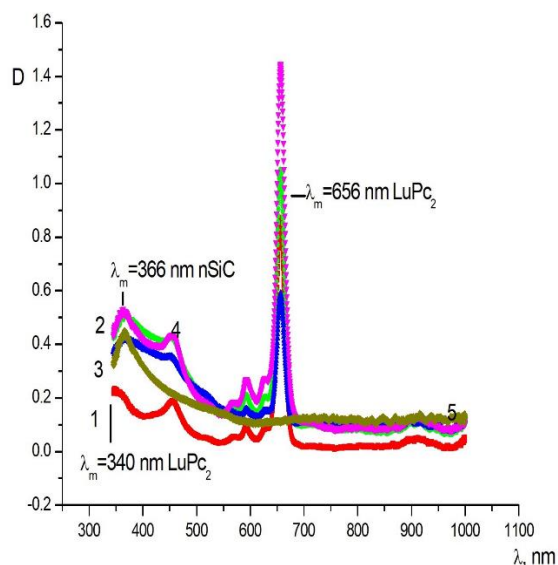


**Fig.1.** Absorption spectra of solutions 1 - LuPc<sub>2</sub> + THF 2 ml, 2 - LuPc<sub>2</sub> + THF 1.5 ml + nSiC + THF 0.5 ml, 3 - LuPc<sub>2</sub> + THF 1 ml + nSiC + THF 1 ml, 4 - LuPc<sub>2</sub> + THF 0.5 ml + nSiC + THF 1.5 ml and 5 - nSiC + THF 2 ml.

A study was made effect of the concentration diphthalocyanine lutetium molecules ( $\pi - \pi^*$  electronic transitions) on the absorption spectra of silicon carbide nanoparticles (electron – hole recombination). It was found that with an increase in the concentration diphthalocyanine lutetium, the amplitude of the absorption spectrum of nSiC increases, which can be explained by the additional absorption on LuPc<sub>2</sub> molecules due to the proximity of the absorption maxima. Thus, it is possible to choose such a metal phthalocyanine whose B-band falls into resonance with the band gap of silicon carbide nanoparticles and thereby increase the absorption by nSiC by an order of magnitude. The following results were obtained: in the resulting solutions, by changing the

concentration of diphthalocyanine lutetium, the absorption on silicon carbide nanoparticles was increased.

This work was supported by Russian Foundation of Basic Research Grant No 18-02-00786 and Program of RAS presidium I.7P.

## References

- [1] Abderrazak H., Hmida E.S. Silicon Carbide: Synthesis and Properties in Properties and Applications of Silicon Carbide, Edited by R. Gerhardt. InTech, Janeza Trdine, pp. 361–388 (2011).
- [2] Borisov A.V., Korel'Chuk M.V., Galanin N.E., Shaposhnikov G.P. Sandwich complexes of lutetium with tetraanthraquinoneporphyrine and asymmetric alkoxy-substituted phthalocyanines. Preparation and spectral properties, Russian Journal of General Chemistry, 84 (5) 953-959 (2014).

## LD-PS-5

### Optical properties of polymer semiconductor

*V. Krasovskii<sup>1</sup>, S. Rasmagin<sup>1</sup>*

<sup>1</sup>*Prokhorov General Physics Institute- Russian Academy of Sciences, Laser physics, Moscow, Russian Federation*

Currently, along with the use of inorganic semiconductors in microelectronics, organic semiconductors, such as the PEDOT – PSS copolymer, are being successfully developed and investigated [1]. In this work, we investigated the optical and electrophysical properties of a high-molecular-weight semiconductor polyvinyl chloride-polyacetylene (PVC-PAC) in order to create organic solar cells. PVC-PAC films prepared as a result of heat treatment of the initial PVC solution in acetophenone solvent at a temperature  $t = 195^{\circ}\text{C}$  and different heating times were prepared [2]. The film thickness was  $300\ \mu\text{m}$ . A study was conducted of the effect of the number of conjugated double bonds of carbon and the associated  $\pi\text{-}\pi^*$  electronic transitions on the photoluminescence spectra and the resistivity of PVC-PAC. cm) decreases, and the peak of the photoluminescence spectra (SF) of the films shift to the long wavelength region. It was found that with an increase in the number of conjugated double bonds of carbon (an increase in heat treatment time), the resistivity of films to the semiconducting state ( $10^3\text{--}10^4\ \Omega\times\text{cm}$ ) decreases, and the peak of the photoluminescence spectra of the films shift to the long wavelength region. The maximum SF peak shift was  $70\ \text{nm}$ . The length of the conjugation chain is determined by the number of conjugated double bonds of carbon. As the conjugation chain length increases  $(\text{-CH=CH-})_n$  in the range  $3.3\text{--}4.5\ \text{nm}$ , the photoluminescence emission quantum decreases from  $2.3$  to  $2\ \text{eV}$ , where  $n=5\text{--}7$ . Thus, it is possible to shift the peak of the photoluminescence spectrum by changing the length of the conjugation chain in the PVC-PAC polymer semiconductor.

This work was supported by Russian Foundation of Basic Research Grant No 18-02-00786 and Program of RAS presidium I.7P.

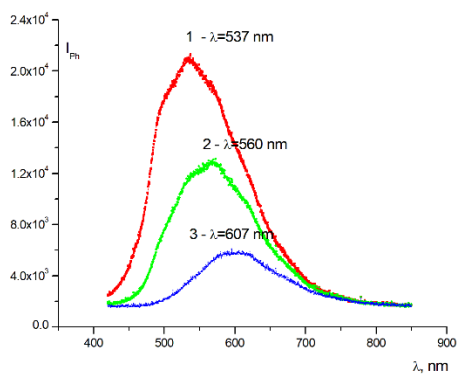


**Fig.1.** Photoluminescence spectra: 1 - PVC-PAC film heat treatment 60 min; 2 - PVC-PAC film heat treatment 180 min; 3 - PVC-PAC film heat treatment 240 min.

The following results were obtained: by changing the number of conjugated carbon double bonds (the length of the conjugation chain), one can regulate the peak of the photoluminescence spectrum in the range of  $537\text{--}607\ \text{nm}$  and the specific resistance in the range  $10^3\text{--}10^4\ \Omega\times\text{cm}$ . This work was supported by Russian Foundation of Basic Research Grant No 18-02-00786 and Program of RAS presidium I.7P.

## References

- [1] Nardes A. M., Kemerink M., Janssen R. A. J. Anisotropic hopping conduction in spin-coated PEDOT:PSS thin films, *Physical review B* 76, 085208 (2007).
- [2] Kryshchak V.I., Rasmagin S.I. Analysis of the properties of dehydrochlorinated polyvinyl chloride films, *The Russian Journal of Applied Physics*, 62 (11) 1689-1691 (2017).

**THz-PS-1****High-sensitive sensor based on a THz asymmetric split-loop resonator with an outer square loop***M.K. Yang<sup>1</sup>, Ch. Kang<sup>2</sup>, H.C. Ryu<sup>1</sup>**<sup>1</sup>Department of IT Convergence Engineering, Sahmyook University, Seoul, 139-742, Korea**<sup>2</sup>Integrated Optics Laboratory, Advanced Photonics Research Institute, Gwangju, 61005, Korea*

Terahertz (THz) technology has received considerable interest because of its potential in a wide variety of applications such as wireless communication, spectroscopy, imaging, and sensing [1, 2]. However, the development of THz devices is very deficient because the electromagnetic properties of most natural materials are not suitable to be used in the THz frequency range. To overcome the limitations of natural materials in the THz band, research on the utilization of metamaterials, which can artificially control electrical and magnetic properties, as devices in the THz band has attracted much attention [3]. We propose a high-sensitive sensor based on an asymmetric split-loop resonator (ASLR) with an outer square loop operating in the terahertz frequency range [4]. Structural asymmetry of the ASLR makes the asymmetric Fano resonance which has a high quality factor compared to the symmetric resonance. The variations of the resonant frequency, transmission coefficient, and quality factor of the ASLR in the Fano resonance were analyzed according to the variation of the structural asymmetry of it. And the surface current density on the ASLR was calculated to analyze the main cause of the variation of transmission characteristics of it. The surface current of ASLR in the Fano resonance showed trapped or quadrupole mode which has a low radiation loss. Therefore, the ASLR operating in the Fano resonance has a high quality factor. The ASLR having a high quality factor can be applied to a high sensitive sensor system because of the high field concentration in the gaps of ASLR metamaterial. The sensitivity of the ASLR was optimized by control of the asymmetry of the ASLR. The performance of the proposed sensor based on the metamaterial was confirmed by characterizing the bovine serum albumin (BSA) having various concentration and thickness using terahertz time-domain spectroscopy. The resonant frequency of the metamaterial was high-sensitively shifted by the variation of the BSA concentration and the thickness of the thin films. The outer square loop attached to the ASLR successfully improved the sensing capability of the ASLR. The proposed high-sensitive sensors based on the terahertz ASLR metamaterial could be used for the detection of biological and chemical sensing

**References**

- [1] P. U. Jepsen, D. G. Cooke, M. Koch, "Terahertz spectroscopy and imaging: Modern techniques and applications," *Laser. Photon. Rev.* 5, 124–166 (2011).
- [2] M. Tonouchi, "Cutting-edge terahertz technology," *Nat. Photonics* 1, 97–105 (2007).
- [3] M. Choi, S. H. Lee, Y. Kim, S. B. Kang, J. Shin, M. H. Kwak, K. Y. Kang, Y. H. Lee, N. Park, B. Min, "A terahertz metamaterial with unnaturally high refractive index," *Nature* 470, 369–373 (2011).
- [4] D. J. Park, J. H. Shin, K. H. Park, and H. C. Ryu, "Electrically controllable THz asymmetric split-loop resonator with an outer square loop based on VO<sub>2</sub>," *Optics Express* 26, 17397 (2018).

**THz-PS-2****Determination of changes in the ratio of water / fat in adipose tissue when heated using terahertz technology**

*I. Yanina*<sup>1,2</sup>, *V. Nikolaev*<sup>2,3</sup>, *O. Zakharova*<sup>2,3</sup>, *A. Borisov*<sup>2,4</sup>, *V. Kochubey*<sup>1,2</sup>, *Y. Kistenev*<sup>2,4</sup>,  
*V. Tuchin*<sup>1,2,5</sup>

<sup>1</sup>*Saratov State University National Research University, Research-Educational Institute of Optics and Biophotonics, Saratov, Russian Federation*

<sup>2</sup>*Tomsk State University National Research University, Interdisciplinary Laboratory of Biophotonics, Tomsk, Russian Federation*

<sup>3</sup>*Institute of Strength Physics and Materials Science of SB RAS, Laboratory of Molecular Imaging and Photoacoustics, Tomsk, Russian Federation*

<sup>4</sup>*Siberian State Medical University, Department of Physics and Mathematics, Tomsk, Russian Federation*

<sup>5</sup>*Institute of Precision Mechanics and Control RAS, Laboratory of Laser Diagnostics of Technical and Living Systems, Saratov, Russian Federation*

Terahertz (THz) spectroscopy allows one to determine the complex refractive index of the medium under study, which is important for creating a functional THz -tomograph with high sensitivity to changes in the concentration of metabolites and accurate marking of the boundaries of the pathological process. Therefore, the development of spectroscopic methods for studying biological tissues in the THz -frequency range, providing detection and visualization of metabolic and pathological processes, has caused great interest in recent years, especially as an additional channel for obtaining information in multimodal systems in combination with optical methods [1,2]. The contrast between healthy and diseased tissue in the THz region is due to both the change in water content [3-5] and the difference in the properties of adipose and muscle tissue and their structure [6-8]. The difficulty of interpreting measurements and the transition from these measurements to in vivo diagnostics is caused by various reasons, for example, diffusion into a sample of saline during storage, changes in the level of hydration during the measurement, effects of scattering [9]. The purpose of this study was to study the effect of temperature change on the water / lipid ratio in adipose tissue in the terahertz range.

We used pig abdominal adipose tissue. The number of samples is 10. The thickness of the samples should be about 1 mm. Sample sizes were 1 cm<sup>2</sup>. The study of fat cells was carried out in vitro.

The temperature varied from 25°C to 70°C. A thermistor was used to samples heating. The sample is clamped between two sheets of fluoroplastic, 2 × 1.5 cm in size. The thermistor was placed on the instrument stage. Measurements were performed using a real-time terahertz spectrometer (EKSPLA, Lithuania). The application "THzSpectrometer 2D" was used.

It was found the changes in the ratio of water / fat in adipose tissue when heated using terahertz technology.

The authors would like to acknowledge the support from RFBR grant No. 18-52-16025 (IYuY, VVN, VIK and VVT), the National Research Tomsk State University Academic D.I. Mendeleev Fund Program (IYuY, VVN, VIK, VVT and YuVK), Fundamental Research Program of the State Academies of Sciences for 2013-2020, line of research III.23.a (VVN).

## References

- [1] S. J. Oh, J. Kang, I. Maeng, J.-S. Suh, Y.-M. Huh, S. Haam, J.-H. Son, Nanoparticle-enabled terahertz imaging for cancer diagnosis, *Opt. Express*, vol. 17, is. 5, pp. 3469–3475 (2009).
- [2] C. S. Joseph, R. Patel, V. A. Neel, R. H. Giles, A. N. Yaroslavsky, Imaging of ex vivo nonmelanoma skin cancers in the optical and terahertz spectral regions, *J. Biophoton.*, pp. 1–10 (2012).
- [3] S. Fan, Y. He, B. S. Ung, E. Pickwell-MacPherson, The growth of biomedical terahertz research, *J. Phys. D.*, vol. 47, no. 37, Article ID 374009 (2014).
- [4] P. C. Ashworth, E. Pickwell-MacPherson, E. Provenzano, S. E. Pinder, A. D. Purushotham, M. Pepper, V. P. Wallace, Terahertz pulsed spectroscopy of freshly excised human breast cancer, *Opt. Express*, vol. 17, is. 15, pp. 12444-12454 (2009).
- [5] J. H. Son, Terahertz electromagnetic interactions with biological matter and their applications, *J. Appl. Phys.*, vol. 105, is. 10, Article ID 102033 (2009).
- [6] Y. He, B. S. Ung, E. P. Parrott, A. T. Ahuja, E. Pickwell-MacPherson, Freeze-thaw hysteresis effects in terahertz imaging of biomedical tissues, *Biomed. Opt. Express*, vol. 7, is. 11, pp. 4711-4717 (2016).
- [7] S. Sy, S. Huang, Y. X. Wang, J. Yu, A. T. Ahuja, Y. T. Zhang, E. Pickwell-Macpherson, Terahertz spectroscopy of liver cirrhosis: investigating the origin of contrast, *Phys. Med. Biol.*, vol. 55, no. 24, pp. 7587-7596 (2010).
- [8] F. Wahaia, G. Valusis, L. M. Bernardo, A. Almeida, J. A. Moreira, P. C. Lopes, J. MacUtkevic, I. Kasalynas, D. Seliuta, R. Adomavicius, R. Henrique, M. H. Lopes, Detection of colon cancer by terahertz techniques, *J. Mol. Struct.*, vol. 1006, is. 1-3, pp. 77-82 (2011).
- [9] Y. Sun, M. Y. Sy, Y.-X. Wang J., A. T. Ahuja, Y.-T. Zhang, E. Pickwell-MacPherson, A promising diagnostic method: Terahertz pulsed imaging and spectroscopy, *World J. Radiol.*, vol. 3, is. 3, pp. 55-65 (2011).

**THz-PS-3****Generation of tunable THz radiation at the difference frequency in a single crystal ZnGeP<sub>2</sub> when pumped by two-frequency radiation at wavelengths ~ 2.12 μm***A.Sirotkin<sup>1</sup>**<sup>1</sup>GPI Institute of General Physics RAS, OK, Moscow, Russian Federation*

THz-radiation in ZnGeP<sub>2</sub> single crystal with pumping by double frequency radiation of optical parametric oscillator in wavelength range ~ 2.12 μm based on KTP crystal with sizes 7'5'10 mm, cut by angle  $\theta \sim 51.5^\circ$  relatively Z-axis in XY-plane was experimentally obtained. Intracavity pumping of OPO was carrying out by electro optical (EO) shutter. Maximum average power of THz radiation, achieved in the experiment, consisted ~ 3.3 nW ( $l= 181 \mu\text{m}$ ) (with pulse frequency repetition 800 Hz, pulse duration 10 ns, pulse energy 1 mJ). THz radiation tuning in ~ 120-270 μm wavelength range was realized. Whereby, tuning range was limited just by ZnGeP<sub>2</sub> single crystal aperture.

**B-PS-1****Determination of stress-related characteristics of blood vessel walls using endoscopic optical coherence elastography**

*A. Potlov<sup>1</sup>, S. Frolov<sup>1</sup>, T. Frolova<sup>1</sup>, S. Proskurin<sup>1</sup>*

*<sup>1</sup>Tambov State Technical University, Biomedical Engineering, Tambov, Russian Federation*

An original approach to assess the stress-related properties of large blood vessel walls is described. Structural images of the investigated part of the blood vessel wall are sequentially obtained using endoscopic optical coherence tomography (EOCT) before the deforming impact and during the process of the deforming impact. Pulse wave is used as the deforming force. The surface area of the deforming force is considered to be equal to the scanning area of an EOCT system. Structural images specific test points are determined corresponding to the moments of systole and diastole. The above points are grouped in pairs. For each pair the vector value of the relative displacement is calculated. Then, the displacement values are independently resolved into components. The longitudinal displacements for each pair of the test points are considered to be equal to the projections of the vectors on the Y-axis. Sizes of the deformable region are calculated by combining the longitudinal displacements for all pairs of the test pixels. The transverse displacements and transverse dimensions for the X-axis are to be found the same way. Further, the values of Young's modulus and Poisson's ratio are calculated using the classical formulas.

The presented approach can be used in analyzing atherosclerotic plaque *in vivo*, determining the likelihood of correct deployment of the flow-diverter, assessing the accuracy of the flow-diverter deployment *post factum*, predicting the duration of the positive effect of stenting of the cerebral artery with aneurysm *post factum* and the feasibility of further surgical procedures.

This work was supported by the Russian Science Foundation (RSF project 16-15-10327).

**B-PS-2****Numerical simulation of optical coherence tomography interference signal occurring in the intravascular space**

*A. Potlov<sup>1</sup>, S. Frolov<sup>1</sup>, S. Proskurin<sup>1</sup>*

*<sup>1</sup>Tambov State Technical University, Biomedical Engineering, Tambov, Russian Federation*

An original approach to numerical simulation of the biological fluids flow through the scanning plane of an optical coherence tomography (OCT) system is described. The proposed approach includes the generation of a geometric layout of the biological object under study; Monte Carlo simulation of the photon migration process in a geometric layout; variation of the characteristics of the section of the geometric layout corresponding to the intravascular space; the interference signals (A-scans) simulation. A sketch of structure was used as a source of information about the geometry of the investigated biological object. This sketch was subjected to posterization, manual identification of structures, their encoding and assigning to tabular optical properties. Numerical simulation of the photon migration and A-scans were realized using classical Monte-Carlo technique. Optical properties of a part of a geometric layout corresponding to the lumen of a blood vessel constantly vary in such a way as to simulate fluctuations of erythrocytes or their aggregation in blood plasma. Moreover, the speed of these fluctuations in different parts of the vascular bed is chosen in such a way as to correspond to the desired shape of the flow velocity profile. If the flow is laminar (parabolic profile), then the rate of fluctuations decreases from the center of the vessel to the walls. In case of turbulent flow, the local velocities of fluctuations form cork-shaped profiles of various geometries.

The proposed approach can be used for developing highly effective algorithms of estimating the relative and absolute blood flow velocity using Doppler OCT systems.

This work was supported by the Russian Foundation for Basic Research (RFBR project 18-01-00786 A).

**B-PS-3****Resting-state functional connectivity revealed by optical neural and hemodynamic signals***J. Lu<sup>1</sup>, B. Li<sup>1</sup>, P. Li<sup>1</sup>**<sup>1</sup>Huazhong University of Science and Technology,  
Wuhan National Laboratory for Optoelectronics, Wuhan, China*

Coherent low-frequency (<0.1 Hz) hemodynamic fluctuations have been shown to reflect resting-state functional connectivity (RSFC) [1], and the patterns of the RSFC closely resemble the signals observed during functional tasks [2-3]. The RSFC integrity appears to be essential for the maintenance of normal brain functions [4] and changes in RSFC are often associated with neuropsychiatric disorders, such as Alzheimer's disease and depression. The RSFC obtained by spontaneous hemodynamic signals is used to indirectly characterize the neural functional connectivity based on neurovascular mechanisms. However, the neurovascular uncoupling may occur under some pathological conditions [5] and whether the RSFC evaluated by spontaneous hemodynamic fluctuations is still a reliable indicator of neural functional connectivity needs to be investigated. The objective of the present study was to compare the hemodynamic RSFC with the neural RSFC under the condition of neurovascular uncoupling produced by cortical spreading depression (CSD) in mice. The hemodynamic RSFC was obtained by using optical intrinsic signal imaging and the neural RSFC was accessed by using voltage-sensitive dye imaging. Seven recordings of resting-state VSD imaging were performed for each mouse (n = 8). One recording was performed before CSD, and others were performed 10 min after CSD to eliminate the interference from the propagation dynamics of CSD. Each recording (t0-t6) lasted for 180 s to ensure the emergence of stable functional networks, and the time interval between the recordings was 10 min. In addition, among five of these mice, functional activations were studied by the electrical stimulation of the hindlimbs. Another four mice (n = 4) were taken as the VSD control group to explore the effects of bleaching on the VSD signals. The experimental operations were the same as the resting-state VSD imaging, but no CSD was elicited. The results showed that during the periods of neurovascular uncoupling after CSD, although reduced correlations between the bilateral cortexes and the increased correlations within the unilateral cortex were found both in the neural and the hemodynamic RSFC, the neural RSFC was altered to a lesser extent and recovered much faster. This study helps to understand the effects of neurovascular uncoupling on the neural and the hemodynamic RSFC and may provide a reference for analyzing the hemodynamic RSFC of diseases associated with neurovascular uncoupling.

**References**

- [1]. Biswal, B., Yetkin, F.Z., Haughton, V.M., Hyde, J.S., 1995. Functional connectivity in the motor cortex of resting human brain using echo-planar MRI. *Magn Reson Med* 34, 537-541.
- [2]. Fox, M.D., Raichle, M.E., 2007. Spontaneous fluctuations in brain activity observed with functional magnetic resonance imaging. *Nat Rev Neurosci* 8, 700-711.
- [3]. Vincent, J.L., Patel, G.H., Fox, M.D., Snyder, A.Z., Baker, J.T., Van Essen, D.C., Zempel, J.M., Snyder, L.H., Corbetta, M., Raichle, M.E., 2007. Intrinsic functional architecture in the anaesthetized monkey brain. *Nature* 447, 83-86.
- [4]. Pizoli, C.E., Shah, M.N., Snyder, A.Z., Shimony, J.S., Limbrick, D.D., Raichle, M.E., Schlaggar, B.L., Smyth, M.D., 2011. Resting-state activity in development and maintenance of normal brain function. *Proc Natl Acad Sci U S A* 108, 11638-11643.

- [5]. Piilgaard, H., Lauritzen, M., 2009. Persistent increase in oxygen consumption and impaired neurovascular coupling after spreading depression in rat neocortex. *J Cereb Blood Flow Metab* 29, 1517-1527.

**B-PS-4****Optical clearing of human gingival mucosa: in vitro studies**

A.A. Selifonov<sup>1,2</sup>, V.V. Tuchin<sup>1,3,4,5</sup>

<sup>1</sup>Saratov State University, Chair of Optics and Biophotonics, Saratov, Russian Federation

<sup>2</sup>Saratov State Medical University, Department of Dentistry, Saratov, Russian Federation

<sup>3</sup>ITMO University, Chair of Optics and Biophotonics, St. Petersburg, Russian Federation

<sup>4</sup>Institute of Precision Mechanics and Control of the Russian Academy of Sciences,  
Chair of Optics and Biophotonics, Saratov, Russian Federation

<sup>5</sup>Tomsk State University, Chair of Optics and Biophotonics, Tomsk, Russian Federation

Due to the significant development of various optical technologies and methods used both for non-invasive diagnostics of biological tissues and for optimized protocols of photodynamic therapy, photothermal destruction, optical biopsy, tomography, and etc., the problem of increasing the depth of light penetration in biological tissue is relevant. An opportunity to change optical parameters of the top layers of tissues reversibly (reduction of the scattering properties), in particular in stomatology, can expand methods of diagnostics and therapy [1]. Very often hyperosmotic agents, such as glucose, sorbitol, glycerol, polyethylene glycol, propylene glycol, dimethyl sulphoxide, and isosmotic solutions, such as X-ray contrast substance iohexol, etc. are used as optical clearing agents (OCAs) [2,3]. In this work, the effective diffusion coefficient of 40%-glucose-aqueous solutions in human gum mucous tissue was determined *in vitro*. The method is based on the registration of the kinetics of changes in the spectra of diffuse reflection and the application of the free diffusion model. The effectiveness of the optical clearing of the human gum mucous tissue in the stage of completion of the process of diffusion of 40%-glucose-aqueous solutions was also determined. Due to the use of hyperosmotic agents (for example, glucose), under conditions of applicability of the method of optical clearing (OC), it is possible to increase the penetration depth of laser radiation into biological tissue, which is important for the diagnosis and therapy of oral diseases in the early stages.

The work was supported by grant of the Russian Federation Governmental grant 17-00-00272 (17-00-00275 (K)).

**References**

- [1] D. K. Tuchina, P. A. Timoshina, V. V. Tuchin, A. N. Bashkatov, and E. A. Genina. IEEE J. Select. Tops Quant. Electron. 2019. 25 (1), 7200508.
- [2] Carneiro I., Carvalho S., Henrique R., Oliveira L. M., Tuchin V. V. A robust ex vivo method to evaluate the diffusion properties of agents in biological tissues, J. Biophotonics. 2019, 12:e201800333.

**B-PS-5****Photothermal effect of gold nanoparticles in various modifications and infrared (808 nm) laser radiation on *S. aureus****E. Tuchina*<sup>1</sup>, *V. Tuchin*<sup>2</sup><sup>1</sup>*Saratov State University, Biological, Saratov, Russian Federation*<sup>2</sup>*Saratov State University, Physics, Saratov, Russian Federation*

Gold nanoparticles (GNPs), due to the high variety of possible forms, tunable physical properties, including the absorption wavelength in the plasmon resonance region, are of great interest to researchers and practitioners in solving problems of microbiology and ecology. GNPs can act not only as independent active agents, but also as intermediaries for targeted delivery of drugs and active molecules, as well as to combine these two properties [1-4]. A large number of studies are devoted to the photothermal effects of gold nanoparticles in combination with laser radiation on microorganisms. The result depends on the shape and optical properties of the nanoparticles, their functionalization and the parameters of the selected radiation [1-7].

In our previous studies, it was shown that GNP in combination with red (625 nm) or infrared (IR, 805 nm) radiation leads to a reduction in the number of such microorganisms as *S. epidermidis* and *S. aureus* by 80% [8]. At the same time, there was a slight increase in the total temperature of the solutions (by 3-4°C). In another work devoted to the study of the functionalized by immunoglobulins of gold nanostretch in combination with laser (808 nm) radiation for staphylococci, the temperature of the medium was 12-15°C, and the death of bacterial populations reached 97% [9].

In this study the effect of infrared laser radiation (808 nm) of different fluence rates on the bacteria *Staphylococcus aureus* 209 P, incubated in solutions of gold nanocubes, nanorods and on glass substrates with fixed nanodiscs, was studied. Radiation with a power density of 60 mW/cm<sup>2</sup> in combination with nanocubes caused the death of 50% of the bacterial population after 30 min of exposure, in combination with nanostructures - 56%. An increase in the temperature of suspended matter after irradiation was found of no more than 5-6°C. Radiation with a power density of 400 mW/cm<sup>2</sup> caused a pronounced inhibition of the viability of bacterial cells – by 81% after 30 min. Incubation of microorganism suspensions on the surface of glass substrate containing gold nanodiscs during irradiation (808 nm, 400 mW/cm<sup>2</sup>) resulted in 99% of bacterial cell death.

**References**

- [1] Huang Y.Y., Sharma S.K., Carroll J., Hamblin M.R, Biphasic Dose Response Low Level Light Therapy – An Update // Response. – 2011. Vol. 9. – P. 602–618.
- [2] Yin R., Agrawa T., Khan U., Gupta G.K., Rai V., Huang Y.-Y., Hamblin M.R. Antimicrobial photodynamic inactivation in nanomedicine: small light strides against bad bugs, // Nanomedicine (Lond). – 2015. Vol. 10(15). – P. 2379-2404.
- [3] Hamblin M.R. Antimicrobial photodynamic inactivation: a bright new technique to kill resistant microbes // Current Opinion in Microbiology. – 2016. – Vol. 33– P. 67-73.
- [4] Karimi M., Zangabad P. S., Ghasemi A., Amiri M., Bahrami M., Malekzad H., Asl H.G., Mahdiah Z., Bozorgomid M., Ghasemi A., Reza M., Boyuk R.T., Hamblin M.R. Temperature-Responsive Smart Nanocarriers for Delivery of Therapeutic Agents: Applications and Recent Advances // ACS Appl. Mater. Interfaces. – 2016. – Vol. 8. – P. 21107-21133.

- [5] Wainwright M., Maish T., Nonell S., Plaetzer K., Almeida A., Tegos G., Hamblin M. R. Photoantimicrobials-are we afraid of the light? // *The Lancet Infectious Disease*. – 2017. – Vol. 17(2). – P. 49-55.
- [6] Hamblin M.R. Mechanisms and applications of the anti-inflammatory effects of photobiomodulation // *AIMS Biophys.* – 2017. – Vol. 4. – P. 337-361.
- [7] Tsai S.R., Hamblin M.R. Biological effects and medical applications of infrared radiation // *J. Photochem. Photobiol. B.* – 2017. – Vol. 170. – P. 197–207.
- [8] Tuchina E.S., Ratto F., Khlebtsov B.N., Centi S., Matteini P., Rossi F., Fusi F., Khlebtsov N.G., Pini R., Tuchin V.V. Combined near infrared photothermolysis and photodynamic therapy by association of gold nanoparticles and an organic dye // *Proc. of SPIE: Plasmonics in Biology and Medicine VIII.* – 2011. Vol. 7911. – P. 79111C-1-7.
- [9] Tuchina E.S., Petrov P.O., Ratto F., Centi S., Pini R., Tuchin V.V. The action of NIR (808nm) laser radiation and gold nanorods labeled with IgA and IgG human antibodies on methicillin-resistant and methicillin sensitive strains of *Staphylococcus aureus*// *Proc. SPIE 9324: Biophotonics and Immune Responses X.* – 2015. – Vol. 93240X. – P. 1-10.

**B-PS-6****comparative study of multivariate analysis methods of blood raman spectra classification was performed**

*L. Bratchenko<sup>1</sup>, I. Bratchenko<sup>1</sup>, A. Lykina<sup>1</sup>, M. Komarova<sup>1</sup>, D. Artemyev<sup>1</sup>, O. Myakinin<sup>1</sup>, A. Moryatov<sup>2</sup>, I. Davydkin<sup>3</sup>, S. Kozlov<sup>2</sup>, V. Zakharov<sup>1</sup>*

*<sup>1</sup>Samara University, Department of Laser and Biotechnical Systems, Samara, Russian Federation*

*<sup>2</sup>Samara State Medical University, Department of Oncology, Samara, Russian Federation*

*<sup>3</sup>Samara State Medical University, Department and Clinic of Hospital Therapy, Samara, Russian Federation*

Pathosis of the human body leads to changes in body fluids biochemical composition. Currently used biochemical analysis of body fluids are notable for low-informative value to identify certain localization of pathologies. An alternative to biochemical methods is analysis by optical methods. Raman spectroscopy allows for the evaluation of blood characteristics at the molecular level. Raman blood spectra are characterized by multicollinearity feature and presence of autofluorescent background and noises of different nature. Selection of methods for experimental data processing of blood spectra is crucial for obtaining statistically reliable information about a pathological process in the body. Therefore, in this paper we examine various approaches to multidimensional analysis of blood samples of various size and perform statistical processing of experimental data from Raman scattering of blood by Factor analysis, Logistic regression, Discriminant analysis, Classification tree, Projection to latent structures discriminant analysis (PLS-DA) and Soft independent modelling of class analogies (SIMCA) to discriminate blood samples according to the pathology type. The analysis of the discussed multivariate methods for processing blood spectra obtained by cost-effective Raman setup in a clinical setting demonstrates that 1) the PLS-DA method (sensitivity 0.75, specificity 0.81) turned out to be the most optimal approach to blood samples classification by cancer localization; 2) the most optimal approach for blood samples classification by the presence of hyperproteinemia is the logistic regression method (sensitivity 0.89, specificity 0.99). In general, the selected multivariate methods may be a reliable tool for analyzing the body fluids spectral characteristics.

**B-PS-7****Laser additive formation of hybrid tissue-engineering matrices for the reconstruction of complex skeletal tissues**

N. Minaev<sup>1</sup>

<sup>1</sup>*Federal Scientific Research Centre “Crystallography and Photonics” of Russian Academy of Sciences, Institute of Photon Technologies, Moscow-Troitsk, Russian Federation*

Technologies for laser formation of tissue-engineered structures are the current method of modern regenerative medicine. The report presents the results of the development of an approach to laser additive formation of tissue equivalents for the task of restoring degenerative-dystrophic diseases of cartilage articulated with bone tissue. In the developed approach, it is proposed for the first time to use a combination of different laser prototyping technologies: the method of surface-selective laser sintering of polymer powder to form a porous scaffold simulating a three-dimensional structure of bone tissue, and a Laser Induced Forward Transfer method (LIFT) for cartilage cells and chondrospheres for the formation of conjugate cartilage equivalent. The use of distilled water as a sensitizer in combination with infrared laser radiation from a thulium laser (1.94  $\mu\text{m}$ ) distinguishes the method developed by us. The process does not use potentially dangerous toxic fillers (carbon, nanoparticles) and allows the use of modified polymer particles saturated with biologically active substances sensitive to high temperatures. The laser-induced transfer method allows precise positioning of cells encapsulated in a hydrogel or multicellular spheroids in a three-dimensional space to form high-density cell layers with a high regenerative potential. The practical results of the development of scaffolds by the method of surface-selective laser sintering and the results of their functionalization with cellular material using LIFT technology, as well as original laser three-dimensional printing systems of their own design are presented.

This work was supported by the Ministry of Science and Higher Education within the State assignment FSRC «Crystallography and Photonics» RAS and Russian Science Foundation (Project No. 18-32-20184)

**B-PS-8****Probe-based confocal laser endomicroscopy for cellular imaging**

*Q. Liu*<sup>1,2,3</sup>, *L. Fu*<sup>1,2,3</sup>

<sup>1</sup>*Huazhong University of Science and Technology, WNLO, Wuhan, China*

<sup>2</sup>*Britton Chance Center for Biomedical Photonics, Wuhan National Laboratory for Optoelectronics-Huazhong University of Science and Technology, Wuhan, Hubei 430074, China*

<sup>3</sup>*MoE Key Laboratory for Biomedical Photonics, School of Engineering Sciences, Huazhong University of Science and Technology, Wuhan, Hubei 430074, China*

Probe-based confocal laser endomicroscopy (pCLE) is an endoscopic modality that obtains very high magnification and resolution images of the mucosal layer of the gastrointestinal tract, which presenting cell morphology with a highly consistent with biopsy pathology. pCLE will be helpful for ‘*in vivo* biopsy’ and for early diagnosis of gastrointestinal diseases.

We developed a visible pCLE that a 488 nm laser source was used for tissue illumination, with detection of the tissue fluorescence through a pinhole aperture subsequently. The visible light imaging probe with outer diameter of 2.6 mm is composed of a fiber bundle and a high-NA miniature objective, enabling real-time imaging of colon mucosa of C57BL/6 mice with lateral resolution of 1.4  $\mu\text{m}$  and field of view of 300  $\mu\text{m} \times 300 \mu\text{m}$  at the depth of 150  $\mu\text{m}$  below the surface. However, it is difficult to observe the structures under lamina propria using visible pCLE, because of the intense scattering of visible light.

Aiming to achieve deep-tissue imaging at cellular resolution, we developed a near-infrared pCLE with a 2.6 mm diameter optical fiber probe. It can achieve real-time deep imaging with a higher contrast, lateral resolution of 1.55  $\mu\text{m}$  and field of view of 330  $\mu\text{m} \times 330 \mu\text{m}$  at the depth of 300  $\mu\text{m}$ . The ability of deep tissue imaging for the near-infrared pCLE has been demonstrated by mouse esophageal imaging at different depths. The deep imaging of ulcerative colitis shows the capability of this system for disease diagnosis in deep-layer tissues.

In summary, we will present two prototypes of pCLE with different laser sources, which can be compatible with biopsy channel of conventional endoscopy with the ability of the detection of gastrointestinal diseases.

**B-PS-9****Space-selective tailoring of porous glass matrix density via femtosecond laser pulses**

*Z. Lijing<sup>1</sup>, R. Zakoldaev<sup>1</sup>, S. Maksim<sup>1</sup>, V. Veiko<sup>1</sup>*

*<sup>1</sup>ITMO University, Department of Laser Systems and Technologies, Sanct-Petersburg, Russian Federation*

In the past decade, high silica porous glass (PG) has been successfully demonstrated as a functional platform for fabrication of fluidics devices, sensors, and for host of active centers such as Bi, Er, etc. [1,2]. In particular, gas analysis based on a PG has recommended the following ratio: one glass plate applies for one type of detected gas [3], i.e. one functional platform occupies the whole PG plate. Thus, the integration of several functional platforms at one PG plate remains a technological problem.

Our team develops ways and methods for density control of PG by utilization of ultrashort laser pulses providing local heating inside the material, leading to local density change classified by four types: pores collapse (so-called “densification”), rarefaction, voids appearance and channel formation [4]. The investigation of the morphological properties, material density especially for densification type, and its tailoring remains a present task. Local control of PG matrix density will open the way for integration of photonic elements (waveguides, splitters, and combiners) and fluidic structures (molecular barriers, solution separators) in single PG platform.

In this work, densified regions which work as waveguides inscribed by femtosecond laser pulses (1035 nm, 220 fs, 1 MHz) were adopted for investigation of refractive index change ( $\Delta n$ ) based on a measured near field distribution of guiding mode. By correlating  $\Delta n$  with the change of PG matrix density, i.e. positive  $\Delta n$  means densification and negative  $\Delta n$  indicates rarefaction of glass matrix, we found a “core-cladding” structure of these waveguides in the cross-section, where a rarefaction region surrounds a densified region and they act as a core and cladding respectively.

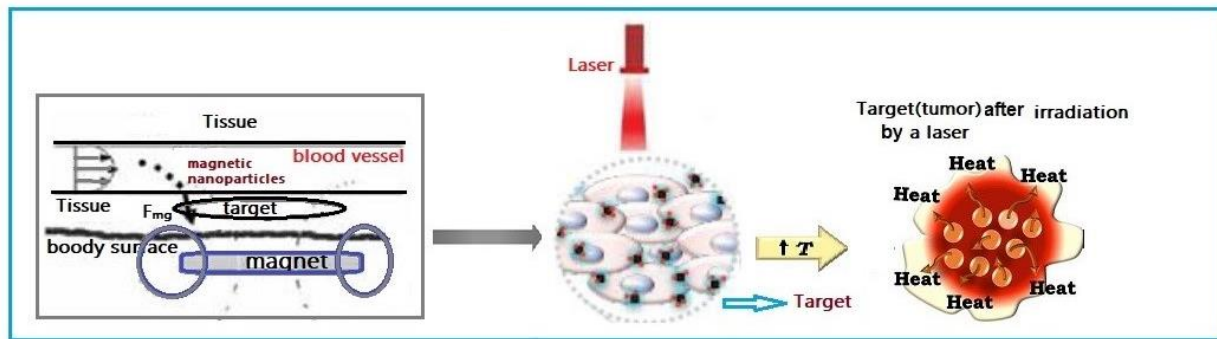
**References**

- [1] Sugioka, Koji, etc. *Lab on a Chip* 14, no. 18 (2014): 3447-3458.
- [2] Iskhakova, Liudmila D., etc. *Journal of Non-Crystalline Solids* 503 (2019): 28-35.
- [3] Maruo, Yasuko Yamada. *Sensors and Actuators B: Chemical* 126, no. 2 (2007): 485-491.
- [4] V. P. Veiko, etc. *Laser Phys. Lett.* 13, 055901 (2016).

**B-PS-10****Numerical simulation for magnetic nanoparticles drug delivery with laser photothermal therapy***S. Salem<sup>1</sup>**<sup>1</sup>Saratov state university, physics faculty, Capanov, Russian Federation*

This work will discuss about principle of magnetic targeting, mechanism of magnetic targeted drug delivery, magnetic nanoparticles in targeted drug delivery in the presence of magnetic field. Magnetically targeted drug delivery by particulate carriers is an efficient method of delivering drugs to localized disease sites such as tumours. High concentrations of chemotherapeutic or radiological agents can be achieved near the target site without any toxic effects to normal surrounding tissue. The magnetic nanoparticles as drug carriers provide huge opportunities in cancer treatment. The use of such carriers in targeted therapy considerably reduces the side effects of conventional chemotherapy. The magnetic drug targeting enables the fast and precise location of drug in the body with the use of external magnetic field.

Also using laser beam for destructive and killing the tumor cells and this occurs by increasing the temperature of tumor cells. This therapy used laser beam which illuminates through cells and generates temperature helping to destroy the tumor cells. In the present study, combination between laser irradiation together with a magnet (which help the magnetic nanoparticle directed toward the target (tumor), and by using the laser beam which the source for energy the tumor damaged and destroyed. The equation of motion describing the problem was solved numerically. Description for the model given by Figure 1.

**Fig. 1.**

**Keywords:** Magnetic nanoparticles, magnetic targeting delivery system, magnetic field, laser heating, computational modeling.

**B-PS-11****spectral features of conventional Raman spectroscopy and autofluorescence analysis of human skin in patients with kidney failure were studied**

*L. Bratchenko<sup>1</sup>, I. Bratchenko<sup>1</sup>, D. Artemyev<sup>1</sup>, O. Myakinin<sup>1</sup>, V. Grishanov<sup>1</sup>, D. Pimenova<sup>2</sup>, P. Lebedev<sup>2</sup>, V. Zakharov<sup>1</sup>*

*<sup>1</sup>Samara University, Laser and Biotechnical Systems Department, Samara, Russian Federation*

*<sup>2</sup>Samara State Medical University, Department of Internal Medicine, Samara, Russian Federation*

Kidney failure leads to the breakdown of water, electrolyte, nitrogen and other metabolic disorders in the human body. Such changes are closely related to the skin condition and affect its component composition. A pathogenesis study demonstrated the accumulation of advanced glycation end-products (AGEs) in the vascular wall, vital organs tissues and skin in patients with severe stages of chronic kidney disease. Improving the diagnostic characteristics and more detailed analysis of pathologically-associated changes in the skin component composition are possible by utilizing the Raman spectroscopy (RS) and autofluorescence (AF) analysis. Therefore, the aim of this work is in vivo optical skin analysis in hemodialysis patients by means of AF in visible region and RS in NIR region.

Studies were performed for two subject's groups. The first group included 85 hemodialysis patients with kidney failure. 79 healthy volunteers constituted a second (control) group. The excitation of the skin AF response was stimulated by the light emitting diode in the 300-420 nm range. Detection of AF spectra was performed at the range of 435-600 nm. Along with AF measurements a backscattered signal was registered in order to compensate the individual differences in the optical properties of the skin. To study skin Raman spectral features the stimulation of collected spectra was performed by the laser module (LML-785) with central wavelength 785 nm. The Raman probe (RPB785) allows for focusing of the exciting radiation, collecting and filtering of the scattered radiation. The collected signal was decomposed into a spectrum using a portable spectrometer (QE65Pro). The spectra were recorded in the spectral range 780-1050 nm.

Firstly, we analyzed data on AF, while the target group is characteristically different by the presence of kidney failure and by level of average age. In order to discrimination target and control group the autofluorescence data is subjected to logistic regression analysis. The analysis demonstrated the detection of subjects associated with increased content of AGE products in the skin with specificity of 0.93, sensitivity of 0.82 and accuracy of 0.88. The PLS-DA analysis of skin Raman spectra set was carried out to determine the target group. The specificity, sensitivity and accuracy of identifying subjects with an elevated AGE-level by analyzing the skin Raman characteristics were 0.98, 0.88 and 0.95, respectively.

As expected, utilizing the combination of RS and AF analysis may improve the accuracy of detecting the AGEs products in the skin. Accuracy, sensitivity and specificity of the analysis are sufficient for clinical setting, which makes it a potential basis for screening AGE-associated diseases (for example, cardiovascular diseases) and methods for monitoring the status of hemodialysis patients.